

FERRY LANDING DESIGN CRITERIA II: VESSEL CHARACTERISTICS AND HOW THEY INFLUENCE FERRY LANDING DESIGN

WA-RD 267.2

Final Technical Report
October 1993



**Washington State
Department of Transportation**

Washington State Transportation Commission
Transit, Research, and Intermodal Planning (TRIP) Division
in cooperation with the U.S. Department of Transportation
Federal Highway Administration

TECHNICAL REPORT STANDARD TITLE PAGE

1. REPORT NO. WA-RD 267.2	2. GOVERNMENT ACCESSION NO.	3. RECIPIENT'S CATALOG NO.	
4. TITLE AND SUBTITLE FERRY LANDING DESIGN CRITERIA II: VESSEL CHARACTERISTICS AND HOW THEY INFLUENCE FERRY LANDING DESIGN		5. REPORT DATE October 1993	
		6. PERFORMING ORGANIZATION CODE	
7. AUTHOR(S) Barbara Adele Scarpelli Charles T. Jahren		8. PERFORMING ORGANIZATION REPORT NO.	
9. PERFORMING ORGANIZATION NAME AND ADDRESS Washington State Transportation Center (TRAC) University of Washington, JE-10 The Corbet Building, Suite 204; 4507 University Way N.E. Seattle, Washington 98105		10. WORK UNIT NO.	
		11. CONTRACT OR GRANT NO. Agreement T9233, Task 23	
12. SPONSORING AGENCY NAME AND ADDRESS Washington State Department of Transportation Transportation Building, MS 7370 Olympia, Washington 98504-7370		13. TYPE OF REPORT AND PERIOD COVERED Final Technical Report	
		14. SPONSORING AGENCY CODE	
15. SUPPLEMENTARY NOTES This study was conducted in cooperation with the U.S. Department of Transportation, Federal Highway Administration.			
16. ABSTRACT <p style="text-align: center;">Information is provided that will help ferry landing designers understand how vessel characteristics affect berthing maneuvers. Such information will assist in the development of improved ferry landing designs and operating policies. The study includes a literature review, mathematical modeling, a review of physical model tests, and sea trials. Full-scale measurements were also collected with global positioning (GPS) equipment. The results show that physical model tests, sea trials, and full-scale measurements provide useful information on vessel stopping and turning characteristics. Efforts to mathematically model vessel deceleration produced limited success. Recommendations are given for further full-scale tests to assist in defining vessel maneuverability in a variety of berthing situations.</p>			
17. KEY WORDS Vessels, port design, ferry, ferry landing design, ferry terminal design, fender design, berthing, global positioning systems, sea trials, physical modeling, mathematical modeling.		18. DISTRIBUTION STATEMENT No restrictions. This document is available to the public through the National Technical Information Service, Springfield, VA 22616	
19. SECURITY CLASSIF. (of this report) None	20. SECURITY CLASSIF. (of this page) None	21. NO. OF PAGES 253	22. PRICE

Final Technical Report
Research Project T9233, Task 23
Ferry Landing Design Criteria — Phase II

**VESSEL CHARACTERISTICS AND HOW THEY
INFLUENCE FERRY LANDING DESIGN**

by

Barbara Adele Scarpelli
Research Assistant
University of Washington

Charles T. Jahren
Assistant Professor of Civil Engineering
University of Washington

Washington State Transportation Center (TRAC)
University of Washington, JE-10
The Corbet Building, Suite 204
4507 University Way N.E.
Seattle, Washington 98105

Washington State Department of Transportation
Technical Monitor
Charles R. Cook
Terminal Construction Engineer
Marine Division, WSDOT

Prepared for

Washington State Transportation Commission
Department of Transportation
and in cooperation with
U.S. Department of Transportation
Federal Highway Administration

October 1993

DISCLAIMER

The contents of this report reflect the views of the authors, who are responsible for the facts and the accuracy of the data presented herein. The contents do not necessarily reflect the official views or policies of the Washington State Transportation Commission, Department of Transportation, or the Federal Highway Administration. This report does not constitute a standard, specification, or regulation.

TABLE OF CONTENTS

<u>Section</u>	<u>Page</u>
Summary	vii
Chapter 1. Introduction	1
Background	1
Study Overview	2
Chapter 2. Research Approach	5
Background	6
Mathematical Model	8
Stopping Distance/Collision Avoidance	18
Actual Full-scale Measurements	24
Summary of Methodology	27
Chapter 3. Findings	31
Introduction	31
Scenarios	32
Information from Sea Trials	42
Actual Full-scale Measurements	43
Stopping Distance/Collision Avoidance	62
Chapter 4. Conclusions and Recommendations	71
Conclusions	71
Recommendations	73
Reference Book on Vessel Characteristics	73
Full-scale Measurements	74
Summary	77
References	79
Bibliography	81
Appendix A. Vessel Characteristics	A-1
Basic Parameters	A-1
Resistance	A-10
Propulsion	A-18
Rudders	A-19
Full-scale Measurements and Sea Trials	A-28

<u>Section</u>	<u>Page</u>
Appendix B. Tables of Kinematic Viscosity and Density of Fresh and Salt Water	B-1
Appendix C. Frictional Resistance and Reynolds Number Sample Calculations.....	C-1
Appendix D. Wave-making Resistance Sample Calculations.....	D-1
Appendix E. Danish Maritime Institute Example Computer Simulation Plot	E-1
Appendix F. $R/Tons$ and V/\sqrt{L} Calculations	F-1
Appendix G. University of Michigan Model Tests.....	G-1
Appendix H. Sea Trials Results for Washington State Ferries.....	H-1
Appendix I. Velocity and Acceleration Sample Calculations.....	I-1
Appendix J. Velocity, Acceleration, and Total Resistance Calculations	J-1
Appendix K. Velocity, Acceleration, and Total Resistance Calculations for Power Reduction Scenarios.....	K-1
Appendix L. Headreach Sample Calculations	L-1
Appendix M. Description of San Juan Islands Sailing.....	M-1

LIST OF FIGURES

<u>Figure</u>		<u>Page</u>
2.1	Calculated Frictional Resistance vs. Velocity for WSF Super Class Ferry.....	9
2.2	Estimated Wave-making Resistance vs. Velocity.....	10
2.3	Calculated Frictional Resistance and Wave-making Resistance vs. Velocity	11
2.4	Calculated Total Resistance vs. Velocity.....	12
2.5	Total Resistance/Displacement vs. Speed-Length Ratio.....	13
2.6	Total Resistance/Displacement vs. Speed-Length Ratio from Physical Model Test Data	16
2.7	Stopping Ships	20
2.8	Ferry Maneuvering Tests	22
2.9	Minimum Turning Path for BUS Design Vehicle.....	23
2.10	Example of Turning Test Results for Washington State Ferries Super Class Ferry MV <i>Yakima</i>	25
2.11	Edmonds to Kingston Ferry Route.....	26
2.12	Sample Velocity vs. Distance Graph.....	28
2.13	Sample Plot of Ferry Path from Kingston to Edmonds.....	29
3.1	Velocity vs. Distance, Full Ahead - Stop.....	33
3.2a	Velocity vs. Distance, Full Ahead - Slow Ahead.....	35
3.2b	Velocity vs. Distance, Full Ahead - Slow Ahead and Full Ahead - Stop	37
3.3	Velocity vs. Distance, Slow Ahead - Slow Astern.....	39
3.4	Velocity vs. Distance, Full Ahead - Full Astern	41
3.5	Selected Ferry Crossings from Kingston to Edmonds	45
3.6	Path of Ferry During Turns with Rudder at 35°	46
3.7	Detail of Right Turn with Rudder at 35°	47
3.8	Detail of Left Turn with Rudder at 35°	48
3.9	Velocity vs. Distance During Sailing Involving Turn with Rudder at 35°	49
3.10	Path of Ferry Involving Right Turn with Rudder at 20°	51
3.11	Path of Ferry During Right Turn with Rudder at 25°	52
3.12	Detail of Right Turn with Rudder at 20° and Throttle at Slow Ahead	53
3.13	Details of Right Turn with Rudder at 25°	54
3.14	Velocity vs. Distance During Sailing Involving Right Turn with Rudder at 20°	55
3.15	Velocity vs. Distance During Sailing Involving Right Turn with Rudder at 25°	56
3.16a	Velocity vs. Distance During Sailing Involving Power Loss.....	57
3.16b	Velocity vs. Distance During Sailing Involving Power Loss (detail of section between 2,000 and 5,000 ft).....	58
3.17a	Velocity vs. Distance During Sailing Involving Power Loss.....	59
3.17b	Velocity vs. Distance During Sailing Involving Power Loss (detail of section between 22,000 and 23,000 ft).....	60
3.18a	Possible Collision Avoidance Path and Possible Turn Avoidance Path	66
3.18b	Possible Turn Avoidance Path	67
3.19	Speed Envelopes for WSF Super Class Ferry.....	69
4.1.	Anticipated Rotational Motion (a) While Berthed and (b) While at Sea.....	78

LIST OF TABLES

<u>Table</u>		<u>Page</u>
3.1	Summary of Full-scale Turning Measurements	61
3.2	Summary of Full-scale Deceleration Measurements.....	61
3.3	AASHTO Stopping Sight Distance (Wet Pavements)	63
3.4	Headreach Calculations for WSF Super Class Ferry	64

SUMMARY

The purpose of this study was to help ferry landing designers understand how vessel characteristics affect berthing maneuvers. This knowledge should assist in improving both ferry landing designs and vessel operating policies.

The study included a literature review, mathematical modeling, and a review of previously performed physical model tests and sea trials. The investigation concentrated on Washington State Ferry's Super Class vessels (capacity-160 automobiles, length-382 ft, beam-73 ft, draft-16 ft, displacement-3,283 long tons). Full-scale measurements were also collected with global positioning system (GPS) equipment. Finally, the research team developed a protocol to assist researchers in making future GPS measurements.

Sea trials provided information on vessel stopping and vessel turning characteristics. The diameter of the turning circle was determined for throttle settings of full ahead and half ahead. The stopping distance from maximum speed using full reverse propulsion was also obtained. From existing Super Class vessel sea trial records, the turning circle was 1,900 ft to 2,600 ft, and the stopping distance was 900 ft.

Mathematical modeling of stopping situations produced similar results for stops using full reverse power. However, modest efforts at mathematical modeling for stops using half astern and slow astern power settings did not produce results that corroborated actual observations. For this reason, the research team recommends that GPS observations be made during stops using half astern and slow astern to improve these mathematical models and to provide empirical data on vessel deceleration characteristics at these throttle settings.

The results of the physical model tests were the preferred source of information for estimating vessel drag for mathematical models. The estimates of Super Class vessel drag obtained from tables in the literature varied considerably from the results of previously performed physical model studies.

The researchers recommend that WSDOT develop a vessel guidebook for ferry landing designers that includes the basic characteristics of all vessels and the results of sea trials and physical model tests. GPS observations should be obtained for distressed vessel situations, such as a vessel attempting to turn with limited or no power, or a vessel drifting with no power under the influence of the wind and current. These observations could be made in open water under safe conditions. The results of these observations could then be analyzed, and ferry landing designs and operating policies could be improved so that operators could better handle distressed vessel situations.

CHAPTER 1

INTRODUCTION

BACKGROUND

Understanding vessel characteristics is a vital part of ferry landing design. The vessel approach path and velocity are influenced by the vessel characteristics. The approach velocity is important because the fender system at the landing facility must absorb the energy associated with the approach velocity; the approach path is important because the placement of the landing structures is dependent upon the location of the ferry during its approach into the berth. (1) Ferry landing structures should be tailored to the velocity and paths of the ferries for which they are designed. Since velocity and approach paths are influenced by ferry characteristics, better understanding of these characteristics can allow the designer to improve the geometric arrangement of landing structures and to select appropriate design berthing forces.

To understand how vessel characteristics influence the vessel approach path near the landing structures, one may examine both the effects of normal berthing maneuvers and the berthing maneuvers of distressed vessels. Examples of distressed vessels are those that are off-course, or those that are experiencing propulsion malfunctions. Because berthing maneuvers involving distressed vessels are rare, it is difficult to study them by observation. Instead, the research team at the University of Washington Department of Civil Engineering analyzed approaches related to these types of berthing maneuvers by using simulation methods. (1)

The objective of the study was to assist ferry landing designers in understanding how vessel characteristics affect berthing maneuvers. This knowledge will allow designers to plan more effective landing structures and to develop appropriate vessel operating policies. Such policies may limit vessel speed and paths; they may also enable

- recommended procedures for future full-scale measurements taken with GPS instrumentation to test other berthing scenarios, or to provide a greater understanding of vessel characteristics and vessel maneuverability;
- recommendations regarding the development of ferry landing design criteria that are similar to some geometric design criteria for roadways;
- recommendations for further research.

CHAPTER 2

RESEARCH APPROACH

Information gleaned from the literature search suggested to the researchers that changes in vessel velocity with respect to time can be estimated if approximate resistance and thrust values are known. Application of this knowledge enables designers to estimate a given vessel's approach velocity in the given circumstances. The literature review also revealed a relationship, known by naval architects, between vessel resistance and vessel velocity. A graph depicting total resistance/tons ($R/Tons$) vs. velocity/length (V/\sqrt{L}) can be prepared for most vessels. A sample curve of this relationship is shown in Figure A.5. (3)

Although mathematical equations can be applied to estimate vessel resistance, the resistance is more accurately obtained from physical model resistance test data. Once vessel resistance is estimated from physical model resistance test results, the total force acting on the vessel can be calculated. Equations of motion can be employed to calculate final velocity from initial vessel velocity. These equations represent a mathematical model to predict the vessel velocity on the basis of vessel characteristics.

Review of existing documentation showed that it is possible to obtain additional information on vessel characteristics by examining the results of sea trials and full-scale measurements. During exploratory full-scale tests, information derived from mathematical models and sea trials was confirmed. Additionally, recommendations for data collection procedures were developed for future full-scale tests.

Demonstrated as part of this study was the principle that design criteria for ferry landing structures can be developed by considering vessel characteristics in a manner similar to that employed in developing design criteria for roadways. However, vessel characteristics should not govern the design of ferry landing structures.

BACKGROUND

Mathematical models created to estimate vessel velocities on the basis of vessel characteristics for specific berthing scenarios will be discussed in the following section. These berthing scenarios represent both normal approaches and approaches that involve vessels in distress. Berthing scenarios studied as part of this project are listed below:

1. a ferry decelerating after a throttle-setting change from full ahead to stop (a distress scenario),
2. a ferry decelerating after a throttle-setting change from full ahead to slow ahead,
3. a ferry decelerating after a throttle-setting change from slow ahead to slow astern,
4. a ferry decelerating after a throttle-setting change from full ahead to full astern,
5. a ferry turning at full-ahead speed resulting from a rudder position change from midships to 35 degrees right,
6. a ferry turning at full-ahead speed resulting from a rudder position change from midships to 35 degrees left,
7. a ferry turning at full-ahead speed resulting from a rudder position change from midships to 25 degrees right, and
8. a ferry turning at slow-ahead speed resulting from a rudder position change from midships to 20 degrees right.

All of the scenarios listed above were tested as part of this study or a previously performed sea trial. Other possible maneuvering scenarios that could be tested in the future include the following:

9. a ferry drifting on a calm day without steering control,
10. a ferry drifting on a windy day without steering control, and
11. a ferry drifting on a windy day with steering control.

Testing procedures for these scenarios will be discussed in Chapter 4.

During the berthing scenarios, evasive maneuvers might aid in preventing or minimizing potential damages. Possible evasive maneuvers are as follows:

1. reversing propulsion to full astern to decelerate the vessel,
2. using the rudder to return to course and avoid collision, and
3. using the rudder to turn the vessel away from the approach path.

Understanding a vessel approach path as the vessel nears the landing facility is important in understanding the berthing scenarios. As part of a continuing research effort at the University of Washington, a preliminary study of the approach paths of WSF ferries was performed. A detailed description of this study is included in Appendix D. The study showed that ferry approach paths can be plotted by using video cameras and simple survey techniques. The study described in Appendix D provided a quick and easy means of estimating a vessel's location within ± 200 feet. (4) The study also recommended the use of the Global Positioning System (GPS) to provide more accurate vessel positioning. A description of the GPS installation on the WSF ferries is also provided in Appendix D. GPS is a measuring system that locates the position of an object on earth by measuring the object's distance from a group of satellites in space. *GPS, A Guide to the Next Utility*, by Jeff Hurn for Trimble Navigation Ltd., provides a more complete description of GPS. (5)

Other research teams have tracked vessel locations with GPS in their studies as well. *Ship Simulation of the Houston Ship Channel, Houston, Texas*, by D.W. Webb and J.C. Hewlett, describes the GPS installation that was used to track two loaded vessels meeting and passing in a constricted channel. (6) The Danish Maritime Institute simulates vessel motion with computer programs. In this application, a vessel captain navigates a simulated path in a laboratory setting. The captain's actions are recorded, and the computer simulation program then plots the course of the simulated path. A more detailed description of the Danish Maritime Institute's facilities is provided in

Reference 2. An example of a plot generated on the basis of the computer simulations are given in Appendix E.

MATHEMATICAL MODEL

As part of this study, $R/Tons$ vs. V/\sqrt{L} curves were generated for WSF Super Class ferries. Curves of $R_f/Tons$ vs. V/\sqrt{L} , $R_w/Tons$ vs. V/\sqrt{L} , both $R_f/Tons$ and $R_w/Tons$ vs. V/\sqrt{L} , and $R_f/Tons$ vs. V/\sqrt{L} generated from calculations by this method are shown in Figures 2.1, 2.2, 2.3, and 2.4, respectively. Additionally, an existing graph of $R_f/Tons$ based on physical model resistance test data for WSF Super Class ferries was reviewed during this study. (Z) This graph is shown in Figure 2.5. The field testing indicated that the resistance values from the physical model test results produce a more accurate estimate of resistance (used to predict vessel velocity) than do the mathematical equations. Although the mathematical equations were found to have shortcomings in this study, they may be useful for other applications. Therefore, the application of these equations for estimating vessel resistance is described in this section.

To develop curves of $R_f/Tons$ vs. V/\sqrt{L} for a WSF Super Class ferry, the Reynolds Number, R , the frictional resistance coefficient, C_f , the frictional resistance, R_f , and the frictional resistance per ton, $R_f/Tons$, were calculated for different velocities using Equations 3, 4, and 5. Summary calculations performed to compute values to develop these curves are provided in Appendix F. The values of $R_f/Tons$ were plotted against values of V/\sqrt{L} for the corresponding velocity. The resulting curve as shown in Figure 2.1 is similar in shape to the published curve for frictional resistance that is presented in Figure A.5. For the range of values of V/\sqrt{L} in Figure 2.1, the $R_f/Tons$ values are similar to those obtained from the published curve shown in Figure A.5.

The research team generated the $R_w/Tons$ vs. V/\sqrt{L} curve shown in Figure 2.2 by using the values of $R_w/Tons$ and values of V/\sqrt{L} obtained from Table A.4. Once plotted, the set of data points were fitted with an exponential regression curve using a least squares fit approximation. The coefficient of correlation for the resulting

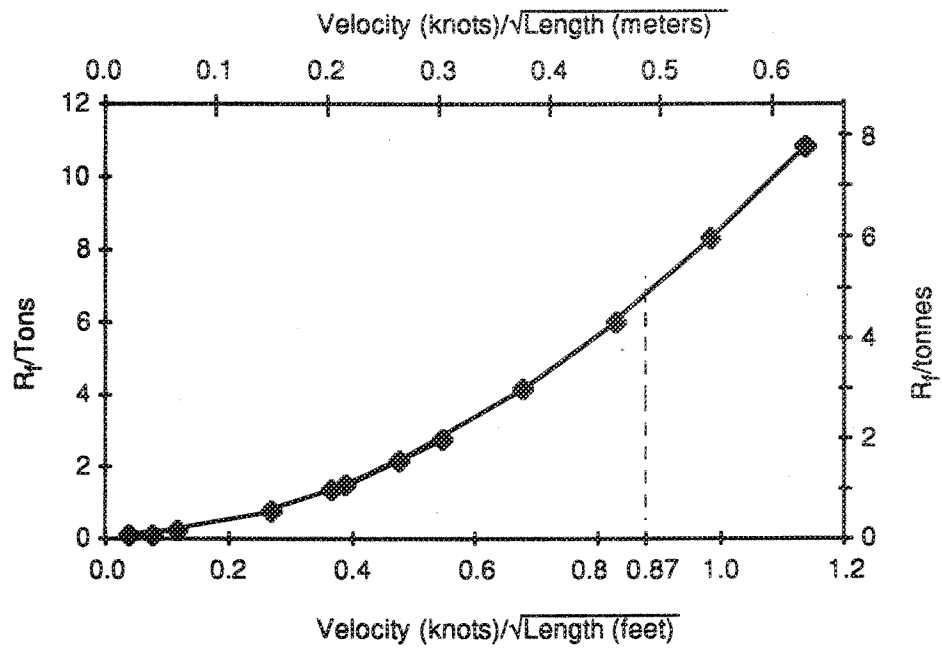


Figure 2.1. Calculated Frictional Resistance vs. Velocity for WSF Super Class Ferry

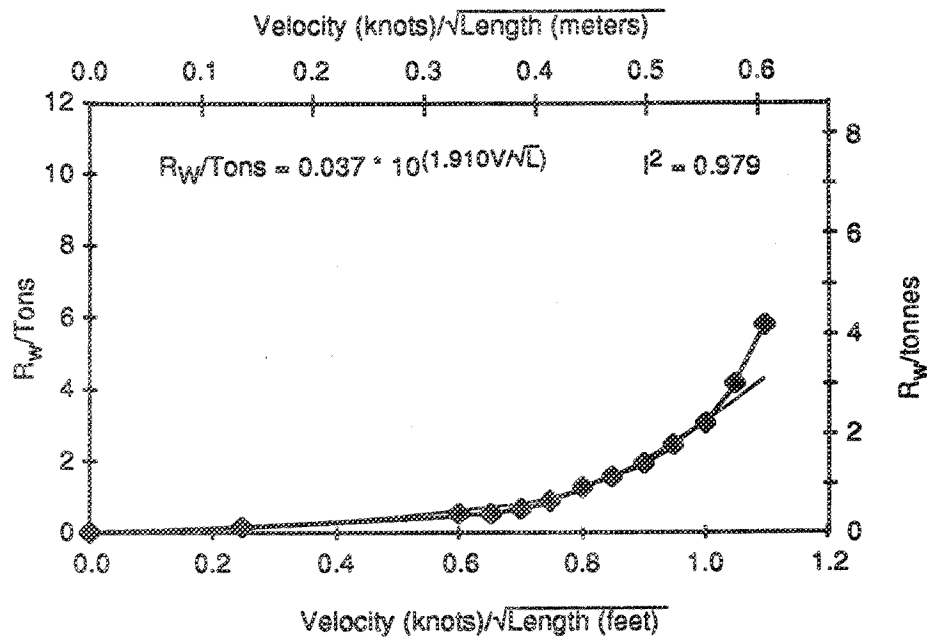


Figure 2.2. Estimated Wave-making Resistance vs. Velocity

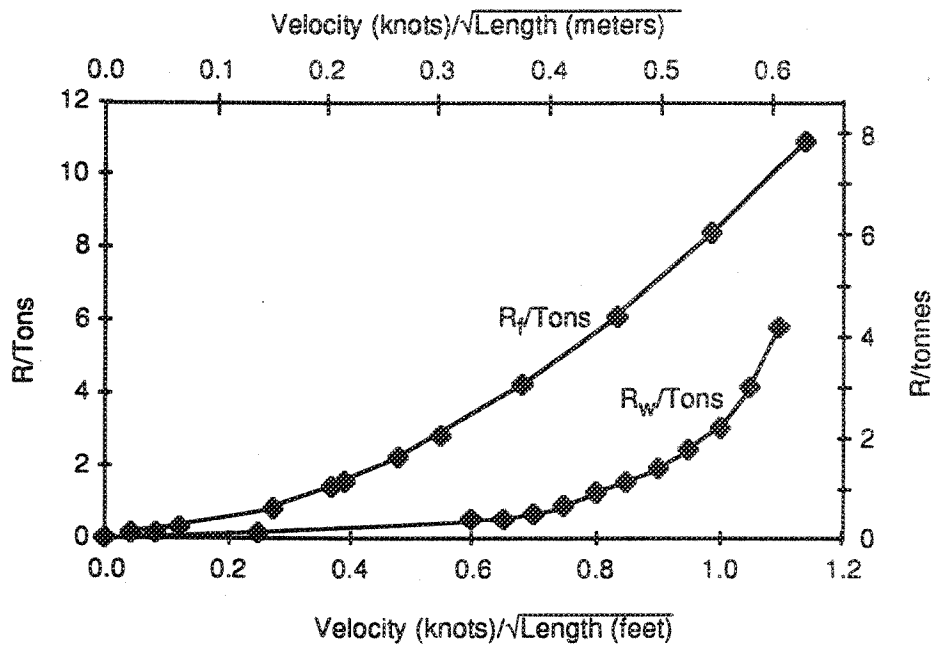


Figure 2.3. Calculated Frictional Resistance and Wave-making Resistance vs. Velocity

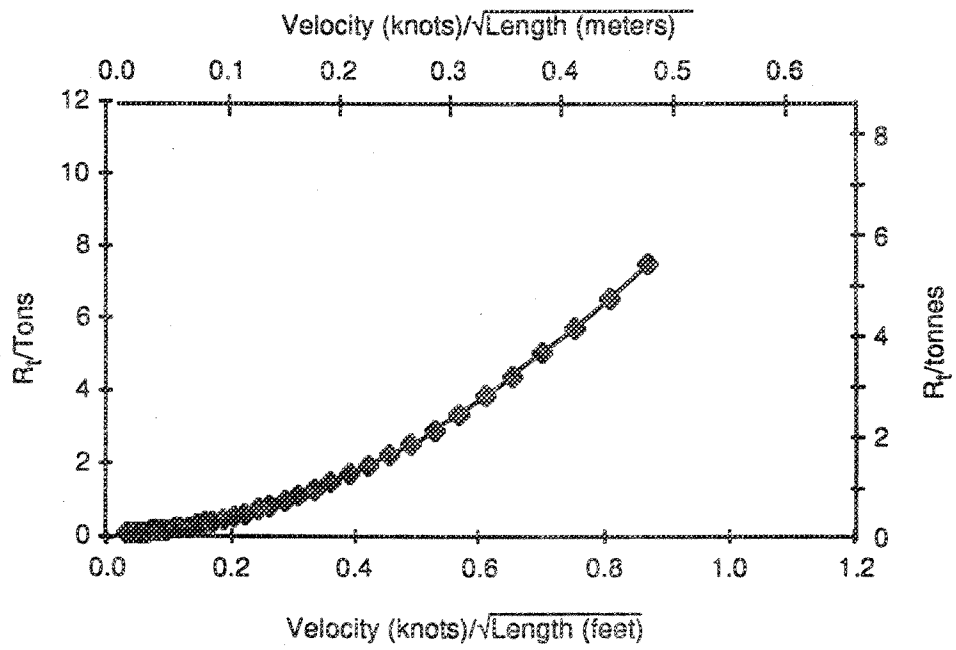


Figure 2.4. Calculated Total Resistance vs. Velocity

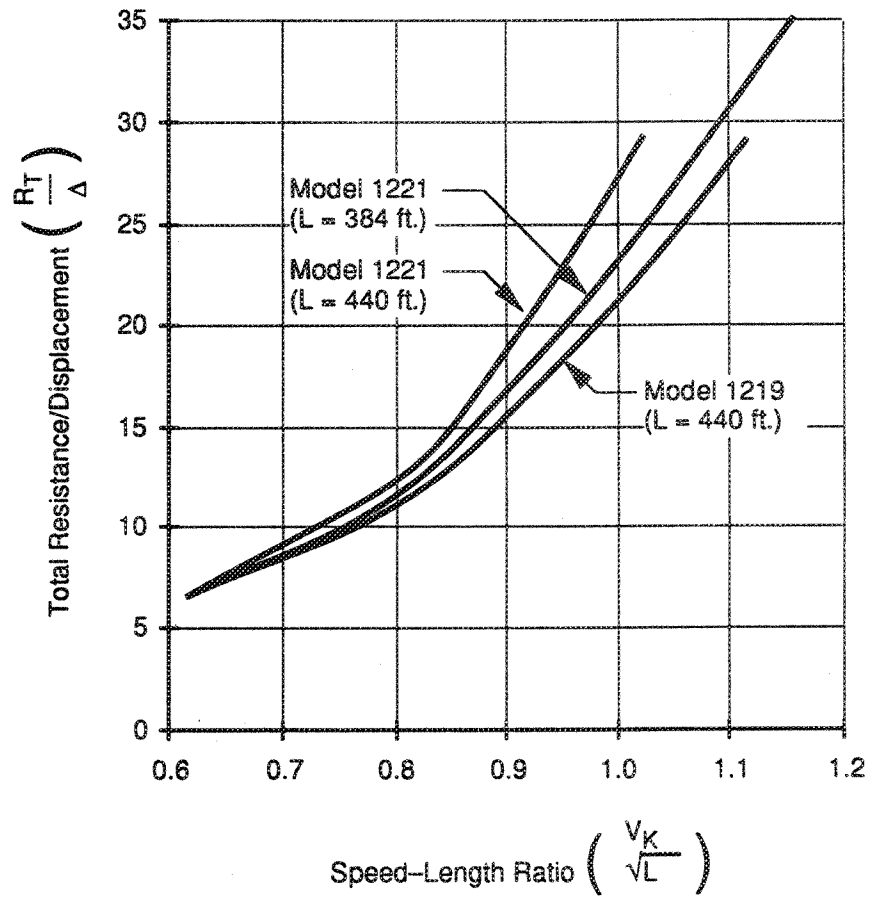


Figure 2.5. Total Resistance/Displacement vs. Speed-Length Ratio (Z)

exponential equation was 0.979, which indicates the curve equation's relative accuracy. A correlation coefficient of 1.00 represents complete accuracy. (8) The resulting curve fit equation is shown on the graph in Figure 2.2 and is described as follows:

$$R_w/Tons = 0.037 * 10^{1.91} * (V/\sqrt{L}) \quad (1)$$

where R_w = wave-making resistance (lbs)

Tons = vessel weight displacement (tons)

V = vessel velocity (knots)

L = vessel length (ft)

For the curve shown in Figure 2.4, $R_f/Tons$ was computed by adding $R_f/Tons$ and $R_w/Tons$ calculated from Equations 5 in Appendix A and 1, respectively. Values of $R_f/Tons$ were plotted against corresponding values of V/\sqrt{L} . The curve in Figure 2.4 is similar in shape, for a similar range of values, to the published curve presented in Figure A.5.

The curve of $R_f/Tons$ vs. V/\sqrt{L} obtained by this method was compared to a graph of $R_f/Tons$ vs. V/\sqrt{L} developed from towing tank model resistance tests. The graph shown in Figure 2.5 presents results of $R_f/Tons$ for ferry model tests performed at the Ship Hydrodynamics Laboratory at the University of Michigan. The tests were performed on a model representing a WSF Super Class ferry. The resistance tests were conducted over a speed range of 13 knots to 23 knots (full-scale). The models were fitted with a dummy hub in place of the stern propeller and a free wheeling bow propeller. (Z) A complete description of the model tests and the test results is given in Appendix G.

A comparison of the two methods of estimating the resistance of a WSF Super Class ferry at full-ahead speed (17 knots or 28.7 ft/sec) renders the following results:

Method	$R_f/Tons$	R_f
Mathematical Model	7.46	24,496.56 lbs
Model Tests	16.66	54,701.21 lbs

The values obtained through the application of mathematical equations to compute values of R_f , R_w , and R_t , differed considerably from the model test results; differences in values for R_w represented the largest differences.

The values of R_f , R_w , and R_t obtained from mathematical equations reflected a simplified approach. Possible sources of error include the following: (1) exclusion of appendage resistance, air resistance, and eddy resistance; and (2) use of approximate methods to calculate the frictional resistance coefficient. In addition, the tabular data pertaining to R_w were developed for vessels other than ferries, and as such, they may not be appropriate for the estimation of R_w for ferries.

The results from the model tests, as presented in Appendix G, were used as part of this study. Values of R_t/Tons obtained from the model test results were plotted against corresponding values of V/\sqrt{L} . The resulting graph is shown in Figure 2.6. An example of the data that were plotted is contained in Appendix G, under the heading, "Table A5." These data were plotted, and the data points were fitted with an exponential regression curve, using a least squares fit approximation. The correlation coefficient for the resulting exponential equation was 1.00, which indicates an excellent fit. (8) However, a more precise fit would be one that passes through the origin. The resulting curve fit equation for the model test data is shown in Figure 2.6 and is as follows:

$$R_t/\text{Tons} = 1.21 * 10^{1.31} * (V/\sqrt{L}) \quad (2)$$

where

- R_t = total vessel resistance (lbs)
- Tons = vessel displacement (tons)
- V = vessel velocity (ft/sec)
- L = vessel length (ft)

In general, these curves are used when velocity is known and resistance is required. However, the curves may also be used to simulate velocity changes. If the vessel's initial velocity is known, then the total resistance at that velocity may be estimated from the curve. The total resistance force is calculated from Equation 2.

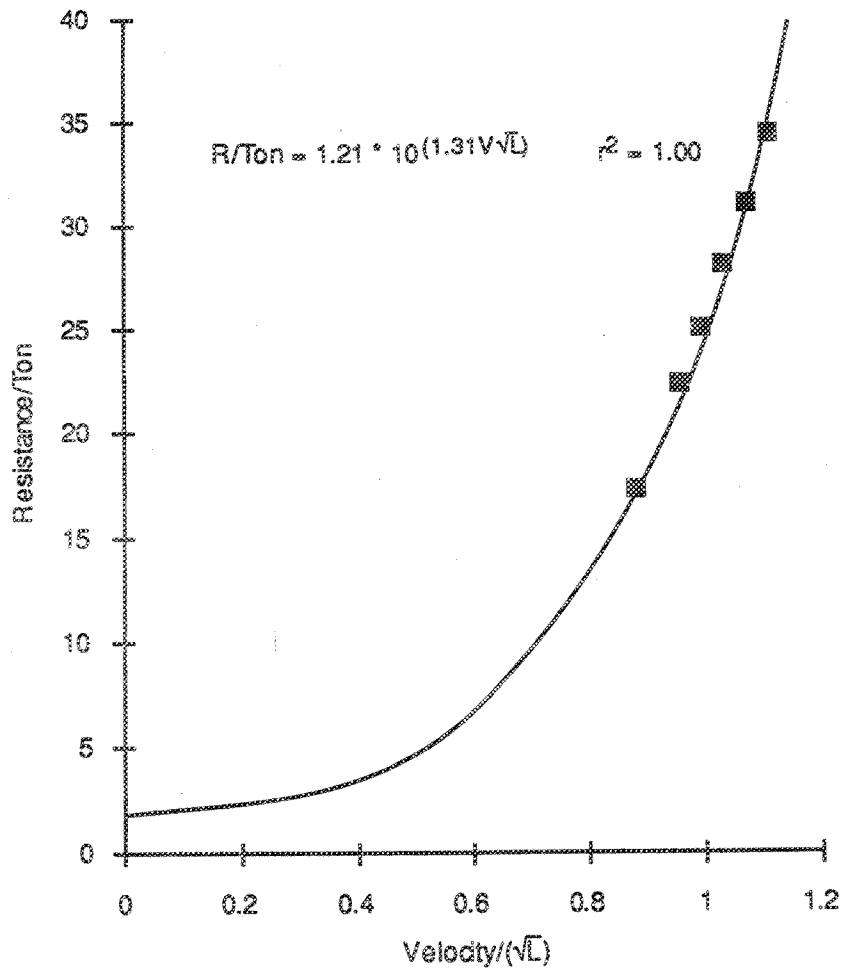


Figure 2.6. Total Resistance/Displacement vs. Speed-Length Ratio from Physical Model Test Data (Z)

This total resistance force represents the drag force on the vessel at a given velocity. If the imbalance between the force created by the propulsion system and the drag force is known, then the vessel's acceleration or deceleration can be calculated. The acceleration or deceleration is calculated from the following equation:

$$A = F/M \quad (3)$$

where A = vessel deceleration (ft/sec²)

F = net force on vessel (lbs)

M = vessel mass (lbs/(ft/sec²))

Apparent vessel mass consists not only of the actual ship mass, but of a certain mass of water surrounding and moving with the ship as well. This mass of surrounding water is referred to as added mass, denoted by the symbol C_m , and is estimated to be in the range of 50 to 80 percent of the actual vessel mass when the vessel is in its final approach maneuver. (9) Added mass applies whenever there is vessel acceleration and not just during the final approach to a landing facility. For the model developed in this study, the vessel was considered to be at a distance from the landing facility, not in its final approach maneuver, and where added mass was not significant. Therefore, the added mass was not considered when the vessel mass was calculated for use in Equation 3. But, added mass is a hydrodynamic property of the vessel that is independent of location.

Velocity as a function of distance can then be computed from equations of motion integrated over a short increment of distance. Velocity can be computed from the following equation:

$$V_1^2 = V_0^2 + 2 * A * s \quad (4)$$

where V_1 = vessel final velocity (ft/sec)

V_0 = vessel initial velocity (ft/sec)

A = vessel acceleration (or deceleration) (ft/sec²)

s = incremental distance travelled (ft)

As the velocity changes, the resistance force changes; therefore, the calculation of V_1 must proceed iteratively. For a given distance, the net vessel force, and therefore the acceleration, are considered to be constant. At the end of the distance interval, the final velocity is calculated from the beginning velocity, the distance travelled, and the net vessel force. The new velocity then represents the beginning velocity for the next distance interval. (10) This model assumes steady-state thrust during the distance travelled and, as such, represents a simplification to vessel deceleration.

STOPPING DISTANCE/COLLISION AVOIDANCE

The principles of geometric alignment of highways are well understood by transportation engineers. Vehicle performance characteristics play an important role in the design of virtually all roadway elements. (11) Current roadway design standards are presented in detail in Reference 12.

Some ferry landing design standards could be developed in a manner similar to the design of roadway standards. For example, practical stopping distance is a concern for designers of both roadways and ferry landing structures. The roadway designer must provide for adequate driver sight distance to permit safe stops. The braking behavior of vehicles is critical in the determination of adequate stopping distance. (11) Similarly, the stopping behavior of a ferry should be of interest to ferry landing designers. However, vessel characteristics should not dictate the design of ferry landing facilities, but be considered in the development of design criteria.

The practical stopping distance used in roadway design is calculated by the following equation:

$$d = V_1^2/30(f) + V_1(t) \quad (5)$$

where d = distance in which vehicle comes to a complete stop (ft)

V_1 = initial velocity (ft/sec)

f = coefficient of friction

t = reaction time (sec)

For safety reasons, a highway design should provide drivers with sufficient sight distance to allow them to safely stop their vehicles to avoid collision with objects obstructing the forward progress of the vehicle. (12)

Vessel designers also define the vessel stopping distance. This distance, known as headreach, provides a measure of the vessel's ability to stop forward progress to avoid collision. Headreach is calculated from the following equation: (13)

$$s = D_i * M * V_1^2 / (2 * R) \quad (6)$$

where s = headreach (ft)

D_i = dynamic potential

M = apparent vessel mass (lb-sec²/ft)

R = vessel resistance (lbs)

V_1 = initial vessel velocity (ft/sec)

Dynamic potential is a dimensionless combination of several variables and is often estimated from curves, as shown in Figure 2.7. Because R varies with V^2 , the curve marked "2" in Figure 2.7 is used to estimate D (V^n indicates use of the curve marked "n"). Dynamic potential is a function of the ratio of the vessel's resistance divided by the astern thrust (R/T). Reaction time and the time required to reach full-astern thrust from ahead thrust are accounted for in the graph presented in Figure 2.7. (13)

The following equation constitutes an approximate method of calculating headreach.

$$s = 80 * V_1^2 * D_i / T + 15 * V_1 \quad (7)$$

where s = headreach (ft)

V_1 = initial vessel velocity (ft/sec)

T_1 = astern thrust (lbs)

D = vessel displacement (tons)

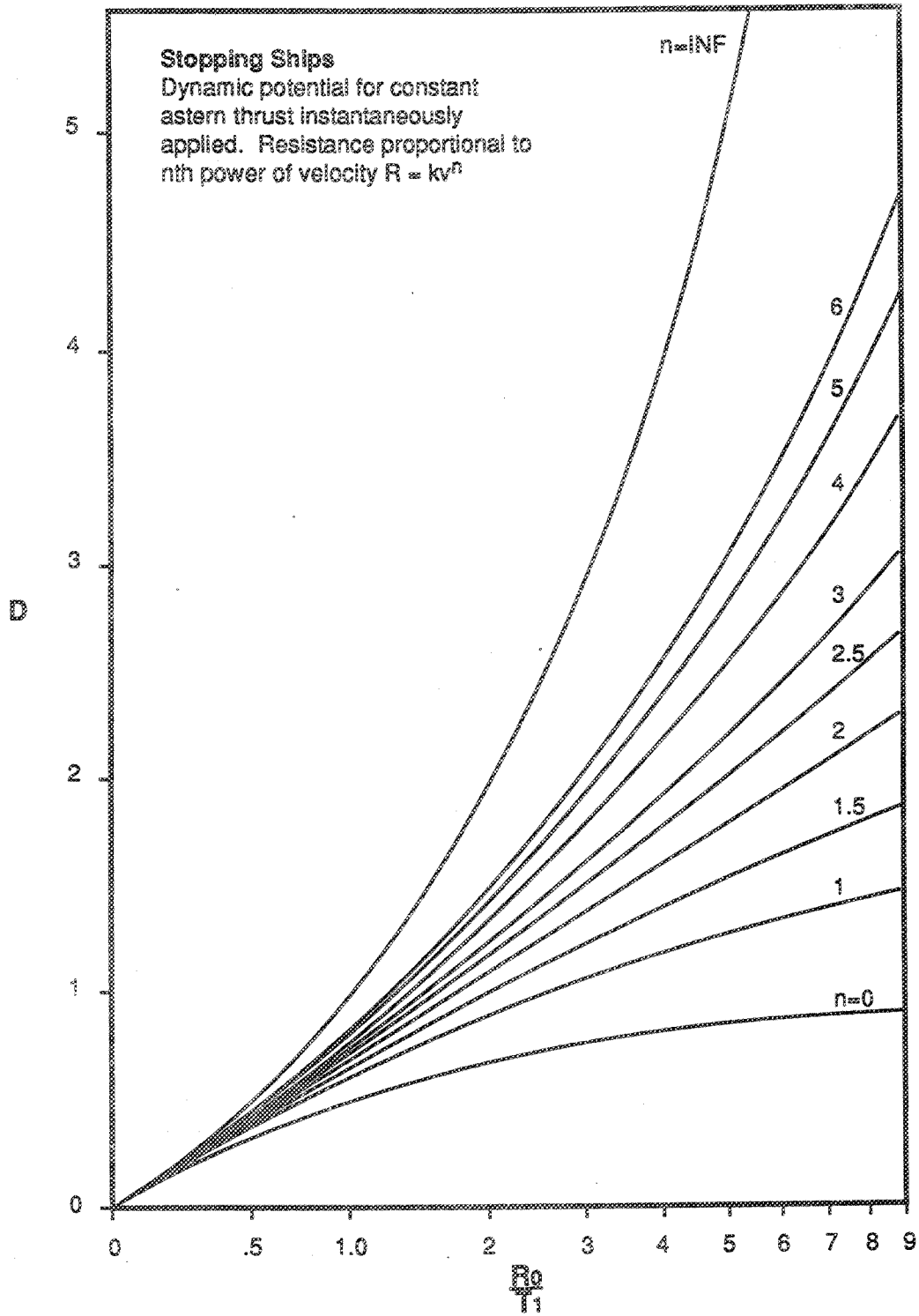


Figure 2.7. Stopping Ships. Dynamic potential for constant astern thrust instantaneously applied. Resistance proportional to nth power of velocity (13)

A further explanation of the derivation of this approximate method is provided in Reference 13. Equation 7 assumes 20 seconds for the time to establish astern thrust. Equation 7 has the advantage of containing only quantities that are readily available.

The headreach used by vessel designers and the stopping distance used by roadway designers are similar. Both enable designers to calculate the distance required to stop the moving vessel, or vehicle, at various speeds. As roadway designers use the safe stopping distance in roadway design, ferry landing designers can use headreach in the development of design criteria for ferry landing structures.

Researchers have studied the stopping characteristics of the ferry MV *Deutschland*. Figure 2.8 shows results of two stopping maneuvering tests with this ferry. These test results furnish general information on stopping times and vessel deceleration. (9) Similar results could be expected for WSF ferries. The graphs in Figure 2.8 indicate that velocity decreases and distance increases with time. This graph also shows that the propeller direction is not reversed instantly, but that it takes approximately 20 seconds before it starts to turn in reverse. Comparison of the two stopping maneuvers reveals that the ferry stops after approximately 600 meters when the initial speed is ahead, but that the ferry stops after approximately 300 meters when the initial speed is astern.

Ferry landing designers are also interested in the turning radius of a vessel. Transportation engineers have long used vehicle turning radius information in their roadway designs. The principal vehicle characteristics affecting horizontal highway design are: vehicle width, wheelbase, and minimum turning radii. Longer vehicles require turning paths of greater widths. A typical minimum turning radius diagram for a BUS design vehicle is depicted in Figure 2.9. In this case, the minimum turning radius and transition lengths are for turns that occur at speeds of less than 10 mph. This radius is considered minimum for this application. The turning dimensions shown in Figure 2.9 were derived from scale models and computer plots. (12)

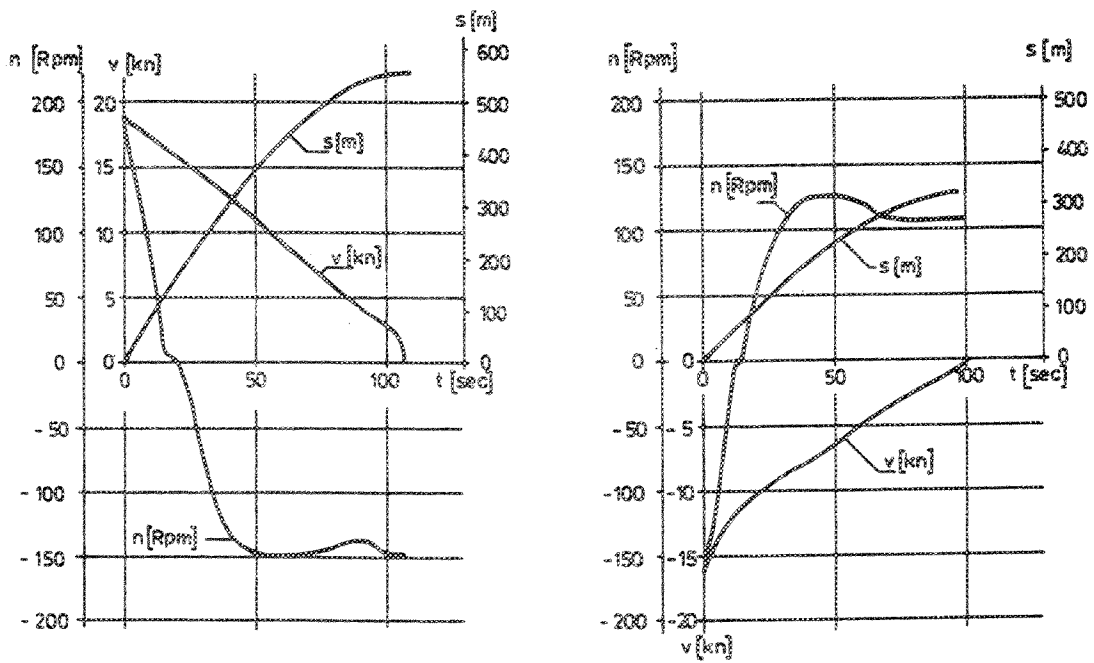
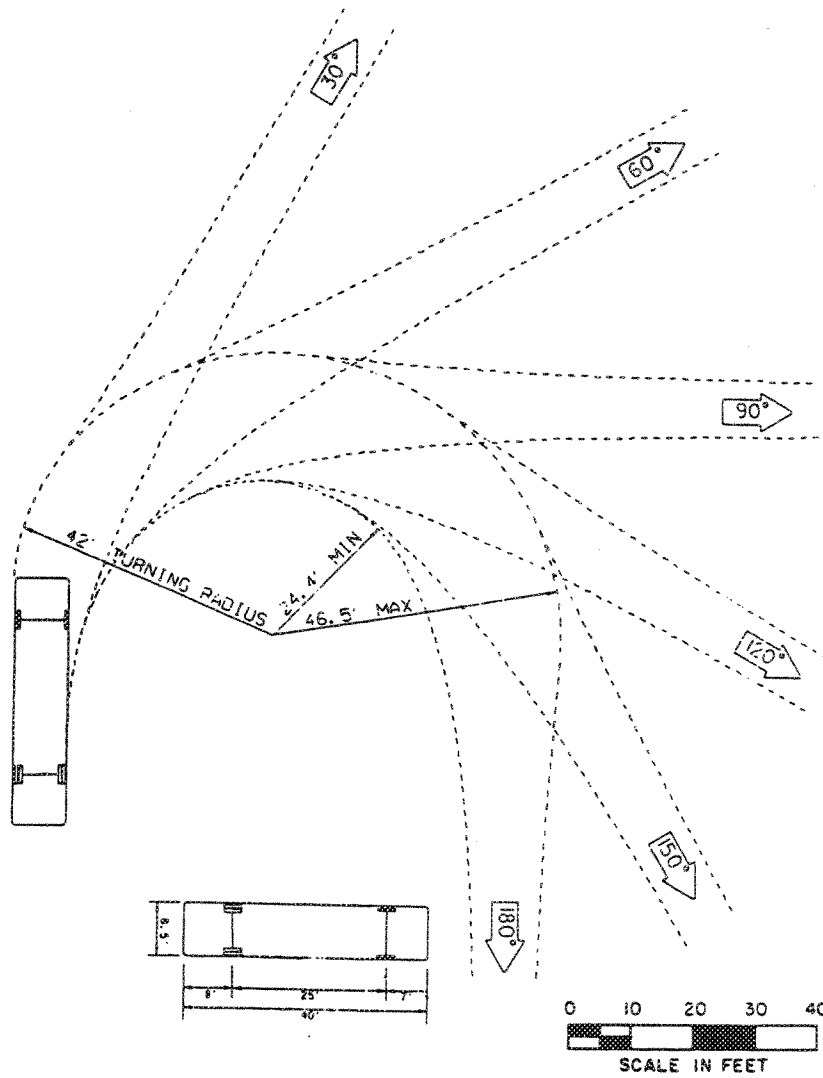


Figure 2.8. Ferry Maneuvering Tests (Q):

(left): Stopping maneuver, initial speed 18.8 knots ahead (9.4 m/sec)

(right): Stopping maneuver, initial speed 15.8 knots astern (7.9 m/sec)

THIS TURNING TEMPLATE SHOWS THE TURNING PATHS OF THE AASHTO DESIGN VEHICLES. THE PATHS SHOWN ARE FOR THE LEFT FRONT OVERHANG AND THE OUTSIDE REAR WHEEL. THE LEFT FRONT WHEEL FOLLOWS THE CIRCULAR CURVE; HOWEVER, ITS PATH IS NOT SHOWN.



Source: Texas State Department of Highways and Public Transportation

Figure 2.9. Minimum Turning Path for BUS Design Vehicle (12)

The turning test results derived from sea trials can provide ferry landing designers with similar turning information. Turning test results provide information related to the vessel turning radius for two different shaft RPMs. Turning test results for the WSF Super Class ferry, *Yakima*, are shown in Appendix H, and an example of turning test results for this ferry are shown in Figure 2.10. The minimum turning radius for the *Yakima* is approximately 1893 feet at a speed of 17 knots. A diagram similar to that shown in Figure 2.9 can be created from this test result. The information gained from turning test results can assist ferry landing designers in developing plans that allow for sufficient turning radii, given operative ferry approach speeds.

ACTUAL FULL-SCALE MEASUREMENTS

As part of this study, full-scale measurements were performed with the WSF Super Class ferry, *Yakima*, using the GPS system, which was referenced previously (Appendix D). These measurements were taken during regular sailings between Edmonds and Kingston. Figure 2.11 shows the location of the terminals at each of these sites and the approximate ferry path on this route. The full-scale tests were exploratory in nature; the research team hoped that the initial round of tests would provide information that would be useful in making recommendations for further full-scale testing.

GPS instrumentation recorded the *Yakima's* position and velocity throughout each sailing. The standard route between Edmonds and Kingston involves travel at constant heading, and also involves heading changes. In particular, the ferry encounters a change of heading into Appletree Cove as it approaches the Kingston terminal. The ferry also changes course from a northeasterly heading (approximately) to an easterly heading (approximately) as it approaches the Edmonds terminal. The location of these heading changes is shown in Figure 2.11. GPS instrumentation tracked the ferry position over the entire sailing.

During the data collection period, the ferry also travelled through nonstandard courses on some sailings. For example, during a demonstration of vessel rudder

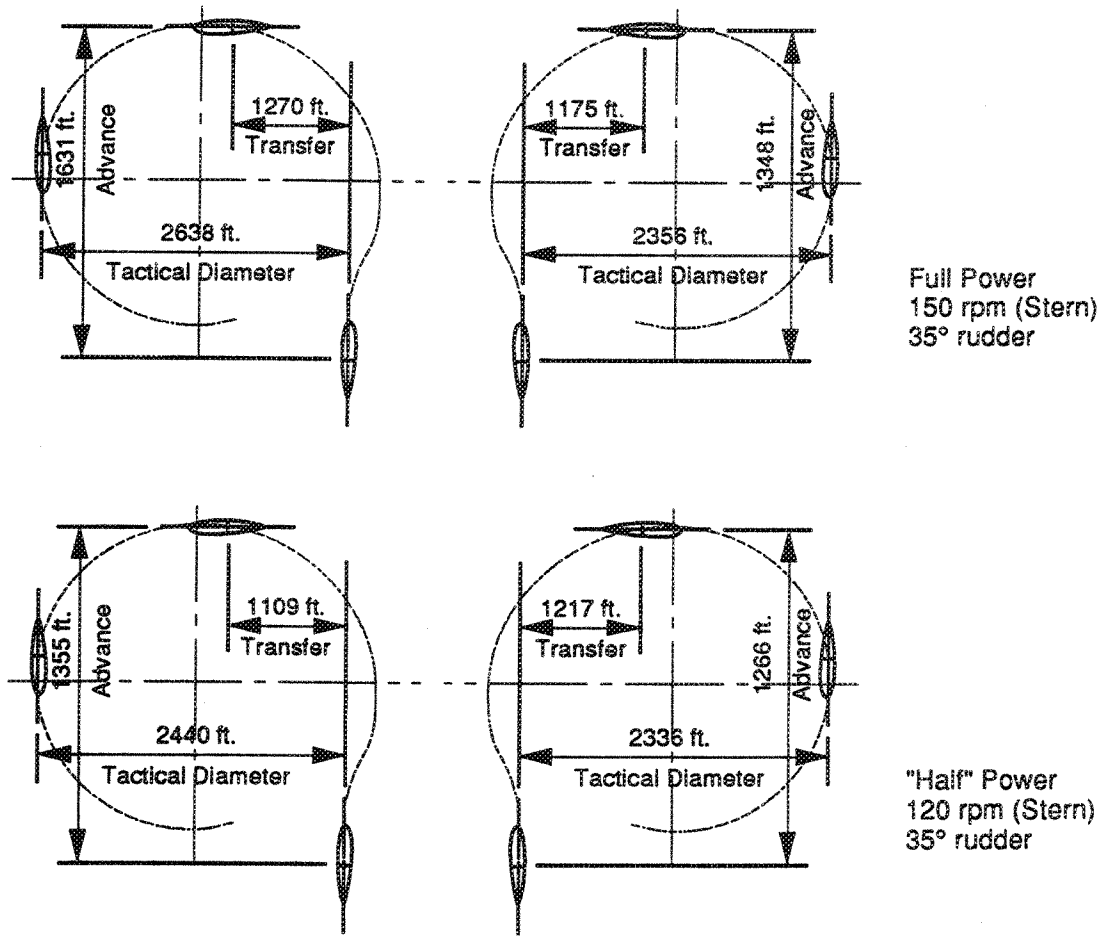


Figure 2.10. Example of Turning Test Results for Washington State Ferries Super Class Ferry MV Yakima (Washington State Ferries)

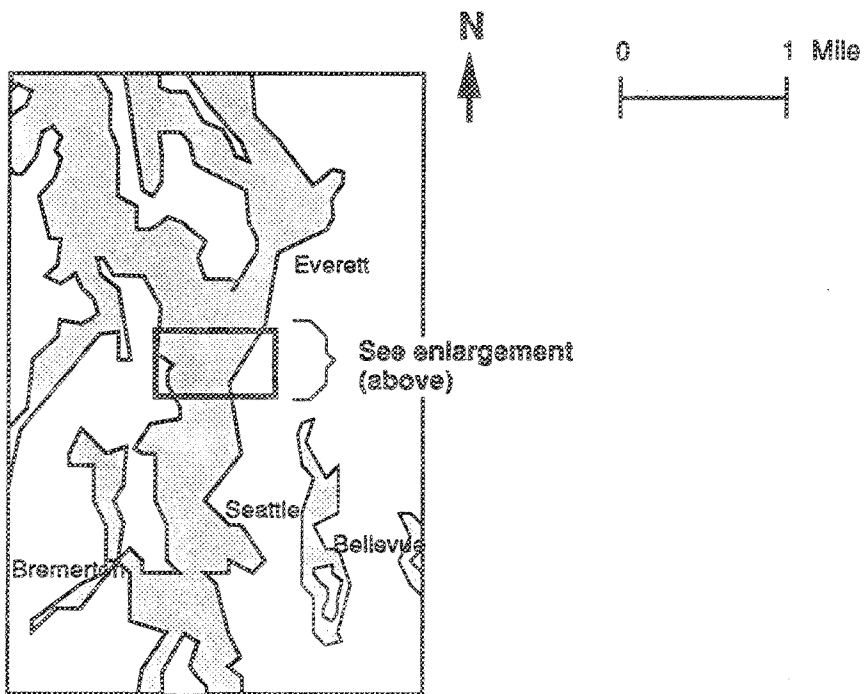
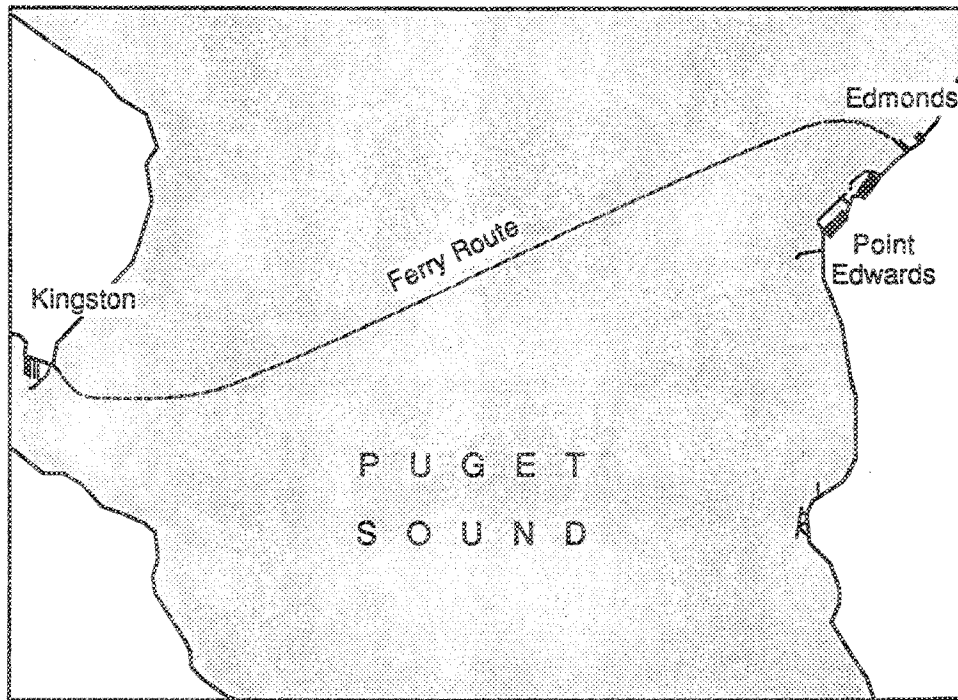


Figure 2.11. Edmonds to Kingston Ferry Route

response, the ferry was turned to the left, to the right, and back on course, when the rudder position was set hard left, hard right, and midships, respectively, while at full-ahead speed. Another example was a 90 degree turn from an easterly direction (approximately) to a northerly direction (approximately) while at full-ahead speed. The vessel rudder response at slow-ahead speed was demonstrated when the captain altered the rudder position on the final approach to the landing facility.

Once measurements had been collected with the GPS instrumentation, the raw data were differentially corrected with Trimble Navigation Ltd.'s POSTNAV II software. Differential correction involves calculating the error associated with the system for a known reference point and applying the correction to the mobile reference point. A more complete description of the POSTNAV II software and differential correction methods is provided in Appendix D. POSTNAV II provides coordinates of the vessel's position, as well as the north and east components of velocity at one-second intervals. Position and velocity results were imported into Microsoft EXCEL for Windows; a spreadsheet was then created. Data manipulation in the spreadsheet resulted in absolute values of distance and net velocity at one-second intervals. The research team generated graphs of velocity vs. distance from the distance and net velocity data. The data were then imported into the AUTOCAD software program, which produced plots of the vessel's path. Examples of the EXCEL graphs and AUTOCAD graphics are shown in Figures 2.12 and 2.13.

SUMMARY OF METHODOLOGY

The methodologies presented in this chapter cover a variety of tasks related to increasing understanding of vessel characteristics and their role in ferry landing design. The selection of possible berthing scenarios and the creation of mathematical models to estimate vessel velocity during these scenarios constitute the first step in this process. Review of existing sea trials results provides additional insight regarding vessel maneuvers. Data gathered during the preliminary full-scale measurements provide a point of comparison for some of the previously developed mathematical models.

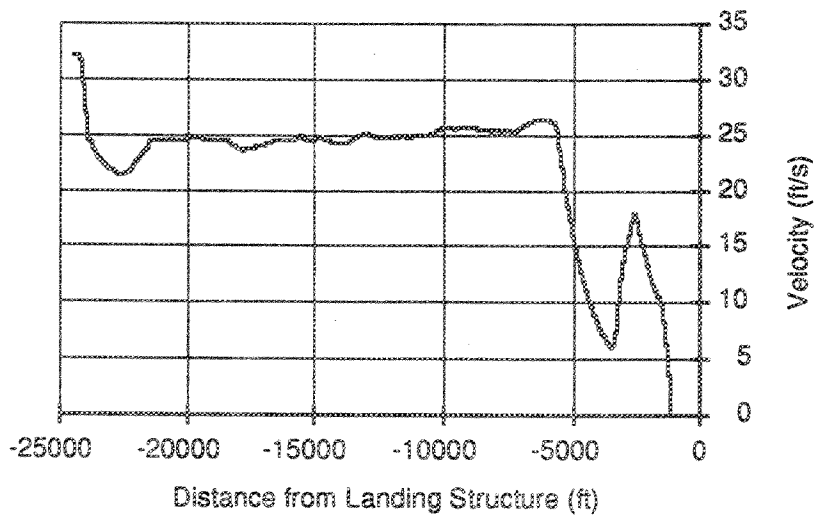


Figure 2.12. Sample Velocity vs. Distance Graph

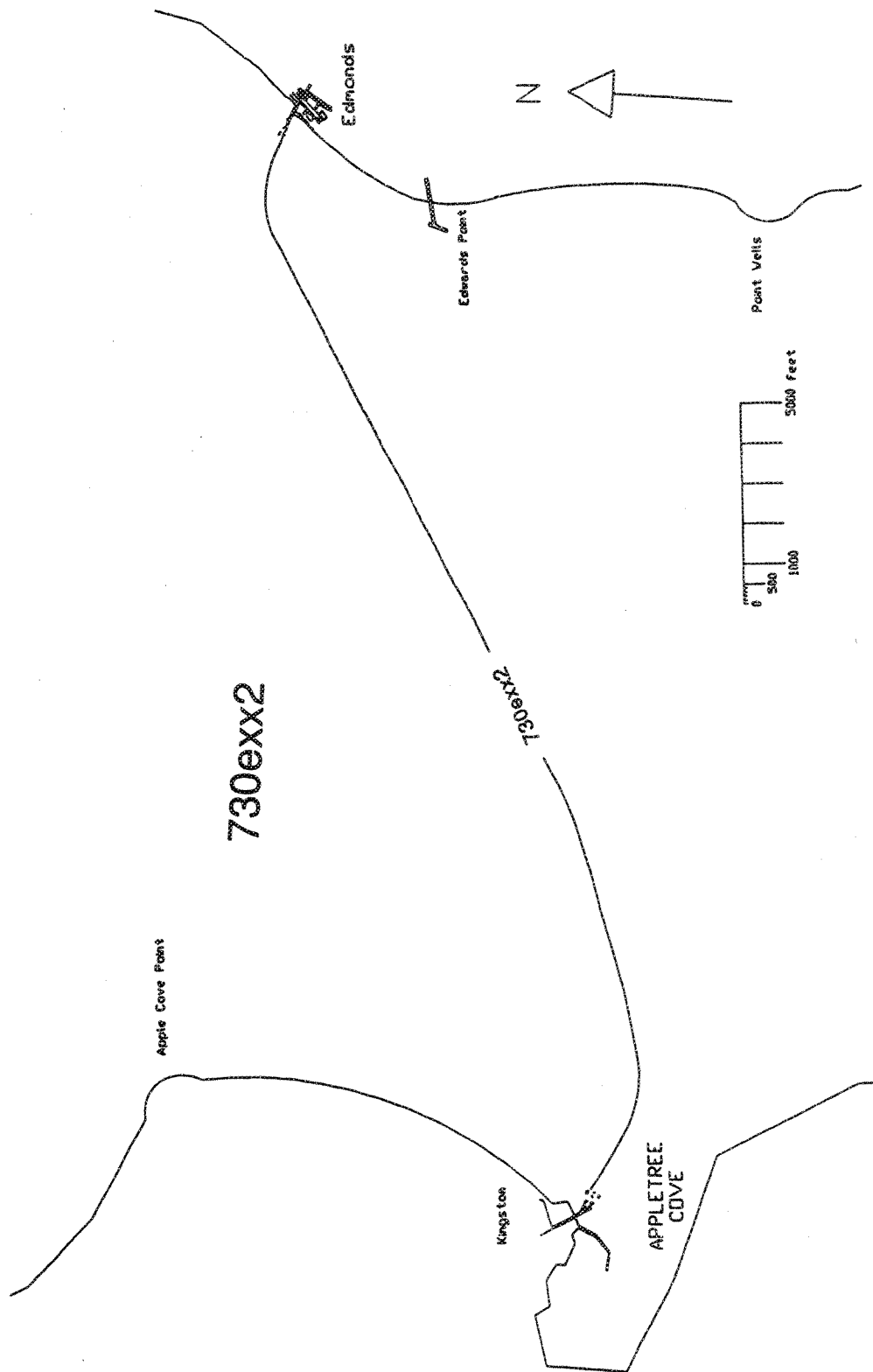


Figure 2.13. Sample Plot of Ferry Path from Kingston to Edmonds

Adaptation of certain sea trials might also offer additional data that would enable ferry landing designers to predict the maneuverability of a distressed vessel. Finally, review of existing geometric roadway design criteria indicates that similar design criteria could be developed for ferry landing facilities. The results of each of these tasks are presented in the following chapter. Recommendations for further research are presented in a subsequent chapter.

CHAPTER 3

FINDINGS

INTRODUCTION

The curves shown in Figures 2.1, 2.2, 2.3, and 2.4 are sources of information that may be used to calculate vessel resistance from the common coefficients and ratios that describe the vessel's form. The results of model resistance tests for WSF Super Class ferries are another source of information regarding the resistance of ferries. The physical model test results are more precise than mathematical equations in estimating vessel resistance for WSF Super Class ferries.

The calculations described in Chapter 2 indicate that velocity can be predicted from the net force on the vessel. The net force used in Equations 3 and 4 is derived from the drag force, which is representative of total resistance. Total resistance is estimated from the vessel characteristics and is calculated using Equation 2. Hence, velocity can be predicted from a given vessel's resistance characteristics. Sample calculations using Equations 2, 3, and 4 are shown in Appendix I. Scenarios described in the next section show results of the application of these mathematical models, which depict the deceleration characteristics of WSF Super Class ferries.

The existing sea trials results are another source of information useful in understanding vessel maneuverability. Stopping distance and turning characteristics reported in the sea trials results can be compared to results obtained with mathematical models. The sea trials results offer insight with respect to other vessel maneuvers that could provide ferry landing designers with additional information.

Full-scale measurements provide a source of data that can be used to test the validity of the mathematical models. The research team observed turns and decelerations during six trips on board a WSF Super Class ferry, under normal operating conditions. These observations were compared to sea trials results and mathematical models.

Comparing data collected during actual maneuvers with mathematical model simulations constitutes a credible way of verifying the validity of the mathematical model simulations. The preliminary full-scale measurements that were completed as part of this study provide another source of information about further testing applications. Full-scale measurements provide data related to actual vessel maneuvers in actual sea conditions.

Current principles of geometric roadway design provide yet another source of information useful in developing design criteria for ferry landing facilities. Design criteria for ferry landings could be developed in a manner similar to that of geometric roadway design principles by considering vessel characteristics. Ultimately, the research team set limits for approach paths and speed limits for approaches on the basis of the principles just described, the results from mathematical models, and on sea trials results.

SCENARIOS

Berthing scenarios were created to simulate simple berthing maneuvers. Four such scenarios were created; they are listed below.

- power reduction from full ahead to stop while on course,
- power reduction from full ahead to slow ahead while on course,
- power reduction from slow ahead to slow astern while on course, and
- power reduction from full ahead to full astern while on course.

The first berthing scenario represents a vessel travelling at full ahead that loses power. When power is unavailable, it is assumed that the propellers rotate without providing thrust or drag, and that the vessel is slowed by its hull resistance alone. Thus, the net vessel force defined in Equation 2 becomes the vessel drag force because the propulsion force is zero. A graph of velocity vs. distance for this scenario (full ahead to stop) is shown in Figure 3.1. The calculations required to determine the values used to create this graph are detailed in Appendix J.

The graph in Figure 2.1 can be used to develop design criteria. For example, the graph shows that the ferry slows from 17 knots to 12 knots in approximately 1500 feet (or

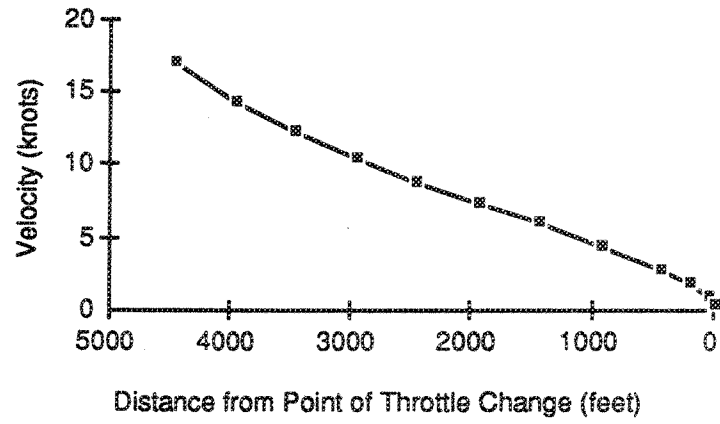


Figure 3.1. Velocity vs. Distance, Full Ahead - Stop

approximately one quarter mile). WSF ferries adopt what is known as the "one-quarter-mile rule", which suggests that the power should be reduced from full ahead to slow ahead at approximately one quarter mile from the landing structure. The ferry is brought to a stop by reverse power when the ferry is within a boat length from the dock. If this rule is followed, then the closest that a ferry would come to a dock at the full speed of 17 knots, is one quarter mile. If the ferry lost power and could only coast in the last quarter mile, then the ferry would reach the landing structure at a velocity of 12 knots, as reflected in Figure 3.1.

Another scenario was created to simulate a vessel decelerating from a reduction in power from full ahead to slow ahead. This scenario is relevant because it simulates the WSF "one-quarter-mile rule" situation described above.

The vessel steady-state velocity at slow ahead was estimated from the vessel's R_t vs. V/\sqrt{L} curve. The ferry travels at 17 knots at full ahead. The force required to overcome total resistance at 17 knots is 55,000 lbs (from Appendix J); thus, 55,000 lbs must be the propulsive force at full ahead. The shaft RPM for full ahead is 150 RPM; the shaft RPM for slow ahead is 50 RPM. From the graph of speed vs. shaft RPM given in Appendix H, the velocity corresponding to 50 RPM is 5 knots. Using this velocity, Equation 2 results in a resistance of 10,500 lbs. Therefore, for a steady state velocity of 5 knots (50 RPM), the thrust is 10,500 lbs.

With $V_0 = 17$ knots as the initial velocity, calculations using Equation 4 were repeated to predict the velocity from resistance characteristics for the scenario of a vessel decelerating from full ahead to slow ahead. For the purpose of performing these calculations, it is assumed that the force or resistance changes from 55,000 lbs to 10,500 lbs. Actually, the thrust may drop below 10,500 lbs while the propeller RPM and vessel speed are adjusting to the new steady state condition. If this is true, the calculated speeds would be higher than the actual speeds. This would result in conservative design criteria. A graph of velocity vs. distance for this scenario is shown in Figure 3.2a. The

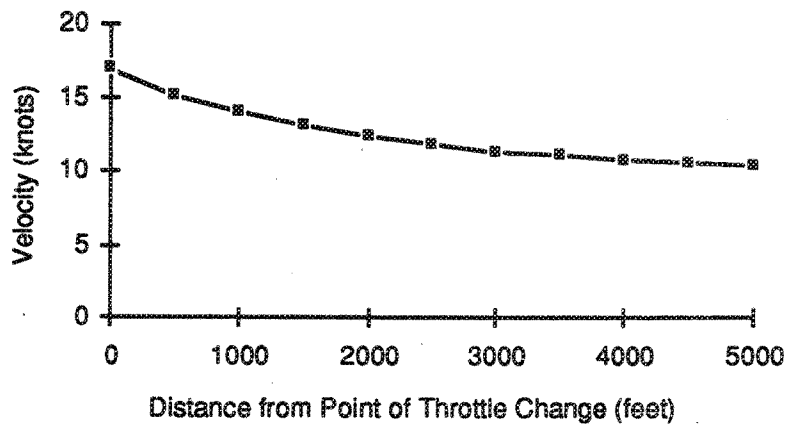


Figure 3.2A. Velocity vs. Distance, Full Ahead - Slow Ahead

calculations required to determine the values used to create this graph are shown in Appendix K. In the first 500 ft of travel, the velocity change is similar to that of the previous scenario, shown in Figure 3.1.

The simulation of the power reduction from full ahead to slow ahead indicates that, after initial noticeable deceleration, the vessel is slowed very gradually. The initial noticeable deceleration is to be expected because the wave-making and friction resistance forces are great, and as such, slow the vessel. As the vessel speed decreases, the wave-making and friction resistance forces decrease rapidly and are not as effective in decelerating the vessel. (14)

The graph shown in Figure 3.2a can also be used to develop design criteria for ferry landing structures. This graph is useful because it shows the speeds that can be expected during a normal approach. The locations of the landing structures are known, and the velocity of the ferry as it passes these locations can be estimated. According to this graph, if the ferry reduced power to slow ahead at one quarter mile from the landing facility, travelled to within one boat length of the facility, and was not able to decelerate further, then the graph indicates that the ferry would be travelling at a speed of approximately 13 knots when it approached the landing facility. Although the ferry does not decelerate significantly past this speed, it does retain steering control while at slow-ahead speed.

The graphs shown in Figures 3.1 and 3.2a can be combined to illustrate the slowing characteristics of a WSF Super Class ferry. An example of such a graph is shown in Figure 3.2b. This graph indicates that the ferry decelerates at a similar rate for the first 500 feet of travel for the two scenarios. After the first 500 feet of travel, the scenario representing a power reduction from full ahead to slow ahead shows less deceleration. Therefore, if the ferry is within 500 feet of the landing structure and travelling at full-ahead speed, a throttle setting of slow ahead, or stop, does not significantly change the ferry's deceleration. The advantage of using the slow ahead

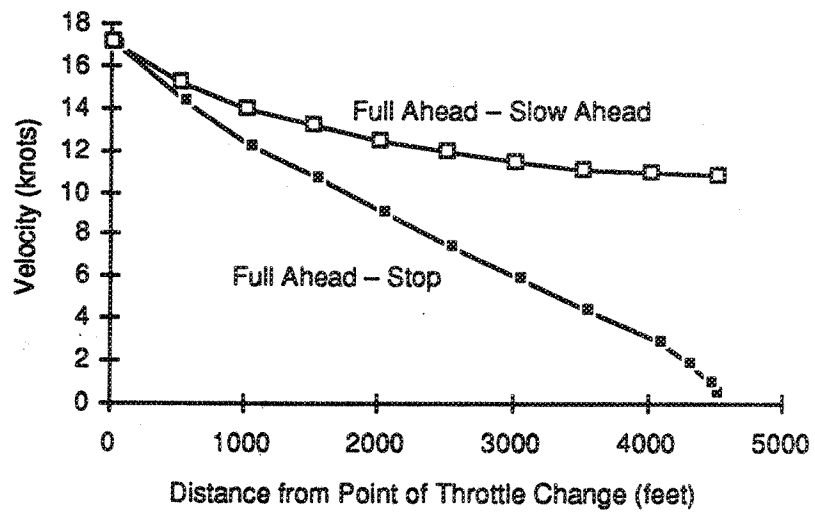


Figure 3.2B. Velocity vs. Distance, Full Ahead - Slow Ahead and Full Ahead - Stop

throttle setting is that the ferry retains steering control even at close proximity to the landing structure.

A third scenario was created to simulate a vessel decelerating after a change in power from slow ahead to slow astern. This scenario is a relevant one, since WSF ferries decrease velocity as they near the dock by reversing power. Slow astern is the first reverse power setting, and is usually applied when the ferry is within approximately one boat length from the dock. Using $V_0 = 13.0$ knots as the initial velocity, calculations using Equation 4 were repeated to predict velocity from resistance characteristics for the scenario involving a vessel decelerating from slow ahead to slow astern. The initial velocity of 13.0 knots, as estimated from Figure 3.2a, is the velocity after approximately 1,000 feet of travel, which is equivalent to two-and-one-half boat lengths. WSF ferries usually travel two to three boat lengths at slow ahead speed before applying reverse power. The reverse power setting to slow astern is often made at one boat length from the landing facility. These calculations assume that the vessel develops the steady state reverse thrust of 10,500 lbs immediately after the throttle setting is changed. However, a real propeller requires time to reverse its motion, and the non-steady thrust probably differs from the steady state thrust. A full-scale test could not be found for comparison. Therefore, one must view the following results with caution. A graph of velocity vs. distance for this scenario is provided in Figure 3.3. The calculations required to determine the values used in creating this graph are shown in Appendix K. This graph shows that the vessel could decelerate from 13.0 knots to 8.0 knots (23.6 ft/sec to 13.5 ft/sec) in approximately 1,400 feet if the power setting were changed from slow ahead to slow astern with no further reverse propulsion.

A fourth scenario was created to simulate a vessel decelerating from a change in power from full ahead to full astern. This scenario is relevant since it is similar to a crash stop test. The crash stop test, explained elsewhere in this report, provides information on vessel stopping ability. During the crash stop test, the power setting is changed from full

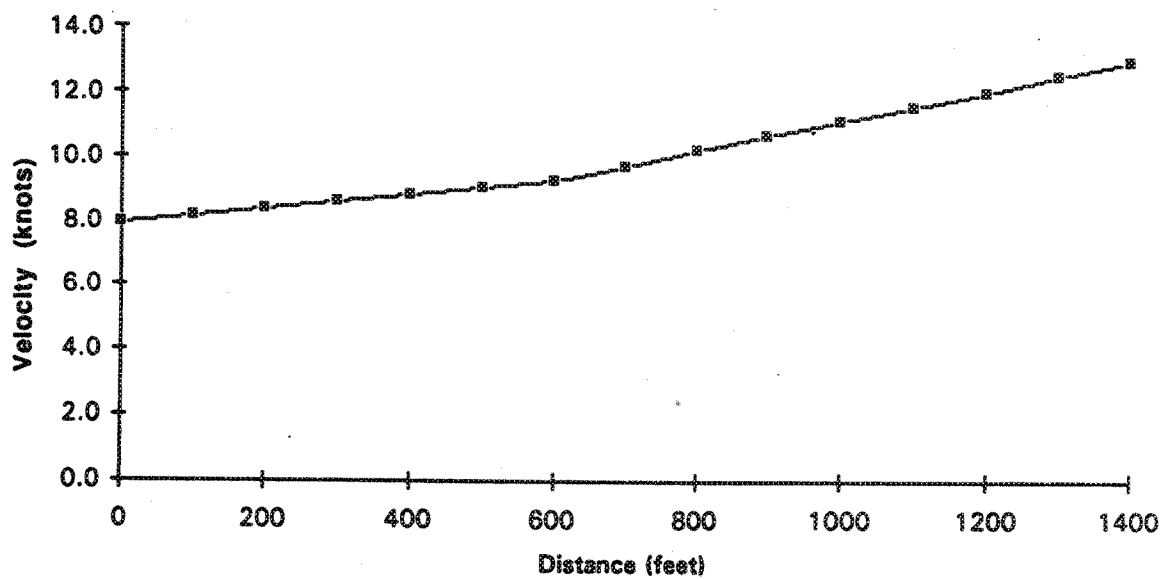


Figure 3.3. Velocity vs. Distance, Slow Ahead — Slow Astern

ahead to full reverse, and the time and distance required to stop the vessel are recorded. (See Reference 15 for a complete description of a crash stop test and Appendix H for a description of the crash stop test procedures adopted by WSF.)

The vessel steady-state velocity at full ahead is 17 knots, and the total resistance at this velocity is 55,000 lbs (from Appendix J). The propulsive force available at full ahead is 55,000 lbs, as described previously. This thrust is achieved when the shaft speed is 150 RPM, which is the shaft speed that corresponds to full ahead. For full-astern power, the shaft speed is 180 RPM; the corresponding velocity is 18 knots. The propulsive force available at steady state velocity at full astern is 70,000 lbs, as calculated from Equation 2.

Using $V_0 = 17$ knots as the initial velocity, calculations using Equation 4 were repeated to predict the velocity from resistance characteristics for the scenario of a change in power from full ahead to full astern. A graph of velocity vs. distance for this scenario is given in Figure 3.4. The calculations required to determine values used in creating this graph are shown in Appendix K. This graph indicates that a WSF Super Class vessel could decelerate from a velocity of 16.3 knots to 6.3 knots (27.5 feet/sec to 10.6 feet/sec) in a distance of approximately 800 feet. The crash stop test for the WSF Super Class vessel, included in Appendix H, indicates that the vessel decelerates from 16.3 to 6.3 knots in 892 feet. The difference could be due to the time required for the propeller's rotation to change from ahead to astern motion.

Information from the graph in Figure 3.4 should be useful to ferry landing designers. Figure 3.4 can be used to estimate velocity for ferries that cannot decelerate in accordance with normal operating procedures. If, for example, the ferry passes the one quarter mile point and does not reduce power to slow ahead, but is forced to use full astern power, then the graph indicates that the ferry could slow to a velocity of approximately 0.5 knots in 1,000 feet.

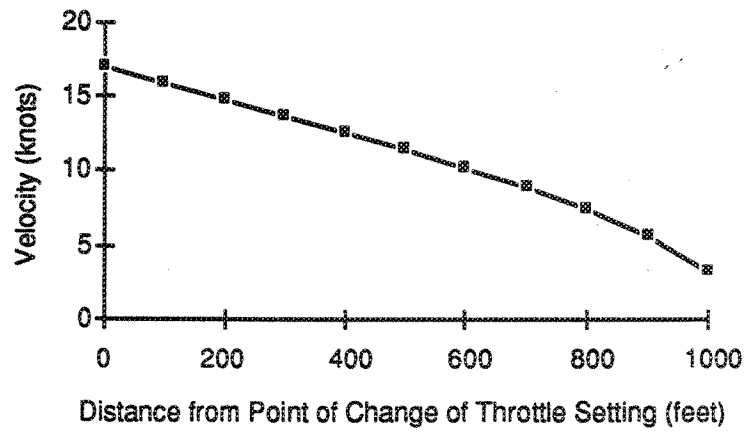


Figure 3.4. Velocity vs. Distance, Full Ahead - Full Astern

INFORMATION FROM SEA TRIALS

Appendix H contains a detailed example of sea trials results, as well as a single page summary. The page entitled "Super Class Maneuvering Data" shows turning maneuver results for each pilot house, opposite turn directions, and throttle settings. Also shown in this document are crash stop test results for two throttle settings, and speed vs. shaft RPM graphs. This document provides ferry landing designers with information, simply presented, that should be useful in developing design criteria for ferry landing aids. The sea trials results for the WSF Super Class ferry, MV *Yakima*, contained in Appendix H, include speed trial, turning maneuver, and crash stop measurements; each of which is described in the following paragraphs.

Results from the speed trials, often summarized and presented graphically, provide information on the steady-state velocity for a given shaft RPM. During the berthing maneuver the throttle setting is altered as necessary to bring the vessel to a stop at the landing structure. As described previously in this report, vessel power is generally altered from full ahead, to slow ahead, to slow astern during a WSF ferry's normal landing facility approach. For each throttle setting, the RPM is known; thus, the steady-state velocity may be estimated from the graph.

Results from the turning maneuver (also referred to as the turning circle) provide data regarding speed loss, time to change heading (15), the tactical diameter, advance, and transfer (Figure 2.10). The results from the turning maneuver are reported for 150 RPM and 120 RPM, and for both stern and bow machinery. They should allow designers to predict possible vessel approach paths and to make suggestions about the placement of landing aids. After reviewing turning circle results, it may also be possible to estimate translational velocity loss, and to estimate how quickly a vessel could change heading for a possible evasive maneuver.

Vessel rudder response, at a specified power setting, is tested by measuring the time and heading change for given rudder angles. Rudder response is measured in a different manner than the turning maneuver. Rudder response is measured with the zigzag test. A complete description of both test procedures is given in References 15 and 16. Typical zigzag test results are shown in Figure A.11. Information gleaned from rudder response tests is also useful in the study of possible berthing scenarios. If, for example, a vessel approaching the landing facility deviates from the normal course because of wind or current, then application of rudder can allow the vessel to correct its course prior to a collision. Knowing the rudder response would aid in the path correction.

If a vessel approaching a landing facility is travelling at a higher than normal speed, then a series of turns could aid in reducing the vessel's velocity. A series of zigzags may be used as an evasive maneuver to slow the vessel. Hence, knowing the velocity loss in a turn is germane to the study of evasive scenarios. An example of velocity loss in a series of turns is shown in Figure A.12.

The results from the crash stop/emergency stop test provide quantitative measures of the minimum distance in which the vessel can be stopped in case of emergency. (15) Ferry landing designers could use this information to estimate the distance from which a vessel can avoid collision with the landing structures during a berthing maneuver by relying on full-astern power to stop the vessel. Since this is not the normal approach procedure, it represents a maneuver involving a vessel in distress. Hence, the results of the crash stop test could provide useful information with respect to simulation of berthing scenarios.

ACTUAL FULL-SCALE MEASUREMENTS

Data from actual full-scale measurements were analyzed to provide recommendations for future full-scale tests. The full-scale measurements also provided a means of verifying the results of the mathematical models for specific scenarios. The tests were conducted during regular sailings; the sailings that were studied are plotted and

shown in Figure 3.5, each denoted with a code name to distinguish each sailing. The code name indicates the date, destination (E = Edmonds, K = Kingston), and letter combinations representing different captains.

The specific vessel maneuvers analyzed include the following:

- turn resulting from a rudder position change to 20 degrees left while at slow-ahead speed;
- turn resulting from a rudder position change to 35 degrees left and 35 degrees right while at full-ahead speed;
- turn resulting from a rudder position change to 25 degrees left while at full-ahead speed; and
- coast resulting from loss of shaft RPM.

Figure 3.5, although general in nature, provides information regarding the possible range of approach paths to a specific location. This information could be used in developing design criteria related to the layout of new facilities.

The path of the ferry executing turns resulting from hard left (35 degrees) and hard right (35 degrees) rudder settings at full-ahead speed is shown in Figure 3.6. Detailed ferry paths at the location of each turn are shown in Figures 3.7 and 3.8. A graph of velocity vs. distance for this sailing is shown in Figure 3.9.

The graphs and plots shown in these figures reflect that the ferry had a turning rate of 25.5 ft/degree and a velocity loss of 3.8 ft/sec when the rudder position was 35 degrees left at full-ahead speed. The same graphs and plots indicate that the ferry had a turning rate of 18.3 ft/degree and a velocity loss of 5.9 ft/sec when the rudder position was 35 degrees right at full-ahead speed. The differences in the turning rate and velocity loss for these turns in opposite directions on the same sailing could be due to conditions that were not recorded, such as wind direction, wind speed, and current.

The information in Figures 3.6, 3.7, 3.8, and 3.9 could also be used to develop design criteria for ferry landing facilities. Knowledge of the distance required to execute

Vessel rudder response, at a specified power setting, is tested by measuring the time and heading change for given rudder angles. Rudder response is measured in a different manner than the turning maneuver. Rudder response is measured with the zigzag test. A complete description of both test procedures is given in References 15 and 16. Typical zigzag test results are shown in Figure A.11. Information gleaned from rudder response tests is also useful in the study of possible berthing scenarios. If, for example, a vessel approaching the landing facility deviates from the normal course because of wind or current, then application of rudder can allow the vessel to correct its course prior to a collision. Knowing the rudder response would aid in the path correction.

If a vessel approaching a landing facility is travelling at a higher than normal speed, then a series of turns could aid in reducing the vessel's velocity. A series of zigzags may be used as an evasive maneuver to slow the vessel. Hence, knowing the velocity loss in a turn is germane to the study of evasive scenarios. An example of velocity loss in a series of turns is shown in Figure A.12.

The results from the crash stop/emergency stop test provide quantitative measures of the minimum distance in which the vessel can be stopped in case of emergency. (15) Ferry landing designers could use this information to estimate the distance from which a vessel can avoid collision with the landing structures during a berthing maneuver by relying on full-astern power to stop the vessel. Since this is not the normal approach procedure, it represents a maneuver involving a vessel in distress. Hence, the results of the crash stop test could provide useful information with respect to simulation of berthing scenarios.

ACTUAL FULL-SCALE MEASUREMENTS

Data from actual full-scale measurements were analyzed to provide recommendations for future full-scale tests. The full-scale measurements also provided a means of verifying the results of the mathematical models for specific scenarios. The tests were conducted during regular sailings; the sailings that were studied are plotted and

shown in Figure 3.5, each denoted with a code name to distinguish each sailing. The code name indicates the date, destination (E = Edmonds, K = Kingston), and letter combinations representing different captains.

The specific vessel maneuvers analyzed include the following:

- turn resulting from a rudder position change to 20 degrees left while at slow-ahead speed;
- turn resulting from a rudder position change to 35 degrees left and 35 degrees right while at full-ahead speed;
- turn resulting from a rudder position change to 25 degrees left while at full-ahead speed; and
- coast resulting from loss of shaft RPM.

Figure 3.5, although general in nature, provides information regarding the possible range of approach paths to a specific location. This information could be used in developing design criteria related to the layout of new facilities.

The path of the ferry executing turns resulting from hard left (35 degrees) and hard right (35 degrees) rudder settings at full-ahead speed is shown in Figure 3.6. Detailed ferry paths at the location of each turn are shown in Figures 3.7 and 3.8. A graph of velocity vs. distance for this sailing is shown in Figure 3.9.

The graphs and plots shown in these figures reflect that the ferry had a turning rate of 25.5 ft/degree and a velocity loss of 3.8 ft/sec when the rudder position was 35 degrees left at full-ahead speed. The same graphs and plots indicate that the ferry had a turning rate of 18.3 ft/degree and a velocity loss of 5.9 ft/sec when the rudder position was 35 degrees right at full-ahead speed. The differences in the turning rate and velocity loss for these turns in opposite directions on the same sailing could be due to conditions that were not recorded, such as wind direction, wind speed, and current.

The information in Figures 3.6, 3.7, 3.8, and 3.9 could also be used to develop design criteria for ferry landing facilities. Knowledge of the distance required to execute

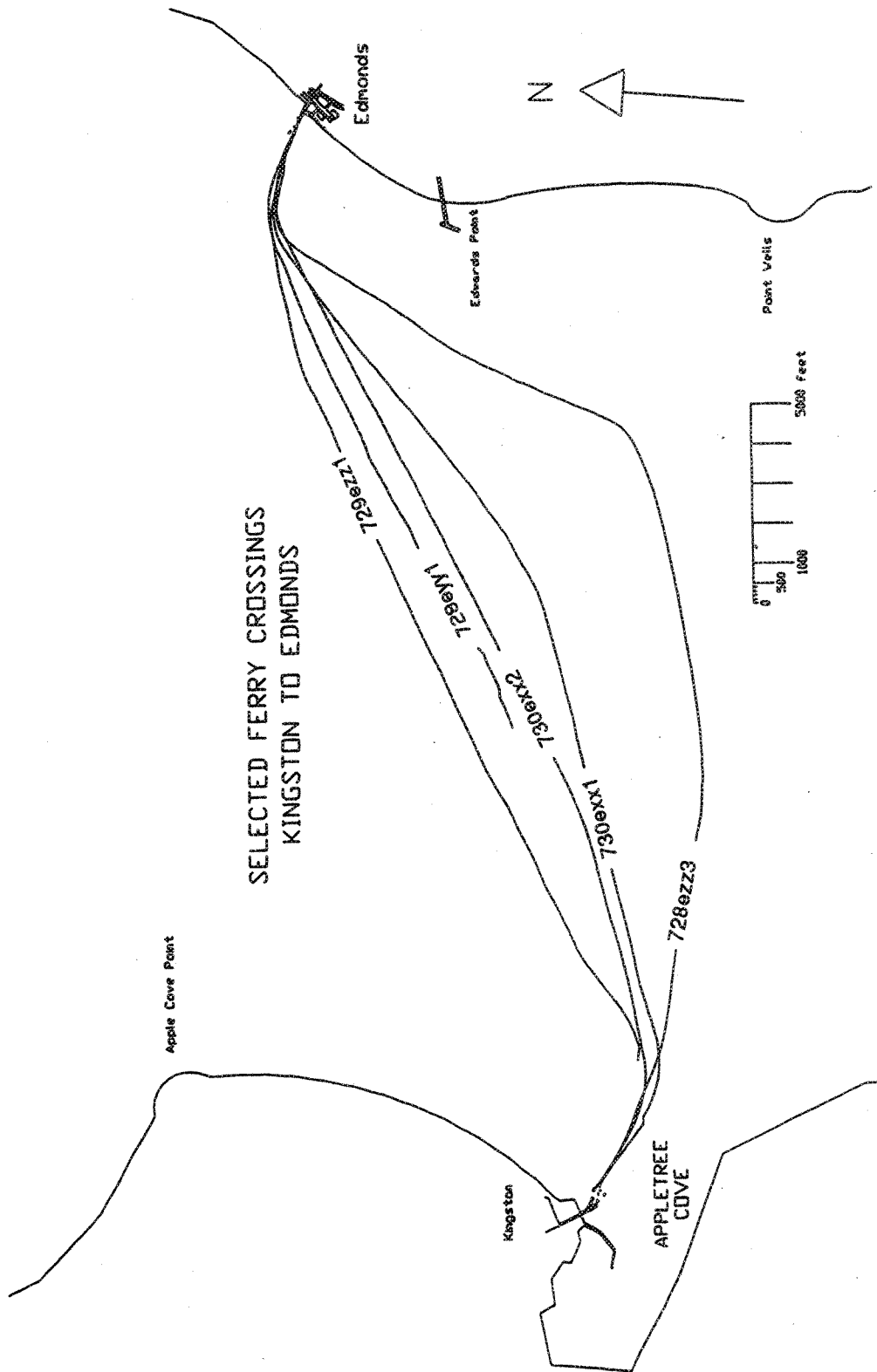


Figure 3.5. Selected Ferry Crossings from Kingston to Edmonds

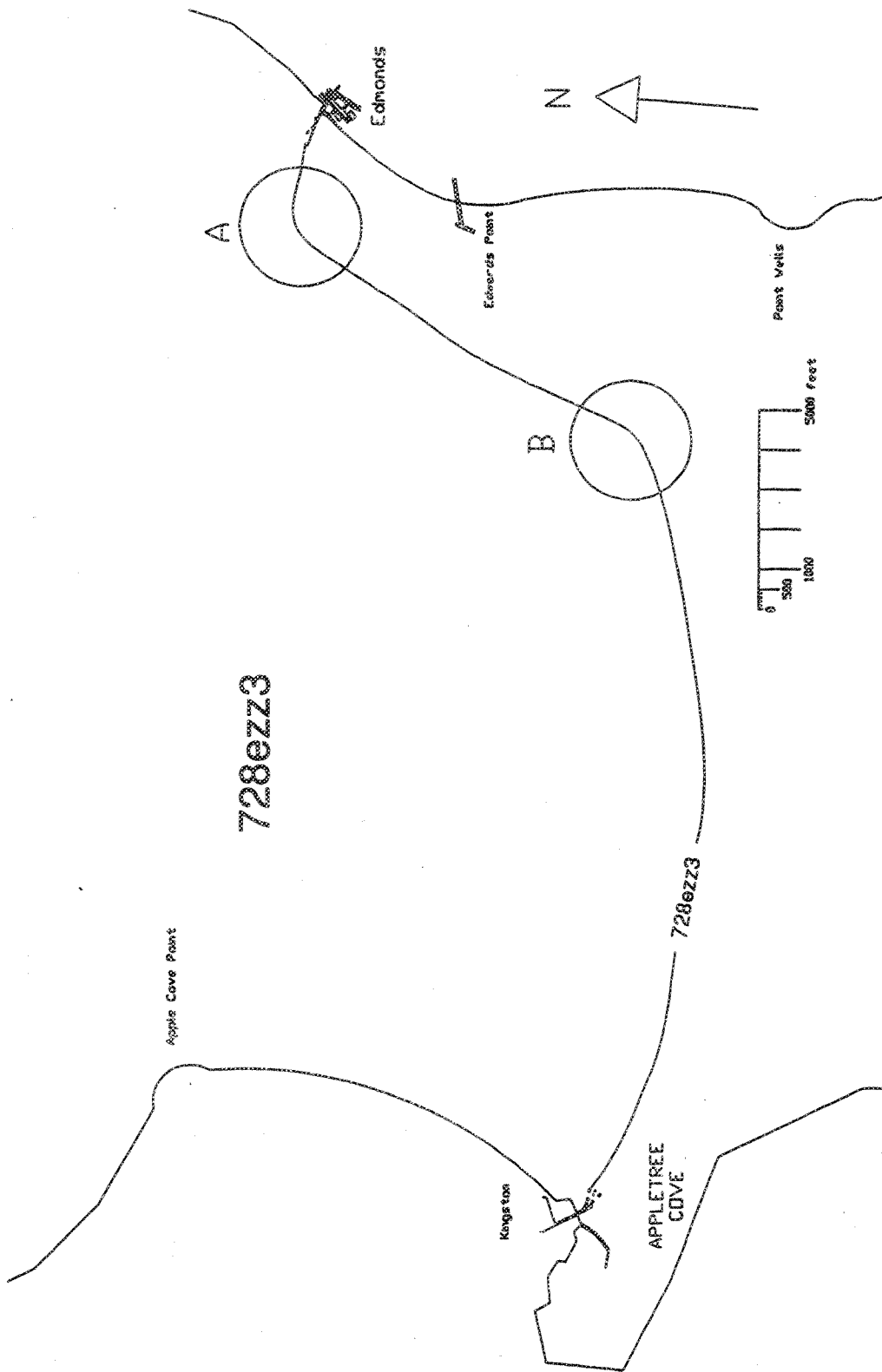


Figure 3.6. Path of Ferry During Turns with Rudder at 35°

728ezz3: Detail A

Throttle Setting: Full Ahead
 Velocity Loss: 5.9 ft/sec
 Rate of Turn: 18.3 ft/Deg

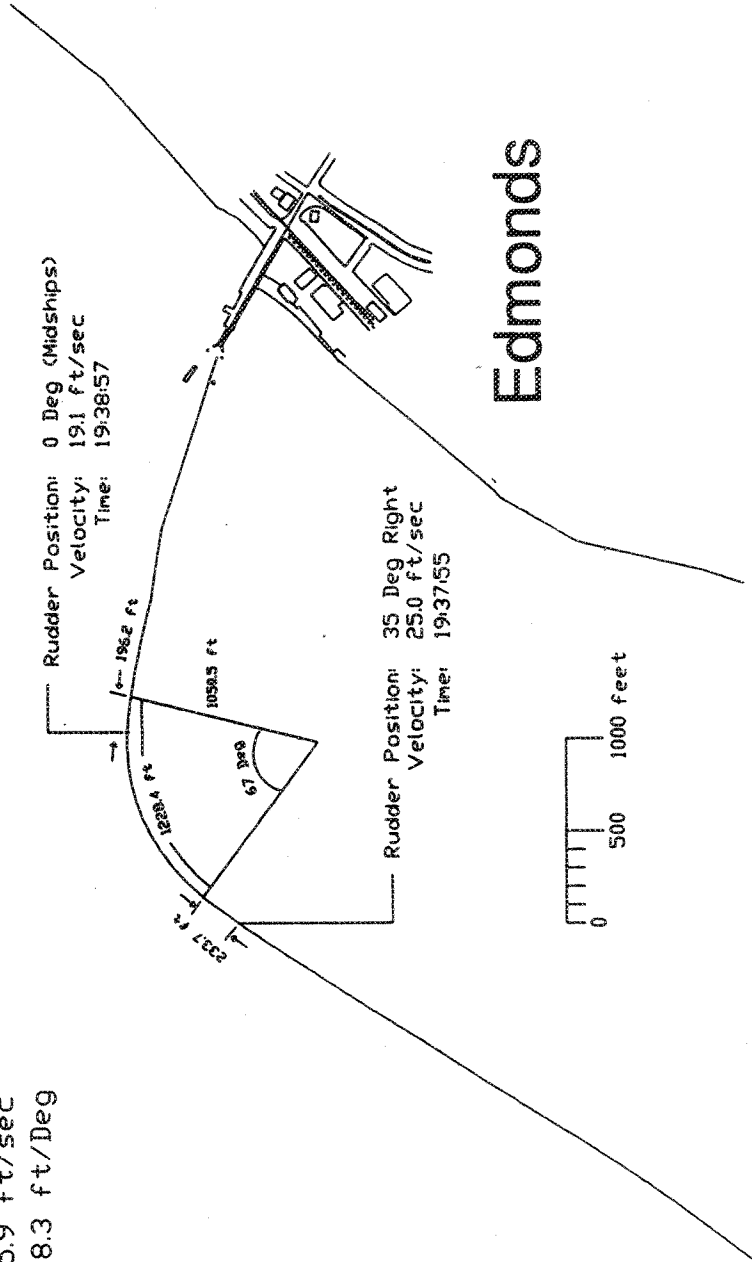


Figure 3.7. Detail of Right Turn with Rudder at 35°

728ez3: Detail B

Throttle Setting: Full Ahead
 Velocity Loss: 3.8 ft/sec
 Rate of Turn: 25.5 ft/Deg

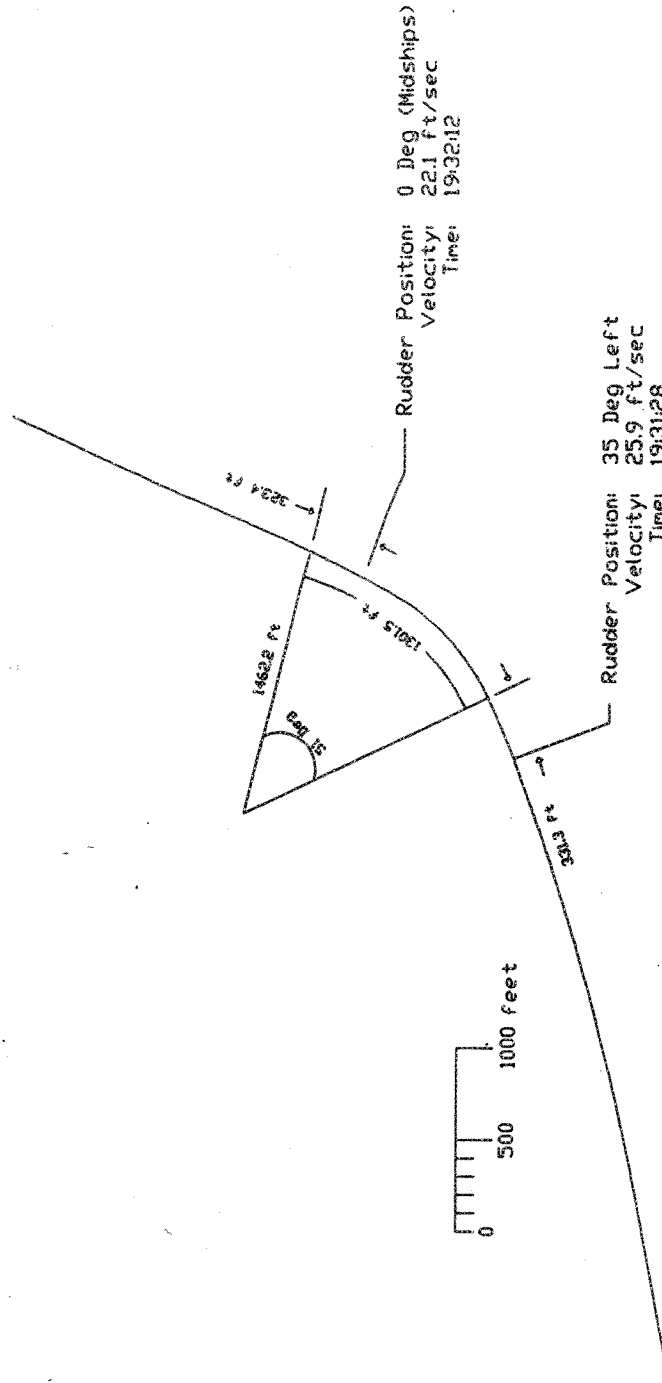


Figure 3.8. Detail of Left Turn with Rudder at 35°

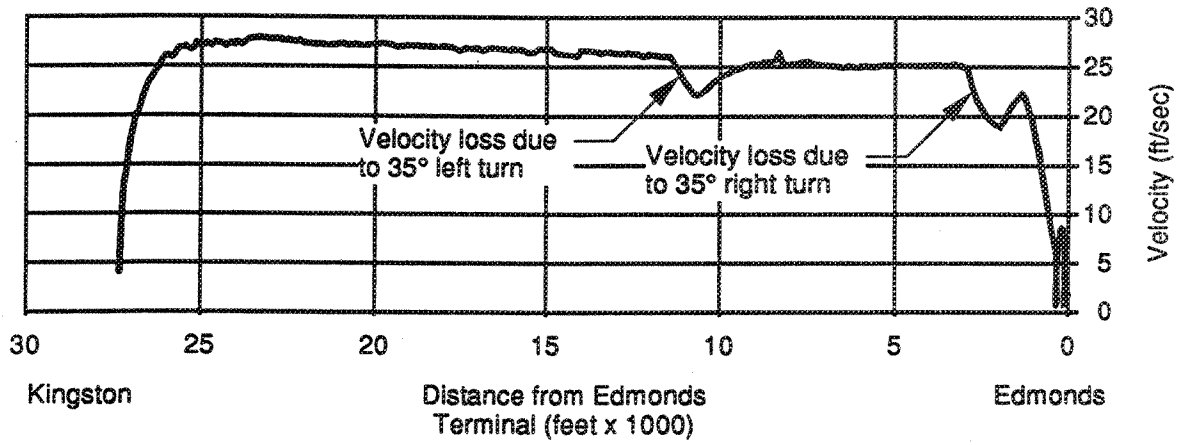


Figure 3.9. Velocity vs. Distance During Sailing Involving Turn with Rudder at 35°

a turn, from the location at which the rudder position is changed, would aid the designer in the layout of new facilities where the approach involves turns around natural features such as rocks, reefs, buoys, and underwater obstructions for one ferry class.

The paths of the ferry executing turns resulting from a rudder setting of 20 degrees left at slow-ahead speed and from a rudder setting of 25 degrees right at full-ahead speed are depicted in Figures 3.10 and 3.11, respectively. Detailed paths of the ferry at the location of each these turns are shown in Figures 3.12 and 3.13. Graphs of velocity vs. distance for each of these sailings are shown in Figures 3.14 and 3.15.

At slow-ahead speed, the ferry had a turning rate of 39.3 ft/degree and a velocity loss of 10.3 ft/sec. At full-ahead speed, the ferry had a turning rate of 31.1 ft/degree and a velocity loss of 2.6 ft/sec for a turn resulting from a rudder position of 25 degrees left. Figures 3.10, 3.11, 3.12, 3.13, 3.14, and 3.15 provide information about turning rates for ferries at both full-ahead speed and slow-ahead speed. These turning rates are valuable because no other source provides information related to 25 degree turns at full-ahead speed or 20 degree turns at slow-ahead speed. Further, no other source provides information on any turns at slow-ahead speeds.

The loss of vessel power, whether intentional or unintentional, may occur during a routine sailing. Figures 3.16a, 3.16b, 3.17a, and 3.17b show graphs of velocity vs. distance for two sailings during which the ferry experienced a loss of power.

Figure 3.16b depicts a loss in power from approximately 150 RPM to 0 RPM; the value of 150 RPM corresponds to a full-ahead throttle setting. In this situation, the velocity decreased from 27.0 ft/sec to 6.0 ft/sec over a distance of approximately 2250 feet. This situation is similar to the scenario represented by the velocity vs. distance graph shown in Figure 3.1. Figure 3.1 depicts a velocity change from 27.0 ft/sec to 6.0 ft/sec in a distance in 2800 feet for a vessel decelerating from a throttle setting change from full ahead to stop (150 to 0 RPM).

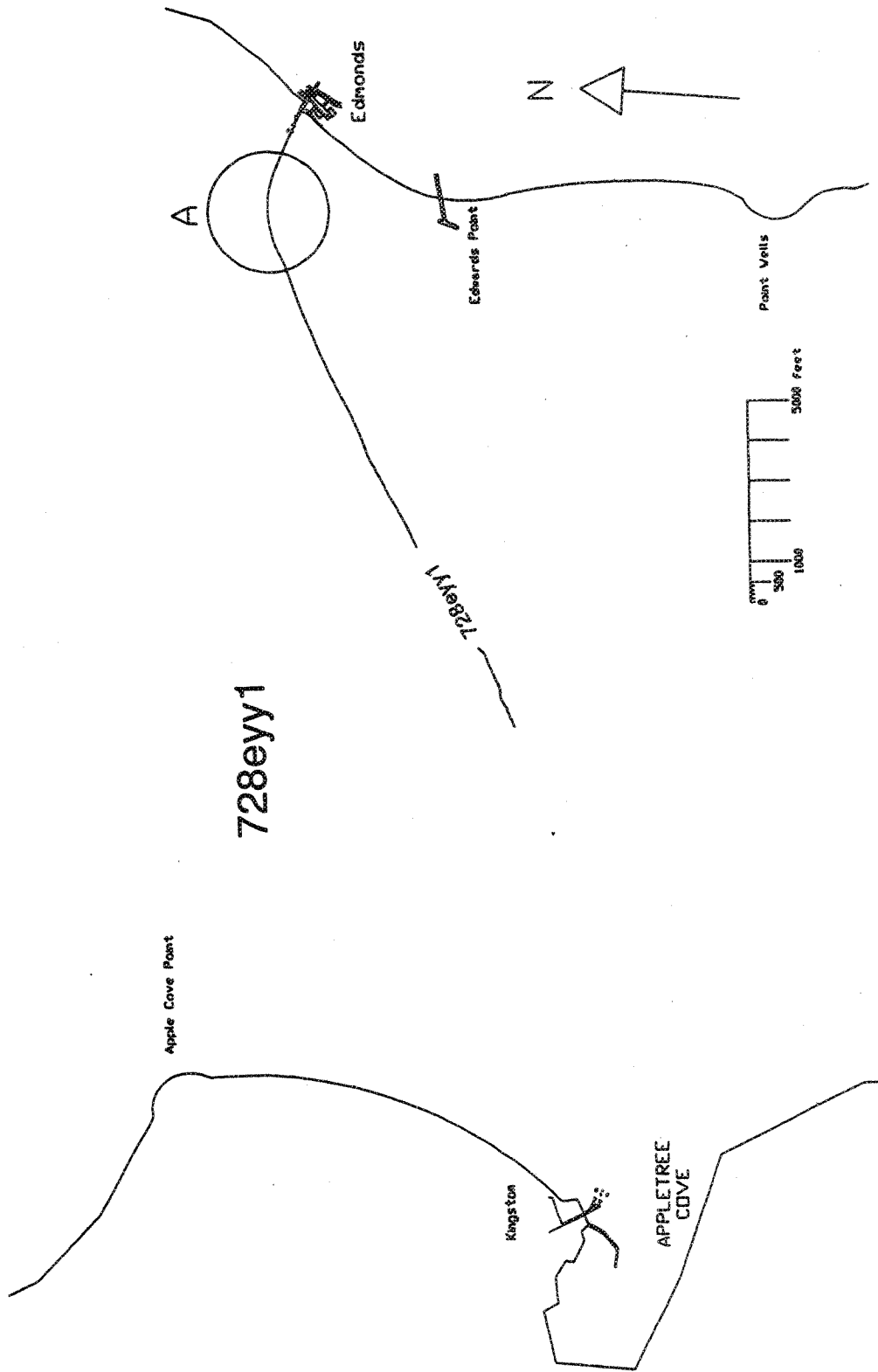


Figure 3.10. Path of Ferry Involving Right Turn with Rudder at 20°

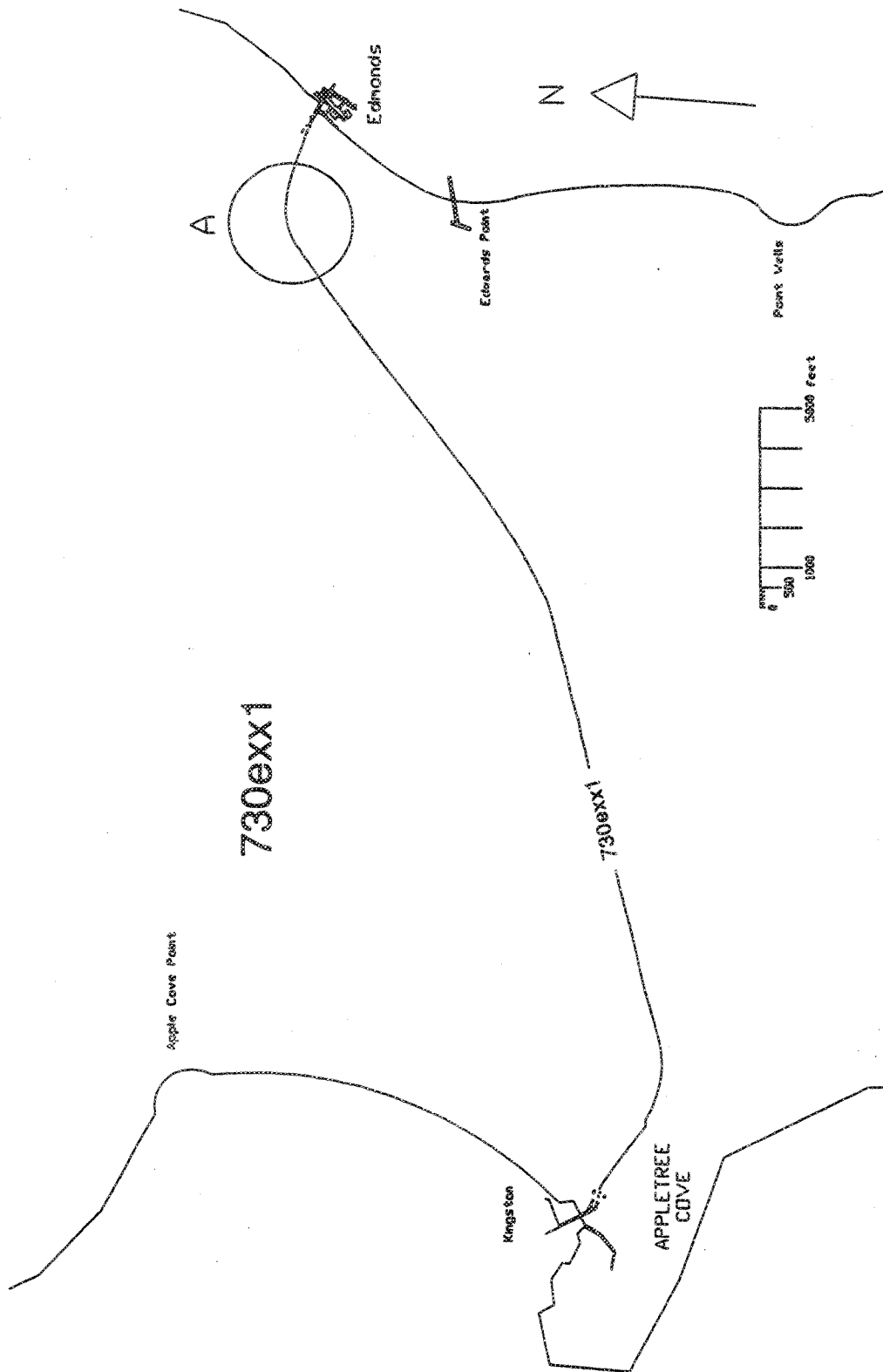
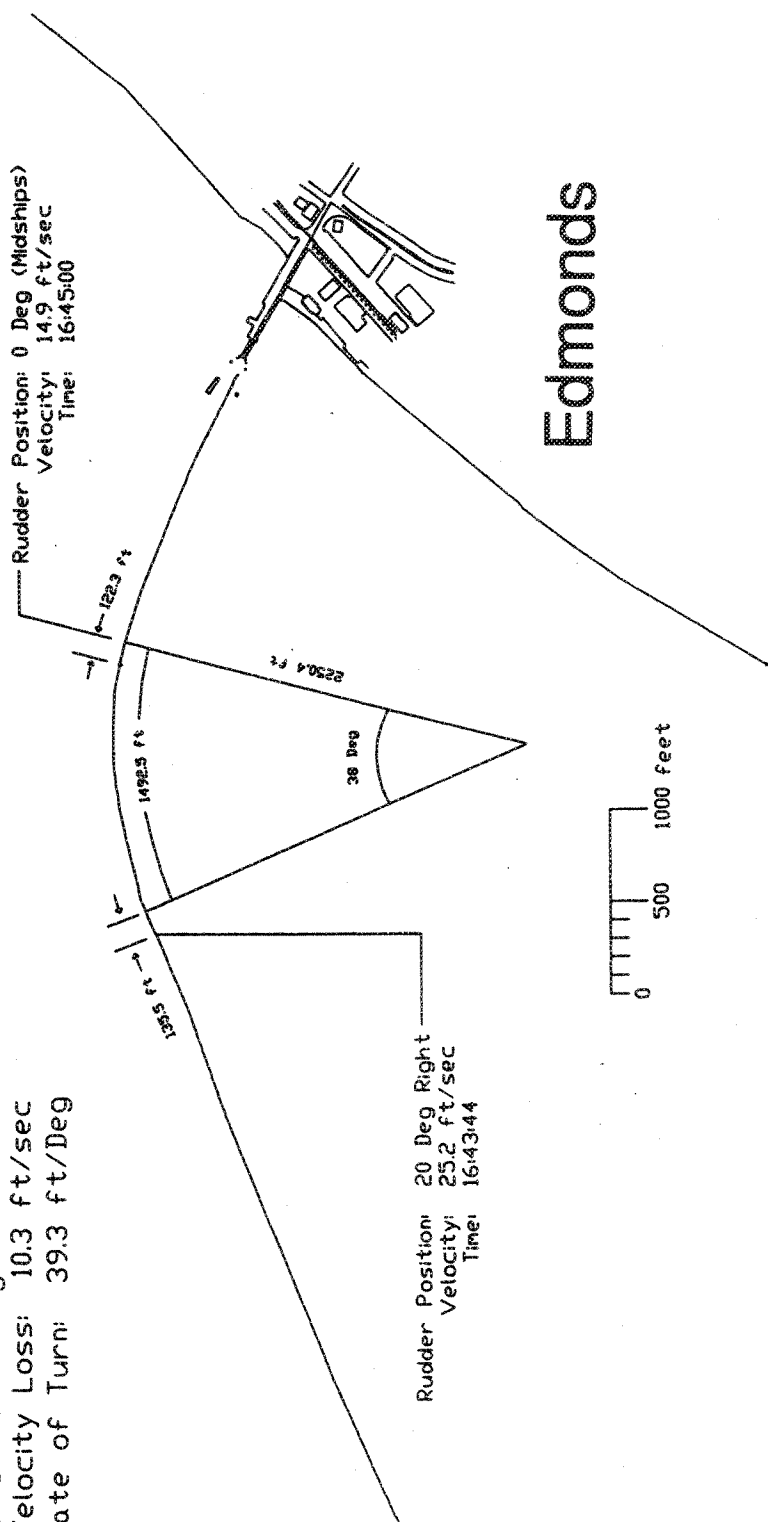


Figure 3.11. Path of Ferry During Right Turn with Rudder at 25°

728ey1: Detail A

Throttle Setting: Slow Ahead
 Velocity Loss: 10.3 ft/sec
 Rate of Turn: 39.3 ft/Deg

Rudder Position: 0 Deg (Midships)
 Velocity: 14.9 ft/sec
 Time: 16:45:00



Rudder Position: 20 Deg Right
 Velocity: 25.2 ft/sec
 Time: 16:43:44

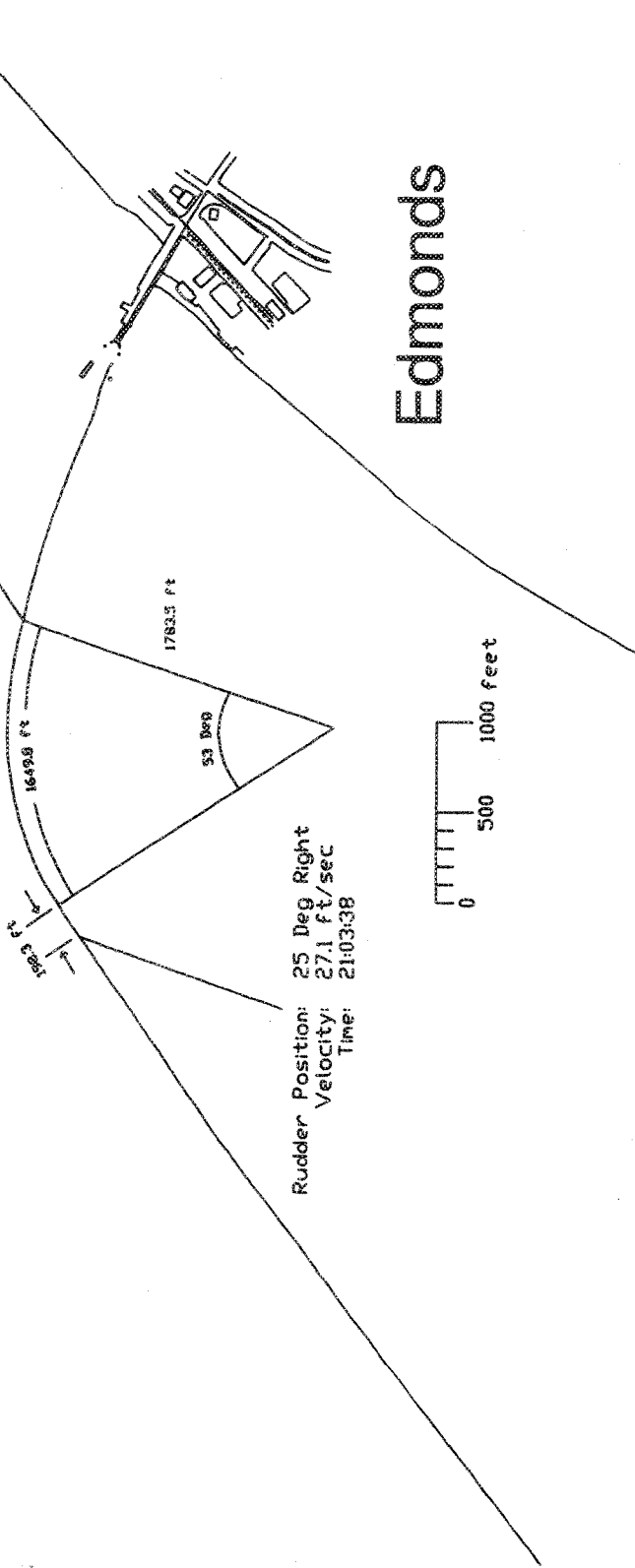
Edmonds

Figure 3.12. Detail of Right Turn with Rudder at 20° and Throttle at Slow Ahead

730exx1: Detail A

Throttle Setting: Full Ahead
 Velocity Loss: 2.6 ft/sec
 Rate of Turn: 31.1 ft/Deg

Rudder Position: 10 Deg Right
 Velocity: 24.5 ft/sec
 Time: 21:04:50



Rudder Position: 25 Deg Right
 Velocity: 27.1 ft/sec
 Time: 21:03:38

Figure 3.13. Detail of Right Turn with Rudder at 25°

VELOCITY VS. DISTANCE

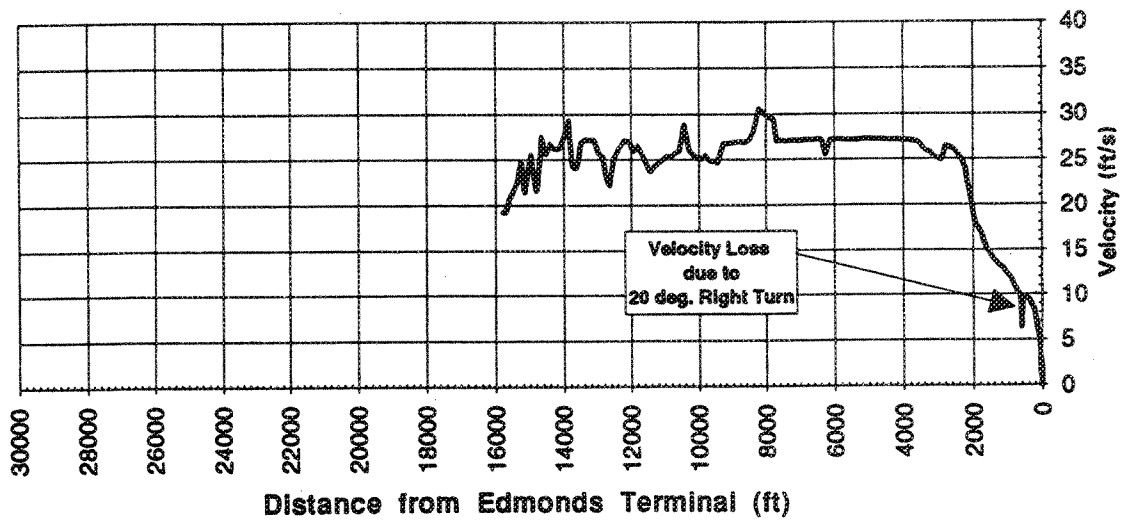


Figure 3.14. Velocity vs. Distance During Sailing Involving Right Turn with Rudder at 20°

VELOCITY VS. DISTANCE

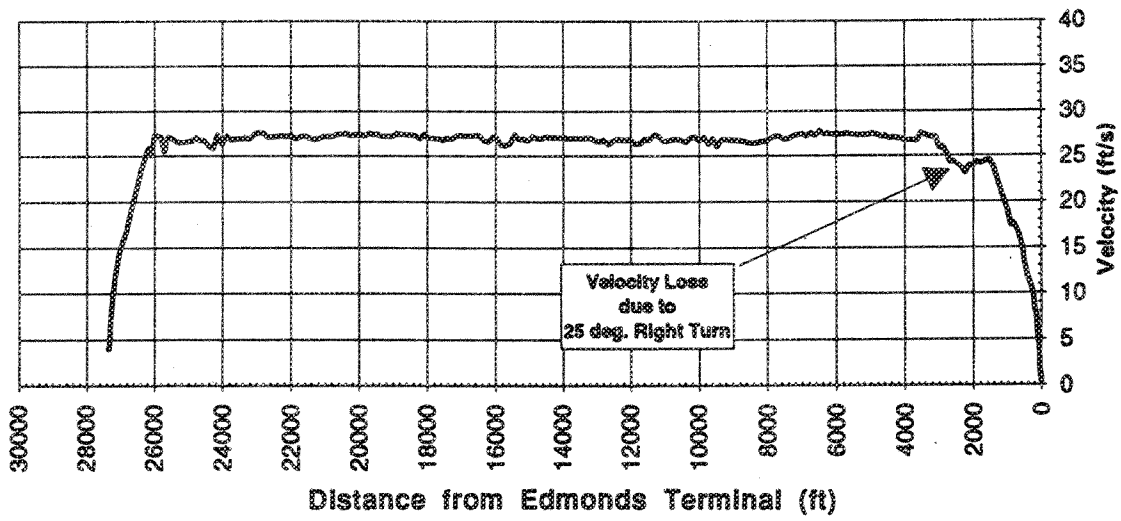


Figure 3.15. Velocity vs. Distance During Sailing Involving Right Turn with Rudder at 25°

VELOCITY VS. DISTANCE

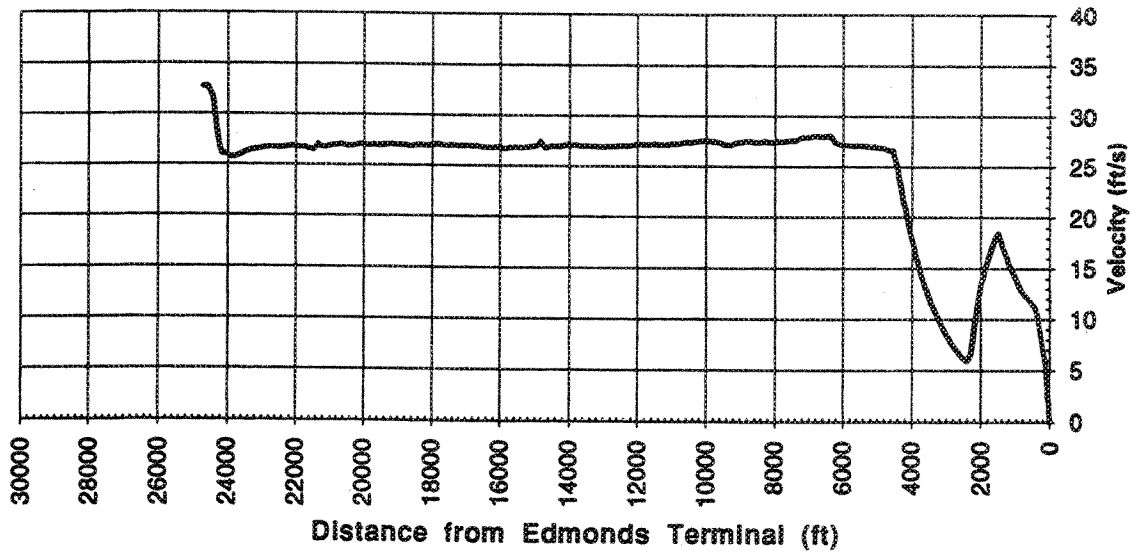


Figure 3.16a. Velocity vs. Distance During Sailing Involving Power Loss

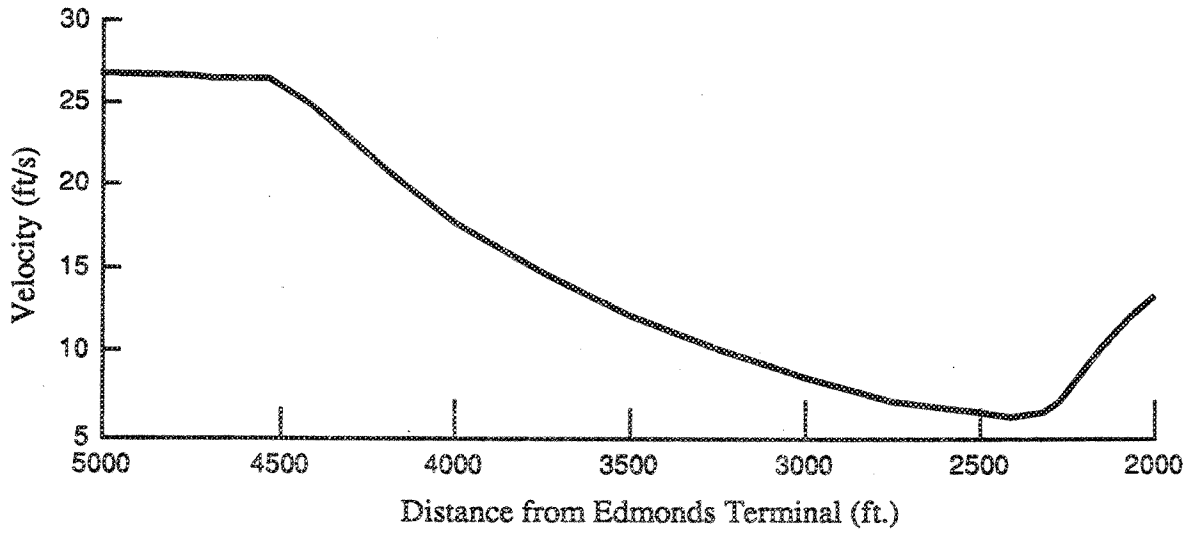


Figure 3.16b. Velocity vs. Distance During Sailing Involving Power Loss (detail of section between 2,000 and 5,000 ft)

VELOCITY VS. DISTANCE

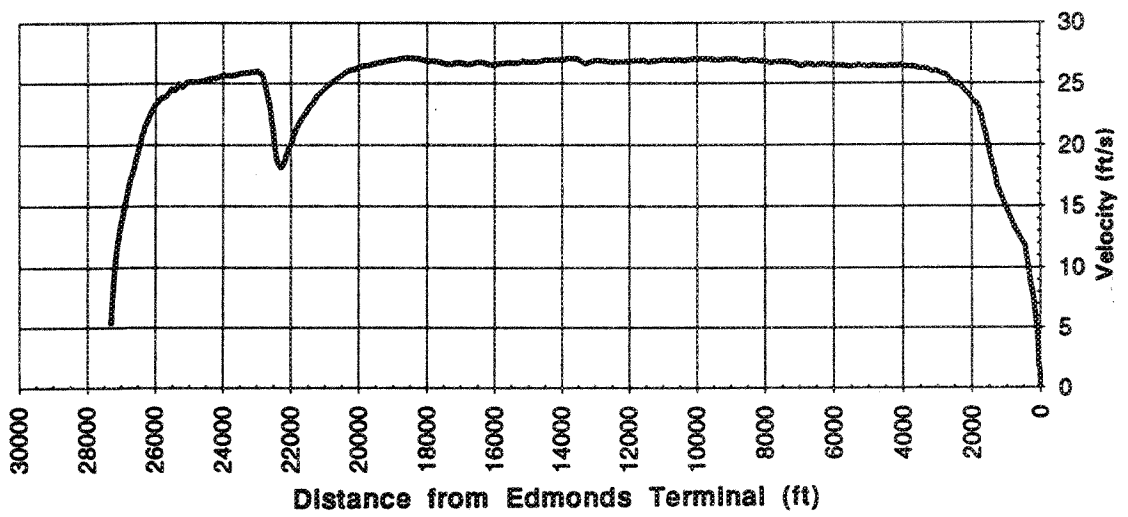


Figure 3.17a. Velocity vs. Distance During Sailing Involving Power Loss

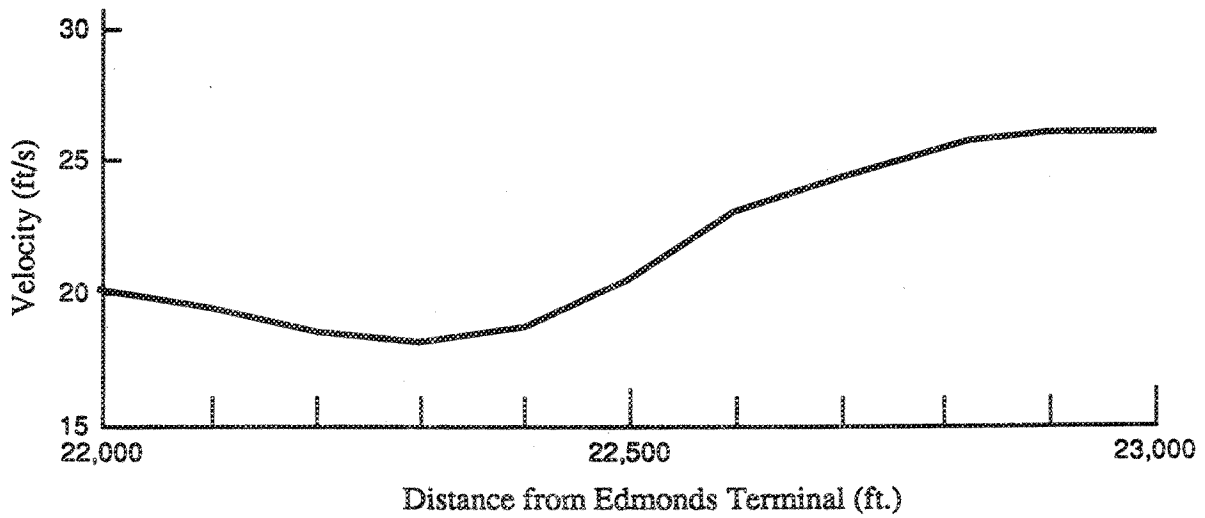


Figure 3.17b. Velocity vs. Distance During Sailing Involving Power Loss (detail of section between 22,000 and 23,000 ft)

Figure 3.17b represents a loss in power from approximately 150 RPM to 0 RPM. In this situation, the ferry's velocity decreased from 26.0 ft/sec to 18.0 ft/sec over a distance of 800 feet. Previous calculations (Figure 3.1) predict a change in velocity from 26.0 ft/sec to 18.0 ft/sec in a distance of 1000 feet for a similar scenario.

The information related to loss of velocity during specific power losses, as shown in Figures 3.16b and 3.17b, could aid in developing ferry landing design criteria. As described in the previous section, this information indicates the stopping abilities of ferries. In a possible evasive maneuver, including the requirement of stopping from full-ahead speed, the distance in which a ferry is able to stop can be obtained from these graphs.

A summary of the results from these preliminary full-scale tests is presented in Tables 3.1 and 3.2.

Table 3.1 Summary of Full-scale Turning Measurements

Run	Throttle Setting	Rudder Position (degrees)	Velocity Loss (ft/sec)	Turning Rate (ft/degree)	Distance to Begin Turning (ft)
728EZZ3A	Full Ahead	35 Left	5.9	18.3	233.7
728EZZ3B	Full Ahead	35 Right	3.8	25.2	331.3
728EYY1	Slow Ahead	20 Right	10.3	39.3	135.5
730EXX1	Full Ahead	25 Right	2.6	31.1	198.3

Table 3.2 Summary of Full-scale Deceleration Measurements

Run	Initial Throttle Setting	Final Throttle Setting	Velocity Loss (ft/sec)	Distance Travelled (ft)
729EZZ1	Full Ahead	Stop	21.0	2250
730EXX2	Full Ahead	Stop	8.0	800

Preliminary full-scale measurements utilizing GPS instrumentation to record position and velocity data have provided information on turning capabilities and vessel deceleration without power. The latter provides a point of comparison with the

mathematical models presented in a previous section. The comparison shows that ferries actually decelerate faster than predicted by simulations based on physical model resistance data. Thus, the calculations provided by Equation 4 give an upper limit for the approach velocity. The full-scale measurements have also provided insight that should prove useful in developing procedures for future tests. Recommendations based on the results of these full-scale measurements are presented in Chapter 4.

STOPPING DISTANCE/COLLISION AVOIDANCE

A review of roadway design criteria provided ideas for developing similar criteria for ferry landing design. In particular, practical stopping distances concern both designers of roadway systems and ferry landing facilities. Stopping sight distance is of most interest to transportation engineers while crash stop distance (or headreach) would be relevant for ferry landing designers and vessel operators. A comparison of these two principles is presented in this section.

Table 3.3 summarizes stopping sight distance design values used by transportation engineers. In highway design, any length of stopping sight distance within the range of values established by Table 3.3 is acceptable for a specific speed. (11) The values in Table 3.3 were computed using Equation 5, which includes allowance for reaction time and for braking distance.

Similar information can be prepared for use by ferry landing designers. For different velocities during a normal approach, the headreach can be calculated from Equation 6 and presented in tabular form. An example of such information, for a WSF Super Class Ferry, is given in Table 3.4. Items included in Table 3.3, but not presented in Table 3.4, are reaction time and braking time. Similar values for these items could be added to Table 3.4. However, Equation 6, and the value of D_i obtained from Figure 2.7, account for the time required for engines to reverse from ahead to astern.

Table 3.4 was developed by calculating headreach for a range of speeds, using Equation 6. Sample calculations used to compute the values in the table are shown in

Table 3.3. AASHTO Stopping Sight Distance (Wet Pavements)

Design Speed (mph)	Assumed Speed for Condition (mph)	Brake Reaction		Coefficient of Friction f	Braking Distance on Level (ft)	Stopping Sight Distance	
		Time (sec)	Distance (ft)			Computed (ft)	Rounded for Design (ft)
20	20-20	2.5	73.3-73.3	0.40	33.3-33.3	106.7-106.7	125-125
25	24-25	2.5	88.0-91.7	0.38	50.5-54.8	138.5-146.5	150-150
30	28-30	2.5	102.7-110.0	0.35	74.7-85.7	177.3-195.7	200-200
35	32-35	2.5	117.3-128.3	0.34	100.4-120.1	217.7-248.4	225-250
40	36-40	2.5	132.0-146.7	0.32	135.0-166.7	267.0-313.3	275-325
45	40-45	2.5	146.7-165.0	0.31	172.0-217.7	318.7-382.7	325-400
50	44-50	2.5	161.3-183.3	0.30	215.1-277.8	376.4-461.1	400-475
55	48-55	2.5	176.0-201.7	0.30	256.0-336.1	432.0-537.8	450-550
60	52-60	2.5	190.7-220.0	0.29	310.8-413.8	501.5-633.8	525-650
65	55-65	2.5	201.7-238.3	0.29	347.7-485.6	549.4-724.0	550-725
70	58-70	2.5	212.7-256.7	0.28	400.5-583.3	613.1-840.0	625-850

Appendix L. The value of D_i was estimated from the graph shown in Figure 2.7, using $R/T = 0.8$. R/T is the ratio of total resistance at the approach velocity to full-astern thrust (54,701/69,752).

The headreach calculated from Equation 6 for a WSF Super Class ferry travelling at full-ahead speed is 1032 feet, as shown in Table 3.4. The stopping distance calculated from the mathematical model presented previously is approximately 1000 feet, as shown in Figure 3.4. Both of these distances are greater than the crash stop distance of 892 feet (for a velocity change from 16 to 6.3 knots) reported in the sea trials results found in Appendix H.

Table 3.4. Headreach Calculations for WSF Super Class Ferry

$$\text{Mass} = 228,382.6 \text{ lb/sec}^2/\text{ft.}$$

$$s = \frac{D_i * M * V^2}{2 * R}$$

V knots	V/√L knots	V fps	R/Ton	R lbs	R/T	D_i	s ft	
17.0	0.9	28.7	16.7	54,716	0.8	0.6	1032.3	(full ahead)
13.0	0.7	22.0	9.0	29,519	0.4	0.4	748.9	(two boat lengths after power reduction from full ahead)
6.25	.32	10.6	3.2	10,429	0.2	0.2	246.1	(slow ahead)

Note: R/Tons calculated from Equation 10, D estimated from Figure 3.7

Headreach values derived from Equation 6 must be used with caution. The headreach values derived from this equation are higher than those predicted from the mathematical models. The mathematical models have been compared to the crash stop results reported in Appendix H and are considered to provide a conservative estimate. Therefore, the values computed from Equation 6 are not precise for WSF Super Class ferries. Possible reasons for these differences could be related to the following factors:

- Equation 6 was derived from information for navy vessels.

- WSF Super Class ferry machinery differs dramatically from the machinery that was assumed to be in use on the vessels upon which Equation 6 was based.
- Graphs such as that shown in Figure 2.7 are not applicable to WSF Super Class ferries with respect to reaction time and time required to achieve astern thrust.
- Graphs used to estimate D_i represent approximate methods.

Vessel stopping distance provides the ferry landing designer with information on the ferry's ability to stop at a given speed. Knowing the distance required to stop enables the designer to establish a location, on the approach path, that could define a collision avoidance point. Figure 3.18a shows such a possible location. If, during a berthing scenario, for example, a ferry travelling at full-ahead loses power control, then the collision avoidance point defines the point at which a ferry must restart its engines and use full-astern power to avoid collision. In the case of the WSF Super Class ferry MV *Yakima*, the collision avoidance point would be 1000 feet from the landing facility. The distance of 1000 feet is the crash stop distance calculated from the mathematical model presented in Chapter 2—Background. This point could also be used to limit vessel velocity during the approach to the landing facility. Specifying that Super Class ferries must reduce power from full ahead at a minimum distance of 1000 feet from the landing structure may, for example, be advisable as an operating procedure. The preceding provides one example of how design criteria could be developed on the basis of stopping distance information. Note, however, that vessel stopping characteristics should not dictate the design but should be considered in developing design criteria.

Turning away from the landing facility to avoid collision requires knowledge of the vessel's turning ability. The results of the turning test, as presented in Appendix H, provide such information. Figure 3.18b indicates the approximate turning radius required by the MV *Yakima*, as described in the turning test results. The MV *Yakima* requires

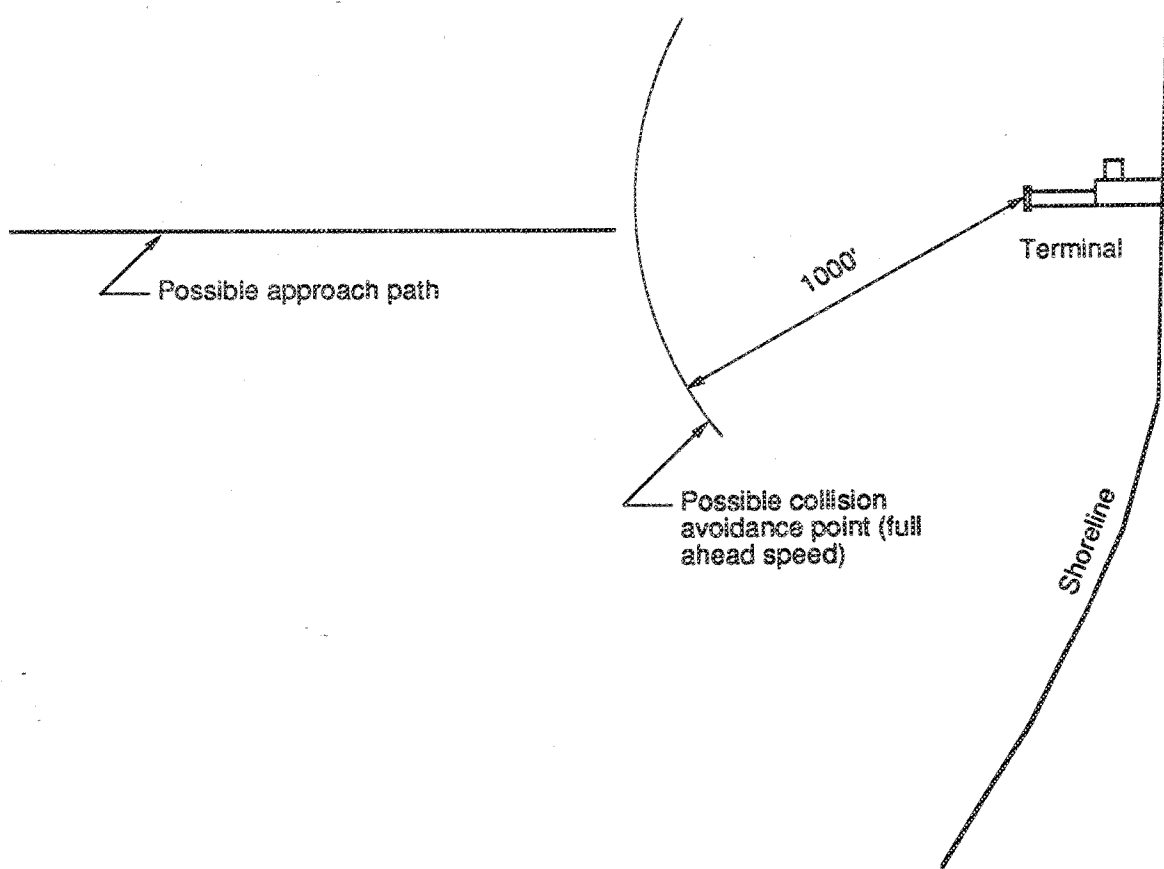


Figure 3.18A. Possible Collision Avoidance Path and Possible Turn Avoidance Path

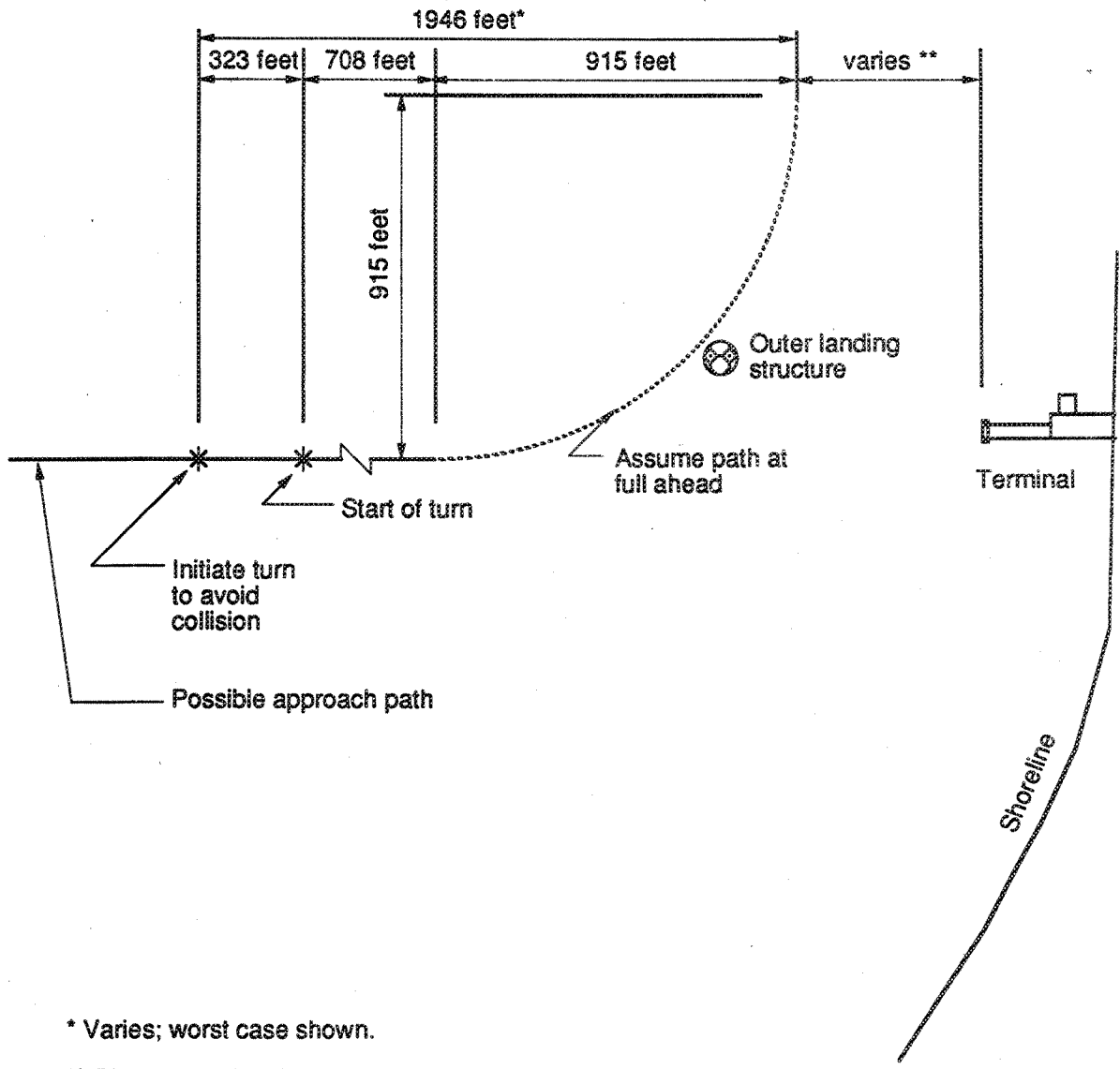


Figure 3.18B. Possible Turn Avoidance Path

approximately 1,946 feet (worst case), along the original heading, from the time the turn is initiated to the time the ferry is turned at right angles to the original path. This ferry also requires approximately 915 feet (worst case), perpendicular to the original heading, from the time the turn is initiated to the time the ferry is turned at right angles to the original path. These values indicate the distance from the landing facility at which this ferry must turn to avoid collision with the landing facility.

Figures 3.10, 3.11, 3.12, 3.13, 3.14, and 3.15 provide yet more information that could be used to develop design criteria. For example, if the approach to a specific landing facility involves a right-hand turn, then the information from these figures will assist the designer in specifying an acceptable approach speed; one that will enable the ferry to decelerate appropriately.

One way to present stopping-distance information for various throttle settings is to generate velocity vs. distance curves for different throttle settings on a single graph. Such a graph is depicted in Figure 3.19 shows. This graph represents stopping distances for a WSF Super Class Ferry, initially travelling at full ahead speed, and experiencing reductions in power to the following throttle settings:

1. full astern,
2. half astern,
3. slow astern, and
4. stop.

Information related to throttle settings 1 and 4 was obtained from Figures 3.4 and 3.1, respectively. Information for settings 2 and 3 was similarly obtained. Velocity vs. distance graphs for each situation were overlaid to create Figure 3.19. These plots may serve as speed envelopes to provide ferry landing designers with valuable information about ferries' deceleration characteristics. For example, consider a ferry travelling at full-ahead speed at a distance of 2,000 feet from the landing structure. A power malfunction forces the ferry to coast. If the engine is not started, then the ferry would

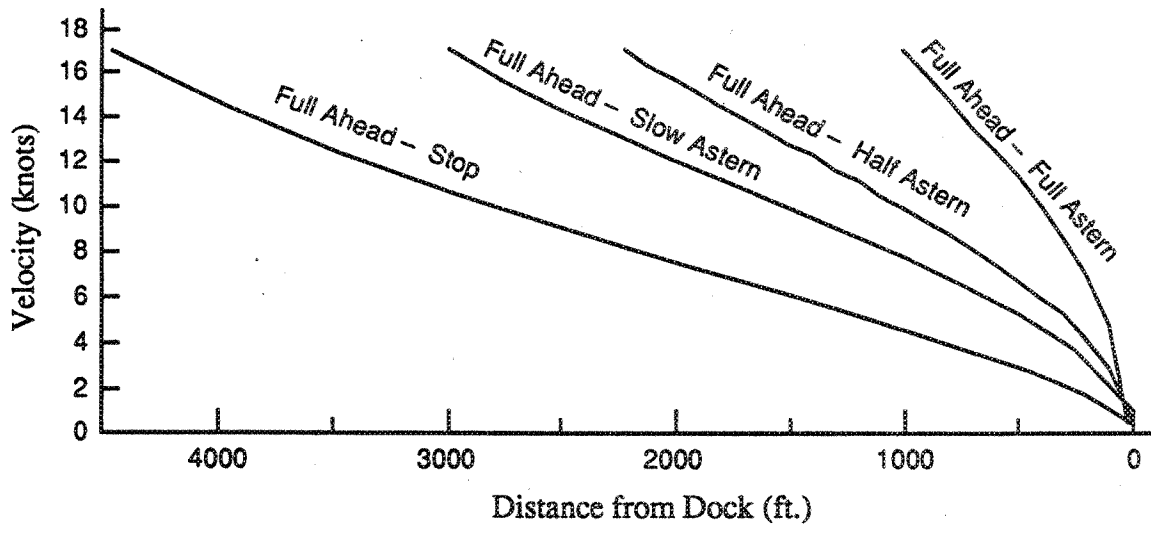


Figure 3.19. Speed Envelopes for WSF Super Class Ferry

coast into the landing structure at a velocity exceeding 8 knots. However, if power could be resumed, then the graph in Figure 3.19 could be used to estimate the minimum amount of coasting distance that the ferry could endure and still experience a safe landing. In the example described, the ferry could coast for 1,500 feet to a speed of approximately 11 knots, use full-astern power, and reduce speed to acceptable ranges within the last 500 feet. In a less extreme example, the ferry could coast for 1,000 feet to a speed of approximately 13 knots, use half-astern power, and reduce speed to acceptable ranges. Hence, the speed envelope curves could be used to develop design criteria for ferry landing facilities.

In Figure 3.19, the curve for stopping at half astern indicates that more than 2,000 ft are required to stop a vessel. This seems unlikely after a comparison is made with the normal stopping procedure. The researchers found WSF vessels start to slow down in preparation for a landing at a distance of 1,500 ft from the dock. The first throttle reduction is from full ahead to slow ahead. At 600 ft to 700 ft from the dock, the throttle is set from slow ahead to slow astern. Within 200 ft from the dock, the throttle is varied as necessary to land the vessel, but full astern is rarely used. This indicates that actual vessels stop in less distance, using primarily the slow ahead, slow astern, and half astern throttle settings.

Figure 3.19 was developed assuming the reverse thrust was 17,000 lbs when the throttle is set at half astern and 10,500 lbs when the throttle is at slow astern. These are thrusts calculated for a steady state speed. Apparently, greater amounts of reverse thrust are obtained during the berthing maneuver. Figure 3.19 should be revised after more information regarding the actual thrust during various parts of the berthing maneuver is obtained. However, the results for stopping at full astern are corroborated by the sea trial crash stop test. Full-scale measurements taken in this study indicate that actual vessels lose speed more quickly than indicated in Figure 3.19, when the throttle is set to the stop position.

CHAPTER 4

CONCLUSIONS AND RECOMMENDATIONS

CONCLUSIONS

A review of the existing literature, sea trials results, physical model resistance tests, full-scale tests, and current roadway design criteria has provided resources for understanding vessel characteristics and how such characteristics may influence the design of ferry landing facilities. Investigation of these resources, and development of mathematical models, have provided tools with which to simulate vessel approaches. The results of these simulations provide information that can be used as design criteria for ferry landing plans. The following list summarizes the results of this study:

- Ferry approach velocities can be estimated using simple, iterative simulations. By knowing the ferry's thrust, resistance, and mass, the acceleration can be estimated for a short distance. Thus, the velocity change can also be estimated. New resistance and acceleration values are determined for the next segment, and the process is repeated. Difficulties in estimating the amount of propeller thrust limits the usefulness of this method. However, the calculated distance for stopping a vessel using full astern thrust and the results of a crash stop test from sea trials corroborated with the results of these calculations.
- Vessel resistance estimates that are based on tabular data found in reference books can not be relied upon to produce simulations that are satisfactory for developing design criteria. Estimates of resistance based on physical modeling results are more reliable.
- In situations where the WSF's "one-quarter-mile" rule is observed, the maximum approach velocity for a WSF Super Class ferry can be estimated

from the simulation methods as 12 knots if the ferry loses power at the one-quarter-mile point.

- By travelling at slow-ahead speed after the one-quarter-mile point, the ferry maintains steering control. Comparing the slow-ahead and stop deceleration curves show that the deceleration characteristics are similar for the initial 500 feet of travel. Thus, the ferry obtains the benefits of deceleration without sacrificing steering control.
- Safe speed vs. distance envelopes, based on stopping distances for various reverse throttle settings, can be developed. These can be used as the basis of operating policies. These envelopes would function in a manner similar to calculations that set roadway speed limits to accommodate stopping distances. To develop such envelopes, further full-scale testing will be required.
- Headreach calculations can be used to define a vessel's stopping distance.
- Sea trials can be used to confirm stopping distance calculations and to provide information on the ferry's turning ability.
- The "advance" dimension is the distance required for a vessel to execute a 90 degree course change. This dimension can be used to estimate the last point at which a vessel may turn to avoid possible collision with the berth.
- A portion of the sea trials turning circles results could be used by designers to map out preliminary approaches to landing facilities that involve turns. This would be similar to the process of developing roadway geometry to accommodate the turning requirements of standard vehicles.
- The research team did not find any information that described the ferry's turning ability at slow-ahead speed or while coasting. Such information would be helpful to evaluate the maneuverability of a distressed vessel.

- The research team found no specific information that would help to predict a distressed vessel's reactions to wind or current.
- Full-scale GPS measurements to track the ferries' paths could be used to obtain information for the two previous items. GPS may also be used during sea trials to track the vessel's location during specific maneuvers.

RECOMMENDATIONS

Reference Book on Vessel Characteristics

The researchers recommend that WSDOT develop a guide book on vessel characteristics to aid ferry landing designs. This guide book should include the following:

- Tables giving basic dimensions and vessel coefficients:
 - capacity,
 - tonnage,
 - length,
 - beam,
 - waterline beam,
 - draft,
 - wetted surface,
 - block coefficient,
 - prismatic coefficient,
 - displacement,
 - mass,
 - power,
 - top speed,
 - RPM at top speed, and
 - power;
- A narrative describing the operation of the steering and propulsion system;

- Drawings of the vessels; and
- Results of sea trials and physical model test.

Full-scale Measurements

Further understanding of vessel characteristics and their influence on ferry landing structure design could be gained by performing full-scale tests using GPS instrumentation. It is expected that the vessel maneuvers similar to those simulated in this study and maneuvers involving more complex motions could be recorded during full-scale tests. Recommendations and suggestions for further tests are presented in this chapter.

Before performing the tests recommended it would be advisable to complete preliminary tests during regular sailings. Data should be collected while the vessel turns or slows during a regular sailing, and then analyzed, using methods similar to those presented in a previous section of this report. An example of a scheduled sailing in the San Juan Islands is provided in Appendix M. During such a sailing, researchers could record and analyze typical maneuvers with GPS instrumentation; they could then compare the results with preliminary mathematical models. A familiarization exercise of this type would be modest in terms of cost and effort, but would allow researchers the opportunity to become familiar with the ferry, the crews, and the data collection procedures.

The preliminary full-scale tests completed as part of this study provided insight into the type and amount of data that should be collected. (See References 15 and 16.) The following should be noted during the data collection process:

- date,
- time,
- captain,
- ship name,
- weather conditions,

sea conditions,
the vessel's heading,
throttle setting,
shaft RPM,
rudder position,
wind speed,
wind direction,
tide,
current,
current direction,
vessel draft,
verbal commands, and
general visual observations.

Researchers could record much of this information directly, with the GPS data, if an electronic interface is provided between the ferry controls and the data recorder. Alternately, researchers could record the data manually. This approach's disadvantages include the possibility of inaccurate and incomplete records as well as the considerable effort required to coordinate manual records with GPS records. If researchers are preoccupied with manual data collection, they will miss opportunities to learn from conversations with the crew on the vessel and from observing general operations. Researchers could collect more complete and accurate records with video cameras. A set of video cameras could be set up to view and record the displayed data, such as tachometer, rudder angle indicator, and gyro (gives vessel's heading readings); the view out the front of the pilot house, and verbal comments. The study described in Reference 6 made use of such video recording equipment.

Full-scale measurements may be used to define vessel deceleration characteristics. Such measurements should include the following:

stop,
slow ahead,
slow astern, and
full astern.

These measurements can be compared to the simulations described in Chapter 3. The preliminary full-scale measurements collected as part of this study and as part of Margaroni and Jahren's study (17) provided sufficient information to imply that these mathematical models were valid for WSF Super Class ferries in some cases, but not valid in other cases. Additional measurements could be taken to improve the mathematical models and to obtain information for additional vessel classes.

Tests described in the previous paragraph could be performed during a regular sailing. For example, the vessel power could be reduced from full ahead to stop, allowing the vessel to coast for a short distance. Vessel power could be reset to full ahead and the regular sailing could be resumed. In addition to full ahead to stop, other variations could be tested. Additional tests would only be a minor disruption, yet they would provide valuable information about the vessel's deceleration characteristics. However, special sailings would be required for more elaborate tests.

To test vessel rudder response, researchers could monitor specific turns with GPS. The results would give vessel heading and speed; vessel turning rate and loss of speed could then be calculated with this information. These tests should be performed at all forward throttle settings. An example would be to perform zigzag tests (described in another section of this report) at full ahead, slow ahead, and without power. The results would give researchers a better understanding of the effects of throttle setting on maneuvers. By collecting data for slow-ahead and stop-throttle positions, researchers could better understand how to maneuver a distressed vessel. Such information is not normally available from sea trials; nor is it covered in the literature.

Researchers could also observe vessel response to wind during special sailings. A test could be performed wherein the throttle is moved from full ahead to stop while the ferry is in a cross wind. This test would provide information about vessel ability to hold a course in a side wind during a propulsion failure. Another test could be performed wherein the stern is moved by wind while the bow is fixed. This would provide information about the rotational motion of the ferry; a berthed ferry can experience this type of motion if it is lying against dolphins on one side and experiences a sudden shift in cross wind. This test could be performed at a location away from the landing facility so that the stern could swing freely. Figure 4.1 shows the anticipated motion of a ferry in such conditions, at both the landing facility and at a location away from the landing facility.

Summary

The simulation methods used to determine deceleration and turning characteristics should be tested for each ferry by taking full-scale measurements. The measurements may be taken far away from the landing structure to minimize the risk of an accident. Some of these tests could be performed during regular sailings with minimal disruption; special sailings may be required for others. GPS instrumentation could be employed to track vessel position, while researchers record other data manually or with video cameras. The results of the tests could be used to validate simulations and to develop design criteria for specific ferries and landings.

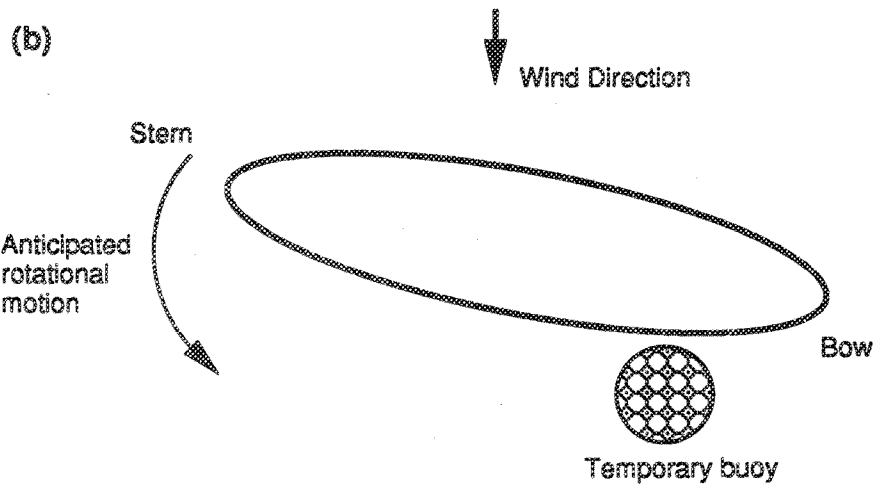
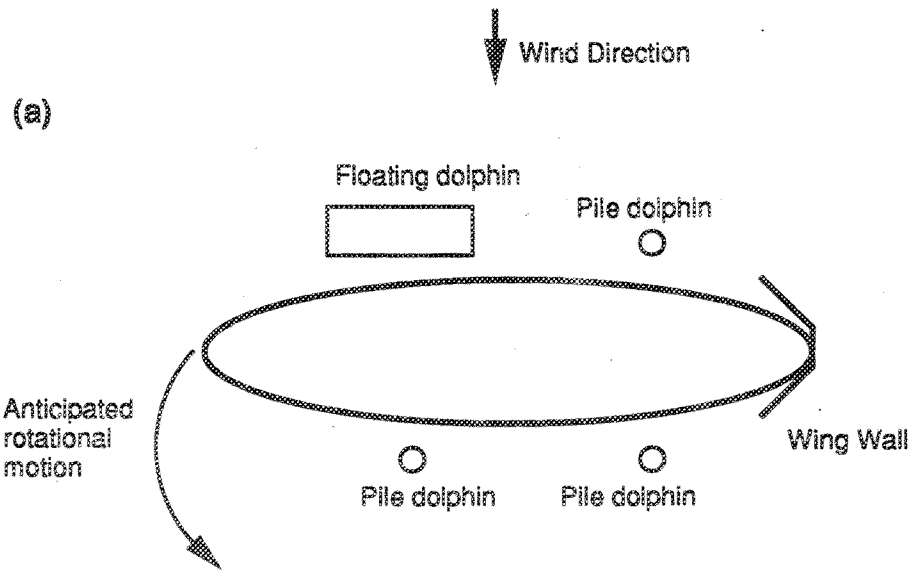


Figure 4.1. Anticipated Rotational Motion (a) While Berthed and (b) While at Sea

REFERENCES

1. Jahren, C.T., Jones R., and Ishii, S. (1992). "Design Criteria for Ferry Landings," *Proceedings, ASCE Ports '92 Conference*.
2. Danish Maritime Institute (1987). *Wind, Sea, Men and Ships — Integrated Maritime Solutions*, Copenhagen, Denmark.
3. Gillmer, T.C. (1970). *Modern Ship Design*, United States Naval Institute, Annapolis MD.
4. Margaroni, S., Jahren, C.T., and Scarpelli, A. (1992). Methods for Tracking Vessel Locations, Working Paper prepared for Washington State Transportation Commission by Washington State Transportation Center, Seattle WA.
5. Hurn, J. (1989). *GPS, A Guide to the Next Utility*, Trimble Navigation Ltd.
6. Webb, D.W. and Hewlett, J.C. (1992). "Ship Simulation of the Houston Ship Channel Houston, Texas," *Proceedings, ASCE Ports'92 Conference*.
7. Snyder, E.D. (1971). *Resistance, Propulsion, and Wake Survey Tests for Two Cross Sound Ferry Boats*, the University of Michigan, College of Engineering, Department of Naval Architecture and Marine Engineering Ship Hydrodynamics Laboratory, Office of Research Administration. Ann Arbor, Michigan
8. Mendenhall, W. (1971). *Introduction to Probability and Statistics*, 3rd edition, Wadsworth Publishing Company, Inc., Belmont CA.
9. PIANC (1984). *Report of the International Commission for Improving the Design of Fender Systems*, Supplement to Bulletin No. 45, Brussels, Belgium.
10. Ishii, S. (1991). "Modifications to Ferry Landings to Accommodate Emergency Landings," Master's Thesis presented to the University of Washington, Seattle, WA.
11. Mannering, F. L. and Kilareski, W. P. (1990). *Principles of Highway Engineering and Traffic Analysis*, John Wiley and Sons, Inc., New York NY.
12. AASHTO (1990). *A Policy on Geometric Design of Highways and Streets* Washington, D.C.
13. SNAME (1957). "Guide to the Selection of Backing Power," Technical and Research Bulletin No. 3-5.
14. Comstock, J.P. (ed.) (1967). *Principles of Naval Architecture*. Society of Naval Architects and Marine Engineers, New York, NY.

15. SNAME, (1966). "Notes on Ship Controllability," Technical and Research Bulletin No. 1-27.
16. SNAME, (1973). "Code for Sea Trials," Technical and Research Code, C-2.
17. Margaroni, S. and Jahren, C.T. (1992). "Vessel Tracking Methods for Ferry Landing Design," Olympia, Washington: Washington State Department of Transportation, Report No. WA-RD 267.1.

BIBLIOGRAPHY

- AASHTO (1990). *A Policy on Geometric Design of Highways and Streets*, Washington, D.C.
- Abkowitz, M.A. (1983). "Measurement of Ship Resistance, Powering, and Maneuvering Coefficients from Simple Trials During a Regular Voyage," *Society of Naval Architects and Marine Engineers Transactions* vol. 96, 97-128.
- Bengsten, K., Corner-Walker, B.P. (1980). "Car Ferry Design and Development," *The Naval Architect*, no. 1.
- Bratteland, E. (1974). "A Survey on Acceptable Ship Movements in Harbours," *The Dock and Harbour Authority*, Volume LV, No.647.
- Brown, P.K., (1967). "Hulls Roll-on Roll-off Services," *The Dock and Harbour Authority*, December, 1967, 251-256.
- Bruun, P. (1985) "Fendering," *The Dock and Harbour Authority* vol. LXU, no. 767.
- Bruun, P. (1981). *Port Engineering*, third edition, Gulf Publishing Company, Houston, TX.
- Comstock, J.P. (ed.) (1967). *Principles of Naval Architecture*. SNAME, New York, NY,
- Dickey, A. (1986). "Ferry Leaves Its Engineers Ashore," *The Engineer* vol. 263, 43
- Doebler, J. (1990). "A Proposal for Installation of Hoistable Upper Car Decks for Issaquah Class Ferries," Master's Thesis presented to the University of Washington, Seattle, WA.
- Eda, H. (1971). "Directional Stability and Control of Ships in Restricted Channels," *SNAME Transactions*, vol. 79, 71-116. New York, NY.
- Fontijn, H.L. (1988). "On the Predication of Fender Forces at Berthing Structures, Part I, Calculating Forces." *Advances on Berthing of Ships and Offshore Structures*, Kluwer Academic Publishers, Norwell, MA.
- Fontijn, H.L. (1988). "On the Prediction of Fender Forces at Berthing Structure, Part II, Ship Berthing Related to Fender Structure," *Advances on Berthing of Ships and Offshore Structures*. Kluwer Academic Publishers, Norwell, MA.
- Gillmer, T.C. (1970). *Modern Ship Design*, United States Naval Institute, Annapolis, MD.
- Guide Specifications and Commentary for Vessel Collision, Design of Highway Bridges, Executive Summary*, vol. 1, 2, Federal Highway Commission (1990).
- Habib, P., Blok, A., Roess, R. (1980). *Functional Designs of Ferries Systems*, Transportation Training and Research Center, New York, NY.

- Hamamoto, M., Hasegawa, K., Iida T. (1988). "On the Technique in the Analyses of Transient Maneuver Tests," *Naval Architecture and Ocean Engineering*, Volume 26, 61-70.
- Hamer, M. (1990). "Two Designs Shortlisted in Search for Safer Ferries," *New Scientist*. Vol 126, 27.
- Hess, T.E. (1988). "Rapid in Field Ferry Berth Construction," *Advances in Berthing and Mooring of Ships and Offshore Structures*, Kluwer Academic Publishers, Norwell, MA.
- Ishii, S. (1991). "Modifications to Ferry Landings to Accommodate Energy Impacts," Master's Thesis presented for the University of Washington, Seattle, WA.
- Ivey, D.L. and Morgan, J.R. (1985). *Safer Timber Utility Poles* vol. 1, Federal Highway Administration.
- Jessup, J.G., Bunck, H.M. (1986). *Analysis of Drummond Island Ferry System*, Michigan Department of Transportation, Ann Arbor, MI.
- Kijima, K., Yasukawa, H. (1985). "Maneuverability of Ships in Narrow Waterways," *Naval Architecture and Ocean Engineering* vol. 23, 25-38.
- Kijima, K. and Qing, H. (1988). "Maneuvering Motion of a Ship in the Proximity of Bankwall," *Naval Architecture and Ocean Engineering* vol. 26, 1-8.
- Kose, K., Hinata, H., and Hashizume, Y. (1985). "On a New Mathematical Model for Maneuvering Motions in Low Speed," *Naval Architecture and Ocean Engineering*, vol. 23, 15-24.
- Lamb, H. (1932). *Hydrodynamics*, Cambridge University Press, Cambridge, MA.
- Landsberg, A.C. (1983). "Design and Verification for Adequate Ship Maneuverability," *Society of Naval Architects and Marine Engineers Transactions* vol. 91, 351-401.
- Lindell, G.A. (1964). "The Wellington Rail Road Ferry Terminal," *The Dock and Harbour Authority*, June 1964, 36-42.
- Lunde, J.K. (1957). "The Linearized Theory of Wave Resistance and Its Application to Ship Shaped Bodies in Motion on the Surface of a Deep, Previously Undisturbed Fluid," *SNAME Technical and Research Bulletin* no. 1-18, New York, NY.
- Mannering, F.L., and Kilareski, W.P., *Principles of Highway Engineering and Traffic Analyses*, John Wiley & Sons, Inc.
- Maxwell, C. and Wheeler, B.E. (1964). "The Picton Rail Road Ferry Terminal," *The Dock and Harbour Authority*, September 1964, 138-143.
- Middendorp, P. (1981). "Fender Forces from Berthing Ships," *The Dock and Harbour Authority*, 160-162.
- Naval Civil Engineering Laboratory (1989). *Prestressed Concrete Fender Piles: Fender System Design*, CR 89.005

- Nece, R.E., McCaskin, M.R., Christensen, D.R. (1985). *Ferry Wake Study*, Washington State Department of Transportation, Olympia, WA.
- "New Ferry Terminal at Southampton," *The Dock and Harbour Authority*, October 1964, 189-193.
- Nickum, W.C., and Sons (1968). Ferry Study Engineering Report Number 3425 for Washington State Highway Commission Department of Highways.
- PIANC (1984). "Report of the International Commission for Improving the Design of Fender Systems," *PIANC Supplement to Bulletin 45*, Brussels, Belgium.
- PIANC (1991). "Danish Ferry Terminals," *PIANC Bulletin 72*, Brussels, Belgium.
- PIANC (1949). Account of the XVIIth Congress.
- PIANC (1953). Report of the Work of the XVIIIth Congress.
- PIANC (1957). Report of Proceedings of XIXth Congress.
- PIANC (1961). Report of Proceedings of XXth Congress.
- PIANC (1969). Report of Proceedings of XXIIth Congress.
- PIANC (1985). Report of Proceedings of 26th Congress.
- PIANC (1990). Report of Proceedings of 27th Congress.
- Porter, R.B., Muir, I.S. (1969). "The Tynes's New Car Ferry Terminal," *The Dock and Harbour Authority*, May 1966, 68-72.
- Reid Crowther and Partners Limited (1989). *Alternate Berthing Structure Study*.
- "Ro-Ro Gathers Momentum," *The Naval Architect*, Sept. 1976.
- Roess, R., Grealy, P., Berkowitz, C. (1982). *Some Critical Aspects of Ferry Systems*, Maritime Administration, Washington, DC.
- Rogge, T. (1964). "Ferry Berthing Installations, Six Basic Types of Structures," *The Dock and Harbour Authority*, vol. XLV, no. 533, 358-361.
- Rossell, H.E. (ed.) (1942). *Principles of Naval Architecture*, SNAME, New York, NY.
- Russell, R.C.H. (1971). "Model Investigations of Berthing Impacts," NATO Advanced Study Institute on Analytical Treatment of Problems of Berthing and Mooring Ships, ASCE, New York, NY.
- Saunders, H.E. (1957). *Hydrodynamics in Ship Design*, SNAME New York, NY.
- Smith, C. (1966). "Pilotage Dynamics," *The Dock and Harbour Authority*, April 1966, 397-400.

- SNAME (1957). "Guide to the Selection of Backing Power," *SNAME Technical and Research Bulletin* no. 3-5, New York, NY.
- SNAME (1963). "How to Use SNAME Small Craft Data Sheets for Design and Resistance Prediction," *Technical and Research Bulletin*, no. 1-23.
- SNAME (1966). "Notes on Ship Controllability," *Technical and Research Bulletin*, no. 1-27.
- SNAME (1973). "Code for Sea Trials," Technical and Research Code No. C-2.
- Sommet, J.,(1971). "The Added Mass of a Ship in Longitudinal Oscillation," NATO Advanced Study Institute on Analytical Treatment of Problems of Berthing and Mooring Ships, ASCE, New York, NY.
- Svendsen, I.A. (1973). "Ship Maneuvres in Harbours, an Analysis of Forces and Types of Maneuvres," NATO Advanced Study Institute on Analytical Treatment of Problems in the Berthing and Mooring of Ships, ASCE, New York, NY.
- Svendsen, I.A. (1974). "Ship Maneuvres in Harbours", *The Dock and Harbour Authority* vol. LV, 171-174.
- Synder, E.D. (1971). *Resistance, Propulsion, and Wake Survey Tests for Two Cross Sound Ferry Boats*, Office of Research Administration, Ann Arbor, MI.
- Taylor, D.W.C. (1943). *The Speed and Power of Ships*, United States Maritime Commission, Washington, DC.
- Taylor, G.R. (1976). "Ro/Ro Ships - State of the Art in Australia," *Marine Technology*, vol 13, no. 4, 343-370.
- Technical Standards for Port and Harbour Facilities in Japan (1980). Bureau of Ports and Harbours, Ministry of Transport, Tokyo, Japan.
- "The Standardization of Ferry Terminals" *The Dock and Harbour Authority*, May 1966, 13-18.
- Todd, F.H., (1964). "Tables of Coefficients for A.T.T.C. and I.T.T.C. Model Ship Correlation and Kinematic Viscosity and Density of Fresh and Salt Water," *SNAME Technical and Research Bulletin*, no. 1-25, New York, NY.
- Tyrell, B.G. (1966). "Mooring Dolphins — Evaluation of Forces and Principles of Design," *The Dock and Harbour Authority*, vol. 47, 115.
- Vasco Costa, F. (1964). "The Berthing Ship," *The Dock and Harbour Authority* vol. 45, 90-94.
- Vasco Costa, F. (1971). "Mechanics of Impact and Evaluation of the Hydrodynamic Mass Analytical Study of the Problem of Berthing," NATO Advanced Study Institute on Analytical Treatment of Problems of Berthing and Mooring Ships, ASCE, New York, NY.

- Veda S. (1988). "Distribution of Berthing Speed and Eccentricity Factor of VLCC Investigated in Japan," *Advances in Berthing and Mooring of Ships and Offshore Structures*, Kluwer Academic Publishers, Norwell, MA.
- Veda S. (1988). "The Virtual Mass Coefficient of Berthing Ships," *Advances in Berthing and Mooring of Ships and Offshore Structures*, Kluwer Academic Publishers, Norwell, MA.
- Veloso Gomes, F.F.M. (1988). "Ships and Berth Structure Interaction," *Advances in Berthing and Mooring of Ships and Offshore Structures*, Kluwer Academic Publishers, Norwell, MA.
- Viggosson, G. (1988). "Field Observations of Ship Behavior at Berth," *Advances in Berthing and Mooring of Ships and Offshore Structures*, Kluwer Academic Publishers, Norwell, MA.
- Washington State Ferries Management Information. (1964).
- Webb, D.W., and Helwlett, J.C. (1992). "Ship Simulation of the Houston Ship Canal, Houston, Texas," *Proceedings, ASCE Ports '92 Conference*.
- Weeks, J. (1972). Propulsion and Auxillary Electrical Systems on the New 440' Cross Sound Ferries for the State of Washington.
- Williams, A. (1983). Development of Hull Forms for Ro-Ro (Roll-on/Roll-off) Ships and Ferries, Swedish Maritime Research Center.
- Wood, D.J.D., (1964). "New Terminals for Woolwich Ferry," *The Dock and Harbour Authority*, December 1964, 234-239.
- Wood, D.J.D., (1969). "Roll on/Roll off Ferry Terminal at Cork," *The Dock and Harbour Authority*, June 1969, 47-49.
- Wurzel, Paul, (1966). "Lake Victoria Wagon Ferry Scheme", *The Dock and Harbour Authority*, vol. XLVII, 138-147.

APPENDIX A
VESSEL CHARACTERISTICS

APPENDIX A

VESSEL CHARACTERISTICS

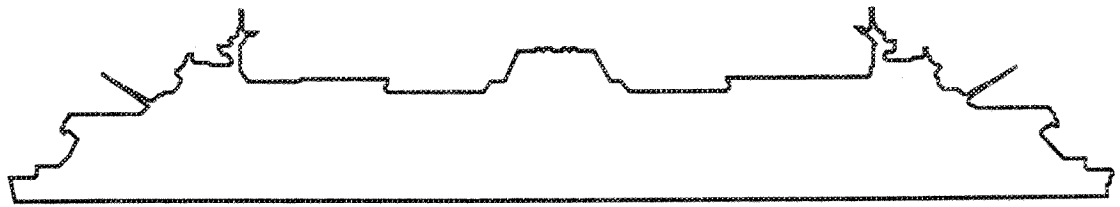
A preliminary investigation relating to vessel characteristics was performed to find information concerning the relationship between the vessel approach velocity and vessel characteristics; and between vessel steering response and vessel characteristics. The researchers anticipated that this information could be used to develop design criteria for ferry landing facilities. The study included a literature search related to vessels generally, and a literature search related specifically to ferries.

Automobile ferries differ from other vessels. Their distinctive characteristics include permanent fendering extending around the hull, a low length to width ratio, vehicle decks above the waterline, and loading/unloading at the bow and/or stern. Because ferries normally operate on inflexible schedules, they require high horsepower to displacement ratios to ensure that crossing times are met under adverse weather conditions. The hull shape and the propulsive arrangement must be selected carefully so that the vessel can perform at required speeds with minimum horsepower. A combination of low resistance and high propulsive efficiency is attained by proper matching of the hull and the propeller.

As part of this study, hypothetical berthing scenarios were developed using the vessel characteristics of Washington State Ferry (WSF) Super Class ferries. Figure A.1 shows each WSF vessel by class, complete with information related to year it was built, its length, speed, automobile capacity, and passenger capacity.

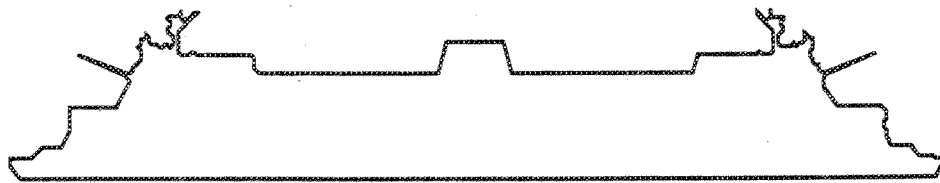
BASIC PARAMETERS

The shape of the surface of a ship's hull determines its form. Ship form is expressed in terms of typical coefficients and/or ratios. These coefficients are calculated



Jumbo Class

Name MV	Place Built	Year Built	Length	Beam	Draft	Auto Clear	Speed (Knots)	Main Engines	Type of Propulsion	Capacity Cars/ Pass.	Tons Gross/Net
Spokane	Seattle	1972	440'	87'	18'	15'	18	4	Diesel-Elec.	206/2000	3246/1198
Walla Walla	Seattle	1972	440'	87'	18'	15'	18	4	Diesel-Elec.	206/2000	3246/1198



Super Class

Name MV	Place Built	Year Built	Length	Beam	Draft	Auto Clear	Speed (Knots)	Main Engines	Type of Propulsion	Capacity Cars/ Pass.	Tons Gross/Net
Hyak	San Diego	1967	382'2"	73'2"	17'3"	16'	7	4	Diesel-Elec.	160/2500	2704/1214
Kaleetan	San Diego	1967	382'2"	73'2"	17'3"	16'	7	4	Diesel-Elec.	160/2500	2704/1214
Yakima	San Diego	1967	382'2"	73'2"	17'3"	16'	7	4	Diesel-Elec.	160/2500	2704/1214
Elwha	San Diego	1967	382'2"	73'2"	17'3"	16'	7	4	Diesel-Elec.	160/2500	2704/1214



Issaquah Class

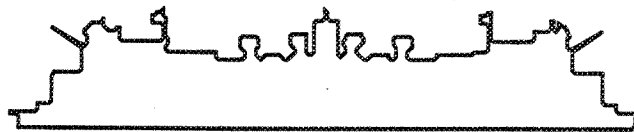
Name MV	Place Built	Year Built	Length	Beam	Draft	Auto Clear	Speed (Knots)	Main Engines	Type of Propulsion	Capacity Cars/ Pass.	Tons Gross/Net
Issaquah	Seattle	1979	328'	78'	15'6"	16'	16	2	Diesel	100/1200	2469/1749
Kittitas	Seattle	1980	328'	78'	15'6"	16'	16	2	Diesel	100/1200	2469/1756
Kitsap	Seattle	1980	328'	78'	15'6"	16'	16	2	Diesel	100/1200	2475/1756
Cathlamet	Seattle	1981	328'	78'	15'6"	16'	16	2	Diesel	100/1200	2477/1772
Chelan	Seattle	1981	328'	78'	15'6"	16'	16	2	Diesel	100/1200	2477/1772
Sealth	Seattle	1982	328'	78'	15'6"	16'	16	2	Diesel	100/1200	2477/1772

Figure A.1. Washington State Ferry Vessel Specifications



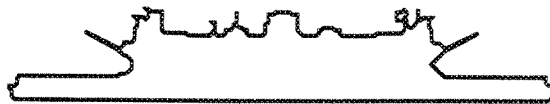
Evergreen State Class

Name MV	Place Built	Year Built	Length	Beam	Draft	Auto Clear	Speed (Knots)	Main Engines	Type of Propulsion	Capacity Cars/ Pass.	Tons Gross/Net
Evergreen State	Seattle	1954	310'	73'	15'	12'6"	13	2	Diesel-Elec.	100/1000	1495/1017
Klahowya	Seattle	1958	310'2"	73'2"	15'6"	13'10"	13	2	Diesel-Elec.	100/1140	1334/907
Tillikum	Seattle	1959	310'2"	73'2"	15'6"	13'10"	13	2	Diesel-Elec.	100/1140	1334/907



Steel Electric Class & Reburished Steel Class

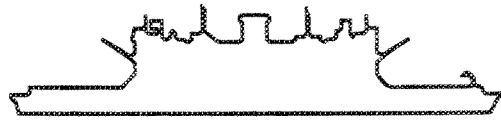
Name MV	Place Built	Year Built	Length	Beam	Draft	Auto Clear	Speed (Knots)	Main Engines	Type of Propulsion	Capacity Cars/ Pass.	Tons Gross/Net
Quinault	Oakland	1927/58	256'	73'10"	12'	13'10"	12	2	Diesel-Elec.	75/665	1368/930
Illahee	Oakland	1927/58	256'2"	73'10"	12'	13'10"	12	2	Diesel-Elec.	75/600	1369/931
Nisqually	San Fran.	1927/58	256'	73'10"	12'	13'10"	12	2	Diesel-Elec.	75/665	1368/930
Klickitat	San Fran.	1927/58 /81	256'	73'10"	12'	13'10"	12	2	Diesel-Elec.	75/600	1431/973



Rhododendron

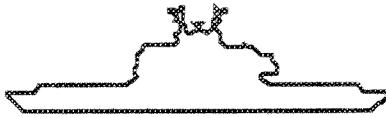
Name MV	Place Built	Year Built	Length	Beam	Draft	Auto Clear	Speed (Knots)	Main Engines	Type of Propulsion	Capacity Cars/ Pass.	Tons Gross/Net
Rhododendron	Baltimore	1947	225'9"	63'	8'6"	12'8"	12	2	Diesel	65/546	937/435

Figure A.1. Washington State Ferry Vessel Specifications (cont.)



Olympic

Name MV	Place Built	Year Built	Length	Beam	Draft	Auto Clear	Speed (Knots)	Main Engines	Type of Propulsion	Capacity Cars/ Pass.	Tons Gross/Net
Olympic	Baltimore	1938	207'6"	62'	6'6"	12'6"	11	1	Diesel	55/605	773/308



Hiyu

Name MV	Place Built	Year Built	Length	Beam	Draft	Auto Clear	Speed (Knots)	Main Engines	Type of Propulsion	Capacity Cars/ Pass.	Tons Gross/Net
Hiyu	Portland	1987	150'	63'1"	11'3"	18'	10	2	Diesel	40/200	498/338

Figure A.1. Washington State Ferry Vessel Specifications (cont.)

from the following basic parameters:

- L = designed waterline length
- T = draft (vertical distance) from the bottom of the ship to the waterline
- B = beam, or breadth at the waterline
- D = volume displacement at draft T
- W = weight displacement at draft T
- A_m = area of midsection at draft T
- A_w = area of waterplane at draft T

The following coefficients and ratios are most commonly used to describe the ship's form:

- midship coefficient $C_m = A_m/(B*T)$
- block coefficient $C_b = D/(L*B*T)$
- prismatic coefficient $C_p = D/(A_m*L) = C_b/C_m$
- waterline coefficient $C_{wp} = A_w/(B*L)$
- length - beam ratio = L/B
- length - draft ratio = L/T
- beam - draft ratio = B/T
- displacement - length ratio = $D/(L)^3$
- speed - length ratio = V/\sqrt{L} (note: V = velocity (knots), L = length (feet))

The naval architect determines basic ship parameters during the design process. In addition to being used by the naval architect during the design, the parameters are also used to express characteristics of the ship's form, to calculate propulsion, and to estimate the vessel resistance to motion. Figures A.2 and A.3 illustrate basic ship parameters. (A1) Table A.1 lists some basic ship parameters for WSF Super Class ferries, as well as other parameters germane to this study.

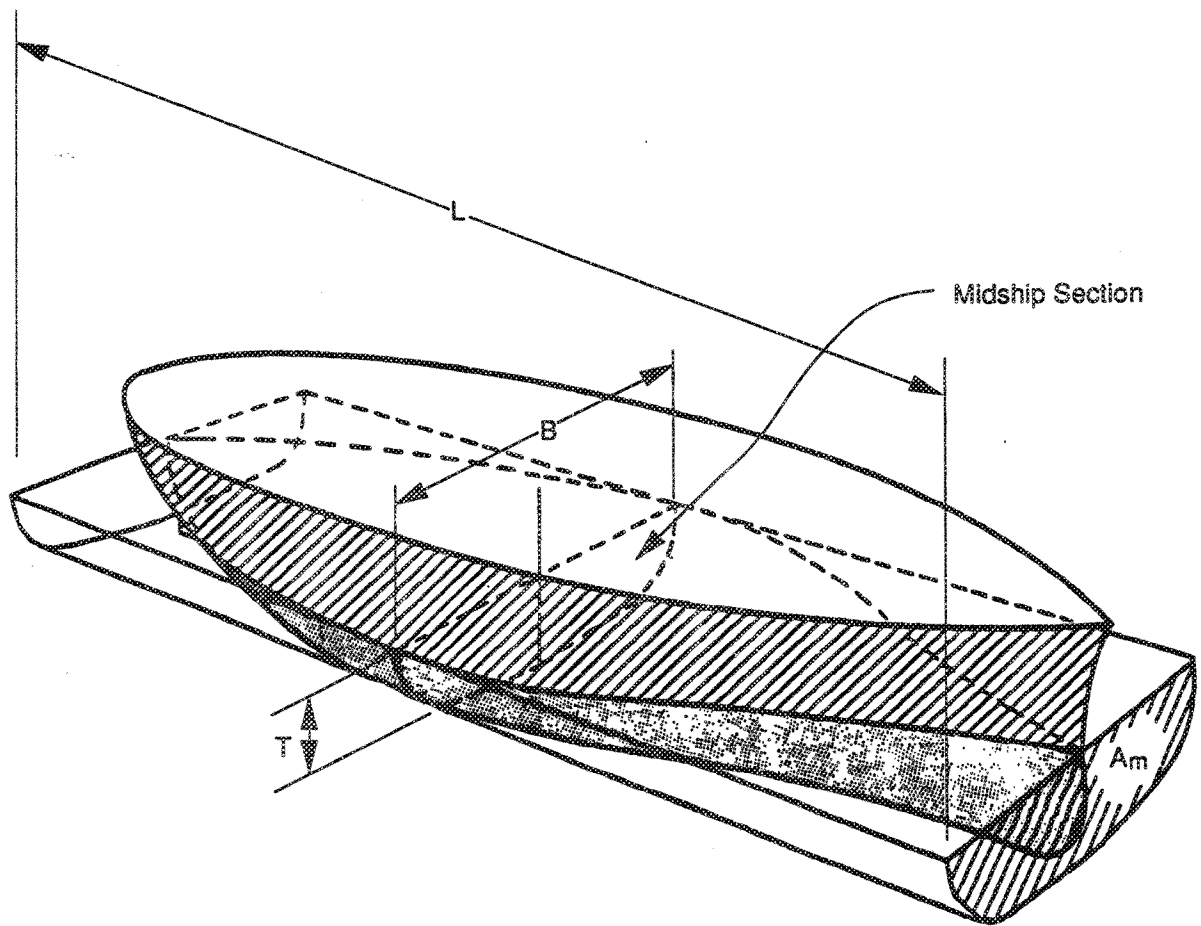


Figure A.2. Basic Vessel Parameters [Ref. 1]

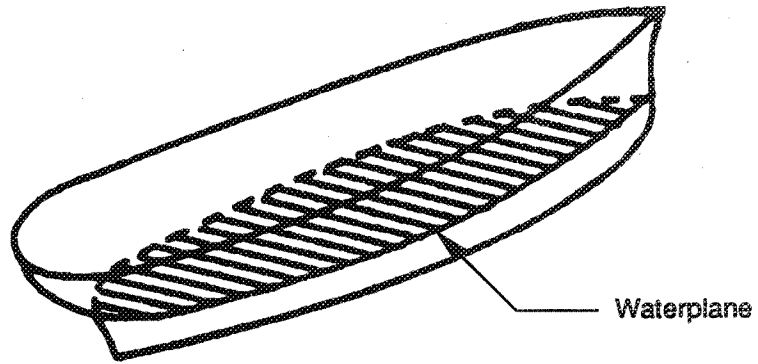


Figure A.3. Vessel Waterplane [Ref. 1]

Table A.1 Vessel Data for WSF Super Class Ferries

Description	Value	Source
Length L	382.25 ft	WSF Brochure
Volumetric Displacement D	114905 ft ³ of sea water	Calculated from Equation 1
Weight Displacement W	3283 tons	Reference (7)
Mass W/g	228382.6 lb/ft/sec ²	Calculated
Prismatic Coefficient C _p	0.5409	Reference (8)
Block Coefficient C _b	0.3439	Reference (8)
Beam B	73.2 ft	WSF Brochure
Waterline Beam B	53.0 ft	Estimated
Draft T	17.25 feet	WSF Brochure
Wetted Surface S	18706 ft ²	Approximated from Equation 2
Density of sea water ρ	1.9905 lb sec ² /ft ⁴	Appendix B
Kinematic Viscosity of sea water ν	1.279x10 ⁻⁵ ft ² /sec	Appendix B
Gravitational Constant g	32.2 ft/sec ²	Constant

The weight displacement of a given vessel constitutes that vessel's actual weight. The volumetric displacement is the volume of salt water that equals the vessel weight (salt water displaced by the vessel). The weight displacement and the volumetric displacement are related by the following equation (A1):

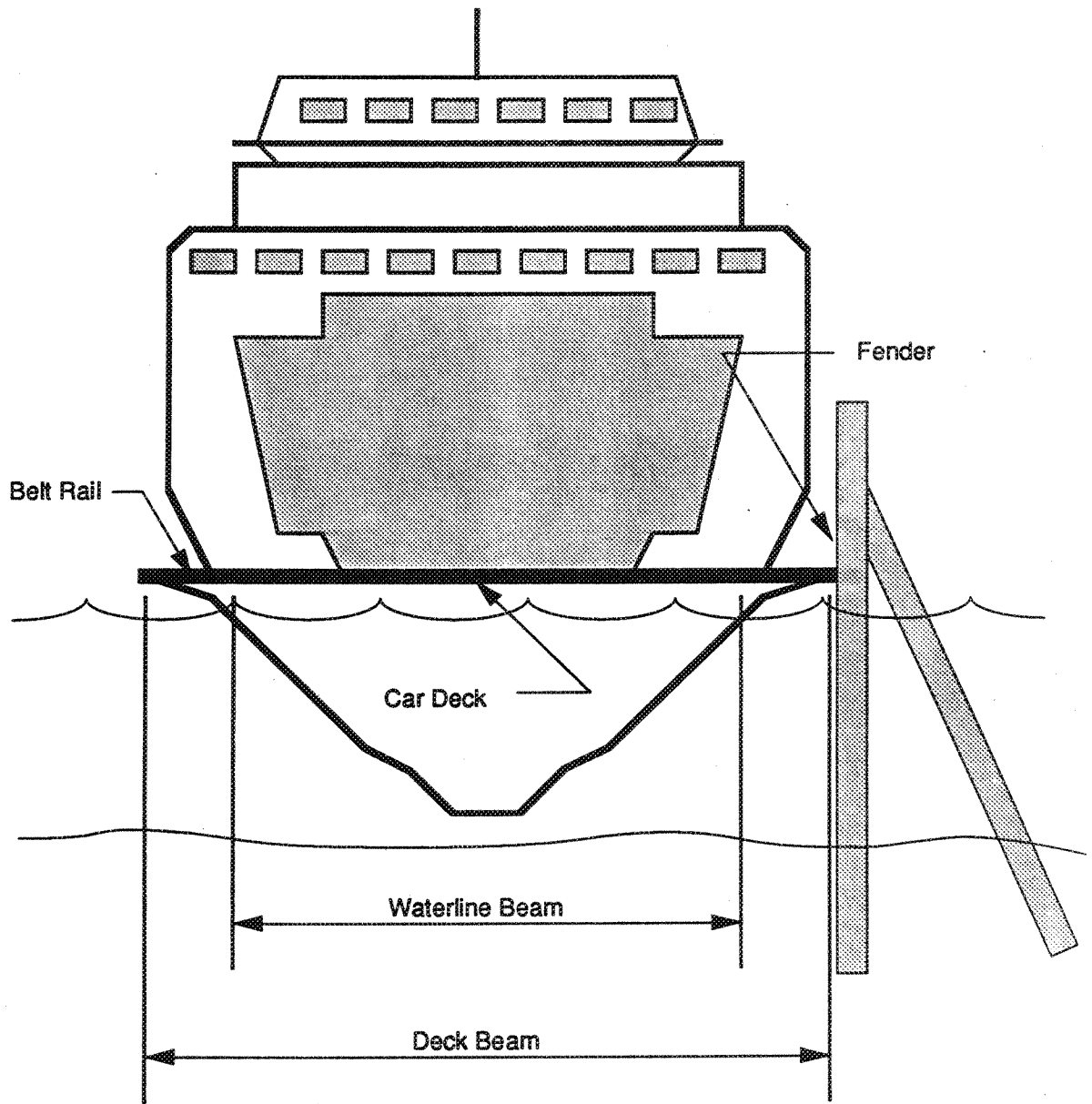
$$D = 35 (W) \tag{1}$$

where D = volumetric displacement (ft³)

W = weight displacement (tons)

35 = conversion of ft³ seawater/tons (1 ton = 2240 lbs)

A vessel's beam constitutes its widest breadth and is usually located at the waterline. For most vessels the waterline breadth is the only breadth describing a vessel. However, ferries are unusual in that their widest breadth is located at the vehicle deck, just above the waterline. This breadth is greater than the breadth measured at the waterline. Both the breadth of the vessel at the widest point (the vehicle deck) and the breadth of the vessel at the waterline describe the vessel's beam. Figure A.4 illustrates the difference between these two parameters.



CROSS-SECTIONAL VIEW

Figure A.4. Vessel Beams

The wetted surface is a vessel's total area of outer surface that is in contact with the water.

The wetted surface can be approximated by the following equation (2):

$$S = 1.7 * L * T + D/T \quad (2)$$

where S = vessel wetted surface (ft²)

L = vessel length (ft)

D = vessel volumetric displacement (ft³)

T = vessel draft (ft)

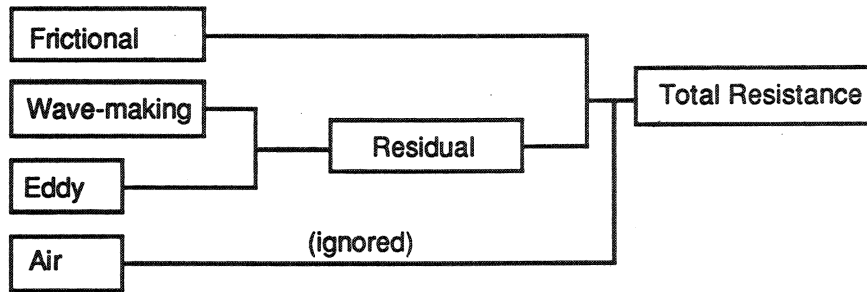
The block coefficient, C_b , is the ratio of the volume displacement of the molded form of a vessel (up to a given waterline) to the volume of a rectangular solid whose length is equal to the waterline length, whose breadth is equal to the molded breadth at that waterline, and whose depth is equal to the molded draft of the vessel up to that waterline. Values of C_b vary from about .38 for high-powered yachts to about .80 for slow-speed cargo vessels. C_b for WSF Super Class ferries is 0.3439. The midship coefficient, C_m , is the ratio of immersed area of the midship section to the area of the circumscribing rectangle, the width of which is the molded beam at the waterline, and the depth of which is the molded draft at the waterline for which C_m is calculated. The prismatic coefficient, C_p , is the ratio of the volume of the displacement of the molded form of a vessel (up to a given waterline) to the volume of a solid that has a length equal to the load waterline length and a constant cross-sectional area equal to that of the vessel's midship section up to the given waterline. C_p expresses and measures the vessel's fineness longitudinally. (2)

RESISTANCE

A vessel's resistance is defined as the force required to tow the vessel at a given speed in smooth water. Vessel resistance to motion through water must be overcome by an equal and opposite propelling force to move the vessel forward. Vessel total resistance consists of four main components: 1) frictional resistance, 2) wave-making

resistance, 3) eddy resistance, and 4) air resistance. Wave-making resistance and eddy resistance combined constitute residual resistance. (2)

Two of these components, residual resistance and frictional resistance, make up the majority of total resistance. Although wind affects the vessel's maneuvers, it has little effect on the resistance that must be overcome by propulsive force. Therefore, it is not considered further in this report. Total resistance is determined by adding frictional resistance to residual resistance. The majority of the residual resistance is wave-making resistance, not eddy resistance (flow separation or form drag effects). Hence, for the purpose of this investigation, residual resistance is assumed to consist of wave-making resistance only, and total resistance is assumed to consist of frictional resistance and wave-making resistance combined ($R_t = R_f + R_w$).



The relationship between frictional and wave-making resistance is illustrated in Figure A.5. (1)

Frictional resistance is the resistance to the motion of the hull through a viscous fluid; it is the largest single component of vessel total resistance and is a result of tangential fluid forces. Frictional resistance accounts for 80 percent to 85 percent of total resistance in slow-speed ships (vessels with speed/length ratios of less than 0.5, such as freighters) and accounts for 50 percent of total resistance in high-speed ships (vessels with speed/length ratios of greater than 0.5, such as passenger liners). (2) Figure A.5 shows the proportions of wave-making resistance and frictional resistance for given speed/length ratios. (1)

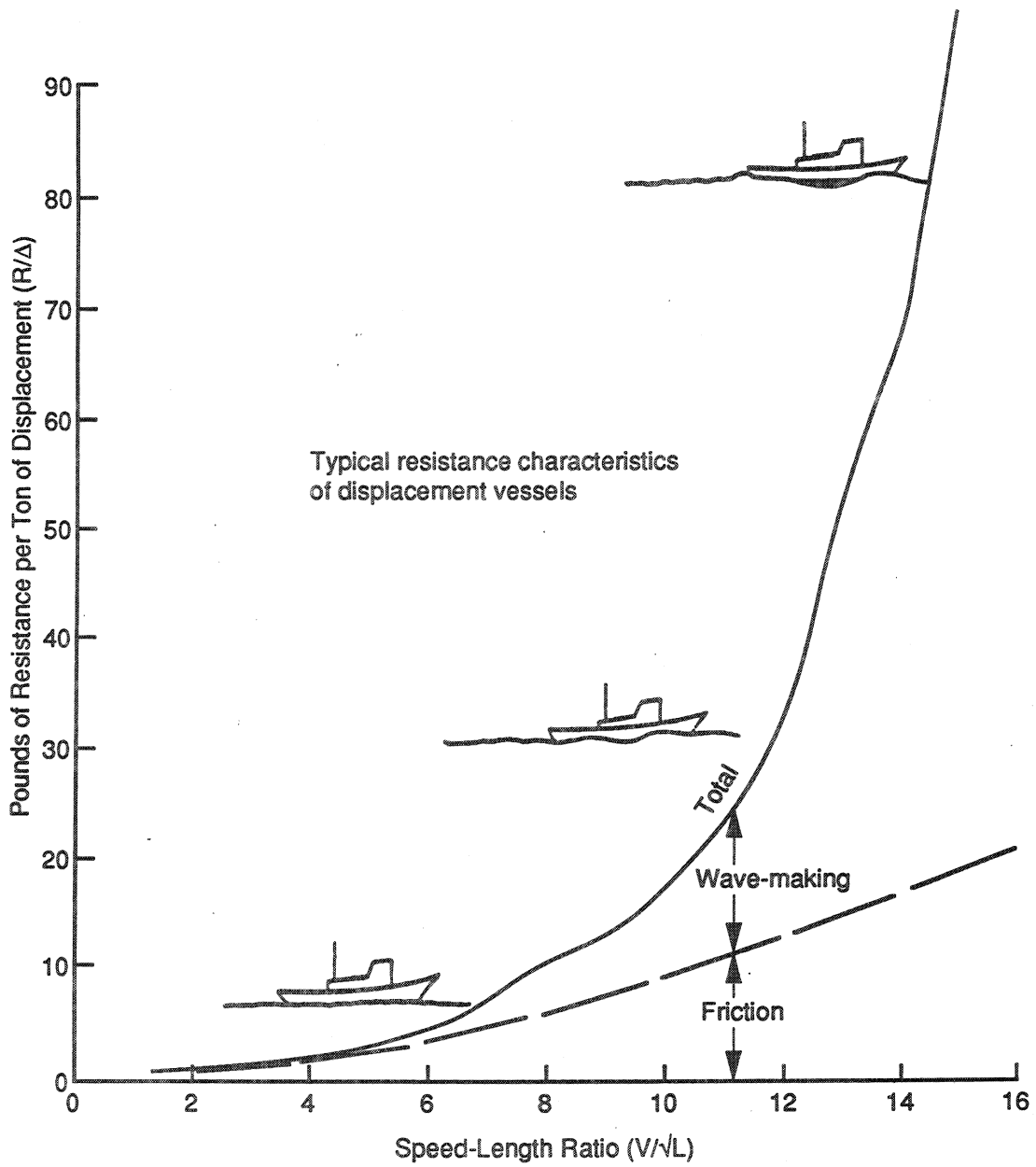


Figure A.5. Resistance vs. V/\sqrt{L} in a Characteristic Speed-Power Curve for a Displacement Ship (Note the ship-wave profiles) [Ref. 1]

Operating at their maximum speed, WSF Super Class ferries have a speed/length ratio of 0.87. The speed/length ratios for other WSF ferries, travelling at maximum speed, are shown in Table A.2

Table A.2. Speed/Length Ratios for WSF Ferries

Class	Maximum Speed	Length	V/\sqrt{L}
Jumbo	18 knots	440.0 ft	0.86
Super	17 knots	382.25 ft	0.87
Issaquah	16 knots	328.0 ft	0.88
Evergreen State	13 knots	310.0 ft	0.74
Refurbished Steel Electric	12 knots	256.0 ft	0.75
Rhododendron	12 knots	229.75 ft	0.79
Olympic	11 knots	207.5 ft	0.76
Hiyu	10 knots	190.0 ft	0.73

Frictional resistance is a function of the surface roughness, the area of surface, the velocity of the fluid over the surface, and the density of the fluid. The Reynolds Number governs the frictional resistance of a vessel. The Reynolds Number is a parameter that can be calculated from the speed of the vessel and the kinematic viscosity of the sea water. The Reynolds Number is calculated from the following equation:

$$R = V * L / \nu \quad (3)$$

where R = Reynolds Number

V = vessel velocity (ft/sec)

L = vessel length (ft)

ν = kinematic viscosity of sea water (ft²/sec)

Hence, the Reynolds Number can be easily calculated from known quantities. The Reynolds Number is mathematically related to frictional resistance by the frictional resistance coefficient. The frictional resistance coefficient is calculated from the Reynolds Number according to the following equation (2):

$$C_f = 0.075 / (\log(R) - 2)^2 \quad (4)$$

where C_f = frictional resistance coefficient

R = Reynolds Number

The frictional resistance can be calculated from the frictional resistance coefficient from the following equation:

$$R_f = C_f * \rho / 2 * S * V^2 \quad (5)$$

where R_f = frictional resistance (lbs)

C_f = frictional resistance coefficient

ρ = density of sea water (lbs*sec²/ft⁴)

V = vessel velocity (ft/sec)

S = vessel wetted surface (ft²)

Sample calculations of the Reynolds Number, the frictional resistance coefficient, and frictional resistance are provided in Appendix C.

The wave-making resistance portion of a ship's residual resistance is the result of fluid pressures acting normally on all parts of the hull, and is the net and aft force on a ship due to these fluid pressures. Wave-making resistance depends on the vessel's shape and on its waterline and transverse sections. The Froude Number, which governs the vessel's wave-making resistance, can be calculated from the vessel's speed, length, and gravitational constant. However, the calculation of the wave-making resistance is complex and cannot be computed directly from the Froude Number. (2) A simplified version of an equation to compute the wave-making resistance is as follows (3):

$$R_w = \frac{4g\rho K_0 A^2}{\pi} \times \int_0^\infty \sin^2\left(\frac{1}{2}K_0 L C_p \cosh u\right) \times e^{-2K_0 f \cosh^2 u} \cosh^2 u du \quad (6)$$

where R_w = wave-making resistance

C_p = prismatic coefficient

g = acceleration of gravity (ft/sec²)

ρ = density of sea water (lb-sec²/ft⁴)

- K_o = g/c^2
- c = vessel velocity (ft/sec)
- A = area of midship section (ft²)
- L = vessel length (ft)
- f = depth of velocity source (or sink) under the free surface of the fluid (ft)
- u = horizontal component of the absolute fluid velocity (ft/sec)

Reference 3 provides a complete description of the above variables. The computation detailed above was considered too complex for the purpose of this study. (3) A simpler and commonly accepted method for estimating wave-making resistance is the use of published tabular data; the research team used this approach in this study. The table used in an attempt to estimate wave-making resistance in this study is shown in Tables A.3 and A.4. (4) Sample calculations related to the use of the table are provided in Appendix D. As explained in the Research Approach section, values used from these tables underestimated wave-making resistance for the WSF Super Class ferry.

The B/T ratio determines which table to use to estimate wave-making resistance; one must know the vessel's waterline beam and draft to use this ratio. Different tables are available for different B/T ratios. The vessel's prismatic coefficient, C_p , determines which group of data within the table is applicable, and the ratio of $D/(.01)(L)^3$ determines which horizontal row is appropriate for the vessel. With this information, the vessel's Residual Resistance/Ton can be determined for a given value of V/\sqrt{L} . For reasons discussed earlier, this study considers residual resistance to consist of wave-making resistance only; hence, values read directly from the table were interpreted to be R_w /Tons.

A vessel's wave-making resistance is sensitive to the effects of shallow water. (2) In shallow water, restricted passage for water flow around the hull brings about greater water velocities, greater pressure differences, and waves of greater height. At vessel

Table A.3. Residual Resistance per Ton (R_r , Δ), Taylor's Standard Series ($B/H = 2.25$) (4)

$V\sqrt{L}$	0.60	0.65	0.70	0.75	0.80	0.85	0.90	0.95	1.00	1.05	1.10	
1	$\Delta/(L/100)^3$											
0.50	50	0.41	0.50	0.69	0.85	1.10	1.20	1.40	1.65	2.00	3.15	5.25
	100	0.53	0.67	0.91	1.09	1.25	1.55	1.75	2.00	2.60	3.95	7.00
	150	0.62	0.78	0.99	1.20	1.40	1.80	2.20	2.55	3.30	4.90	8.40
	200	0.67	0.83	1.03	1.27	1.62	2.20	2.50	3.00	4.00	6.00	9.90
	250	0.71	0.86	1.07	1.29	1.96	2.30	2.90	3.60	4.90	7.50	13.00
0.60	50	0.49	0.62	0.83	1.22	1.61	2.05	2.70	3.80	5.40	6.20	6.80
	100	0.62	0.74	0.99	1.30	1.69	2.15	3.00	4.45	6.70	8.10	9.20
	150	0.68	0.83	1.05	1.34	1.71	2.20	3.20	4.85	7.60	9.00	10.60
	200	0.72	0.88	1.09	1.35	1.74	2.30	3.35	5.20	8.10	9.60	11.00
	250	0.74	0.92	1.12	1.36	1.79	2.48	3.60	5.60	8.50	10.00	11.50
0.70	50	0.80	1.02	1.32	1.83	2.34	3.35	4.70	7.30	11.50	14.30	15.00
	100	0.81	1.03	1.32	1.83	2.46	3.50	5.30	8.90	15.60	20.00	22.40
	150	0.81	1.03	1.33	1.83	2.46	3.50	5.45	9.75	17.80	24.00	28.20
	200	0.82	1.04	1.33	1.83	2.46	3.50	5.50	10.30	19.00	26.80	33.00
	250	0.83	1.06	1.34	1.83	2.50	3.65	5.50	10.60	20.00	28.90	35.70
0.80	50	1.00	1.27	2.00	3.52	6.70	9.30	10.30	13.20	19.30	25.50	28.00
	100	1.00	1.27	2.00	3.52	6.70	10.50	12.00	15.60	24.70	35.30	43.50
	150	1.00	1.27	2.00	3.52	6.70	10.90	12.50	16.80	26.70	40.20	52.50
	200	1.00	1.27	2.00	3.52	6.70	11.10	12.80	17.35	27.70	42.00	57.50
	250	1.00	1.27	2.00	3.52	6.70	11.30	13.20	17.60	28.30	41.50	58.50

Note:

R_r = residual resistance (lb.)

V = speed (knots)

Δ = displacement (tons (2,240 lb.))

L = length (ft.)

B = beam (ft.)

i = prismatic longitudinal coefficient (also known as C_p)

H = draft (ft.)

Table A.4. Residual Resistance per Ton (R_r , Δ), Taylor's Standard Series ($B/H = 3.75$) (4)

V/\sqrt{L}	0.60	0.65	0.70	0.75	0.80	0.85	0.90	0.95	1.00	1.05	1.10	
1	$\Delta/(L/100)^3$											
0.50	50	0.46	0.52	0.67	0.88	1.20	1.55	1.90	2.40	3.00	4.10	5.80
	100	0.72	0.93	1.16	1.46	1.85	2.40	2.90	3.45	4.30	5.70	8.50
	150	0.80	1.02	1.32	1.73	2.20	2.90	3.50	4.20	5.20	7.20	11.30
	200	0.86	1.05	1.38	1.81	2.30	3.20	3.80	4.45	5.70	8.20	13.10
	250	0.89	1.08	1.43	1.90	2.47	3.40	4.02	4.65	6.50	8.70	14.30
0.60	50	0.55	0.72	0.91	1.28	1.70	2.20	2.80	4.00	5.35	6.60	8.10
	100	0.73	0.92	1.21	1.52	1.85	2.50	3.40	4.85	7.10	9.15	11.10
	150	0.83	1.05	1.37	1.69	2.15	2.70	3.60	5.30	7.80	10.30	12.70
	200	0.88	1.13	1.48	1.88	2.30	2.85	3.80	5.50	8.00	10.80	13.70
	250	0.93	1.20	1.51	1.93	2.45	3.00	4.00	5.60	8.40	11.30	14.20
0.70	50	0.89	1.16	1.66	2.34	3.20	4.40	6.00	8.80	12.20	15.60	17.30
	100	1.00	1.35	1.81	2.52	3.30	4.60	6.60	9.80	15.70	21.20	25.20
	150	1.03	1.39	1.87	2.55	3.35	4.70	6.80	10.60	17.40	24.30	29.20
	200	1.05	1.40	1.86	2.50	3.35	4.65	6.80	10.70	17.50	-	-
	250	1.08	1.41	1.84	2.49	3.35	4.60	6.50	10.30	16.70	-	-
0.80	50	1.63	2.42	3.80	5.60	7.80	10.50	13.50	17.00	22.90	28.20	32.00
	100	1.55	2.35	3.51	5.20	7.75	11.40	15.30	20.30	28.00	37.30	45.00
	150	1.31	1.92	2.77	4.20	6.30	9.70	12.90	17.00	26.00	36.30	
	200	1.27	1.77	2.52	3.60	5.50	8.40	11.00	14.80	23.70		
	250	1.32	1.94	2.50	3.65	6.20	8.20	11.00	14.90	23.70		

Note:
 R_r = residual resistance (lb.) V = speed (knots)
 Δ = displacement (tons (2,240 lb.)) L = length (ft.)
 B = beam (ft.) l = prismatic longitudinal coefficient (also known as C_p)
 H = draft (ft.)

speeds higher than the critical speed (the speed of translation of a wave in the depth of water in question), the increase in shallow water resistance rapidly diminishes to zero, and the vessel may encounter less resistance in shallow water than in deep water. At moderate speeds an effective depth-speed relationship is calculated from the following equation:

$$V = 0.4 \sqrt{g \cdot h} \quad (7)$$

where V = critical vessel speed (knots)

h = depth of water (feet)

g = gravitational constant (ft/sec²)

For power and standardization trials, a location is usually selected wherein the depth of the water is greater than that computed from Equation 7. (1)

PROPULSION

In addition to vessel resistance, the influence of propulsion was also reviewed. Resistance to motion must be overcome by a propelling force. Propeller thrust is the force that overcomes the vessel's resistance. The power necessary to overcome the vessel's resistance is measured in terms of effective horsepower (EHP). EHP is calculated from the vessel's resistance according to the following equation:

$$EHP = R_t \cdot V / 550 \quad (8)$$

where EHP = effective horsepower

R_t = total resistance (lbs)

V = vessel velocity (ft/sec)

550 ft-lb/sec = 1 HP (constant)

Typically, a plot of EHP vs. speed is generated for a vessel in the course of designing that vessel. The curve is refined during the design process as the design itself is refined. A typical curve of EHP vs. speed for a large displacement ship is shown in Figure A.6. (1) Such a curve is then used in power calculations.

EHP varies with total resistance, and hence, with a ship's form. An example of how EHP is affected by changes in vessel parameters is shown in Figure A.7a. (2) The graphs in this figure indicate the variations in EHP for different values of V/\sqrt{L} , B/T , and C_p . The ship from which these curves were generated is similar in length and displacement to WSF Super Class ferries.

With EHP estimated, as from curves in either Figure A.6 or Figure A.7a, R_t can be calculated, and vessel velocity can be estimated from the vessel's resistance vs. speed/length curve. Hence, the EHP curves can be used as a tool to estimate the initial vessel velocity.

The shaft RPMs (which correspond to various throttle settings) for the WSF Super Class ferries that were used in this study are shown in the following table.

Table A.5 Shaft RPMs and Throttle Settings for WSF Super Class Ferries

Throttle Setting	Shaft RPM
Full Ahead	150 RPM
Half Ahead	100 RPM
Slow Ahead	50 RPM
Stop	0 RPM
Slow Astern	60 RPM
Half Astern	100 RPM
Full Astern	Maximum RPM

A graph of velocity vs. shaft RPM for the WSF Super Class MV *Yakima* is shown in Figure A.7b.

RUDDERS

The influence of the rudder and of the rudder-propeller interaction were also reviewed as part of this study. Ferry vessels must have good maneuverability, and as such, generally have larger rudders than do seagoing merchant vessels. (4) The rudder

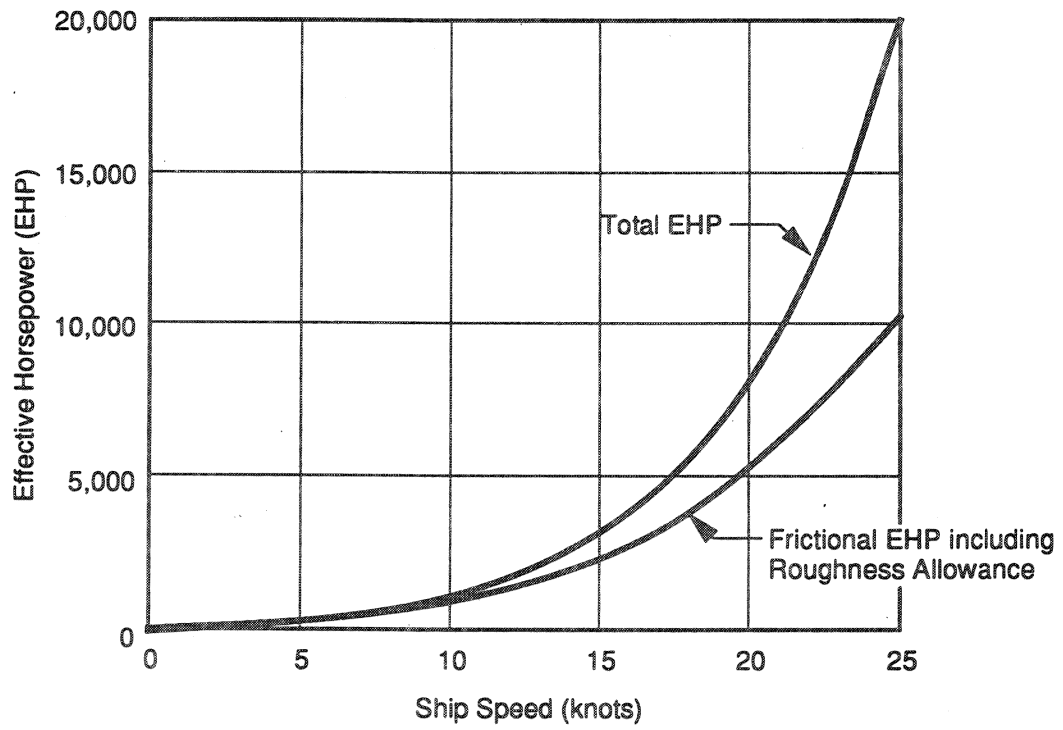


Figure A.6. Typical Curves of Frictional and Total Effective Horsepower vs. Speed for a Large Displacement Ship (1)

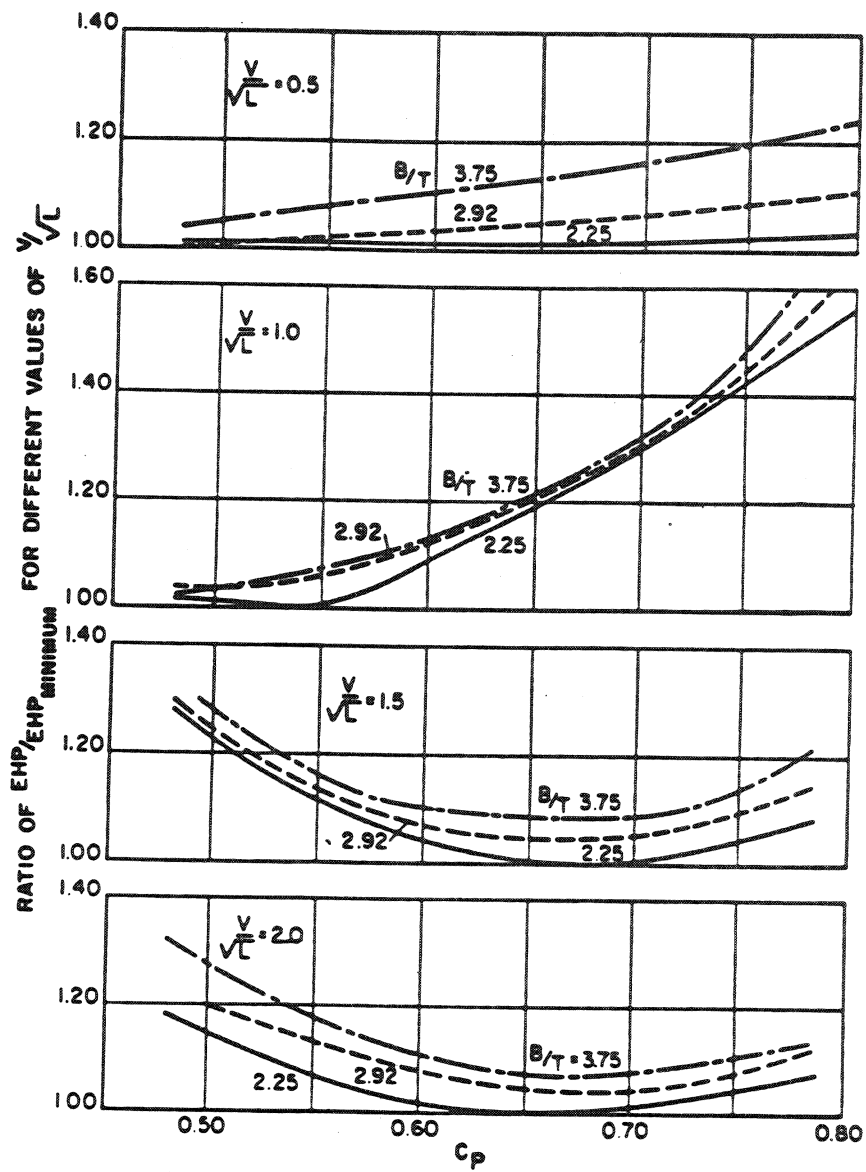


Figure A.7a. Variation in EHP with Change of C_p for a 400-ft Ship of 2743 Tons Displacement (2)

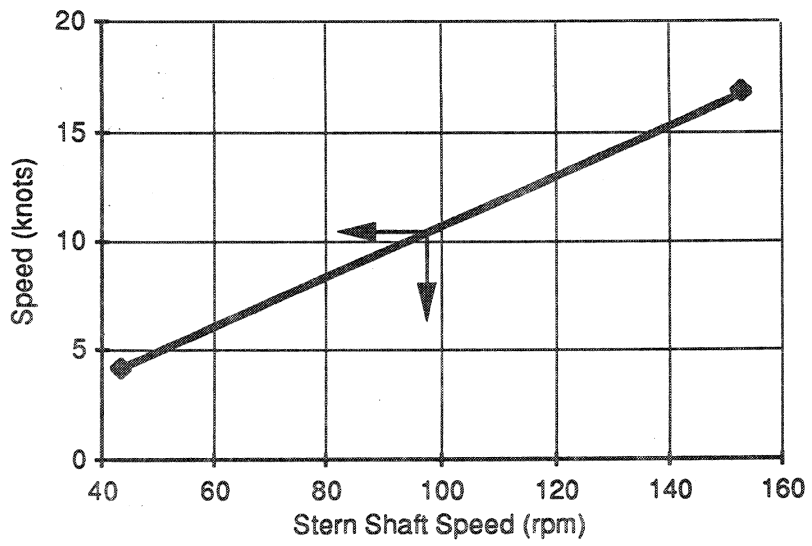


Figure A.7b. Example of Washington State Ferries Super Class Ferry Speed vs. Stern Shaft Speed (rpm) [Washington State Ferries]

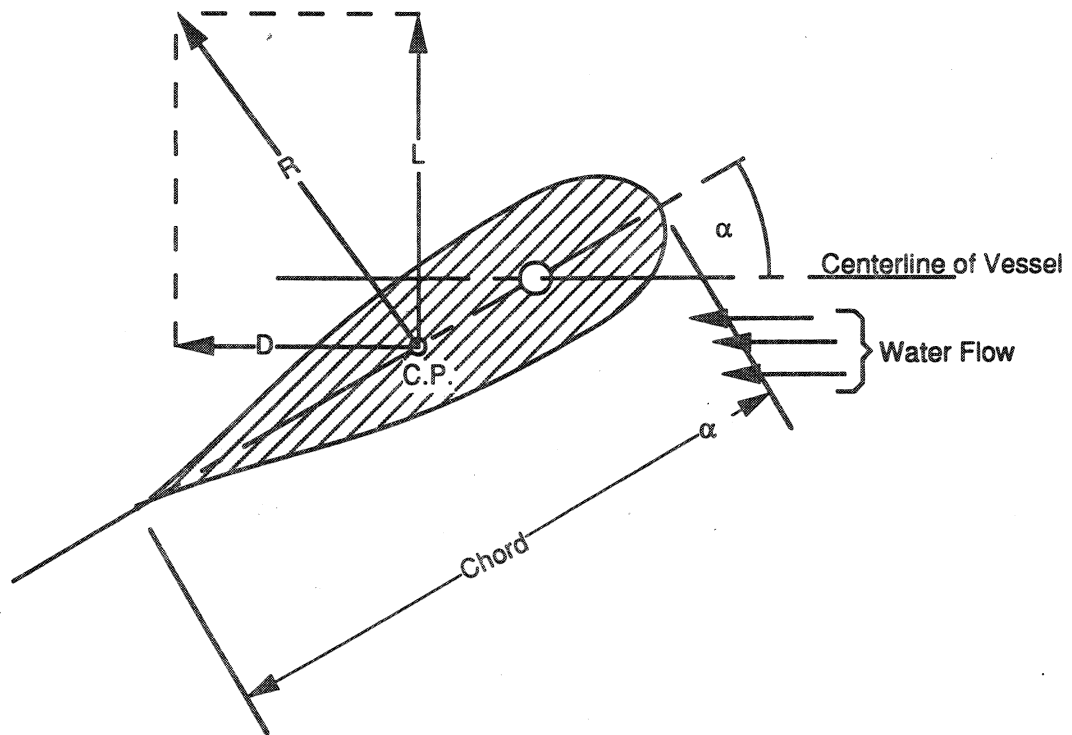
directly influences a vessel's maneuverability; rudder lift and drag forces are created when the rudder angle is changed.

Rudder lift force is the force that is perpendicular to the direction of motion. Rudder drag force is the force that is parallel to the direction of motion. Figure A.8 shows these forces acting on a rudder. These added forces cause the vessel to rotate; this rotation causes changes in the pressure distribution on the hull. A restoring force is generated as a result of the changes in the pressure distribution. When these forces reach equilibrium, the vessel is in a steady state. Figure A.9 shows and explains the motion of a turning vessel. (1) Rudders with a high aspect ratio (rudder height/rudder length) achieve large rudder angles prior to stalling and usually reach greater rudder forces than do low-aspect ratio rudders. Stall is defined as a certain critical rudder angle beyond which the rudder lift force decreases.

The rudder type and rudder attachment to the ship's structure further influence maneuverability. An all movable rudder is the most effective type of rudder. The simple, fully balanced rudder depicted in Figure A.10 is an example of an all movable rudder. The rudder stock, which is the circular, solid shaft from which an all movable rudder is hung, must withstand substantial bending moment and torque moment if the structural support at the bottom is omitted. (2) WSF Super Class ferries are equipped with all movable rudders with bottom support.

Another common type of rudder is the horn rudder, which has fixed and movable portions. The fixed portion of the rudder is referred to as the horn. This type of rudder generally produces a larger control force in the forward direction. (2) An example of a horn rudder is shown in Figure A.10. WSF Jumbo Class ferries are equipped with this type of rudder.

The three general types of rudders are unbalanced, balanced, and semi-balanced. The blade of an unbalanced rudder is entirely after the stock. In a balanced rudder, a portion of the rudder area is ahead of the stock. In a semi-balanced rudder, the area ahead



- α = angle of attack
- Chord = length of rudder
- D = drag force
- L = lift force
- R = total resultant force
- C.P. = center of pressure (point at which resultant forces act)

Figure A.8. Rudder Force Nomenclature (1)

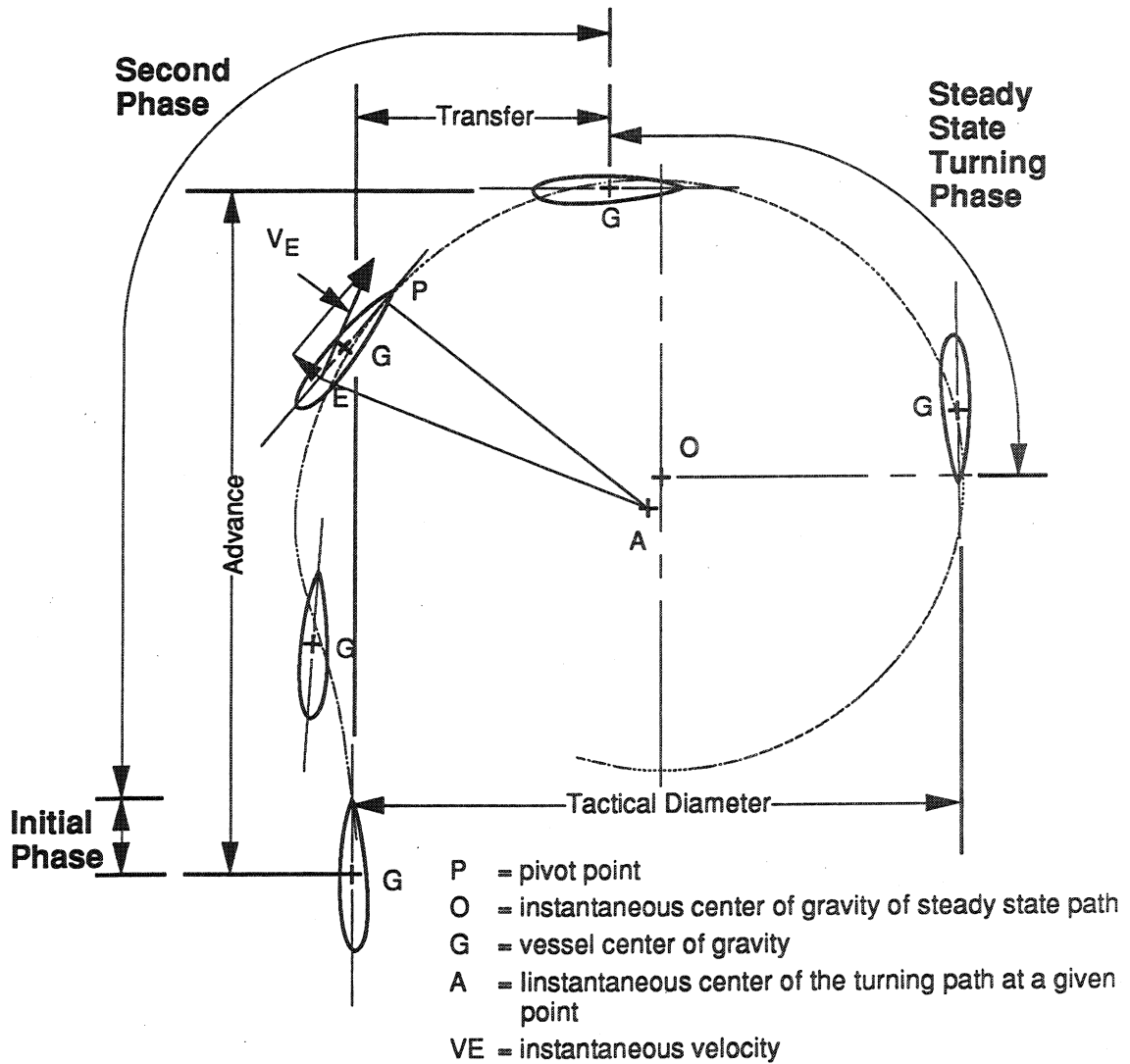


Figure A.9. Motion of Vessel in Turning (1)

Advance = Distance moved by the vessel center of gravity in the direction of the original course from the point where the rudder is started over until the heading has changed 90 degrees.

Transfer = Distance moved by the vessel center of gravity at right angles to the original course from the point where the rudder is started over until the heading has changed 90 degrees.

Tactical Diameter = Distance at right angles to the original course gained by the vessel center of gravity in turning 180 degrees.

Phases in a Turn

1. Initial Phase

Turn begins when rudder is put over, vessel accelerates in an outward drift, experiences a reduction in speed, and rotates about a vertical axis in the direction of the desired turn.

2. Second Phase

Pressure distribution on the hull changes to a pressure increase along the outward side of the vessel, creating a force (and couple) which accelerates the turning motion. This accounts for the S-shaped path during the first 90 degrees.

3. Steady State Turning Phase

Equilibrium of forces causes the vessel to settle on the circular portion of the turning path. The vessel continues to be slowed and accelerated toward the center of the turning circle until acceleration and turning radius are constant.

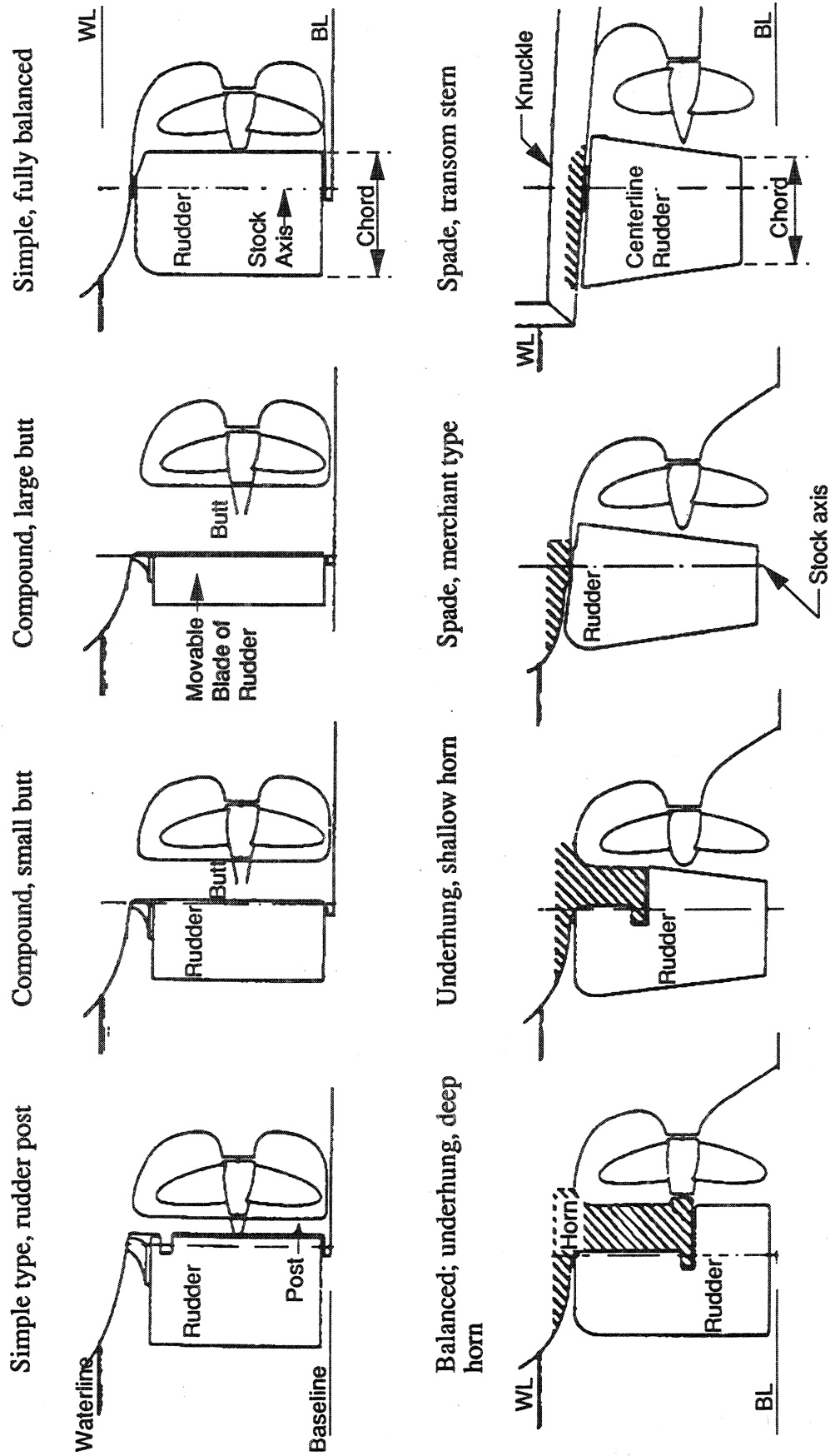


Figure A.10. Various Rudder-fin Combinations [from Transactions, Volume 91, 1993. The Society of Naval Architects and Marine Engineers. New York. 1984.]

of the stock does not extend to the full height of the blade aft of the stock. (1) Examples of each are provided in Figure A.10.

Secure attachment of the rudder to the ship structure improves the rudder's hydrodynamics and provides directional stability. However, turning resistance is increased if a large skeg is provided. A skeg is a foil-like section ahead of the rudder that is securely attached to the ship structure. A large area rudder enhances turning ability but also adds resistance. The fineness of vessel afterbody improves flow to the rudder and improves the rudder's effectiveness. However, the rudder profile should fit with dimensions dictated by the shape of the hull. The rudder should be placed in the propeller race, should have a clearance of at least one propeller radius between the propeller and the rudder. Additionally, the top of the rudder should be as far below the water surface as possible. (2)

Vessel resistance can be reduced by giving careful attention to the design of the rudder and the rudder post. The relative position of the rudders astern of the propeller, the number of propellers, and the depth below the keel line further affect the vessel's maneuverability and resistance. (2)

WSF ferries are equipped with rudders and propellers at each end. For a given direction of travel, the stern propeller pushes the vessel forward, and the stern rudder controls the vessel's heading. At the same time, the bow propeller windmills (rotates without producing thrust) to minimize drag, and the bow rudder is held at midships (the centerline of the ferry). When the ferry is in its final approach to the dock, this situation changes, and the bow propeller provides astern thrust to slow the ferry. The bow rudder can then be used to control the ferry's heading. With propeller wash against the bow rudder, the rudder angle can be set to move the bow of the ferry in the required direction. This enables ferry operators to control the ferry heading with bow and stern rudders.

FULL-SCALE MEASUREMENTS AND SEA TRIALS

Full-scale measurements are tests that are performed with actual vessels in actual sea conditions. The measurements are indicative of the ship's potential in terms of operation and performance. (5) Procedures for full-scale measurements are intended to provide the maximum amount of useful data with the least interference to vessel operations. (2)

In general, full-scale measurements are performed in deep water; however, ferries sometimes dock in shallow water. Vessel response differs considerably between deep and shallow water operations. Discussion of the effects of shallow water on vessel motion can be found in an earlier section of this report, and in References 2 and 5. There is relatively little documentation on vessel response in shallow water because tests are rarely performed in shallow water.

Maneuverability criteria for which full-scale measurements are desirable may be classified into three main categories: turning, maneuvering, and steering. The turning circle, with rudder hard over (maximum rudder angle), is a time-honored way of defining steady-state turning. The ability to initiate and check moderate changes in course is an important vessel characteristic; the well known zigzag maneuver demonstrates this ability. (5) Steering includes elusive characteristics of controllability and is not discussed further in this report.

Routine full-scale measurements are known as sea trials. Common tests and sea trials executed to measure vessel maneuverability are listed below:

- zigzag test
- turning test
- pull out from steady turn
- crash back test
- standardization trials

Zigzag Test

A zigzag (or "Z" maneuver) test consists of a series of predetermined turns in opposite directions. Both rudder position and heading changes are recorded during the test. The zigzag test provides quantitative measures of the rudder's inherent effectiveness in initiating and checking changes in course. In addition to measuring rudder position and corresponding heading changes, the zigzag test measures the velocity loss in a turn. (4) Examples of zigzag test results are shown in Figures A.11 and A.12.

Turning Circle Test

A turning circle test consists of the execution of a full circle at constant power and rudder hard over. The turning test provides quantitative measures of the rudder's effectiveness. Results from the turning test will also define quantities such as transfer and advance. A typical turning circle, complete with definition of transfer and advance, is depicted in Figure A.9.

Pull Out From a Steady Turn Test

A pull out from a steady turn test provides data to determine the rudder setting required to effectively check vessel swing from a steady turning condition. The test involves changing the rudder to an opposite position while the vessel is in a steady turn with constant power. (5)

Crash Back Test

A crash back test measures the total time and distance required for a vessel to stop from full ahead, with full astern power. This stopping distance is defined as headreach. The crash back test is also known as an emergency stop test because it provides quantitative measures of the vessel's ability to stop its forward progress in order to avoid collision or other emergencies. An example of results from a crash back test is given in Figure A.13. The crash back test is also known as a crash stop test.

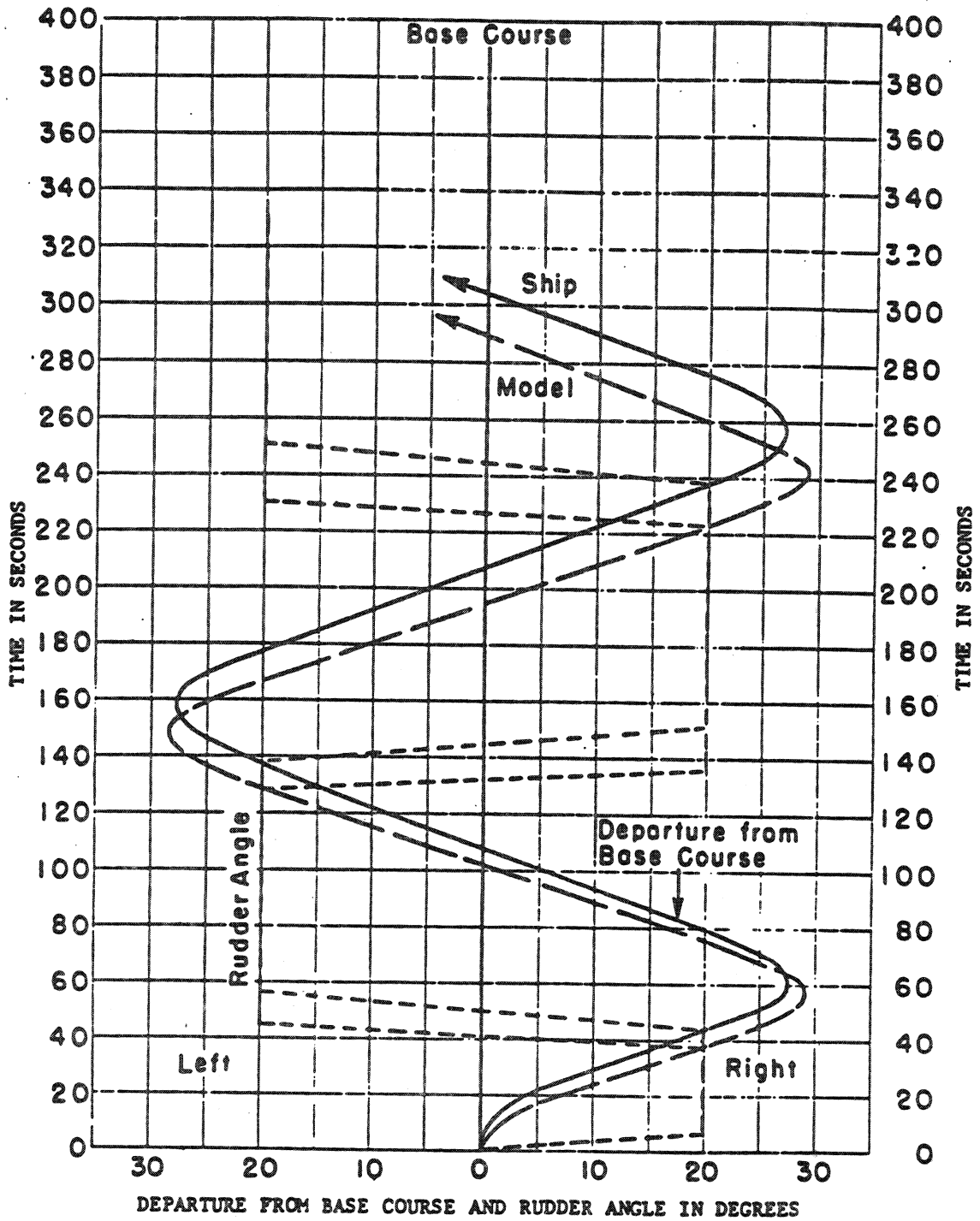


Figure A.11. Zigzag Maneuvers from Trials and Model Test of Single-Screw Ship (Vessel 1) (Approach speed of 15 knots and rudder angle of 20 degrees) (5)

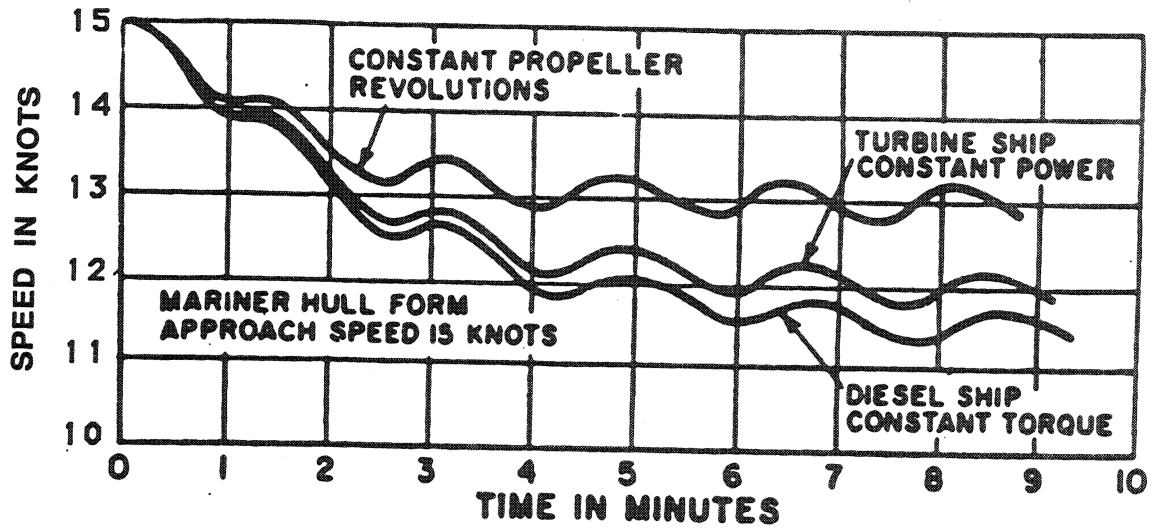


Figure A.12. Time History of Velocity in Zigzag Maneuver Computed for Different Types of Power Plants (2)

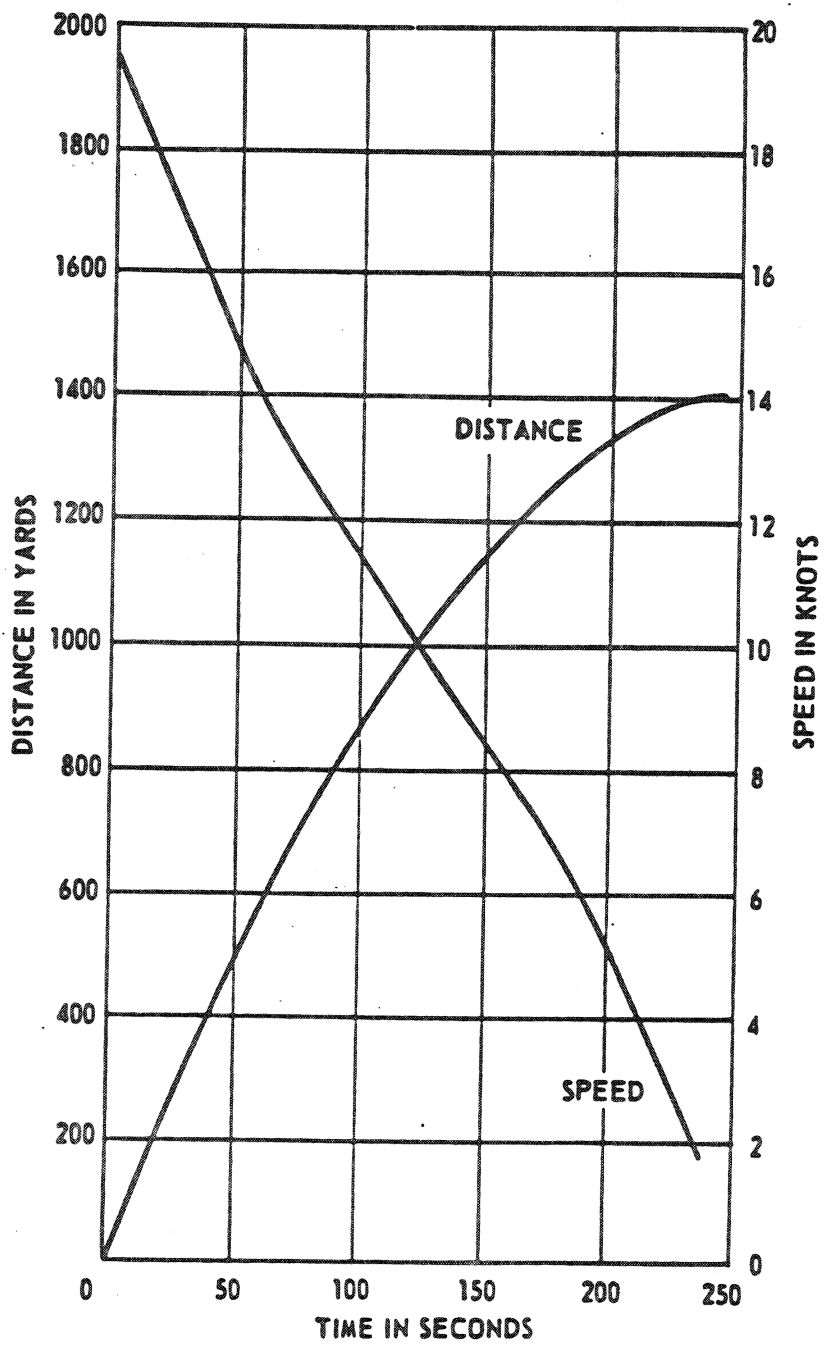


Figure A.13. Deceleration Run Using Full Power Astern (5)

Standardization Trials

Standardization trials (also known as speed trials) comprise a systematic series of runs over a measured distance designed to establish the relationship between speed and shaft RPM. The general plan for conducting standardization trials provides for several consecutive runs at each selected speed point, alternating direction over a constant power. Speeds, power values, and RPM are averaged for each speed point. (6)

REFERENCES

1. Gillmer, T.C. (1970). *Modern Ship Design*, United States Naval Institute, Annapolis MD.
2. Comstock, J.P. (ed.) (1967). *Principles of Naval Architecture*, Society of Naval Architects and Marine Engineers, New York, NY.
3. Lunde, J.K. (1953). *The Linearized Theory of Wave Resistance and Its Application to the Ship Shaped Bodies in Motion on the Surface of a Deep, Previously Undisturbed Fluid*, SNAME Technical and Research Bulletin No. 1-18, New York, NY.
4. Rossell, H.E. and Chapman, L.B. (ed.) (1942). *Principles of Naval Architecture*, Society of Naval Architects and Marine Engineers, New York, NY.
5. SNAME, (1966). "Notes on Ship Controllability," Technical and Research Bulletin No. 1-27.
6. SNAME, (1973). "Code for Sea Trials", Technical and Research Code, C-2.
7. Ishii, S. (1991). "Modifications to Ferry Landings to Accomodate Emergency Landings," Master's Thesis presented to the University of Washington, Seattle, WA.
8. Doeblner, J.K. (1990). "A Proposal for the Installation of Hoistable Upper Car Decks for Issaquah Class Ferries," Master's Thesis presented to the University of Washington, Seattle, WA.

APPENDIX B
TABLES OF KINEMATIC VISCOSITY AND DENSITY OF
FRESH AND SALT WATER

Table B-1. Values of Mass Density for Salt Water (Temperature in F°, ρ in English units of $\frac{\text{lbs sec}^2}{\text{ft}^4}$)

°F	ρ	°F	ρ	°F	ρ
32.	1.9947	51.	1.9923	70.	1.9876
33.	1.9946	52.	1.9921	71.	1.9873
34.	1.9946	53.	1.9919	72.	1.9870
35.	1.9945	54.	1.9917	73.	1.9867
36.	1.9944	55.	1.9916	74.	1.9864
37.	1.9943	56.	1.9912	75.	1.9861
38.	1.9942	57.	1.9910	76.	1.9858
39.	1.9941	58.	1.9908	77.	1.9856
40.	1.9940	59.	1.9905	78.	1.9851
41.	1.9939	60.	1.9903	79.	1.9848
42.	1.9937	61.	1.9901	80.	1.9846
43.	1.9936	62.	1.9898	81.	1.9841
44.	1.9934	63.	1.9895	82.	1.9837
45.	1.9933	64.	1.9893	83.	1.9834
46.	1.9931	65.	1.9890	84.	1.9830
47.	1.9930	66.	1.9888	85.	1.9827
48.	1.9928	67.	1.9885	86.	1.9823
49.	1.9926	68.	1.9882		
50.	1.9924	69.	1.9879		

Table B-2. Values of Mass Density for Salt Water (Temperature in C°, ρ in English units of $\frac{\text{lbs sec}^2}{\text{ft}^4}$)

°C	ρ	°C	ρ
0.	1.9947	16.	1.9901
1.	1.9946	17.	1.9896
2.	944	18.	1.9892
3.	943	19.	1.9887
4.	1.9941	20.	1.9882
5.	1.9939	21.	1.9877
6.	1.9936	22.	1.9871
7.	1.9934	23.	1.9866
8.	1.9931	24.	1.9860
9.	1.9928	25.	1.9854
10.	1.9924	26.	1.9849
11.	1.9921	27.	1.9842
12.	1.9918	28.	1.9836
13.	1.9913	29.	1.9829
14.	1.9910	30.	1.9823
15.	1.9905		

Table B-3. Values of Mass Density for Salt Water (Temperature in C°, ρ in metric units of $\frac{\text{kg sec}^2}{\text{m}^4}$)

°C	ρ	°C	ρ
0	104.83	16	104.59
1	104.82	17	104.56
2	104.81	18	104.54
3	104.81	19	104.52
4	104.80	20	104.49
5	104.79	21	104.46
6	104.77	22	104.43
7	104.76	23	104.40
8	104.74	24	104.37
9	104.73	25	104.34
10	104.71	26	104.31
11	104.69	27	104.28
12	104.68	28	104.24
13	104.65	29	104.21
14	104.61	30	104.18
15	104.61		

Table B-4. Values of Kinematic Viscosity for Salt Water (Temperature in F°, v in English units of $\frac{\text{ft}^2}{\text{sec}} \times 10^5$)

DEG. F	0.0	0.1	0.2	0.3	0.4	0.5	0.6	0.7	0.8	0.9
32.	1.96810	1.96667	1.96525	1.95726	1.95566	1.95505	1.96667	1.96290	1.95936	1.95580
33.	1.93276	1.92873	1.92520	1.92169	1.91819	1.91470	1.91122	1.90775	1.90429	1.90084
34.	1.89740	1.89398	1.89057	1.88718	1.88379	1.88041	1.87704	1.87368	1.87034	1.86700
35.	1.86367	1.86035	1.85705	1.85375	1.85046	1.84718	1.84391	1.84065	1.83741	1.83418
36.	1.83093	1.82771	1.82450	1.82129	1.81810	1.81492	1.81174	1.80858	1.80542	1.80227
37.	1.79916	1.79601	1.79289	1.78978	1.78667	1.78358	1.78050	1.77742	1.77436	1.77130
38.	1.78825	1.78521	1.78218	1.77916	1.77614	1.77314	1.77016	1.76715	1.76417	1.76120
39.	1.73826	1.73528	1.73234	1.72940	1.72647	1.72355	1.72063	1.71773	1.71483	1.71194
40.	1.70906	1.70619	1.70332	1.70047	1.69762	1.69478	1.69194	1.68912	1.68630	1.68349
41.	1.68069	1.67790	1.67512	1.67235	1.66959	1.66684	1.66409	1.66135	1.65861	1.65589
42.	1.65063	1.64776	1.64490	1.64206	1.63924	1.63643	1.63362	1.63082	1.62803	1.62524
43.	1.62631	1.62347	1.62064	1.61782	1.61500	1.61219	1.60939	1.60659	1.60380	1.60101
44.	1.60025	1.59747	1.59470	1.59194	1.58918	1.58643	1.58368	1.58093	1.57818	1.57543
45.	1.57079	1.56799	1.56520	1.56243	1.55967	1.55691	1.55416	1.55141	1.54866	1.54591
46.	1.55007	1.54726	1.54446	1.54167	1.53888	1.53609	1.53330	1.53051	1.52772	1.52493
47.	1.52591	1.52311	1.52032	1.51753	1.51474	1.51195	1.50916	1.50637	1.50358	1.50079
48.	1.50244	1.50012	1.49780	1.49548	1.49316	1.49084	1.48852	1.48620	1.48388	1.48156
49.	1.47956	1.47730	1.47505	1.47280	1.47055	1.46830	1.46605	1.46380	1.46155	1.45930
50.	1.45724	1.45504	1.45283	1.45062	1.44841	1.44620	1.44399	1.44178	1.43957	1.43736
51.	1.43541	1.43326	1.43111	1.42899	1.42685	1.42473	1.42261	1.42049	1.41838	1.41626
52.	1.41618	1.41208	1.40997	1.40791	1.40585	1.40375	1.40169	1.39962	1.39756	1.39551
53.	1.39346	1.39141	1.38937	1.38734	1.38531	1.38328	1.38126	1.37925	1.37724	1.37523
54.	1.37323	1.37124	1.36926	1.36728	1.36530	1.36333	1.36137	1.35941	1.35745	1.35550
55.	1.35355	1.35160	1.34966	1.34772	1.34578	1.34385	1.34192	1.34000	1.33808	1.33617
56.	1.33426	1.33232	1.33038	1.32845	1.32652	1.32459	1.32267	1.32075	1.31883	1.31691
57.	1.31542	1.31356	1.31170	1.30985	1.30801	1.30616	1.30432	1.30249	1.30066	1.29883
58.	1.29701	1.29520	1.29339	1.29159	1.28979	1.28800	1.28621	1.28442	1.28264	1.28086
59.	1.27938	1.27751	1.27565	1.27379	1.27200	1.27024	1.26848	1.26673	1.26498	1.26323
60.	1.26150	1.25976	1.25802	1.25628	1.25457	1.25285	1.25113	1.24942	1.24771	1.24600
61.	1.24430	1.24261	1.24092	1.23923	1.23755	1.23587	1.23420	1.23253	1.23086	1.22920
62.	1.22754	1.22589	1.22424	1.22259	1.22094	1.21930	1.21767	1.21603	1.21440	1.21278
63.	1.21115	1.20953	1.20791	1.20629	1.20467	1.20306	1.20146	1.19985	1.19825	1.19665
64.	1.19506	1.19348	1.19189	1.19032	1.18874	1.18717	1.18561	1.18404	1.18248	1.18092
65.	1.17937	1.17781	1.17624	1.17471	1.17316	1.17162	1.17008	1.16855	1.16701	1.16548
66.	1.16396	1.16244	1.16092	1.15940	1.15790	1.15640	1.15490	1.15340	1.15191	1.15041
67.	1.14892	1.14744	1.14596	1.14448	1.14300	1.14153	1.14006	1.13859	1.13713	1.13566
68.	1.13421	1.13275	1.13130	1.12985	1.12840	1.12696	1.12552	1.12409	1.12265	1.12122
69.	1.11979	1.11837	1.11695	1.11553	1.11411	1.11270	1.11129	1.10988	1.10848	1.10708
70.	1.10568	1.10428	1.10289	1.10150	1.10011	1.09873	1.09735	1.09597	1.09459	1.09322
71.	1.09185	1.09048	1.08912	1.08775	1.08639	1.08504	1.08368	1.08233	1.08098	1.07964
72.	1.07830	1.07696	1.07562	1.07428	1.07295	1.07162	1.07030	1.06897	1.06765	1.06633
73.	1.06502	1.06370	1.06239	1.06109	1.05978	1.05848	1.05718	1.05588	1.05458	1.05329
74.	1.05200	1.05071	1.04943	1.04815	1.04687	1.04559	1.04432	1.04304	1.04177	1.04051
75.	1.03924	1.03798	1.03672	1.03546	1.03421	1.03296	1.03171	1.03046	1.02922	1.02797
76.	1.02673	1.02550	1.02427	1.02304	1.02182	1.02060	1.01937	1.01816	1.01694	1.01573
77.	1.01452	1.01330	1.01209	1.01088	1.00968	1.00847	1.00727	1.00607	1.00487	1.00368
78.	1.00248	1.00129	1.00011	0.99892	0.99774	0.99655	0.99538	0.99420	0.99302	0.99185
79.	0.99069	0.98952	0.98836	0.98720	0.98604	0.98489	0.98374	0.98259	0.98144	0.98029
80.	0.97915	0.97801	0.97686	0.97572	0.97458	0.97344	0.97231	0.97118	0.97004	0.96892
81.	0.96779	0.96667	0.96555	0.96444	0.96332	0.96221	0.96110	0.96000	0.95889	0.95779
82.	0.95669	0.95558	0.95448	0.95338	0.95228	0.95119	0.95009	0.94900	0.94791	0.94683
83.	0.94574	0.94466	0.94359	0.94251	0.94144	0.94037	0.93930	0.93823	0.93717	0.93611
84.	0.93504	0.93398	0.93292	0.93186	0.93080	0.92975	0.92869	0.92764	0.92659	0.92554
85.	0.92450	0.92346	0.92242	0.92138	0.92035	0.91932	0.91829	0.91726	0.91623	0.91521
86.	0.91418	0.91316	0.91213	0.91111	0.91009	0.90907	0.90806	0.90704	0.90603	0.90502

APPENDIX C
FRICTIONAL RESISTANCE AND REYNOLDS NUMBER
SAMPLE CALCULATIONS

This appendix provides sample calculations for the frictional resistance of a WSF Super Class ferry. These calculations are based on Equations 1, 2, and 3. The Reynolds Number is calculated from vessel length and velocity, and from the kinematic viscosity of sea water. The frictional resistance coefficient is computed from the Reynolds Number. Frictional resistance is then calculated from Equation 3, which includes standard parameters such as vessel wetted surface, vessel velocity, and sea water density in addition to the frictional resistance coefficient. Frictional resistance is divided by vessel weight displacement to compute $R_f/Tons$. An initial velocity of 17 knots was used because this value represents the maximum velocity of a Super Class Ferry.

where

$$R = (V)(L)/\nu \quad (1)$$

R = Reynolds Number
V = vessel velocity
L = vessel length
 ν = kinematic viscosity

where

$$C_f = 0.075/(\log(R) - 2)^2 \quad (2)$$

C_f = frictional resistance coefficient
R = Reynolds Number

where

$$R_f = C_f (\rho/2) (S) (V^2) \quad (3)$$

R_f = frictional resistance
 C_f = frictional resistance coefficient
 ρ = density
S = vessel wetted surface

SAMPLE CALCULATIONS — FRICTIONAL RESISTANCE FOR SUPER CLASS FERRIES

1) Reynolds Number

$$R = V * L / \nu$$

R	=	Reynolds Number	variable	
V	=	vessel velocity	variable	ft/sec
L	=	vessel length	fixed	ft
ν	=	kinematic viscosity	fixed	ft ² /sec

Calculate R for V=17 knots

$$17 \text{ knots} = 28.71 \text{ fps}$$

$$R = 28.71 * 382.25 / 1.279 \times 10^{-5}$$

$$R = 8.59E + 08$$

2) Frictional Resistance Coefficient

$$C_f = 0.075 / (\log R - 2)^2$$

C_f	=	frictional resistance coefficient	variable
-------	---	-----------------------------------	----------

Calculate C_f for R=8.59E+08

$$C_f = 0.075 / (\text{LOG}(859000000) - 2)^2$$

$$C_f = 0.00156$$

3) Frictional Resistance

$$R_f = C_f * 0.5 * \rho * S * V^2$$

R_f	=	frictional resistance	variable	lbs
C_f	=	frictional resistance coefficient	variable	
ρ	=	density of sea water	fixed	lbs*sec ² /ft ⁴
S	=	vessel wetted surface	fixed	ft ²
V	=	vessel velocity	variable	ft/sec

Calculate R_f for $C_f=0.00156$, $V=28.71$ ft/sec

$$R_f = 0.00156 * 0.5 * 1.9905 * 18706 * 28.71^2$$

$$R_f = 23939 \text{ lbs}$$

4) Resistance/Tons

$$= R_f/\text{Tons}$$

$$\begin{aligned} R_f &= \text{frictional resistance} \\ \text{Tons} &= \text{vessel displacement} \end{aligned}$$

variable lbs
fixed tons

Calculate R_f/Tons for $R_f = 23939$ lbs

$$R_f/\text{Tons} = 23938.89/3283$$

$$R_f/\text{Tons} = 7.3$$

5) Velocity/ $\sqrt{\text{Length}}$

$$= V/\sqrt{L}$$

$$\begin{aligned} V &= \text{vessel velocity} \\ L &= \text{vessel length} \end{aligned}$$

variable ft/sec
fixed ft

Calculate V/\sqrt{L} for $V=17$ knots

$$V/\sqrt{L} = 17/\sqrt{382.25}$$

$$V/\sqrt{L} = 0.87$$

The fixed values used in the above calculations are from Table C.1, below.

Table C.1 Vessel Data for WSF Super Class Ferries

Description	Value	Source
Length L	382.25 ft	WSF Brochure
Volumetric Displacement D	114905 ft ³ of sea water	Calculated from Equation 1 (App.A)
Weight Displacement W	3283 tons	Reference (1)
Mass W/g	228382.6 lb/ft/sec ²	Calculated
Prismatic Coefficient C _p	0.5409	Reference (2)
Block Coefficient C _b	0.3439	Reference (2)
Beam B	73.2 ft	WSF Brochure
Waterline Beam B	53.0 ft	Estimated
Draft T	17.25 feet	WSF Brochure
Wetted Surface S	18706 ft ²	Approximated from Equation 2 (App. A)
Density of sea water ρ	1.9905 lb sec ² /ft ⁴	Appendix B
Kinematic Viscosity of sea water ν	1.279x10 ⁻⁵ ft ² /sec	Appendix B
Gravitational Constant g	32.2 ft/sec ²	Constant

REFERENCES

1. Ishii, S. (1991). "Modifications to Ferry Landings to Accomodate Emergency Landings," Master's Thesis presented to the University of Washington, Seattle, WA.
2. Doebler, J.K. (1990). "A Proposal for the Installation of Hoistable Upper Car Decks for Issaquah Class Ferries," Master's Thesis presented to the University of Washington, Seattle, WA.

APPENDIX D
WAVE-MAKING RESISTANCE SAMPLE CALCULATIONS

This appendix provides sample calculations for estimating values of beam/draft, displacement/length, and prismatic coefficient. These parameters are necessary in order to estimate wave-making resistance from tables. The beam/draft and displacement/length ratios are computed from basic vessel parameters. The prismatic coefficient is a basic vessel parameter. Once these values are known, then $R_w/Tons$ can be estimated directly from the tables.

SAMPLE CALCULATIONS — WAVE-MAKING RESISTANCE FOR SUPER CLASS FERRIES

1) **Beam/Draft Ratio**

$$= B/T$$

where B = vessel beam fixed ft
 T = vessel draft fixed ft

Calculate B/T for *Yakima*

$$\begin{aligned} B/T &= \frac{53.0}{17.25} \\ B/T &= 3.07 \end{aligned}$$

2) **Displacement/Length Ratio**

$$= \frac{D}{\sqrt[3]{(0.01)(L)}}$$

where D = vessel displacement fixed tons
 L = vessel length fixed ft

Calculate $\frac{D}{\sqrt[3]{(0.01)(L)}}$ for *Yakima*

$$\frac{D}{\sqrt[3]{(0.01)(L)}} = \frac{3283}{\sqrt[3]{(0.01)(382.25)}}$$

$$\frac{D}{\sqrt[3]{(0.01)(L)}} = 58.9$$

3) Prismatic Coefficient

$$= C_p$$

$$C_p = \text{vessel prismatic coefficient} \quad \text{fixed}$$

$$C_p = 0.5409$$

The fixed values used in the calculations above are from Table D.1.

Table D.1 Vessel Data for WSF Super Class Ferries

Description	Value	Source
Length L	382.25 ft	WSF Brochure
Volumetric Displacement D	114905 ft ³ of sea water	Calculated from Equation 1 (App. A)
Weight Displacement W	3283 tons	Reference (1)
Mass W/g	228382.6 lb/ft ³	Calculated
Prismatic Coefficient C _p	0.5409	Reference (2)
Block Coefficient C _b	0.3439	Reference (2)
Beam B	73.2 ft	WSF Brochure
Waterline Beam B	53.0 ft	Estimated
Draft T	17.25 feet	WSF Brochure
Wetted Surface S	18706 ft ²	Approximated from Equation 2 (App. A)
Density of sea water ρ	1.9905 lb sec ² /ft ⁴	Appendix B
Kinematic Viscosity of sea water ν	1.279x10 ⁻⁵ ft ² /sec	Appendix B
Gravitational Constant g	32.2 ft/sec ²	Constant

REFERENCES

1. Ishii, S. (1991). "Modifications to Ferry Landings to Accomodate Emergency Landings," Master's Thesis presented to the University of Washington, Seattle, WA.
2. Doebler, J.K. (1990). "A Proposal for the Installation of Hoistable Upper Car Decks for Issaquah Class Ferries," Master's Thesis presented to the University of Washington, Seattle, WA.

APPENDIX E

**DANISH MARITIME INSTITUTE
EXAMPLE COMPUTER SIMULATION PLOT**

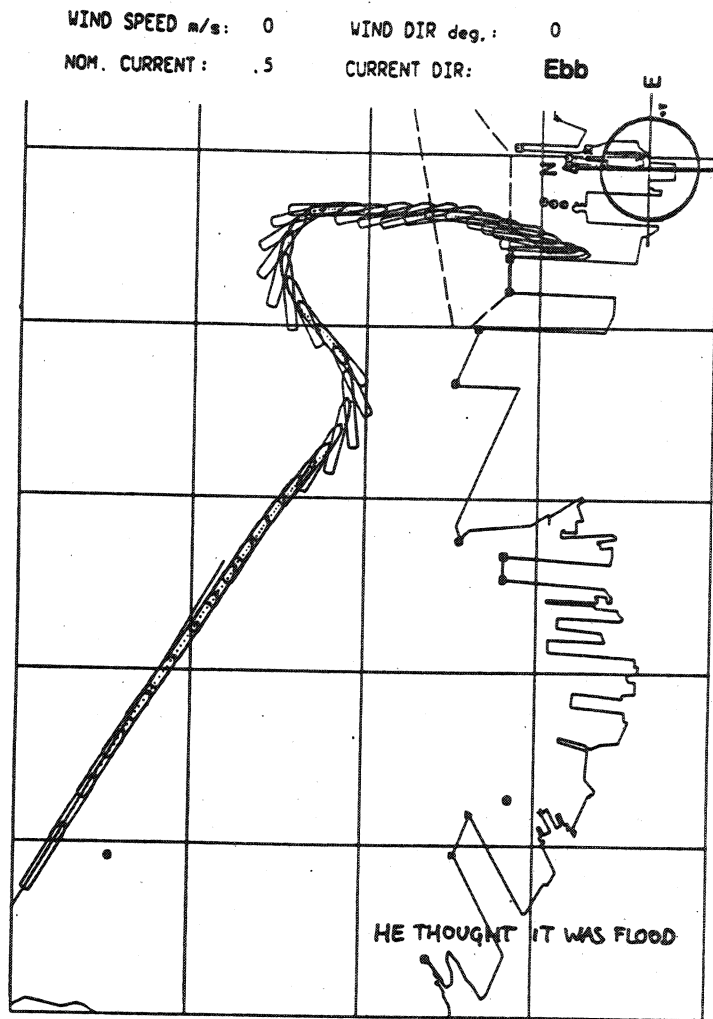


Figure E-1. Simulator Maneuver in Changing Currents (Danish Maritime Institute (1987). *Wind, Sea, Men and Ships — Integrated Maritime Solutions*, Copenhagen, Denmark.)

APPENDIX F
R/TONS AND V/\sqrt{L} CALCULATIONS

The calculations presented in this appendix are representative of those required to compute $R_f/Tons$ for a WSF Super Class ferry travelling at various speeds. The calculations for $R_f/Tons$ are based on Equations 1, 2, and 3. The $R_w/Tons$ values constitute a summary of Table F.1.

where $R = (V)(L)/\nu$ (1)

R = Reynolds Number
 V = vessel velocity
 L = vessel length
 ν = kinematic viscosity

where $C_f = 0.075/(\log(R) - 2)^2$ (2)

C_f = frictional resistance coefficient
 R = Reynolds Number

where $R_f = C_f (\rho/2) (S) (V^2)$ (3)

R_f = frictional resistance
 C_f = frictional resistance coefficient
 ρ = density
 S = vessel wetted surface

Table F.1. Residual Resistance per Ton (R_r , Δ), Taylor's Standard Series ($B/H = 3.75$) (4)

V/\sqrt{L}	0.60	0.65	0.70	0.75	0.80	0.85	0.90	0.95	1.00	1.05	1.10	
1	$\Delta/(L/100)^3$											
0.50	50	0.46	0.52	0.67	0.88	1.20	1.55	1.90	2.40	3.00	4.10	5.80
	100	0.72	0.93	1.16	1.46	1.85	2.40	2.90	3.45	4.30	5.70	8.50
	150	0.80	1.02	1.32	1.73	2.20	2.90	3.50	4.20	5.20	7.20	11.30
	200	0.86	1.05	1.38	1.81	2.30	3.20	3.80	4.45	5.70	8.20	13.10
	250	0.89	1.08	1.43	1.90	2.47	3.40	4.02	4.65	6.50	8.70	14.30
0.60	50	0.55	0.72	0.91	1.28	1.70	2.20	2.80	4.00	5.35	6.60	8.10
	100	0.73	0.92	1.21	1.52	1.85	2.50	3.40	4.85	7.10	9.15	11.10
	150	0.83	1.05	1.37	1.69	2.15	2.70	3.60	5.30	7.80	10.30	12.70
	200	0.88	1.13	1.48	1.88	2.30	2.85	3.80	5.50	8.00	10.80	13.70
	250	0.93	1.20	1.51	1.93	2.45	3.00	4.00	5.60	8.40	11.30	14.20
0.70	50	0.89	1.16	1.66	2.34	3.20	4.40	6.00	8.80	12.20	15.60	17.30
	100	1.00	1.35	1.81	2.52	3.30	4.60	6.60	9.80	15.70	21.20	25.20
	150	1.03	1.39	1.87	2.55	3.35	4.70	6.80	10.60	17.40	24.30	29.20
	200	1.05	1.40	1.86	2.50	3.35	4.65	6.80	10.70	17.50	-	-
	250	1.08	1.41	1.84	2.49	3.35	4.60	6.50	10.30	16.70	-	-
0.80	50	1.63	2.42	3.80	5.60	7.80	10.50	13.50	17.00	22.90	28.20	32.00
	100	1.55	2.35	3.51	5.20	7.75	11.40	15.30	20.30	28.00	37.30	45.00
	150	1.31	1.92	2.77	4.20	6.30	9.70	12.90	17.00	26.00	36.30	
	200	1.27	1.77	2.52	3.60	5.50	8.40	11.00	14.80	23.70		
	250	1.32	1.94	2.50	3.65	6.20	8.20	11.00	14.90	23.70		

Note: R_r = residual resistance (lb.) V = speed (knots)

Δ = displacement (tons (2,240 lb.)) L = length (ft.)

B = beam (ft.) l = prismatic longitudinal coefficient (also known as C_p)

H = draft (ft.)

Table F-2. Resistance Data

Length 382.25 ft
 Displ. 130321 ft³
 Displ. 3283 tons
 Wet Surf 18706 ft²
 Viscosity 1.28E-05 ft²/sec
 Density 1.9905 lb sec²/ft⁴
 Gravity 32.2 ft/sec²

Velocity fps	Velocity knots	Reynolds No.	C _f	R _f	R _f /Tons	V/√L knots	R _w /Displ	V/√L knots
37.0	21.9	1.11E+09	0.00150	38,528	11.7	1.1	0.5	0.6
32.0	19.0	9.56E+08	0.00154	29,342	8.9	1.0	0.5	0.7
27.0	16.0	8.07E+08	0.00157	21,337	6.5	0.8	0.7	0.7
22.0	13.0	6.58E+08	0.00161	14,538	4.4	0.7	0.9	0.8
15.5	9.2	9.26E+08	0.00155	6,911	2.1	0.5	1.2	0.8
12.0	7.1	3.59E+08	0.00175	4,680	1.4	0.4	1.6	0.9
17.8	10.5	5.32E+08	0.00166	9,779	3.0	0.5	1.9	0.9
12.7	7.5	3.80E+08	0.00173	5,203	1.6	0.4	2.4	1.0
8.8	5.2	2.63E+08	0.00182	2,623	0.8	0.3	3.0	1.0
1.3	0.8	3.89E+07	0.00240	76	0.0	0.0	4.1	1.1
2.5	1.5	7.47E+07	0.00217	253	0.1	0.1	5.8	1.1
3.8	2.3	1.14E+08	0.00205	550	0.2	0.1	0.0	0.0
1.3	0.8	3.89E+07	0.00240	76	0.0	0.0		

APPENDIX G

UNIVERSITY OF MICHIGAN MODEL TESTS

(Snyder, E.D. (1971). Resistance, Propulsion, and Wake Survey Tests for Two Cross Sound Ferry Boats, the University of Michigan, College of Engineering, Department of Naval Architecture and Marine Engineering, Ship Hydrodynamics Laboratory, Office of Research Administration. Ann Arbor, Michigan.)

THE UNIVERSITY OF MICHIGAN

COLLEGE OF ENGINEERING

Department of Naval Architecture and Marine Engineering
Ship Hydrodynamics Laboratory



RESISTANCE, PROPULSION, AND WAKE SURVEY TESTS
FOR TWO CROSS-SOUND FERRY BOATS

by

Eric D. Snyder

Project Director: Finn C. Michelsen

for

Philip F. Spaulding and Associates, Inc.
65 Marion Street
Seattle, Washington 98104

Administered through

October 1971

OFFICE OF RESEARCH ADMINISTRATION ANN ARBOR

THE UNIVERSITY OF MICHIGAN
COLLEGE OF ENGINEERING
Department of Naval Architecture and Marine Engineering
Ship Hydrodynamics Laboratory

RESISTANCE, PROPULSION, AND WAKE SURVEY TESTS
FOR TWO CROSS-SOUND FERRY BOATS

by
Eric D. Snyder
Project Director: Finn C. Michelsen

for
Philip F. Spaulding and Associates, Inc.
65 Marion Street
Seattle, Washington 98104

Administered through
Office of Research Administration

October 1971
Ann Arbor

Under authorization from the sponsor, a series of tests was conducted for two design alternatives of a cross-sound ferry boat. A model of each design alternative was constructed of sugar pine to a linear scale ratio of 1:23.430. The first design (UM model 1219) has a length of 440'-0" over all and the model was constructed to the lines shown on Philip F. Spaulding and Assoc., Inc. drawing no. 7048-01-6. The second design (UM model 1221) has a length of 384'-0" over all and the model was constructed to the lines shown on Philip F. Spaulding and Assoc., Inc. drawing no. 7048-01-6, alternative. Model and ship geometric characteristics are given in Tables 1 and 2 for UM models 1219 and 1221, respectively.

As indicated by the sponsor, the 440'-0" design was the primary alternative. Therefore UM model 1219 received more extensive testing than did UM model 1221. The tests conducted with UM model 1219 included resistance and self-propulsion at the design draft of 17'-0"; wake survey at the design speed of 20.5 knots; and an analysis of the vibratory forces and moments induced by the propeller on the stern bearing.

The 384'-0" design alternative (UM model 1221) is intended for possible latter jumboization to a length of 440'-0" by inserting 56'-0" of parallel midbody. Only resistance tests at the 17'-0" design draft were conducted on UM model 1221. However, the model was tested both with and without the parallel midbody.

RESISTANCE AND SELF-PROPULSION TESTS

Resistance and self-propulsion tests were conducted on the models of the two design alternatives for the purpose of determining the resistance properties of the two alternatives and to predict the power requirements of the primary alternative (UM model 1219). Toward this end the following resistance tests were conducted at the 17'-0" design draft over a speed range of 13 knots to 23 knots full scale.

1. UM model 1219
2. UM model 1221
3. UM model 1221 with parallel midbody

A self-propulsion test using a stock model propeller was conducted with UM model 1219 at the 17'-0" design draft over a speed range of 13 knots to 23 knots full scale. The model test conditions with their corresponding full scale values are given in Table 3.

For the resistance tests the models were fitted with rudder, shafting, and a dummy hub in place of the propeller, both at the bow and the stern. For the self-propulsion test a free wheeling model propeller was placed at the bow.

It was felt that the effect of the free wheeling bow propeller was negligible on the resistance. However, in analyzing the results of the self-propulsion test, abnormally high values of thrust deduction were observed. The resistance of the models was then remeasured with a free wheeling bow propeller. The

effect upon resistance was significant. It is felt that the free wheeling bow propeller has enough effect upon the flow around the model to alter the resistance. When the results of the self-propulsion test was re-analyzed using the with-bow-propeller data, the thrust deduction obtained was reasonable.

The results of the resistance tests are presented in Figures 1 through 4. Figures 1 and 2 show the full scale effective horsepower versus speed in knots for UM models 1219 and 1221, respectively. The results of both the tests without the bow propeller and with the bow propeller are presented. Figure 3 shows the total resistance per ton of displacement versus speed-length ratio for the two models without the bow propeller. Figure 4 shows the residuary resistance per ton of displacement versus speed-length ratio for the two models without the bow propeller. All model resistance test data was extrapolated to full scale using the 1957 ITTC friction coefficients with a correlation allowance of 0.0002.

The results of the self-propulsion test are presented on Figures 5 and 6 as curves of full scale power, revolutions per minute, efficiency, wake, and thrust deduction versus speed in knots. The geometric characteristics of the stock model propellers used for the self-propulsion tests and their corresponding full scale values are given in Table 4. Figure 7 shows the open water characteristics of UM propeller 12 which was used for the self-propulsion test. The model test was conducted in

accordance with standard procedure and the results were extrapolated to full size using the thrust identity.

NOMINAL WAKE SURVEY

On the primary design alternative (UM model 1219) the nominal wake was measured in the plane of the propeller. Two separate methods were used. First the wake was measured by means of wake wheels which gave an average wake within a ring of the propeller disk. By this method the average wake as a function of radius is determined. The nominal wake was also measured by means of a 5-hole pitot tube survey which gave a three-dimensional wake for each point in the propeller disk. Both wake surveys were conducted at the design speed of 20.5 knots.

The results of the wake wheel survey are presented in Figure 8 as a curve of Taylor's wake fraction versus the non-dimensional radius. The radial distribution of wake as found from this test was used to design a wake adapted propeller for the subject vessel.

The results of the 5-hole pitot tube wake survey are presented in Figures 9 and 10. Figure 9 shows the transverse wake distribution in the propeller disk. The transverse wake is the vector summation of the tangential and radial components of the wake. Figure 10 shows contours of constant axial wake over the propeller disk. The results of the 5-hole pitot tube wake survey

were used to analysis the vibratory forces and moments induced by the propeller upon the stern bearings.

VIBRATION ANALYSIS

An analysis of the vibratory exciting forces and moments induced by the propeller upon the stern bearing was made for the primary design alternative (UM model 1219). The propeller used in this analysis was designed under consultation with Professor Michelsen of the University of Michigan. The geometric characteristics of the propeller are given in Table 5.

The vibrations analysis was made using an unsteady lifting surface theory and the results are given in Table 6.

TABLE 1

Model and Ship Geometric Characteristics

Sponsor: Philip F. Spaulding & Assoc., Inc.
 Ship type: Cross-Sound Ferry
 UM model no.: 1219
 Scale ratio: $\lambda = 23.430$

	<u>Model</u>	<u>Ship</u>
LOA	18.779 ft	440'-0"
LBP	17.840 ft	418'-0"
B, maximum	3.713 ft	87'-0"
B, @ DWL	2.689 ft	63'-0"
D	1.078 ft	25'-3"
T	0.726 ft	17'-0"

Turbulence Stimulation:

0.036 inch diameter girth wire placed at station 1.

References:

Philip F. Spaulding & Assoc., Inc. drawing no. 7048-01-6.

TABLE 2

Model and Ship Geometric Characteristics

Sponsor: Philip F. Spaulding & Assoc., Inc.
 Ship type: Cross-Sound Ferry
 UM model: 1221
 Scale ratio: $\lambda = 23.430$

	<u>Model</u>	<u>Ship</u>
LOA	16.389 ft	384'-0"
LBP	15.450 ft	362'-0"
B, maximum	3.713 ft	87'-0"
B, @ DWL	2.689 ft	63'-0"
D	1.078 ft	25'-3"
T	0.726 ft	17'-0"

Turbulence Stimulation:

0.036 inch diameter girth wire placed at frame 64.

References:

Philip F. Spaulding & Assoc., Inc. drawing no 7048-01-6
 alternate.

TABLE 3
Test Conditions

MODEL 1219

No. 1: Design Displacement

	<u>Model</u>	<u>Ship</u>
LWL	18.609 ft	436'-0"
T, mean	8.707 in	17'-0"
Trim	even keel	even keel
Displaced Volume	11.518 ft ³	148,153 ft ³
Displacement	717.4 lbs FW @ 68°F	4,233 LTSW
Wetted Surface	46.342 ft ²	25,440 ft ²
C _B	0.317	0.317

MODEL 1221

No. 2: Design Displacement

	<u>Model</u>	<u>Ship</u>
LWL	16.219 ft	380'-0"
T, mean	8.707 in	17'-0"
Trim	even keel	even keel
Displaced Volume	10.132 ft ³	130,321 ft ³
Displacement	631.1 lbs FW @ 68°F	3,723 LTSW
Wetted Surface	39.4 ft ²	21,629 ft ²
C _B	0.320	0.320

No. 3: Design Displacement with 56'-0" Parallel Midbody

	<u>Model</u>	<u>Ship</u>
LWL	18.609 ft	436'-0"
T, mean	8.707 in	17'-0"
Trim	even keel	even keel
Displaced Volume	12.684 ft ³	163,143 ft ³
Displacement	790.0 lbs FW @ 68°F	4,661 LTSW
Wetted Surface	46.8 ft ²	25,692 ft ²
C _B	0.349	0.349

TABLE 4
Propeller Characteristics - Stock Model Propellers

Sponsor: Philip F. Spaulding & Assoc., Inc.
Scale ratio: $\lambda = 23.430$

Bow Propeller - UM Propeller 11

	<u>Model</u>	<u>Ship</u>
Diameter	6.494 in	12'-8"
P/D	1.100	1.100
Z	4	4
MWR	0.235	0.235
A_e/A_o	0.525	0.525
BTF	0.045	0.045
Rake	6 deg.	6 deg.

Stern Propeller - UM Propeller 12

	<u>Model</u>	<u>Ship</u>
Diameter	6.658 in	13'-0"
P/D	1.090	1.090
Z	4	4
MWR	0.246	0.246
A_e/A_o	0.514	0.514
BTF	0.045	0.045
Rake	6 deg.	6 deg.

TABLE 5
Propeller Characteristics - Wake Adapted Design

Sponsor: Philip F. Spaulding & Assoc., Inc.

Diameter	=	13'-0"
mean P/D	=	0.9998
Z	=	4
MWR	=	0.273
A_e/A_o	=	0.557
BTF	=	0.050
Rake	=	3 deg.
design N	=	180 rpm

TABLE 6
Results of Vibration Analysis

Sponsor: Philip F. Spaulding & Assoc., Inc.
UM Model: 1219

Using Wake Adapted Propellers

$V_K = 20.5$ knots $N = 180$ rpm $J_V = 0.8878$

MEAN VALUES

	Force	Moment
Axial	-106,165 lbs	254,135 ft-lbs
Transverse	-5,058 lbs	-18,071 ft-lbs
Vertical	3,526 lbs	-46,879 ft-lbs

VIBRATORY VALUES

	Force	Moment
Axial	8,056 lbs $\theta = 231.4^\circ$	17,174 ft-lbs $\theta = 50.8^\circ$
Transverse	3,858 lbs $\theta = 220.1^\circ$	38,599 ft-lbs $\theta = 215.4^\circ$
Vertical	3,858 lbs $\theta = 310.1^\circ$	38,599 ft-lbs $\theta = 125.4^\circ$

Sign Convension:

Axial positive directed aft

Transverse positive directed to starboard

Vertical positive directed upward

θ = blade angle zero at top dead center positive in clockwise direction when looking forward

Moments follow right hand rule

FIGURE 1

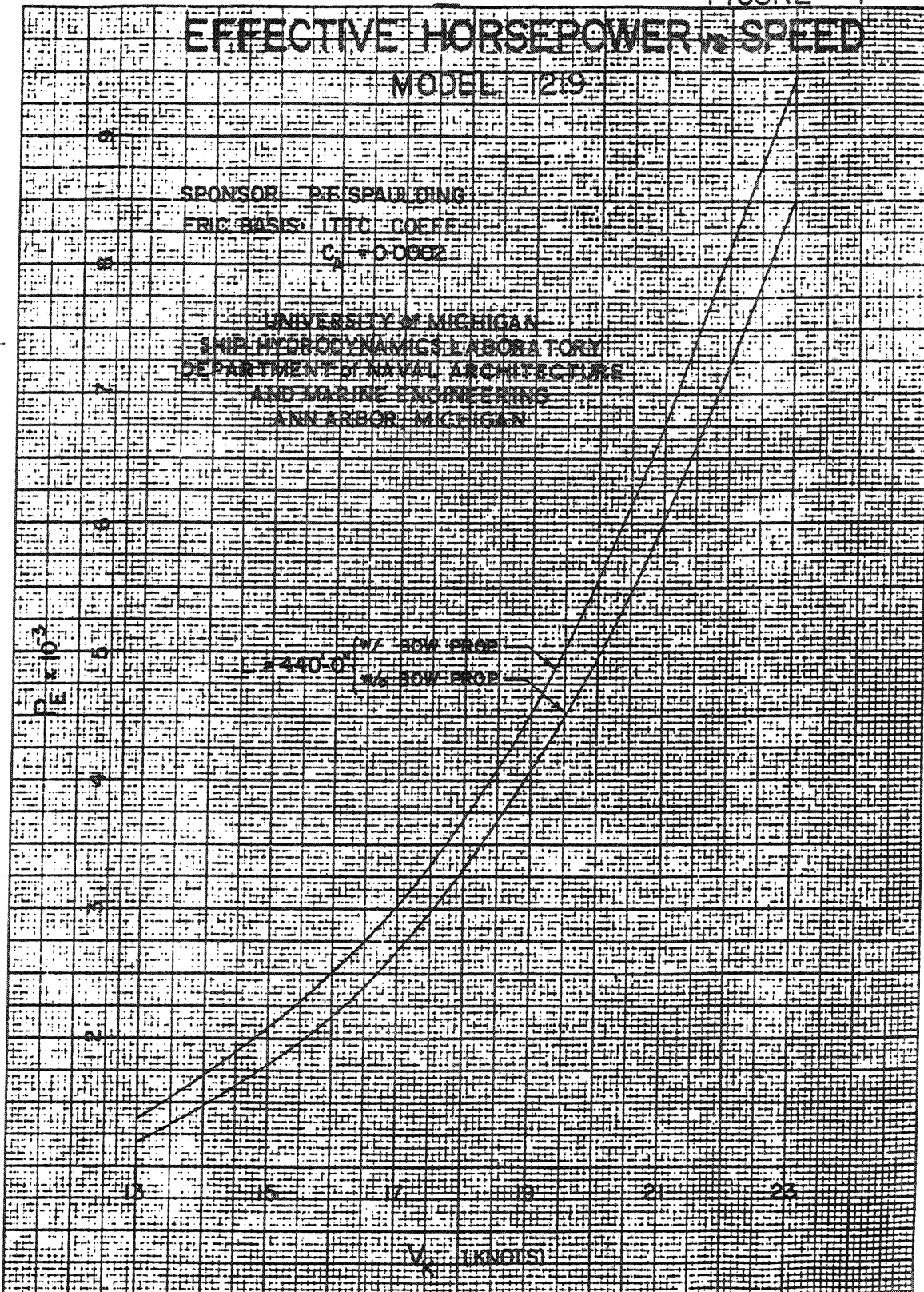
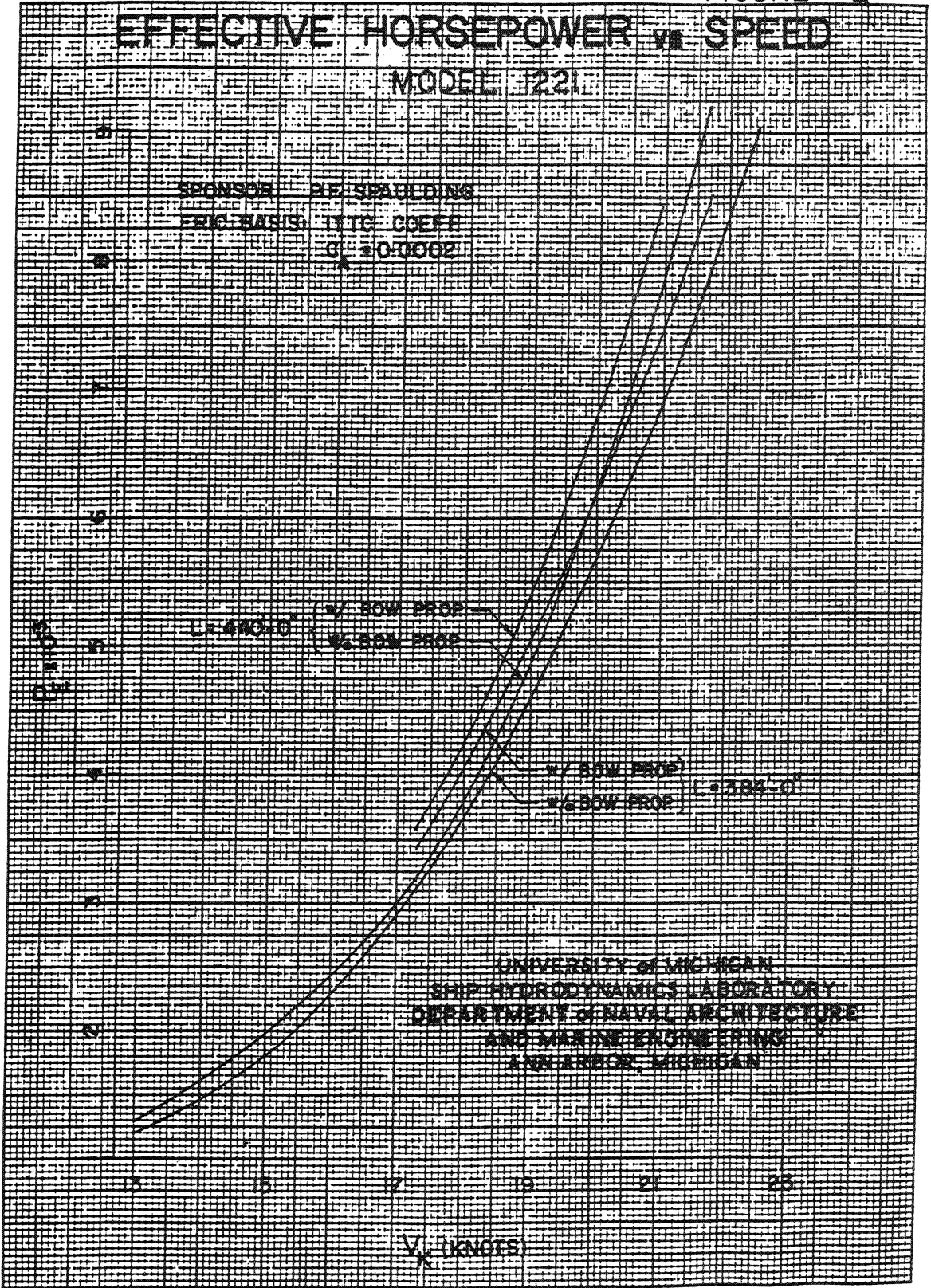


FIGURE 2



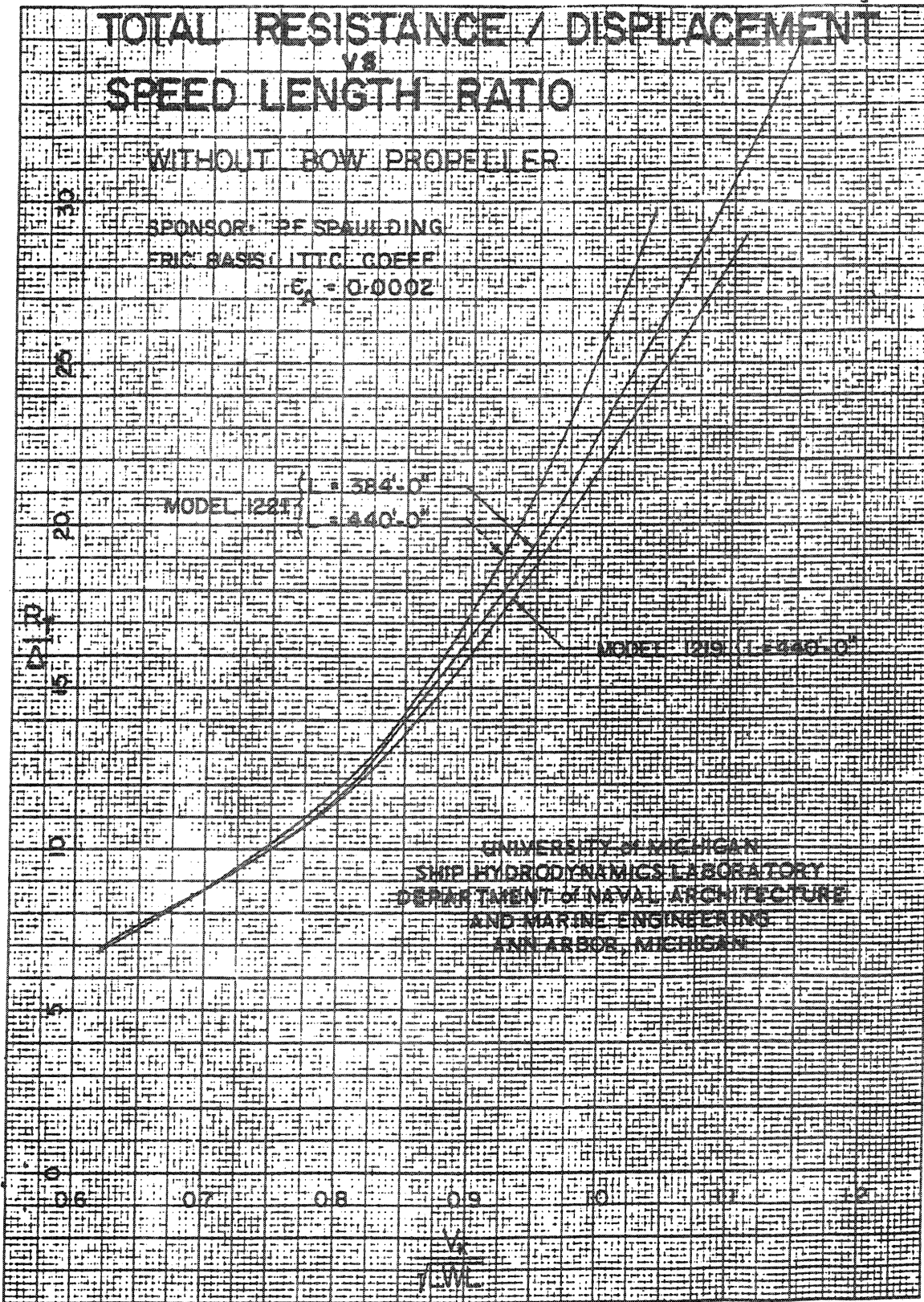
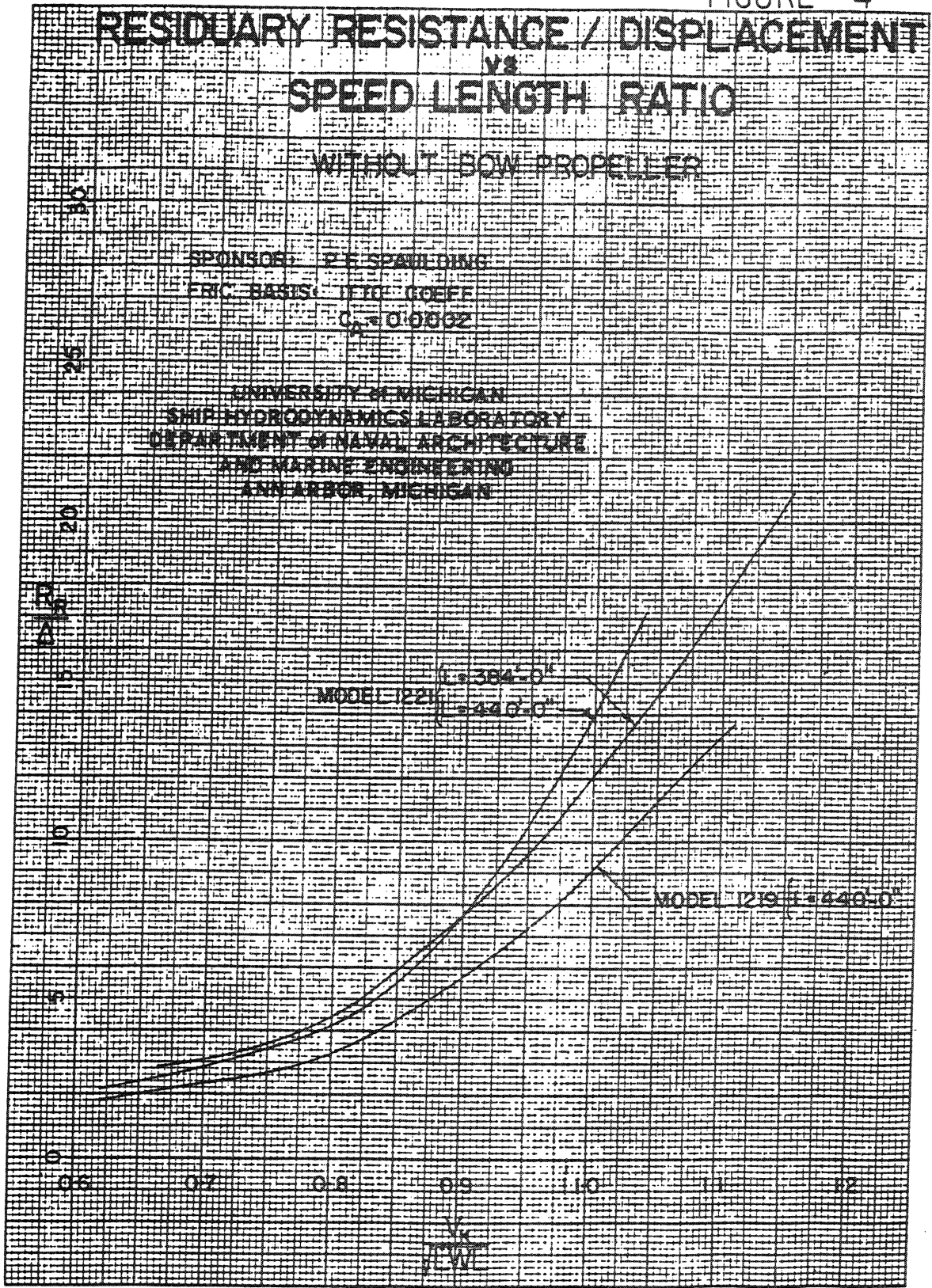


FIGURE 4

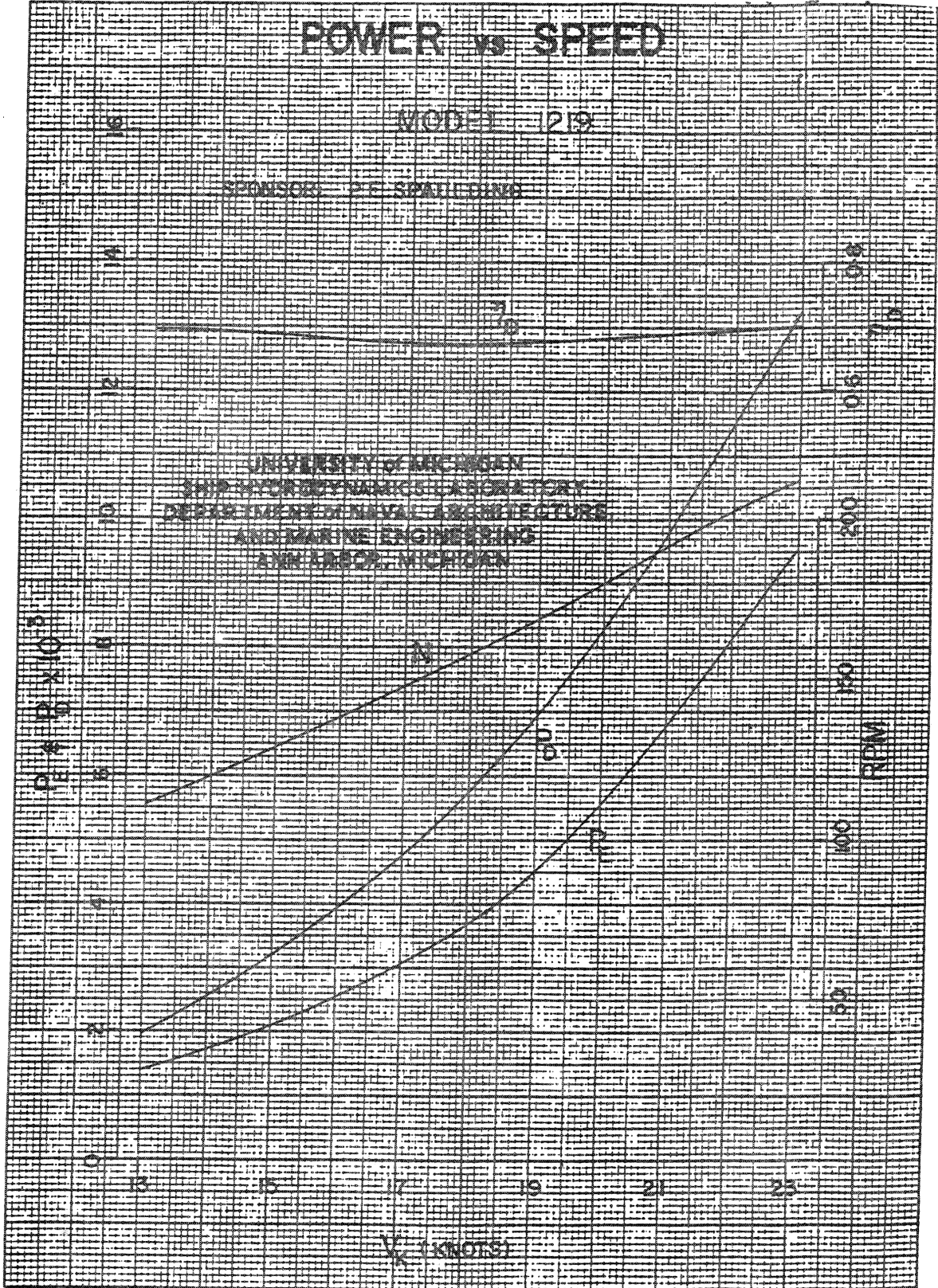


POWER vs SPEED

MODEL 1219

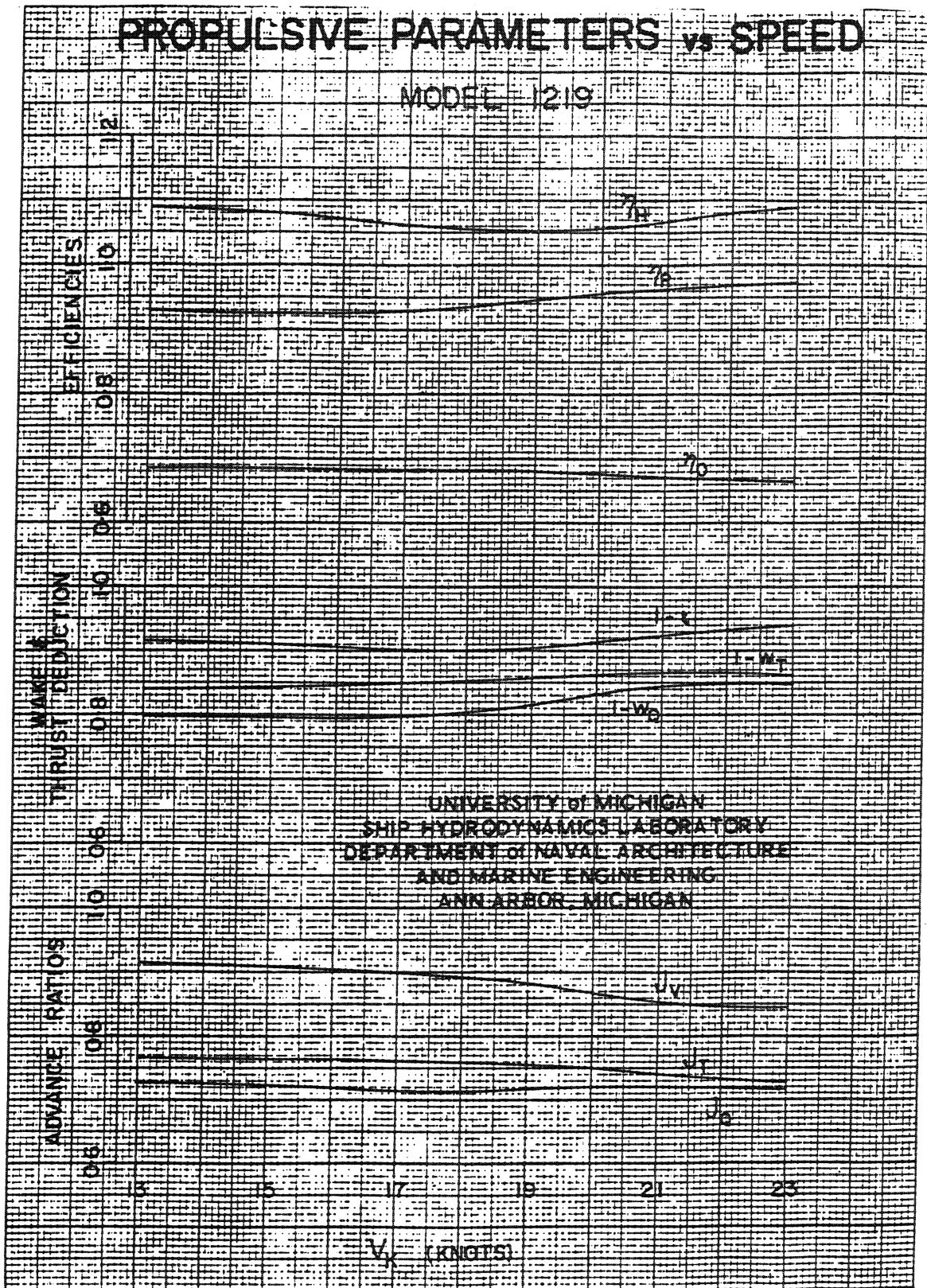
SPONSOR: P.F. SPAULDING

UNIVERSITY OF MICHIGAN
 SHIP HYDRODYNAMICS LABORATORY
 DEPARTMENT OF NAVAL ARCHITECTURE
 AND MARINE ENGINEERING
 ANN ARBOR, MICHIGAN



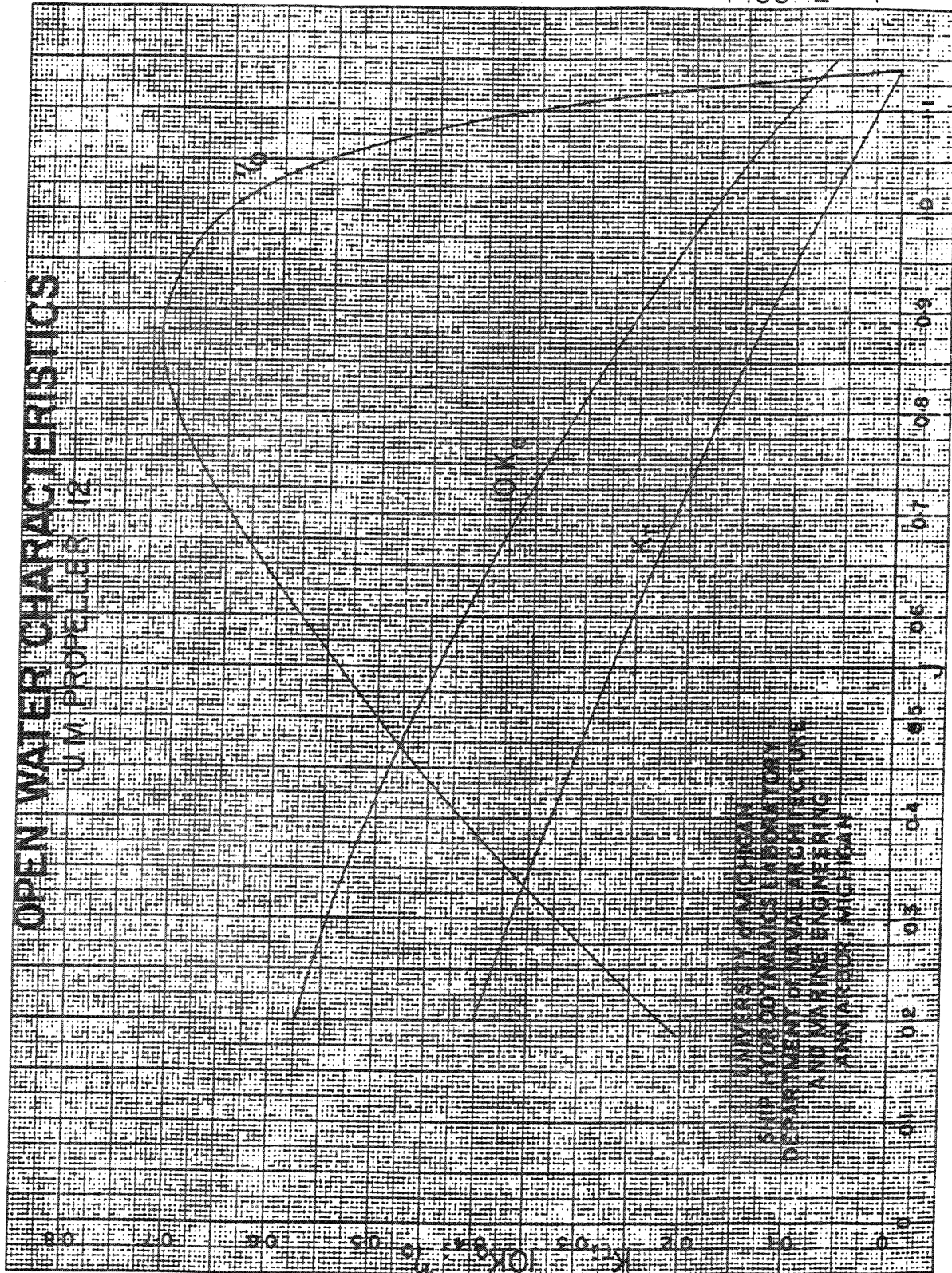
PROPULSIVE PARAMETERS vs SPEED

MODEL 1219



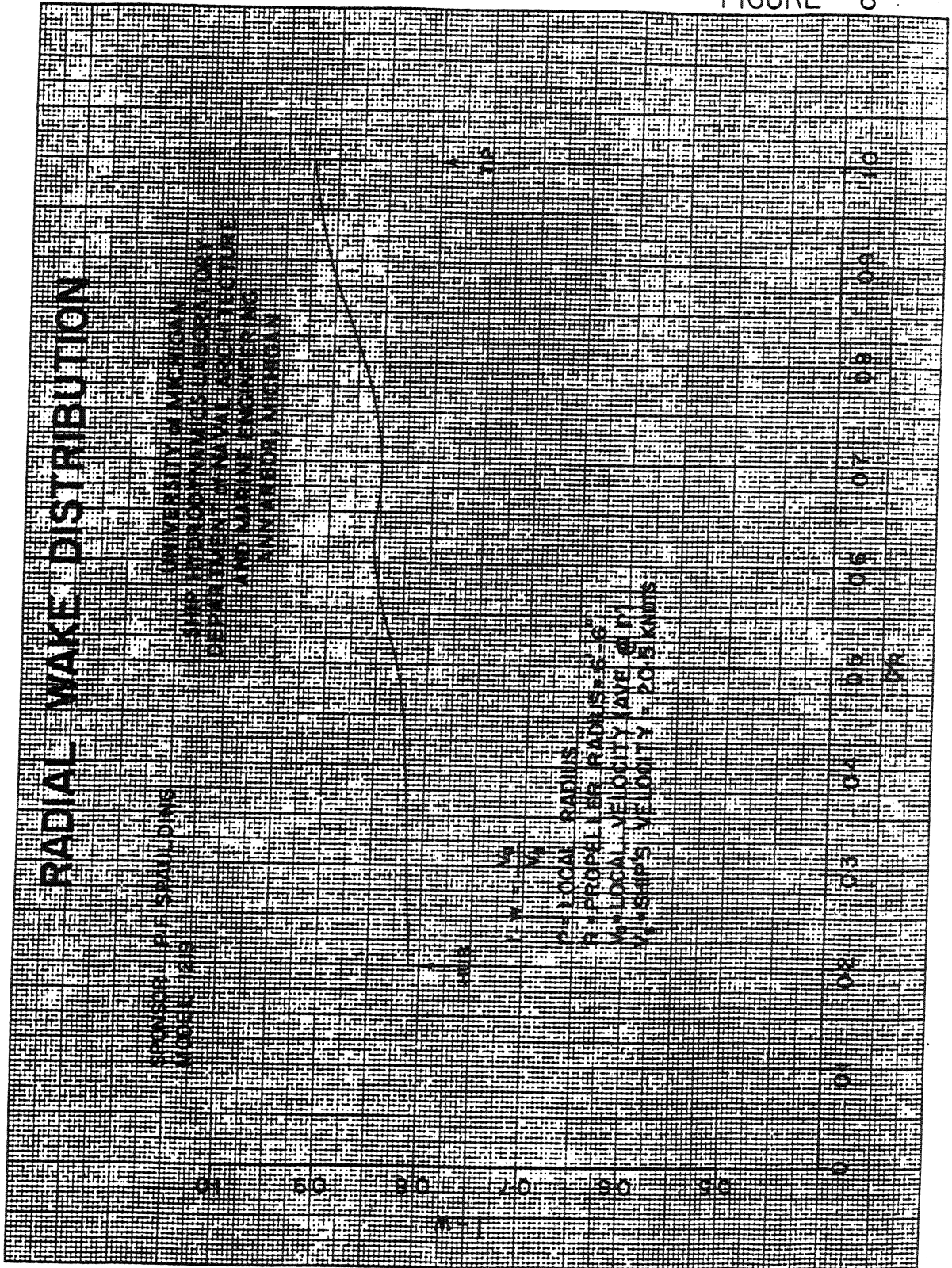
OPEN WATER CHARACTERISTICS

U.M. PROJECT # 12



UNIVERSITY OF MICHIGAN
DEPARTMENT OF MECHANICAL ENGINEERING
ANN ARBOR, MICHIGAN 48106-1324

FIGURE 8

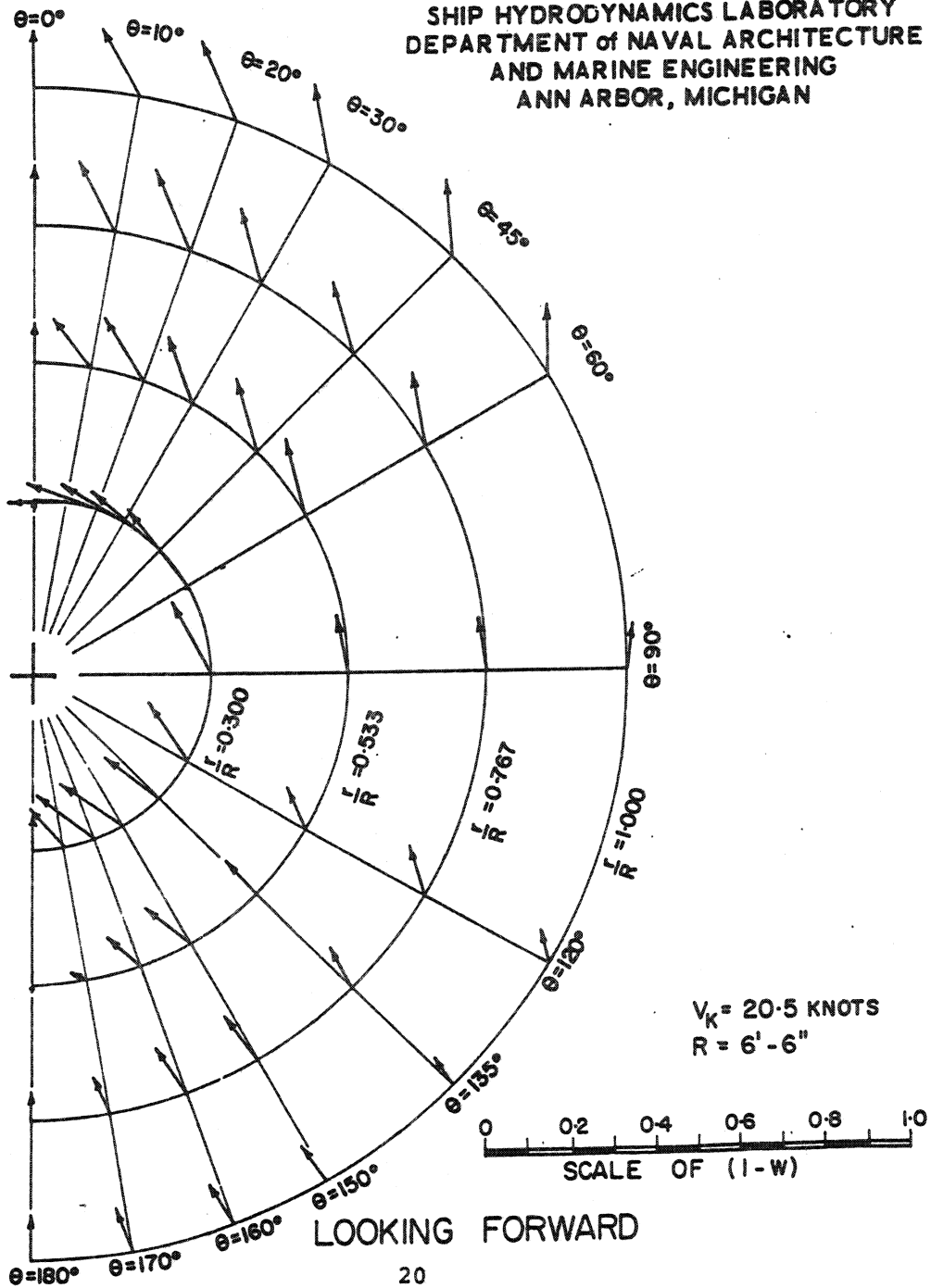


TRANSVERSE WAKE DISTRIBUTION

MODEL 1219

SPONSOR: P.F. SPAULDING

UNIVERSITY of MICHIGAN
SHIP HYDRODYNAMICS LABORATORY
DEPARTMENT of NAVAL ARCHITECTURE
AND MARINE ENGINEERING
ANN ARBOR, MICHIGAN

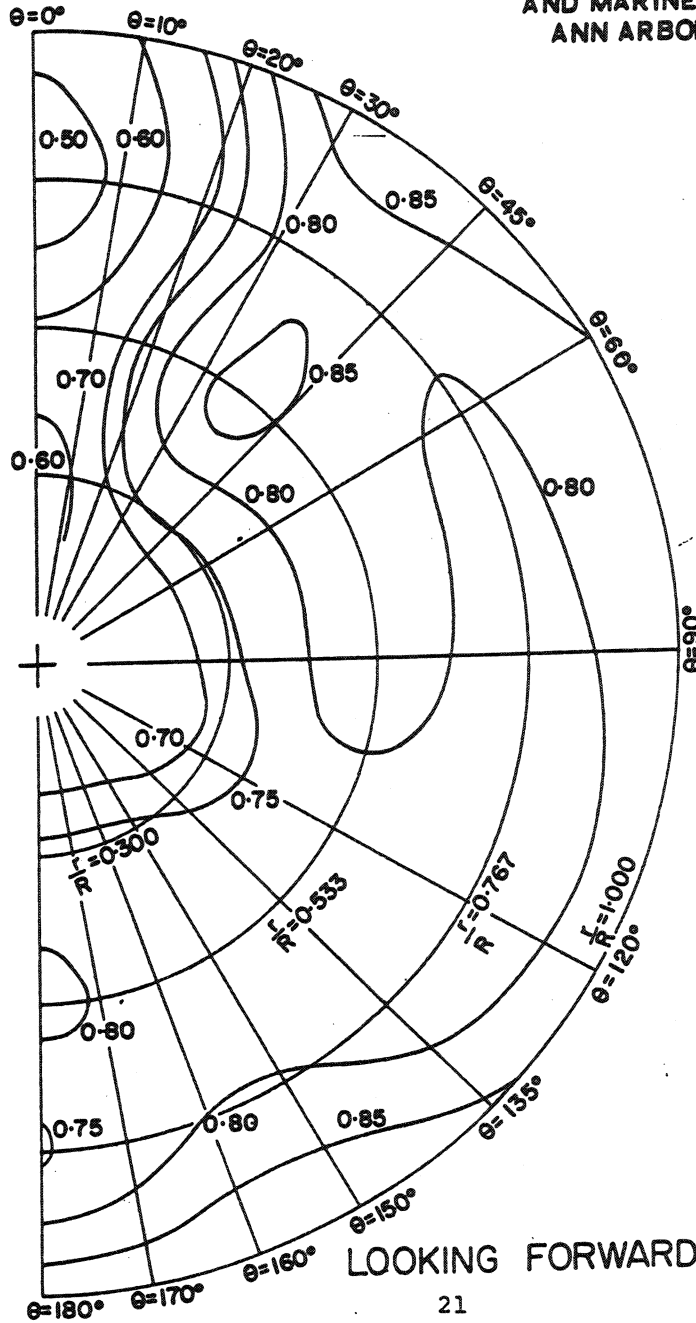


AXIAL WAKE CONTOURS

MODEL 1219

SPONSOR: P.F. SPAULDING

UNIVERSITY of MICHIGAN
SHIP HYDRODYNAMICS LABORATORY
DEPARTMENT of NAVAL ARCHITECTURE
AND MARINE ENGINEERING
ANN ARBOR, MICHIGAN



$V_K = 20.5$ KNOTS
 $R = 6'-6''$

APPENDIX

The Appendix contains:

1. Photograph reduction of the lines of Model 1219
2. Copies of the computer output of the effective horsepower and self-propulsion extrapolation programs.

TABLE A1
Model 1219 Lines

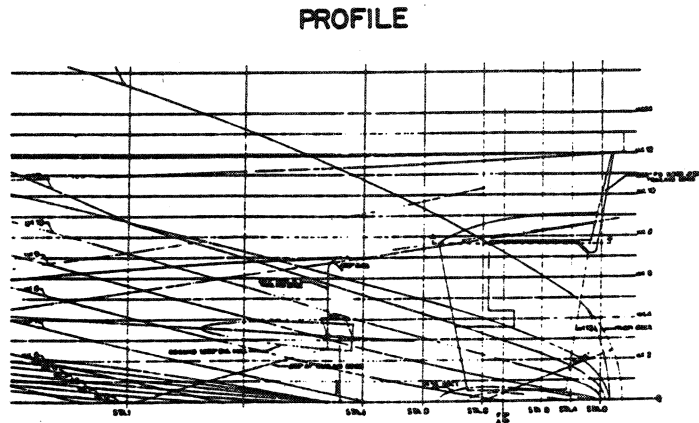
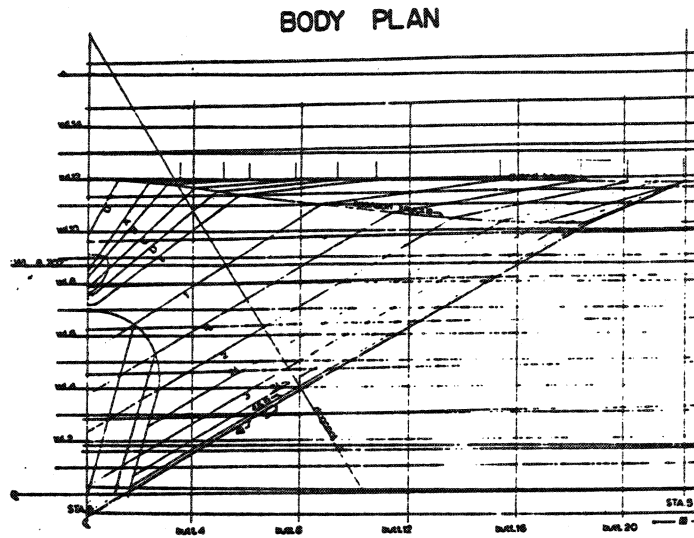


TABLE A2

Model 1219 L = 440'-0"

Without Bow Propeller

SHIP HYDRODYNAMICS LABORATORY
DEPARTMENT OF NAVAL ARCHITECTURE
AND MARINE ENGINEERING
UNIVERSITY OF MICHIGAN
ANN ARBOR, MICHIGAN

EXTRAPOLATION OF MODEL TEST DATA

MODEL TEST DATA						
MODEL NO.	1219	LWL	18.608	VOLUME	11.500	
CONDITION:	EVEN	BEAM	2.688	WET'D SURF	46.342	
LAMDA	29.430	DRAFT FWD	0.725	TEMP	64.00	
FRICTION LINE	ITTC	DRAFT AFT	0.725	RHO	1.9375	
		BLOCK COEF.	0.325	NU*10**5	1.14147	

VM	RTM	RNM/10**6	CTM*1000	CFM*1000	CR*1000
4.514	3.470	7.3578	3.7941	3.1665	0.6276
5.019	4.240	8.1811	3.7500	3.1074	0.6426
5.525	5.060	9.0064	3.6926	3.0553	0.6373
6.033	6.130	9.8342	3.7520	3.0087	0.7433
6.542	7.500	10.6651	3.9031	2.9667	0.9364
6.798	8.250	11.0819	3.9766	2.9472	1.0294
7.054	9.020	11.4996	4.0376	2.9285	1.1091
7.311	9.940	11.9183	4.1423	2.9106	1.2317
7.569	10.870	12.3381	4.2269	2.8934	1.3334
7.827	11.810	12.7589	4.2944	2.8769	1.4175
8.086	12.770	13.1808	4.3510	2.8611	1.4899

VM	SLR	FROUDE NO.	FN**4/CFM	CTM/CFM
4.514	0.620	0.184	0.366	1.198
5.019	0.689	0.205	0.569	1.207
5.525	0.758	0.226	0.851	1.209
6.033	0.828	0.247	1.228	1.247
6.542	0.898	0.267	1.723	1.316
6.798	0.933	0.278	2.022	1.349
7.054	0.968	0.288	2.359	1.379
7.311	1.004	0.299	2.739	1.423
7.569	1.039	0.309	3.164	1.461
7.827	1.074	0.320	3.639	1.493
8.086	1.110	0.330	4.168	1.521

N° 08458

12
11
10
9
8
7
6
5
4

TABLE A2 (CONT.)

SHIP HYDRODYNAMICS LABORATORY
 DEPARTMENT OF NAVAL ARCHITECTURE
 AND MARINE ENGINEERING
 UNIVERSITY OF MICHIGAN
 ANN ARBOR, MICHIGAN

EXTRAPOLATION OF MODEL TEST DATA

SHIP DATA					
MODEL NO.	1219	LWL	435.98	DISP L TSW	4226.
CONDITION:	EVEN	BEAM	62.98	WET'D SURF	25440.
LAMBDA	29.430	DRAFT FWD	17.00	TEMP	59.00
FRICTION LINE	ITTC	DRAFT AFT	17.00	RHO	1.9905
CORR. ALLOW.	0.00020	BLOCK COEF.	0.325	NU*10**5	1.27908

VK	RNS/10**8	CFS*1000	CTS*1000	RTS	EHP
12.936	7.447	1.588	2.416	29195.	1159.
14.383	8.280	1.567	2.410	36002.	1590.
15.834	9.115	1.548	2.386	43198.	2100.
17.290	9.953	1.532	2.475	53428.	2836.
18.751	10.794	1.516	2.653	67353.	3877.
19.483	11.216.	1.509	2.738	75073.	4490.
20.218	11.639	1.502	2.811	82990.	5151.
20.954	12.063	1.496	2.927	92821.	5971.
21.692	12.487	1.489	3.023	102717.	6840.
22.432	12.913	1.483	3.101	112677.	7760.
23.173	13.340	1.477	3.167	122833.	8739.

VK	EHP	SLR	FROUDE NO.	RR/DISP	RT/DISP
12.936	1159.	0.620	0.184	1.795	6.908
14.383	1590.	0.689	0.205	2.272	8.519
15.834	2100.	0.758	0.226	2.731	10.222
17.290	2836.	0.828	0.247	3.797	12.642
18.751	3877.	0.898	0.267	5.626	15.937
19.483	4490.	0.933	0.278	6.678	17.764
20.218	5151.	0.968	0.288	7.747	19.637
20.954	5971.	1.004	0.299	9.241	21.964
21.692	6840.	1.039	0.309	10.722	24.305
22.432	7760.	1.074	0.320	12.189	26.662
23.173	8739.	1.110	0.330	13.673	29.065

STOP OR GO

TABLE A3

Model 1219 L = 440'-0"

With Bow Propeller

SHIP HYDRODYNAMICS LABORATORY
DEPARTMENT OF NAVAL ARCHITECTURE
AND MARINE ENGINEERING
UNIVERSITY OF MICHIGAN
ANN ARBOR, MICHIGAN

EXTRAPOLATION OF MODEL TEST DATA

MODEL TEST DATA					
MODEL NO.	1219	LWL	18.608	VOLUME	11.500
CONDITION:	BOW PROP	BEAM	2.688	WET'D SURF	46.342
LAMDA	23.430	DRAFT FWD	0.725	TEMP	64.00
FRICTION LINE	ITTC	DRAFT AFT	0.725	RHO	1.9375
		BLOCK COEF.	0.325	NU*10**5	1.14147

VM	RTM	RNM/10**6	CTM*1000	CFM*1000	CR*1000
4.514	3.860	7.3578	4.2206	3.1665	1.0540
5.019	4.670	8.1811	4.1303	3.1074	1.0829
5.525	5.570	9.0064	4.0648	3.0553	1.0095
6.033	6.670	9.8342	4.0825	3.0087	1.0738
6.542	8.080	10.6651	4.1737	2.9667	1.0070
6.798	8.900	11.0819	4.2899	2.9472	1.3427
7.054	9.810	11.4996	4.3912	2.9285	1.4627
7.311	10.800	11.9183	4.5007	2.9106	1.5901
7.569	11.850	12.3381	4.6079	2.8934	1.7145
7.827	12.870	12.7589	4.6799	2.8769	1.8029

VM	SLR	FROUDE NO.	FN**4/CFM	CTM/CFM
4.514	0.620	0.184	0.366	1.333
5.019	0.689	0.205	0.569	1.329
5.525	0.758	0.226	0.851	1.330
6.033	0.828	0.247	1.228	1.357
6.542	0.898	0.267	1.723	1.407
6.798	0.933	0.278	2.022	1.456
7.054	0.968	0.288	2.359	1.499
7.311	1.004	0.299	2.739	1.546
7.569	1.039	0.309	3.164	1.593
7.827	1.074	0.320	3.639	1.627

TABLE A3 (CONT.)

SHIP HYDRODYNAMICS LABORATORY
 DEPARTMENT OF NAVAL ARCHITECTURE
 AND MARINE ENGINEERING
 UNIVERSITY OF MICHIGAN
 ANN ARBOR, MICHIGAN

EXTRAPOLATION OF MODEL TEST DATA

SHIP DATA					
MODEL NO.	1219	LWL	435.98	DISP L TSW	4226.
CONDITION:	BOW PROP	BEAM	62.98	WET'D SURF	25440.
LAMBDA	29.430	DRAFT FWD	17.00	TEMP	59.00
FRICTION LINE	ITTC	DRAFT AFT	17.00	RHO	1.9905
CORR. ALLOW.	0.00020	BLOCK COEF.	0.325	NU*10**5	1.27908

VK	RNS/10**8	CFS*1000	CTS*1000	RTS	EHP
12.936	7.447	1.588	2.842	34349.	1364.
14.383	8.980	1.567	2.790	41684.	1841.
15.834	9.115	1.548	2.758	49937.	2427.
17.290	9.953	1.532	2.805	60563.	3215.
18.751	10.794	1.516	2.923	74224.	4273.
19.483	11.216	1.509	3.052	83662.	5004.
20.218	11.639	1.502	3.165	93429.	5799.
20.954	12.063	1.496	3.286	104185.	6702.
21.692	12.487	1.489	3.404	115667.	7703.
22.432	12.913	1.483	3.486	126684.	8724.

VK	EHP	SLR FROUDE NO.	RR/DISP	RT/DISP
12.936	1364.	0.620	0.184	3.014
14.383	1841.	0.689	0.205	3.616
15.834	2427.	0.758	0.226	4.325
17.290	3215.	0.828	0.247	5.485
18.751	4273.	0.898	0.267	7.252
19.483	5004.	0.933	0.278	8.710
20.218	5799.	0.968	0.288	10.217
20.954	6702.	1.004	0.299	11.930
21.692	7703.	1.039	0.309	13.786
22.432	8724.	1.074	0.320	15.503

STOP OR GO

D'06062

UNIVERSITY OF MICHIGAN

12
11
10
9
8
7
6
5
4

TABLE A4

Model 1221 L = 384'-0"

Without Bow Propeller

SHIP HYDRODYNAMICS LABORATORY
 DEPARTMENT OF NAVAL ARCHITECTURE
 AND MARINE ENGINEERING
 UNIVERSITY OF MICHIGAN
 ANN ARBOR, MICHIGAN

EXTRAPOLATION OF MODEL TEST DATA

MODEL TEST DATA					
MODEL NO.	1221	LWL	16.819	VOLUME	10.117
CONDITION:	EVEN	BEAM	2.688	WET'D SURF	39.400
LAMDA	23.430	DRAFT FWD	0.725	TEMP	65.00
FRICITION LINE	ITTC	DRAFT AFT	0.725	RHO	1.9273
		BLOCK COEF.	0.332	NU*10**5	1.12570

VM	RTM	RNM/10**6	CTM*1000	CFM*1000	CR*1000
4.515	3.330	6.5050	4.2804	3.2373	1.0431
5.020	4.020	7.2334	4.1791	3.1762	1.0029
5.528	4.980	7.9640	4.2708	3.1223	1.1485
6.036	6.300	8.6972	4.5302	3.0741	1.4561
6.548	7.810	9.4337	4.7734	3.0306	1.7428
6.804	8.720	9.8032	4.9353	3.0104	1.9250
7.061	9.640	10.1736	5.0660	2.9911	2.0749
7.319	10.610	10.5450	5.1899	2.9725	2.2174
7.577	11.700	10.9172	5.3096	2.9548	2.3848
7.836	12.780	11.2902	5.4534	2.9377	2.5156

VM	SLR	FROUDE NO.	FN**4/CFM	CTM/CFM
4.515	0.664	0.198	0.471	1.322
5.020	0.738	0.220	0.735	1.316
5.528	0.813	0.242	1.098	1.368
6.036	0.887	0.264	1.586	1.474
6.548	0.963	0.287	2.227	1.575
6.804	1.000	0.298	2.615	1.639
7.061	1.038	0.309	3.052	1.694
7.319	1.076	0.320	3.545	1.746
7.577	1.114	0.332	4.097	1.807
7.836	1.152	0.343	4.713	1.856

TABLE A4 (CONT.)

SHIP HYDRODYNAMICS LABORATORY
 DEPARTMENT OF NAVAL ARCHITECTURE
 AND MARINE ENGINEERING
 UNIVERSITY OF MICHIGAN
 ANN ARBOR, MICHIGAN

EXTRAPOLATION OF MODEL TEST DATA

SHIP DATA					
MODEL NO.	1221	LWL	380.01	DISP L TSW	3718.
CONDITION:	EVEN	BEAM	62.98	WET'D SURF	21629.
LAMDA	23.430	DRAFT FWD	17.00	TEMP	59.00
FRICITION LINE	ITTC	DRAFT AFT	17.00	RHO	1.9905
CORR. ALLOW.	0.00020	BLOCK COEF.	0.332	NU*10**5	1.27908

VK	RNS/10**8	CFS*1000	CTS*1000	RTS	EHP
12.940	6.493	1.616	2.859	29395.	1168.
14.389	7.220	1.594	2.797	35560.	1571.
15.842	7.949	1.575	2.724	45054.	2191.
17.301	8.681	1.558	3.214	59067.	3137.
18.766	9.416	1.542	3.485	75351.	4341.
19.501	9.785	1.535	3.668	85453.	5116.
20.238	10.155	1.528	3.803	95626.	5941.
20.976	10.525	1.521	3.938	106401.	6852.
21.717	10.897	1.514	4.099	118702.	7914.
22.459	11.269	1.508	4.224	130812.	9019.

VK	EHP	SLR FROUDE NO.	RR/DISP	RT/DISP
12.940	1168.	0.664	0.198	2.884
14.389	1571.	0.738	0.230	3.429
15.842	2191.	0.813	0.242	4.760
17.301	3137.	0.887	0.264	7.198
18.766	4341.	0.963	0.287	10.136
19.501	5116.	1.000	0.298	12.089
20.238	5941.	1.038	0.309	14.034
20.976	6852.	1.076	0.320	16.113
21.717	7914.	1.114	0.332	18.574
22.459	9019.	1.152	0.343	20.955

STOP OR GO
 F

06254

12
11
10
9
8
7
6
5
4

TABLE A5

Model 1221 L = 384'-0"

With Bow Propeller

SHIP HYDRODYNAMICS LABORATORY
 DEPARTMENT OF NAVAL ARCHITECTURE
 AND MARINE ENGINEERING
 UNIVERSITY OF MICHIGAN
 ANN ARBOR, MICHIGAN

EXTRAPOLATION OF MODEL TEST DATA

MODEL TEST DATA					
MODEL NO.	1221	LWL	16.219	VOLUME	10.117
CONDITION:	BOW PROP	BEAM	2.688	WET'D SURF	39.400
LAMDA	23.430	DRAFT FWD	0.725	TEMP	65.00
FRICTION LINE	ITTC	DRAFT AFT	0.725	RHO	1.9373
		BLOCK COEF.	0.332	NU*10**5	1.12570

VM	RTM	RNM/10**6	CTM*1000	CFM*1000	CR*1000
6.036	6.700	8.6972	4.8178	3.0741	1.7437
6.548	8.410	9.4337	5.1401	3.0306	2.1095
6.804	9.300	9.8032	5.2636	3.0104	2.2532
7.061	10.300	10.1736	5.4128	2.9911	2.4217
7.319	11.280	10.5458	5.5177	2.9725	2.5451
7.577	12.380	10.9172	5.6499	2.9548	2.6951

VM	SLR	FROUDE NO.	FN**4/CFM	CTM/CFM
6.036	0.887	0.264	1.586	1.567
6.548	0.963	0.287	2.227	1.696
6.804	1.000	0.298	2.615	1.748
7.061	1.038	0.309	3.052	1.810
7.319	1.076	0.320	3.545	1.856
7.577	1.114	0.332	4.097	1.912

TABLE A5 (CONT.)

SHIP HYDRODYNAMICS LABORATORY
 DEPARTMENT OF NAVAL ARCHITECTURE
 AND MARINE ENGINEERING
 UNIVERSITY OF MICHIGAN
 ANN ARBOR, MICHIGAN

EXTRAPOLATION OF MODEL TEST DATA

SHIP DATA					
MODEL NO.	1221	LVL	380.01	DISP L TSW	3718.
CONDITION:	BOW PROP	BEAM	62.98	WET'D SURF	21629.
LAMDA	23.430	DRAFT FWD	17.00	TEMP	59.00
FRICITION LINE	ITTC	DRAFT AFT	17.00	RHO	1.9905
CORR. ALLOW.	0.00020	BLOCK COEF.	0.332	NU*10**5	1.27908
WK	RNS/10**6	GFS*1000	GTS*1000	RTS	EHP
17.301	8.681	1.558	3.502	64353.	3418.
18.766	9.416	1.542	3.852	83281.	4798.
19.501	9.785	1.535	3.988	93118.	5575.
20.238	10.155	1.528	4.149	104348.	6483.
20.976	10.525	1.521	4.266	115255.	7422.
21.717	10.897	1.514	4.410	127689.	8513.
WK	EHP	SLR FROUDE NO.	RR/DISP	RT/DISP	
17.301	3418.	0.887	0.264	8.620	
18.766	4798.	0.963	0.287	12.268	
19.501	5575.	1.000	0.298	14.151	
20.238	6483.	1.038	0.309	16.380	
20.976	7422.	1.076	0.320	18.495	
21.717	8513.	1.114	0.332	20.991	

STOP OR GO

TABLE A6

Model 1221 L = 440'-0"

Without Bow Propeller

SHIP HYDRODYNAMICS LABORATORY
 DEPARTMENT OF NAVAL ARCHITECTURE
 AND MARINE ENGINEERING
 UNIVERSITY OF MICHIGAN
 ANN ARBOR, MICHIGAN

EXTRAPOLATION OF MODEL TEST DATA

MODEL TEST DATA					
MODEL NO.	1221	LWL	18.600	VOLUME	12.660
CONDITION:	MIDBODY	BEAM	2.688	WET'D SURF	46.800
LAMDA	23.430	DRAFT FWD	0.725	TEMP	68.00
FRICITION LINE	ITTC	DRAFT AFT	0.725	RHO	1.9367
		BLOCK COEF.	0.348	NU*10**5	1.08042

VM	RTM	RNM/10**6	CTM*1000	CFM*1000	CR*1000
4.513	3.650	7.7738	3.9537	3.1357	0.8180
5.018	4.460	8.6433	3.9080	3.0775	0.8306
5.524	5.440	9.5150	3.9334	3.0261	0.9073
6.032	6.600	10.3897	4.0024	2.9802	1.0222
6.542	8.340	11.2682	4.2997	2.9387	1.3610
6.798	9.460	11.7892	4.5167	2.9194	1.5972
7.055	10.670	12.1514	4.7303	2.9010	1.8294
7.312	12.000	12.5949	4.9519	2.8833	2.0686
7.571	13.580	13.0397	5.1974	2.8663	2.3310

VM	SLR	FROUDE NO.	FN**4/CFM	CTM/CFM
4.513	0.619	0.184	0.369	1.261
5.018	0.689	0.205	0.575	1.270
5.524	0.758	0.226	0.859	1.300
6.032	0.828	0.247	1.239	1.343
6.542	0.898	0.267	1.739	1.463
6.798	0.933	0.278	2.041	1.547
7.055	0.968	0.288	2.382	1.631
7.312	1.004	0.299	2.766	1.717
7.571	1.039	0.309	3.197	1.813

TABLE A6 (CONT.)

SHIP HYDRODYNAMICS LABORATORY
 DEPARTMENT OF NAVAL ARCHITECTURE
 AND MARINE ENGINEERING
 UNIVERSITY OF MICHIGAN
 ANN ARBOR, MICHIGAN

EXTRAPOLATION OF MODEL TEST DATA

SHIP DATA					
MODEL NO.	1221	LWL	436.01	DISP L TSW	4658.
CONDITION:	MIDBODY	BEAM	62.98	WET'D SURF	25692.
LAMDA	23.430	DRAFT FWD	17.00	TEMP	59.00
FRICITION LINE	ITTC	DRAFT AFT	17.00	RHO	1.9905
CORR. ALLOW.	0.00020	BLOCK COEF.	0.348	NU*10**5	1.27908

VK	RNS/10**8	GFS*1000	CTS*1000	RTS	EHP
12.936	7.447	1.588	2.606	31806.	1263.
14.382	8.280	1.567	2.598	39190.	1730.
15.833	9.115	1.548	2.656	48553.	2360.
17.288	9.953	1.532	2.754	60029.	3186.
18.750	10.795	1.516	3.077	78903.	4542.
19.484	11.217	1.509	3.306	91548.	5476.
20.220	11.641	1.502	3.532	105305.	6537.
20.958	12.066	1.496	3.764	120585.	7759.
21.698	12.492	1.489	4.000	138044.	9195.

VK	EHP	SLR FROUDE NO.	RR/DISP	RT/DISP
12.936	1263.	0.619	2.146	6.837
14.382	1730.	0.689	2.693	8.424
15.833	2360.	0.758	3.565	10.436
17.288	3186.	0.828	4.790	12.903
18.750	4542.	0.898	7.501	16.960
19.484	5476.	0.933	9.506	19.676
20.220	6537.	0.968	11.725	22.635
20.958	7759.	1.004	14.244	25.919
21.698	9195.	1.039	17.204	29.672

STOP OR GO

TABLE A7

Model 1221 L = 440'-0"

With Bow Propeller

SHIP HYDRODYNAMICS LABORATORY
 DEPARTMENT OF NAVAL ARCHITECTURE
 AND MARINE ENGINEERING
 UNIVERSITY OF MICHIGAN
 ANN ARBOR, MICHIGAN

EXTRAPOLATION OF MODEL TEST DATA

MODEL TEST DATA					
MODEL NO.	1221	LWL	18.609	VOLUME	12.660
CONDITION:	MID W PRO	BEAM	2.688	WET'D SURF	46.800
LAMDA	33.430	DRAFT FWD	0.725	TEMP	68.00
FRICTION LINE	ITTC	DRAFT AFT	0.725	RHO	1.9367
		BLOCK COEF.	0.348	NU*10**5	1.08042

VM	RTM	RNM/10**6	CTM*1000	CFM*1000	CR*1000
6.032	7.160	10.3897	4.3420	2.9802	1.3618
6.542	9.020	11.2682	4.6503	2.9387	1.7115
6.798	10.170	11.7092	4.8557	2.9194	1.9362
7.055	11.420	12.1514	5.0628	2.9010	2.1618
7.312	12.780	12.5949	5.2738	2.8833	2.3985

VM	SLR	FROUDE NO.	FN**4/CFM	CTM/CFM
6.032	0.828	0.247	1.239	1.457
6.542	0.898	0.267	1.739	1.582
6.798	0.933	0.278	2.041	1.663
7.055	0.968	0.288	2.382	1.745
7.312	1.004	0.299	2.766	1.829

12
11
10
9
8
7
6
5
4

TABLE A7 (CONT.)

SHIP HYDRODYNAMICS LABORATORY
 DEPARTMENT OF NAVAL ARCHITECTURE
 AND MARINE ENGINEERING
 UNIVERSITY OF MICHIGAN
 ANN ARBOR, MICHIGAN

EXTRAPOLATION OF MODEL TEST DATA

SHIP DATA

MODEL NO.	1221	LWL	436.01	DISP L TSW	4652.
CONDITION:	MID W PRO	BEAM	62.98	WET'D SURF	25692.
LAMDA	83.430	DRAFT FWD	17.00	TEMP	59.00
FRICTION LINE	ITTC	DRAFT AFT	17.00	RHO	1.9905
CORR. ALLOW.	0.00020	BLOCK COEF.	0.348	NU*10**5	1.27908

VK	RNS/10**8	CFS*1000	CTS*1000	RTS	EHP
17.288	9.953	1.532	3.093	67432.	3579.
18.750	10.795	1.516	3.488	87898.	5059.
19.484	11.217	1.509	3.645	100929.	6037.
20.220	11.641	1.502	3.864	115220.	7152.
20.958	12.066	1.496	4.086	130896.	8422.

VK	EHP	SLR FROUDE NO.	RR/DISP	RT/DISP
17.288	3579.	0.828	0.247	6.381
18.750	5059.	0.898	0.267	9.433
19.484	6037.	0.933	0.278	11.523
20.220	7152.	0.968	0.288	13.856
20.958	8422.	1.004	0.299	16.460

STOP OR GO

12
11
10
9
8
7
6
5
4

MODEL NUMBER 1219

TEST NUMBER 1

SHIP LENGTH = 436.0 FEET

SPEED. (KNOTS)	RESISTANCE (POUNDS)	RPM	EHP	SHP	PC
11.463	25440.	99.793	895.	1341.	0.6672
13.097	35134.	112.418	1411.	1968.	0.7171
14.731	43552.	126.793	1968.	2835.	0.6942
15.877	50369.	137.284	2450.	3680.	0.6749
17.339	61007.	151.194	3245.	4988.	0.6505
18.743	74201.	165.921	4266.	6424.	0.6641
19.545	84577.	174.526	5071.	7260.	0.6984
20.348	95401.	184.647	5955.	8683.	0.6858
21.293	109293.	196.272	7139.	11578.64	0.6666
21.695	115752.	200.757	7703.	11069.	0.6959
22.382	126183.	207.652	8663.	12576.	0.6889
22.927	134176.	212.499	9436.	13193.	0.7152

SPEED (KNOTS)	TORQUE POUNDS-FT	THRUST POUNDS	I-T	I-WT	I-WO	I-W
11.463	70562.	30161.	0.8579	0.8381	0.7964	0.8172
13.097	91957.	36977.	0.9495	0.8435	0.7983	0.8209
14.731	117480.	46747.	0.9291	0.8489	0.8036	0.8262
15.877	138892.	55297.	0.9072	0.8483	0.7993	0.8238
17.339	173283.	67606.	0.9005	0.8516	0.7832	0.8174
18.743	203347.	80592.	0.9182	0.8697	0.8169	0.8433
19.545	218494.	95102.	0.8905	0.8434	0.8349	0.8392
20.348	246979.	102090.	0.9375	0.8797	0.8315	0.8556
21.293	266864.	117541.	0.9298	0.8833	*****	*****
21.695	289578.	127033.	0.9123	0.8687	0.8636	0.8661
22.382	318081.	129621.	0.9735	0.8972	0.8493	0.8733
22.927	326085.	142316.	0.9425	0.8701	0.8658	0.8680

SPEED	KT	LOKO	JT	JO	JAUG
11.4635	0.1918	0.3452	0.7505	0.7132	0.7318
13.0970	0.1853	0.3545	0.7661	0.7250	0.7455
14.7306	0.1841	0.3588	0.7688	0.7278	0.7483
15.8769	0.1858	0.3590	0.7648	0.7206	0.7427
17.3385	0.1873	0.3693	0.7613	0.7001	0.7307
18.7428	0.1854	0.3598	0.7658	0.7194	0.7426
19.5452	0.1977	0.3495	0.7363	0.7289	0.7326
20.3477	0.1896	0.3529	0.7557	0.7143	0.7350
21.2934	0.1932	0.3500	0.7471	*****	*****
21.6946	0.1996	0.3500	0.7318	0.7275	0.7297
22.3824	0.1904	0.3594	0.7539	0.7136	0.7338
22.9270	0.1996	0.3518	0.7318	0.7282	0.7300

APPENDIX H
SEA TRIALS RESULTS FOR WASHINGTON STATE FERRIES

FOR
WASHINGTON STATE FERRIES
SEA TRIALS

CONDUCTED BY
OFFSHORE SURVEY AND NAVIGATION LIMITED
1974 SPICER ROAD, NORTH VANCOUVER, B.C.
CANADA V7H 1A2
(604) 929-7961

PERSONNEL CONDUCTING TRIALS

IN CHARGE	:	CAPT. JOHN SWANN	O.S.N.L	ON BEHALF OF
TRIALS MASTER	:	MR. FRANK VIBRANS-ENG.	W.S.F.	
COORDINATING	:	CAPT. JOHN PETERSON	W.S.F.	
P.N.S. TECH.	:	CAPT. JOHN SWANN	O.S.N.L.	
SNR. ENGINEER	:	MR. MARK LANZINER	O.S.N.L.	
PROCESSED	:	MR. GREG BLANCHETTE	O.S.N.L.	
	:	MRS. NINA SOO	O.S.N.L.	

M.V. YAKIMA

TUESDAY 20TH MARCH 1984

LOCATION: POSSESSION SOUND

VESSEL CONDITION

DRFT. FWD. : 17'05"
DRFT. AFT. : 17'00"
M'DRFT. : 17'02.5"

TIDAL INEQ.

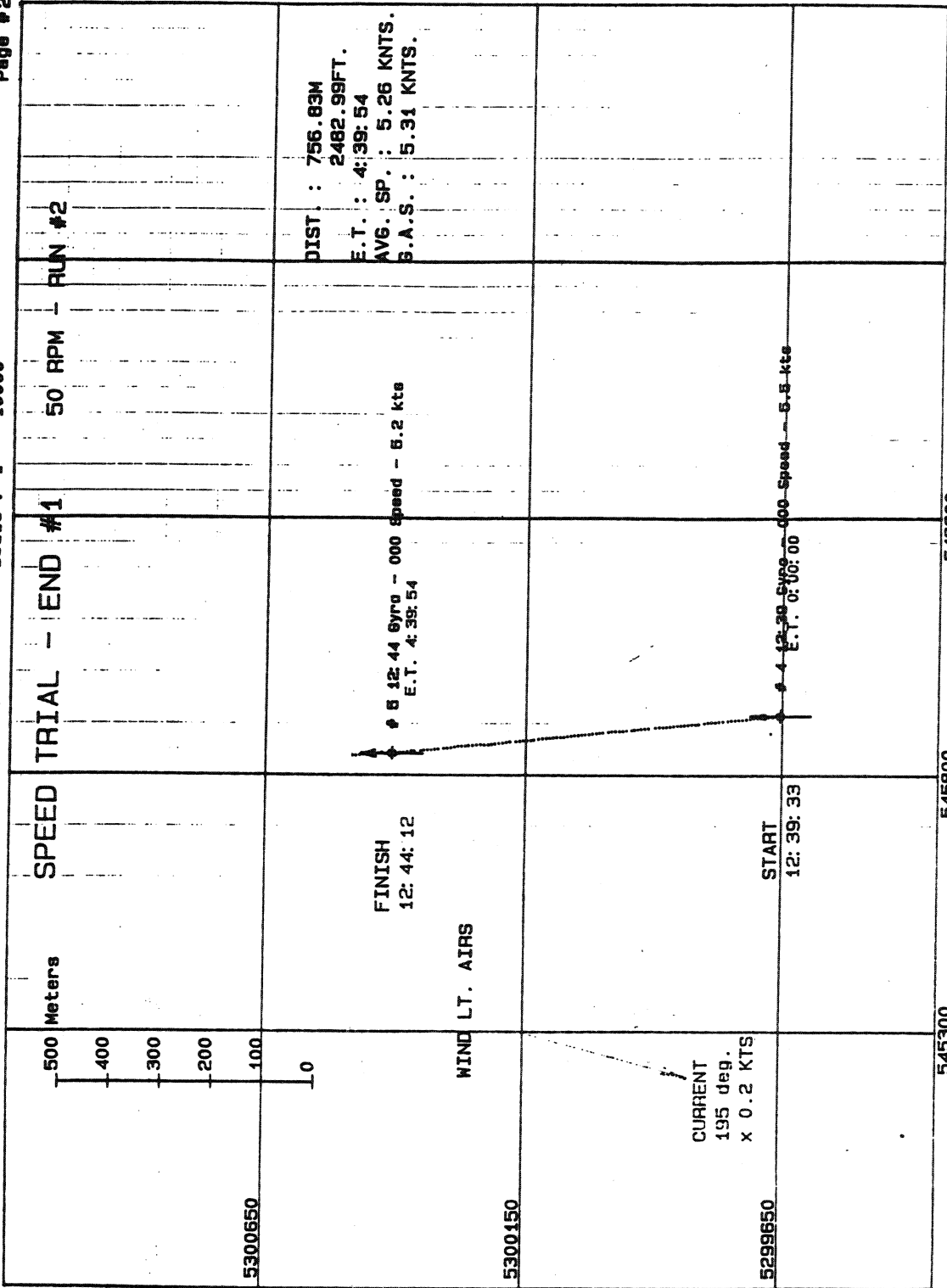
LW. 0136 H
HW. 0648 H
LW. 1409 H
HW. 2004 H

WIND: S x 15 KTS.

SEA: 2' - 3'

WEATHER: 0'CAST WITH RAIN

END #1

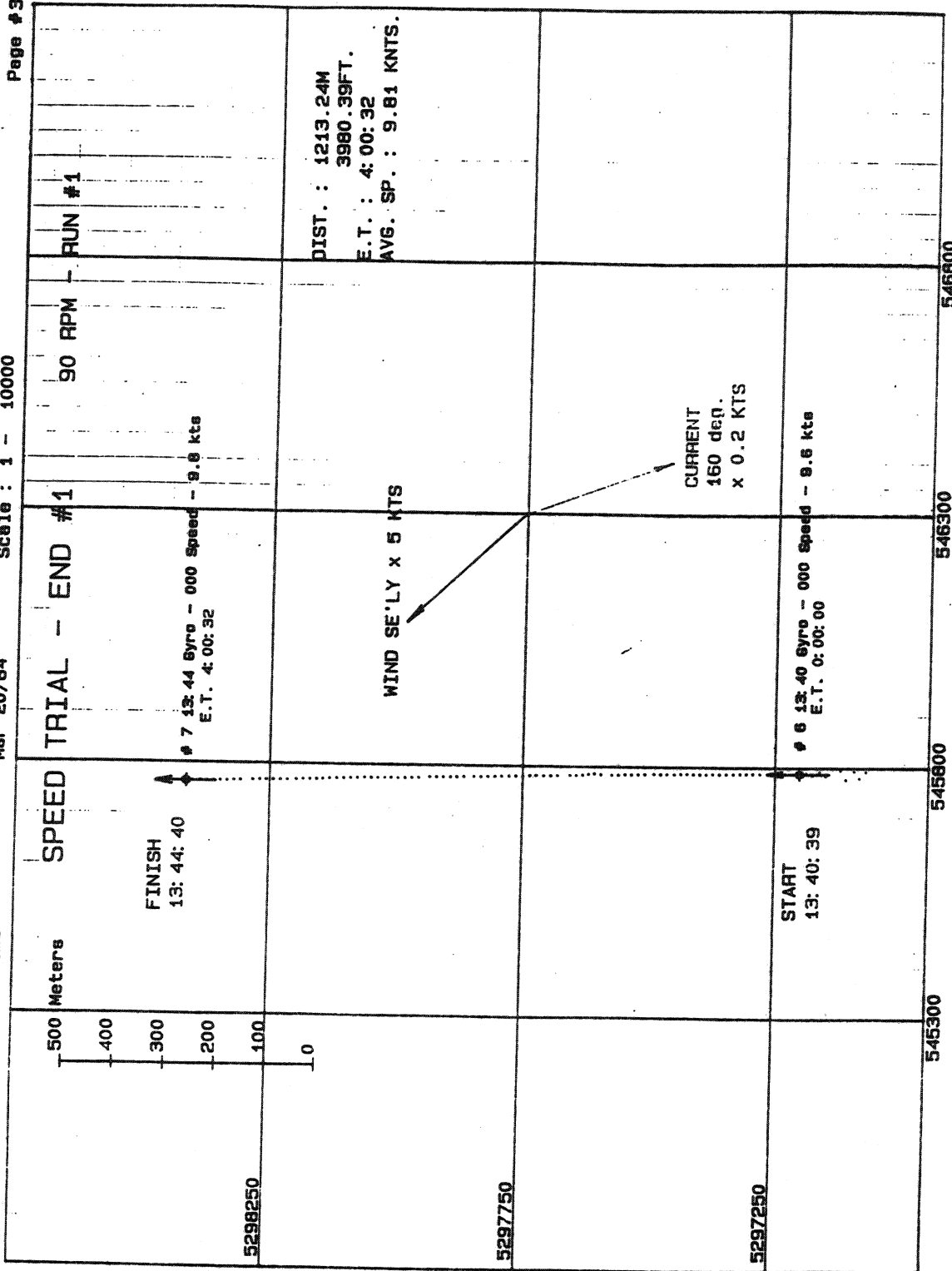


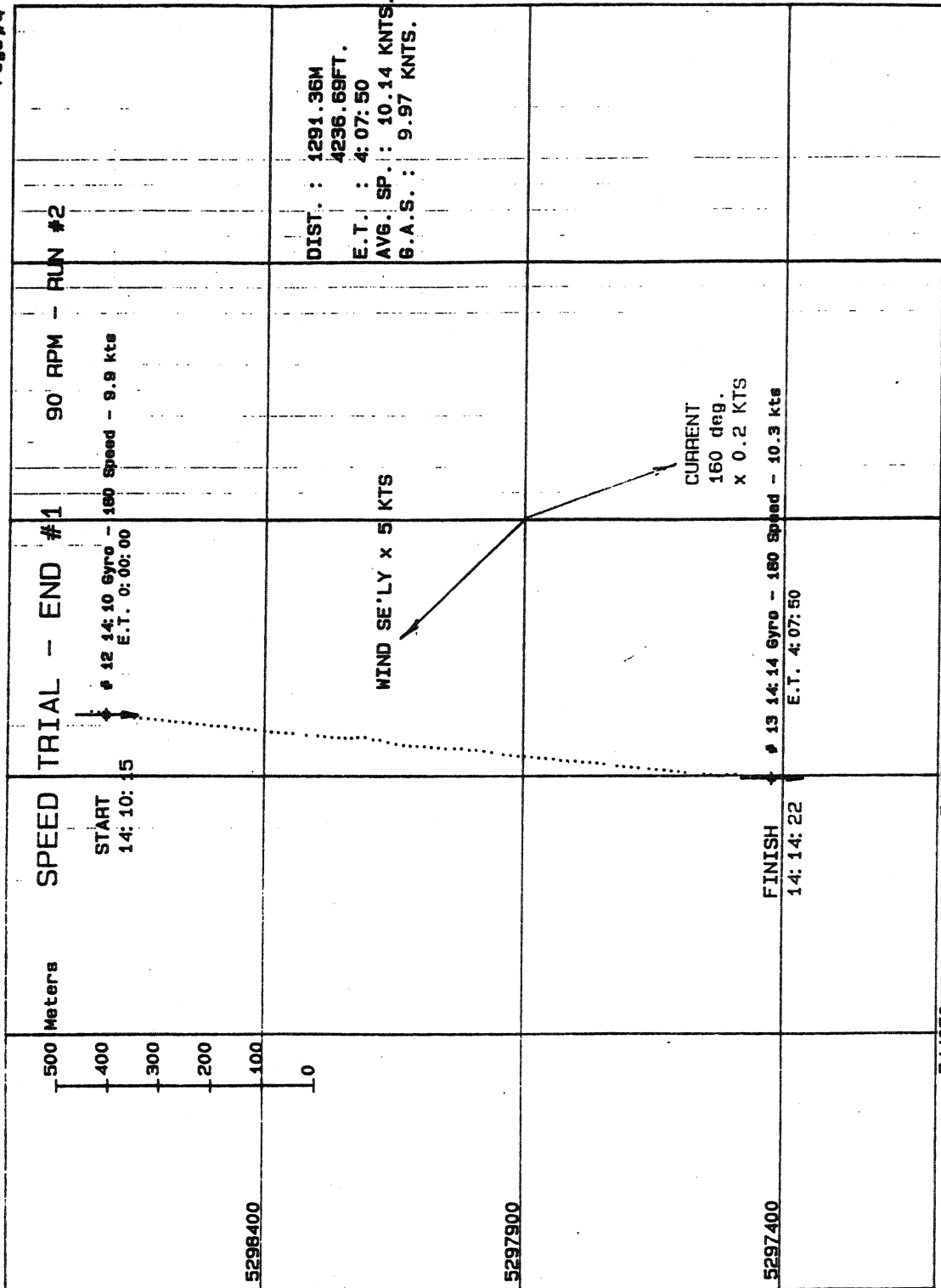
See Trials - M. V. Yakima

Mar 20/84

Scale : 1 - 10000

Page #3





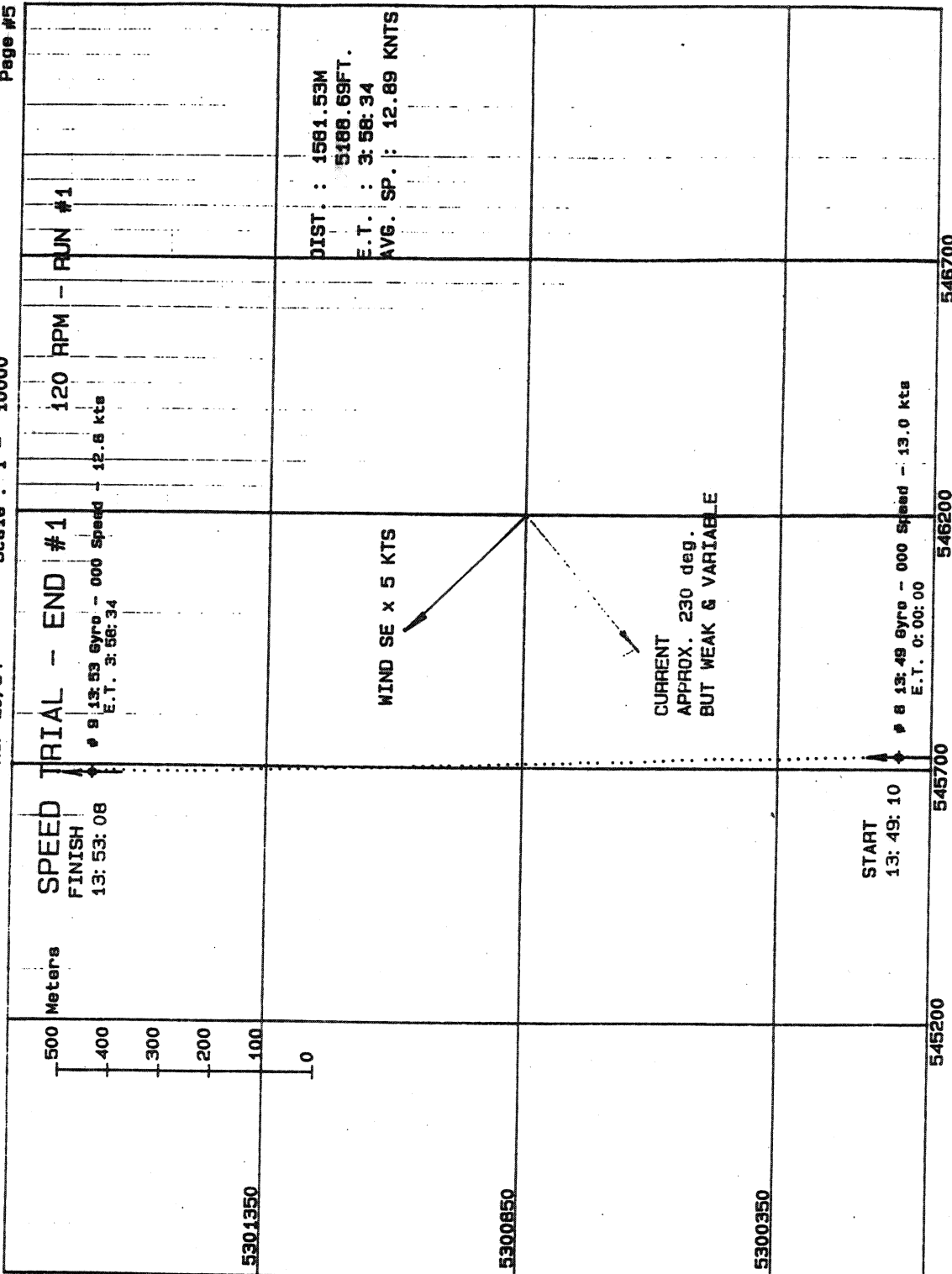
46010

Sea Trials - M. V. Yakima

Mar 20/84

Scale : 1 - 10000

Page #5

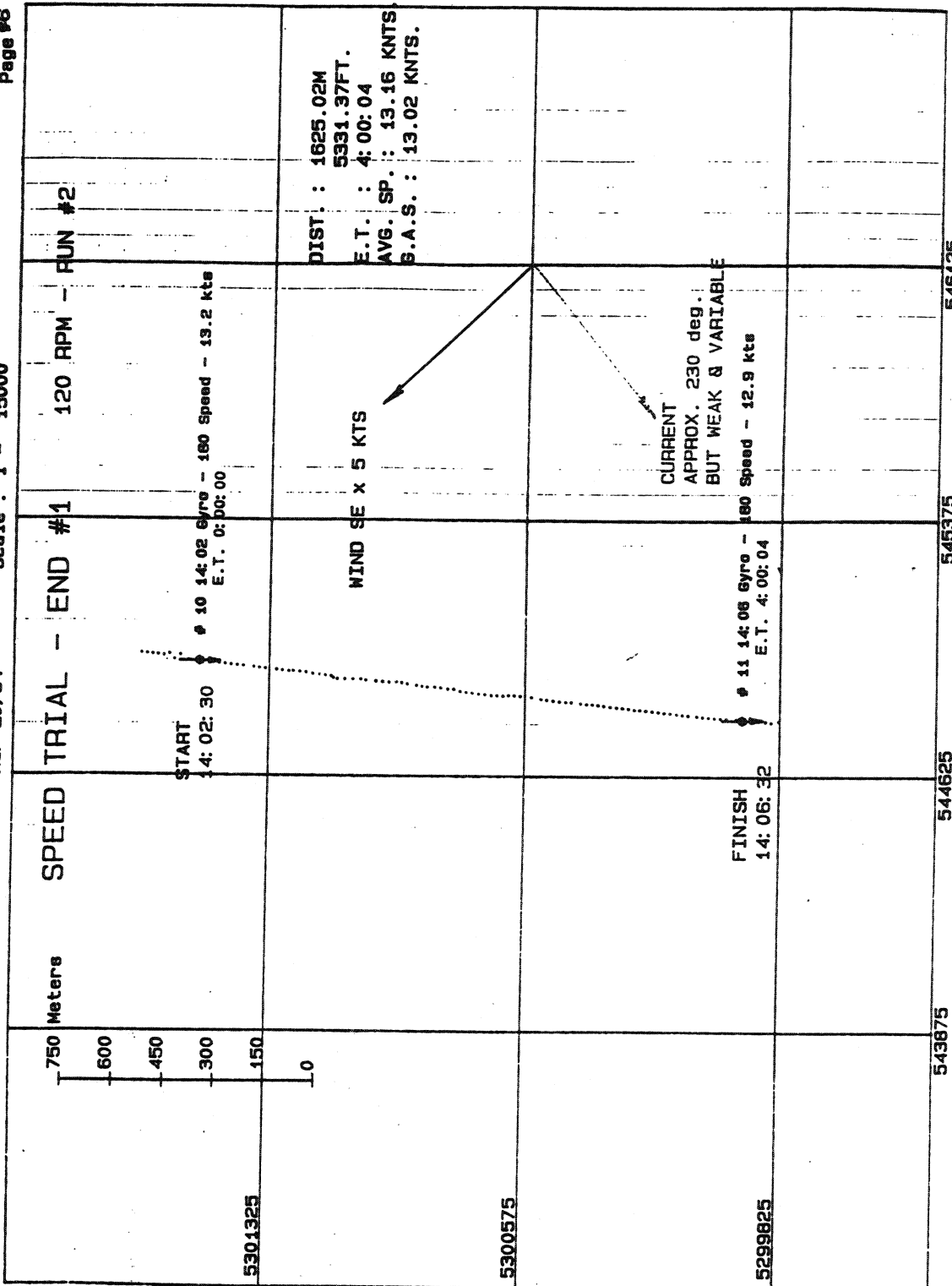


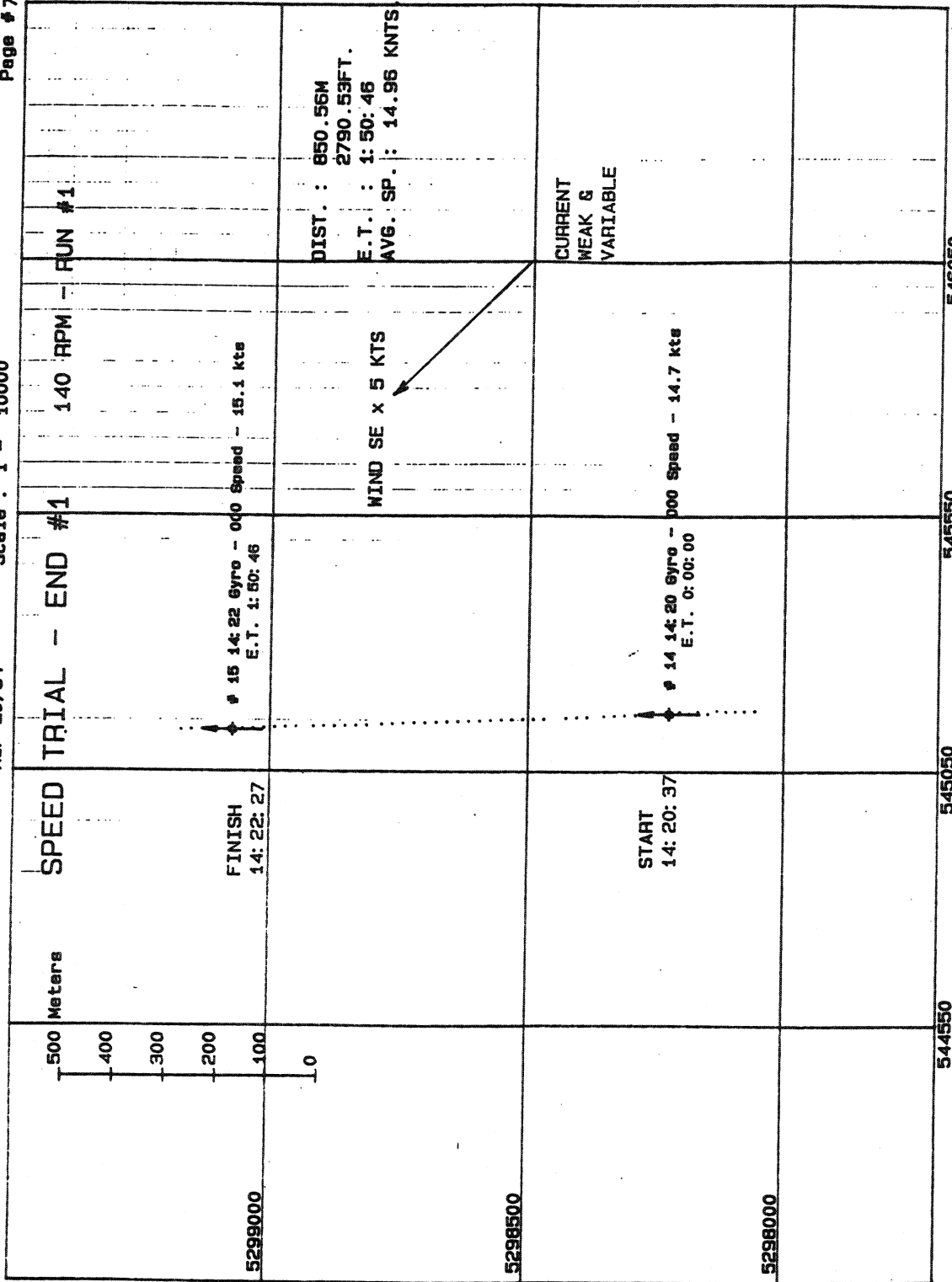
See Trials - M. V. Yakima

Mar 20/84

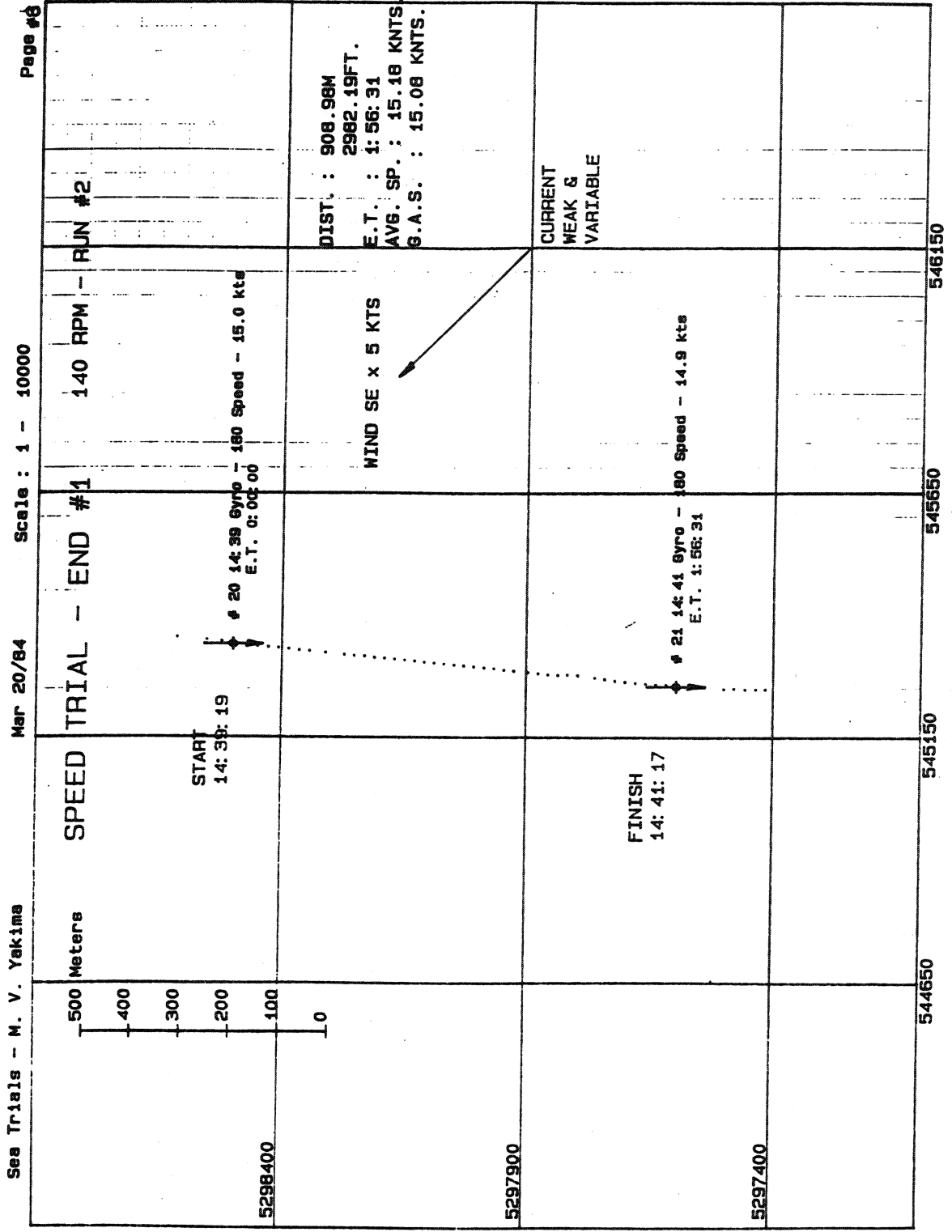
Scale : 1 - 15000

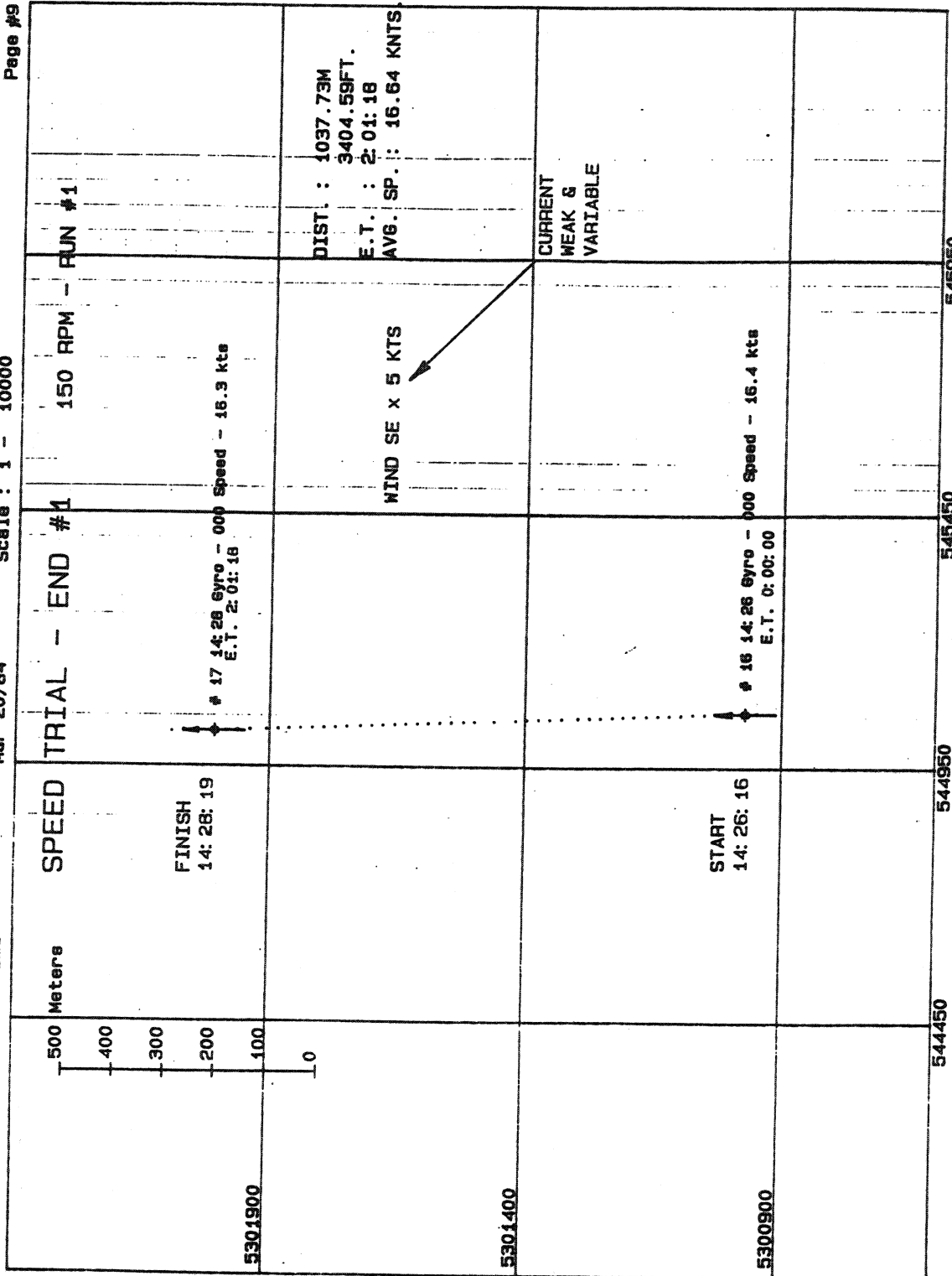
Page #6





461510





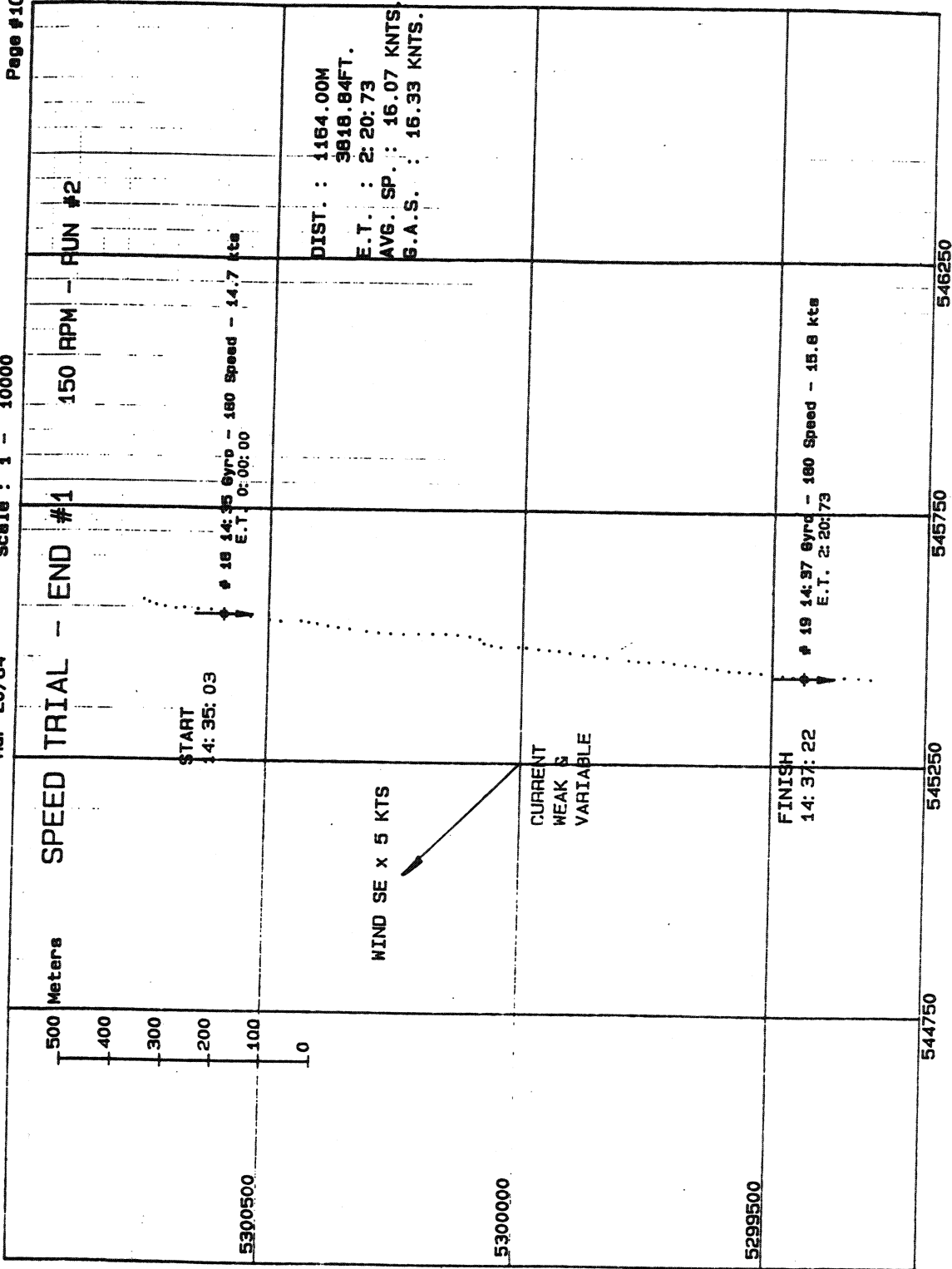
461110

See Trials - M. V. Yakima

Mar 20/84

Scale : 1 - 10000

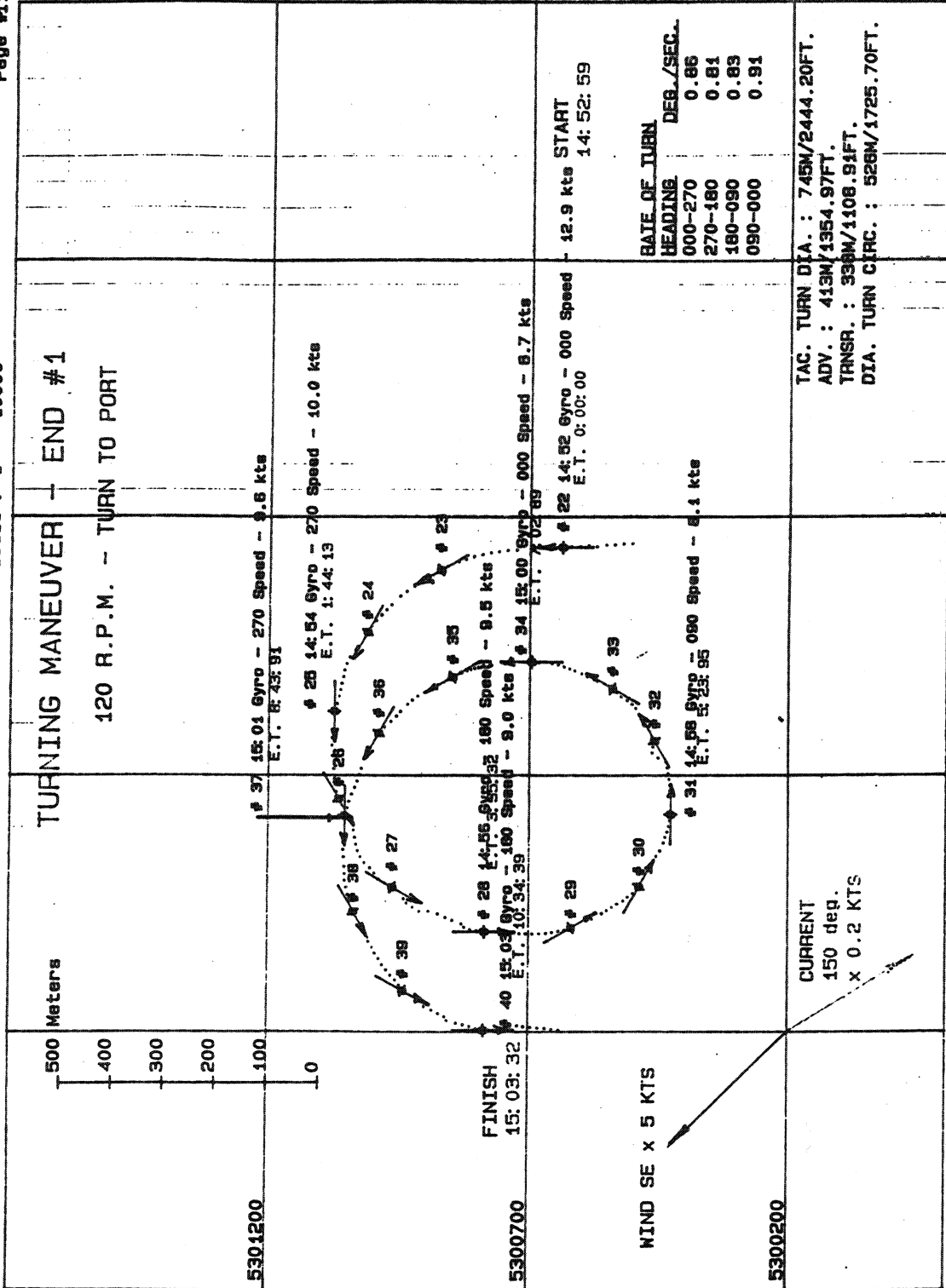
Page #10



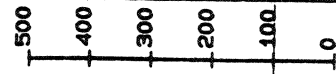
Sea Trials - M. V. Yakima

Mar 20/84

Scale : 1 - 10000

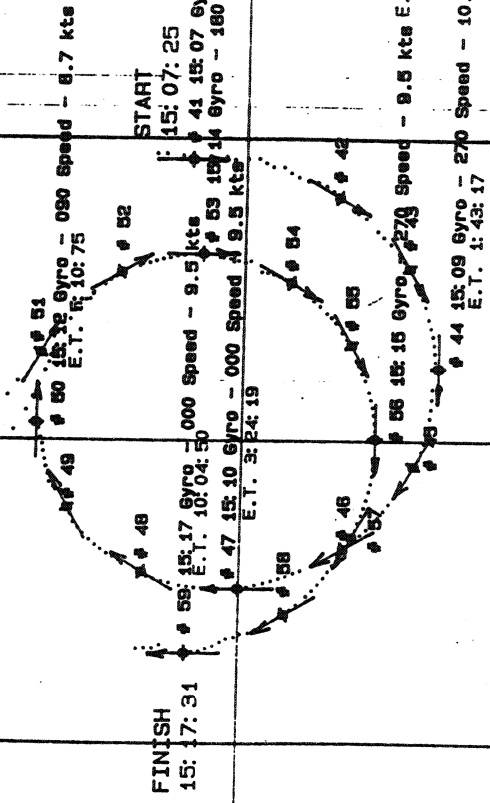


500 Meters



TURNING MANEUVER - END #1
 120 R.P.M. - TURN TO STARBOARD
 WIND SE x 5 KTS

CURRENT
 150 deg.
 x 0.2 KTS



FINISH
 15:17:31

START
 15:07:25

HEADINGS	DEG./SEC.
180-270	0.87
270-000	0.89
000-090	0.84
090-180	0.92

TAC. TURN DIA. : 712M/2395.93FT.
 ADV. : 386M/1266.38FT.
 TRANSR. : 371M/1217.18FT.
 DIA. TURN CIRC. : 557M/1827.41FT.

5299800

5299300

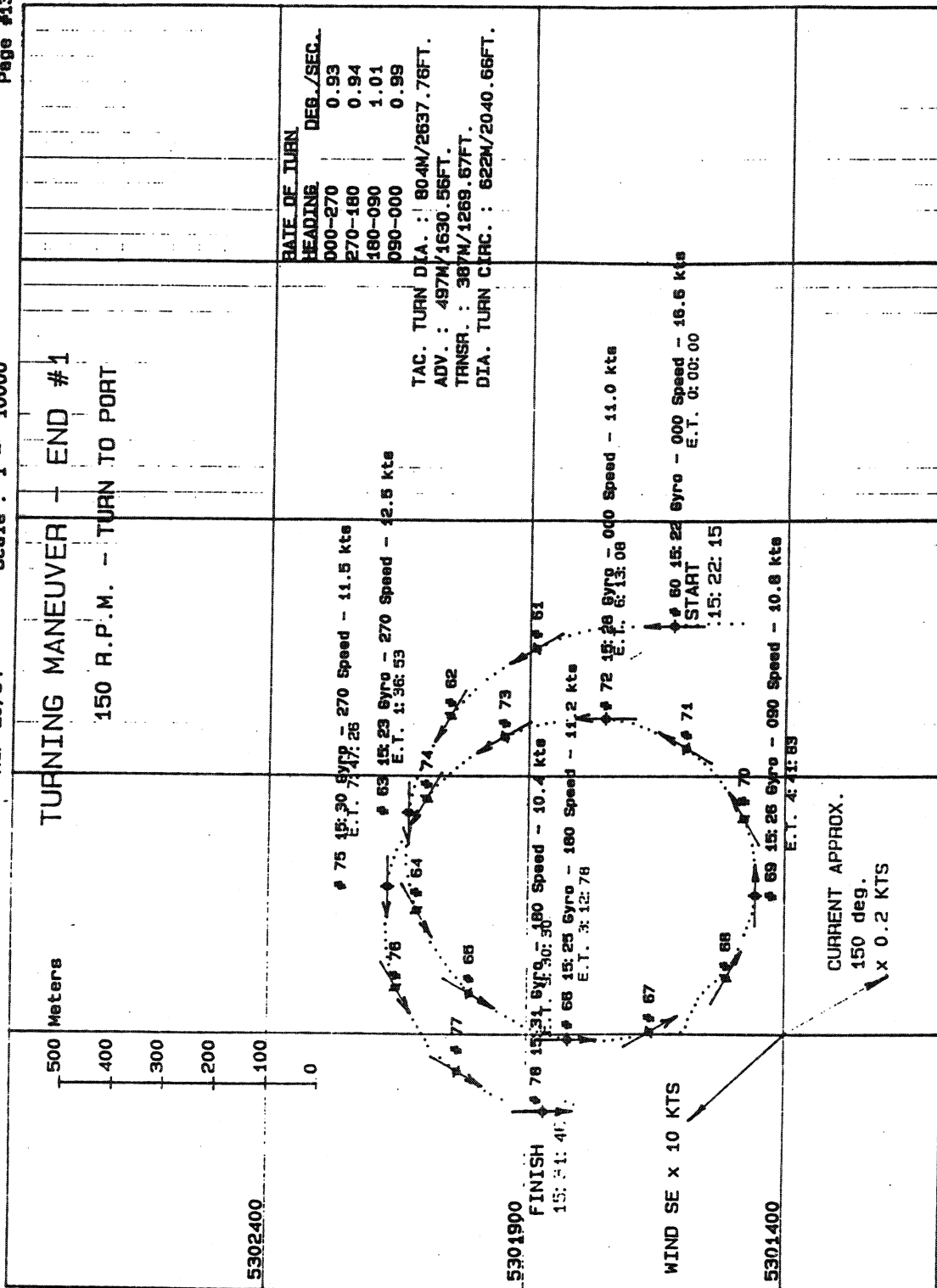
5298800

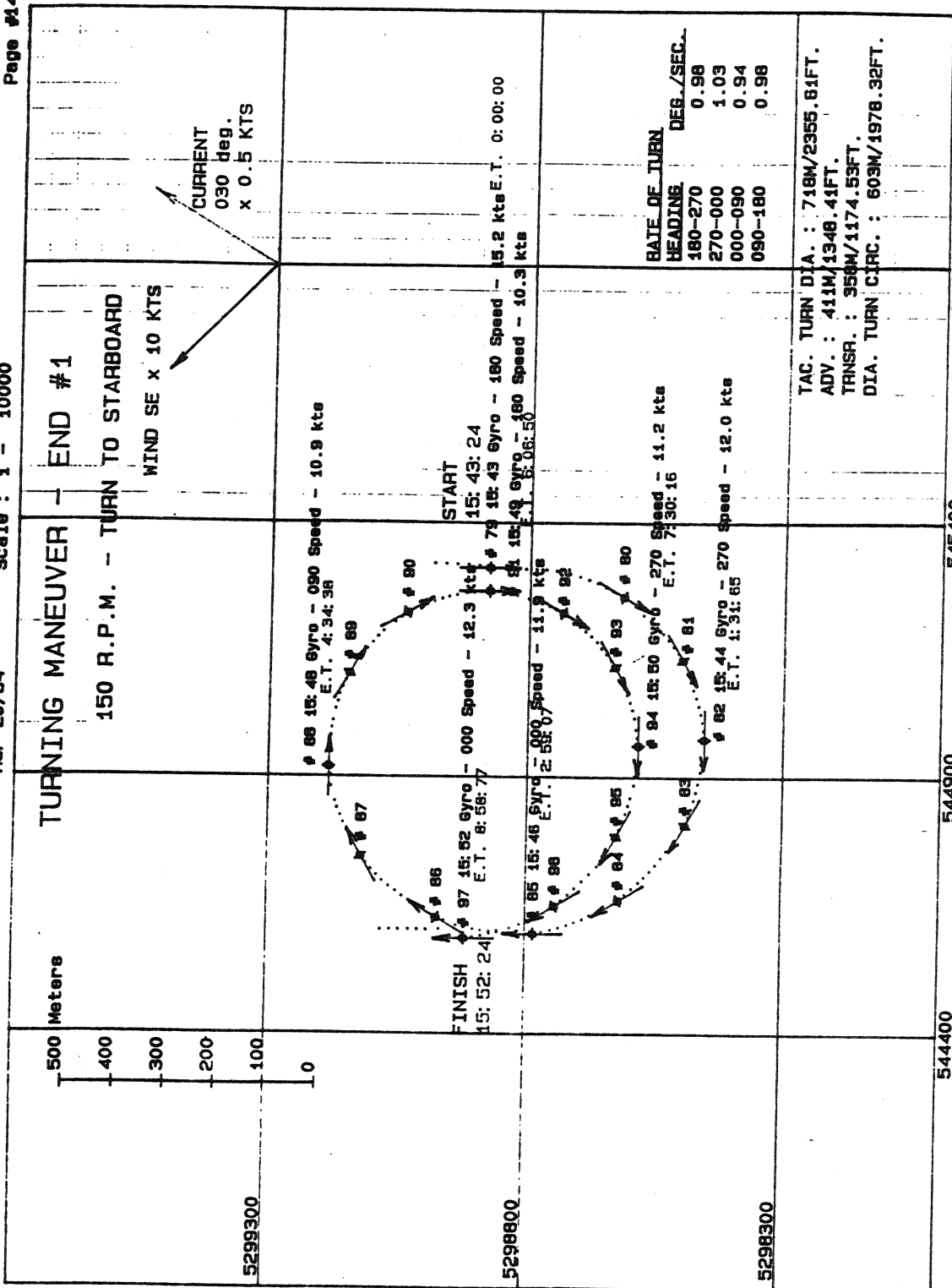
543700

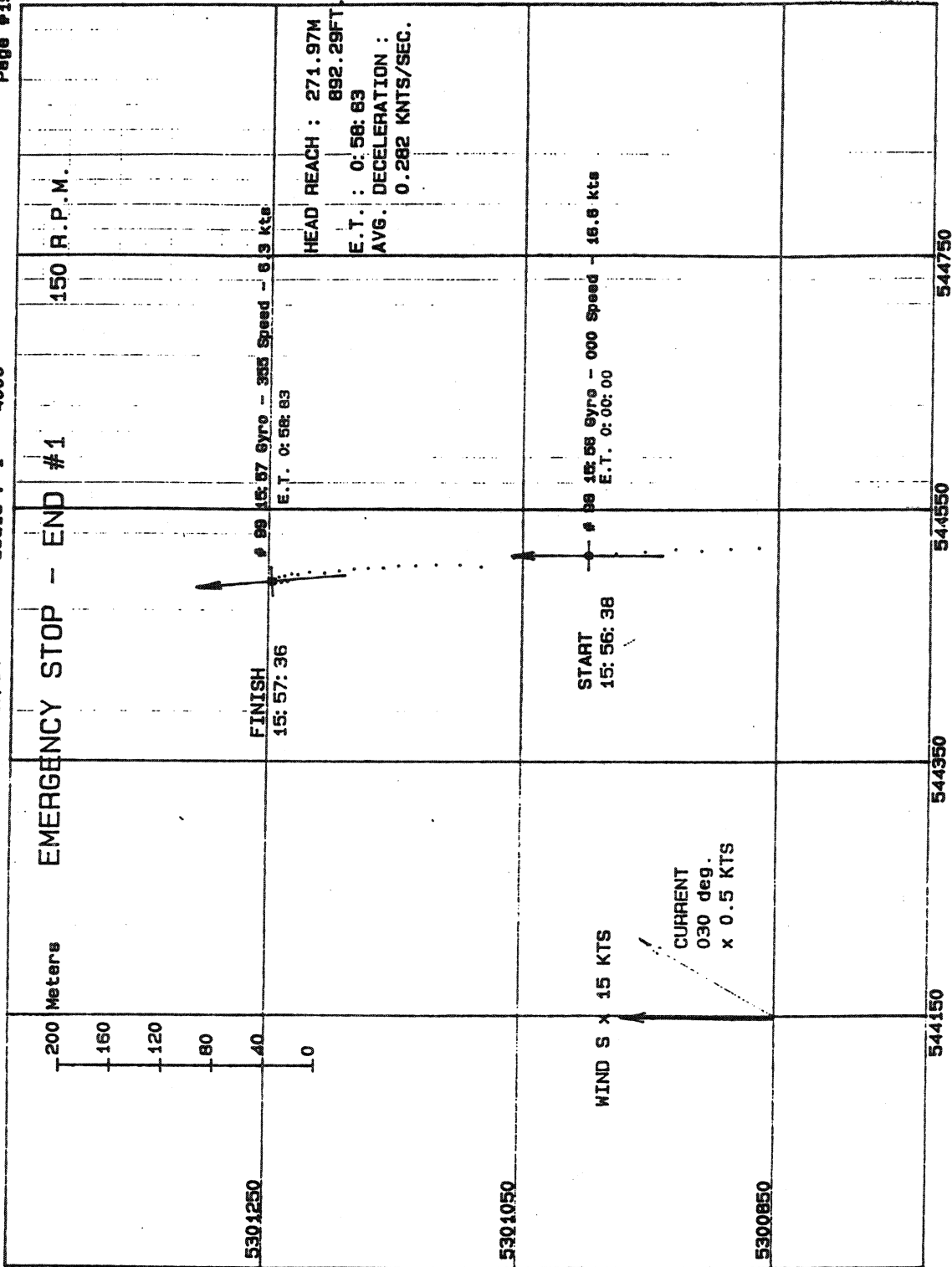
544200

544700

545200







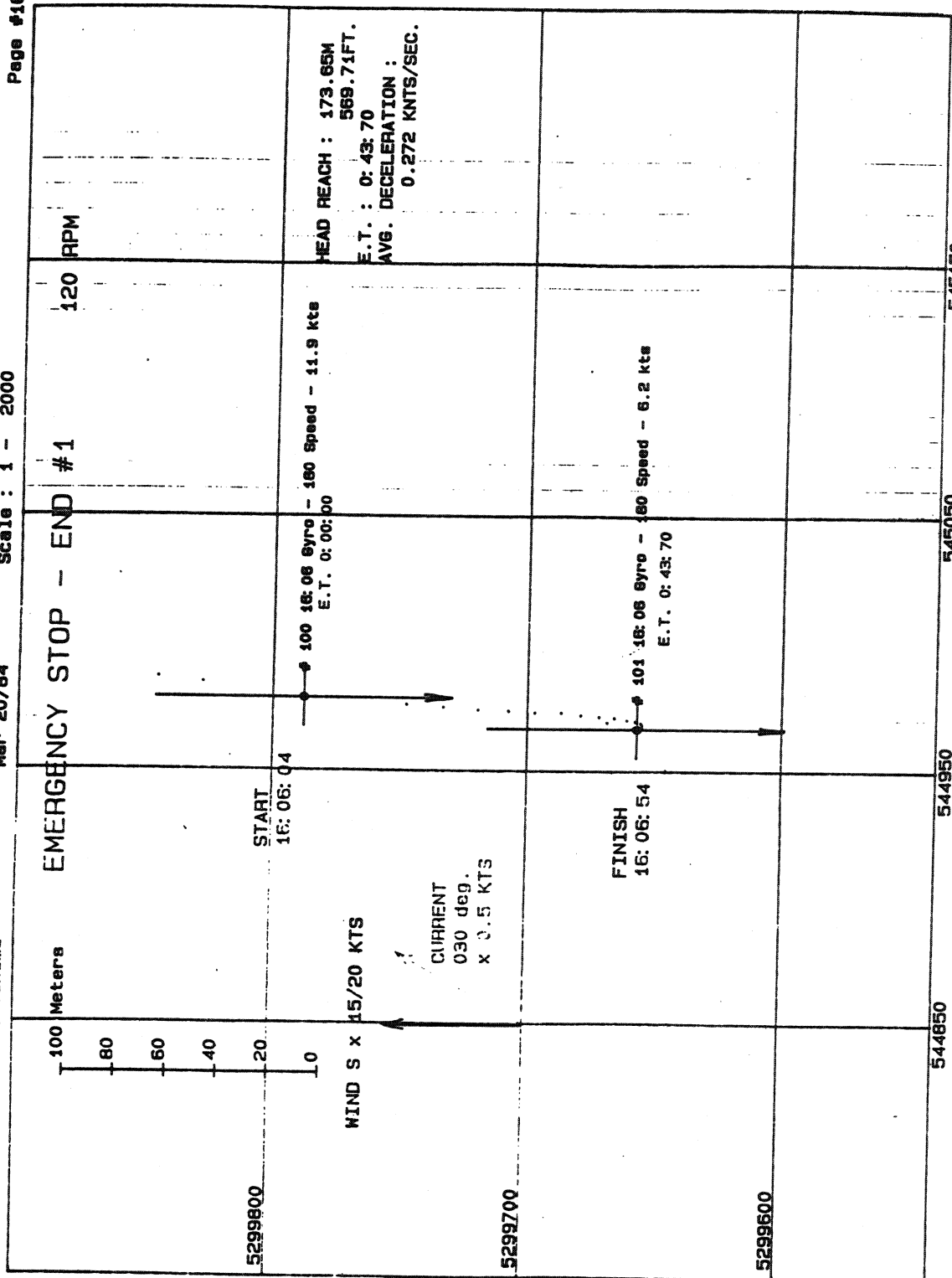
40-1116

Sea Trials - M. V. Yakima

Mar 20/84

Scale : 1 - 2000

Page #16



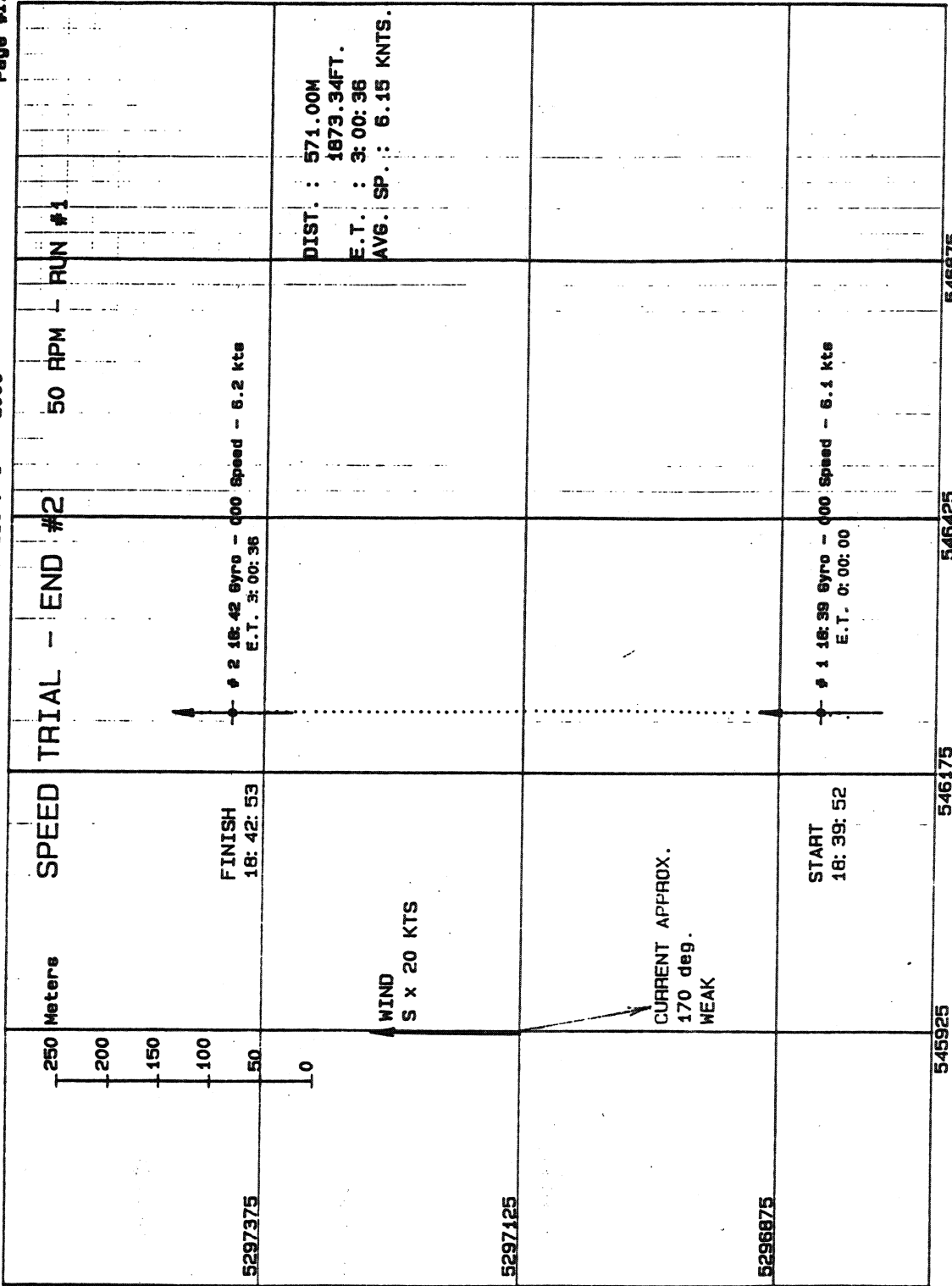
END #2

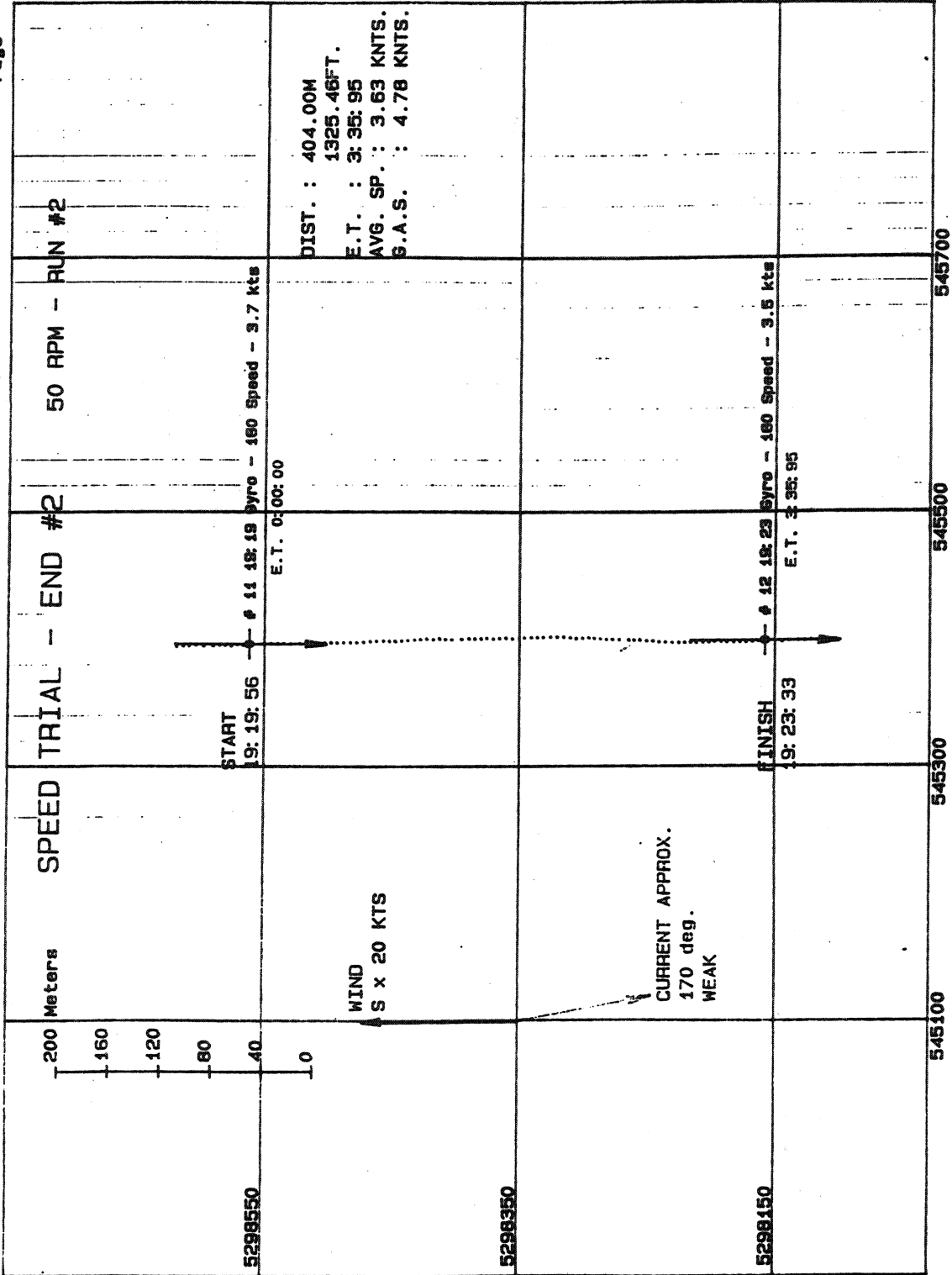
46-1510

See Trials - M. V. Yakima

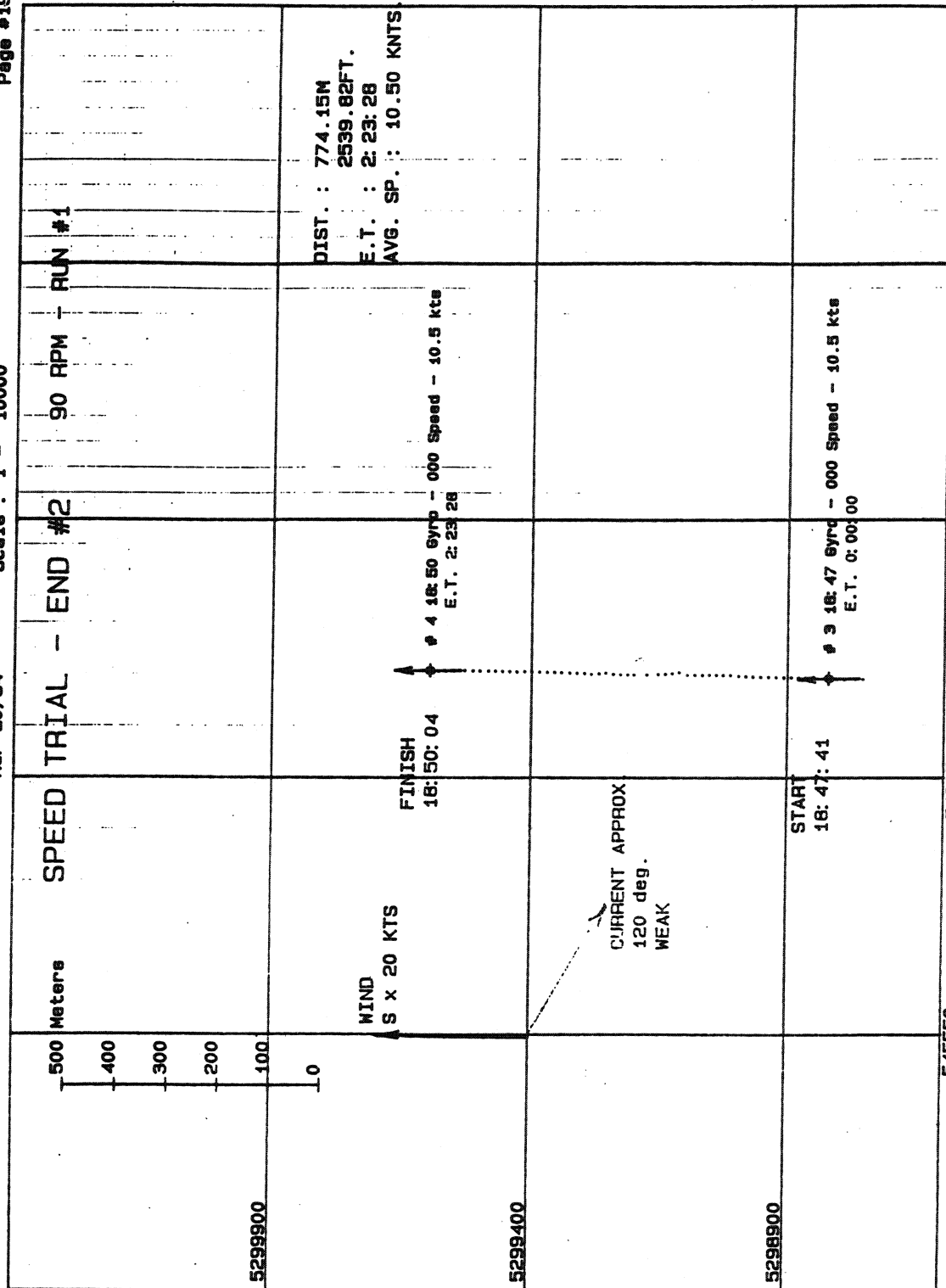
Mar 20/84

Scale : 1 - 5000





431310



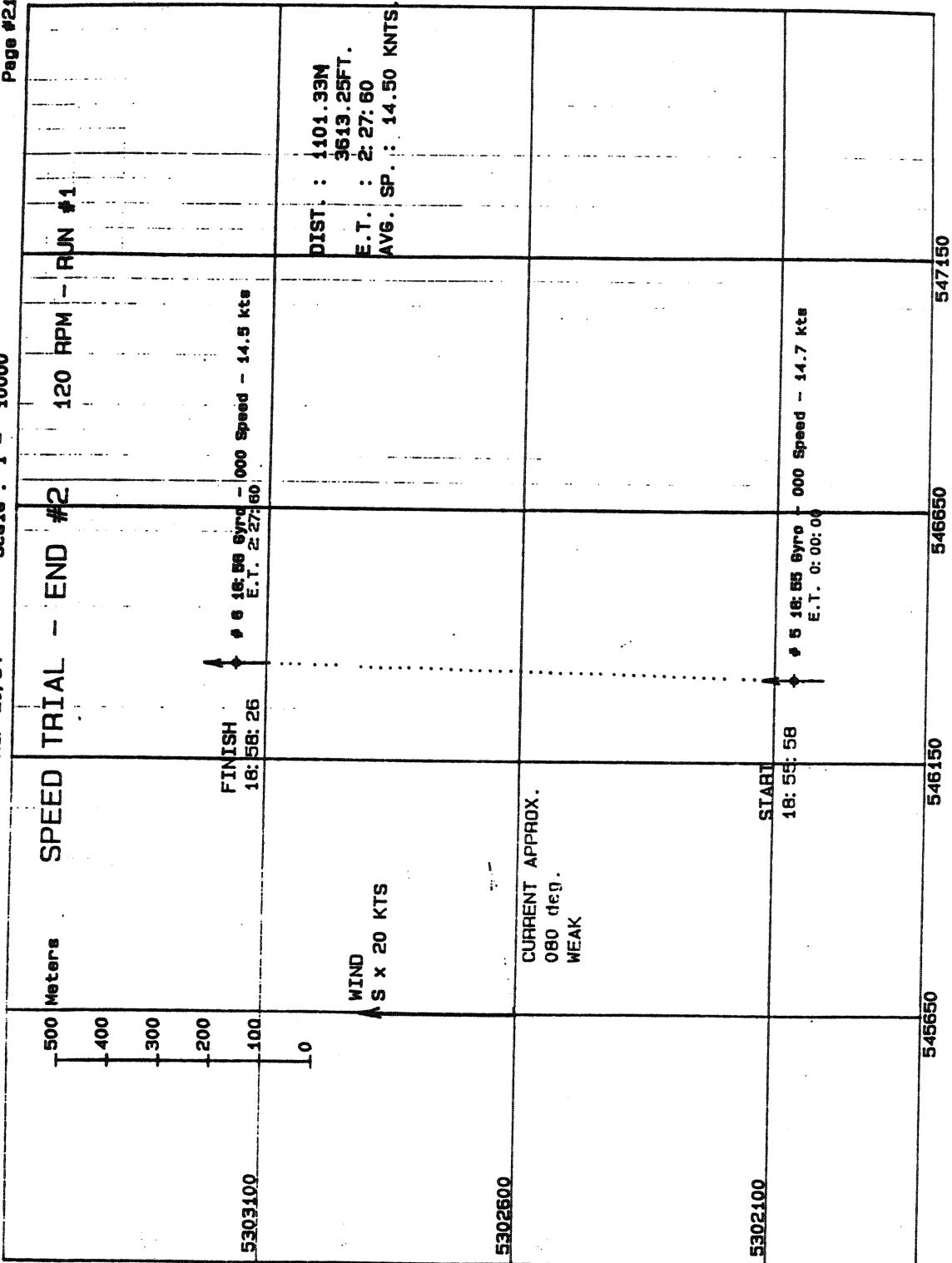
46110

See Trials - M. V. Yakima

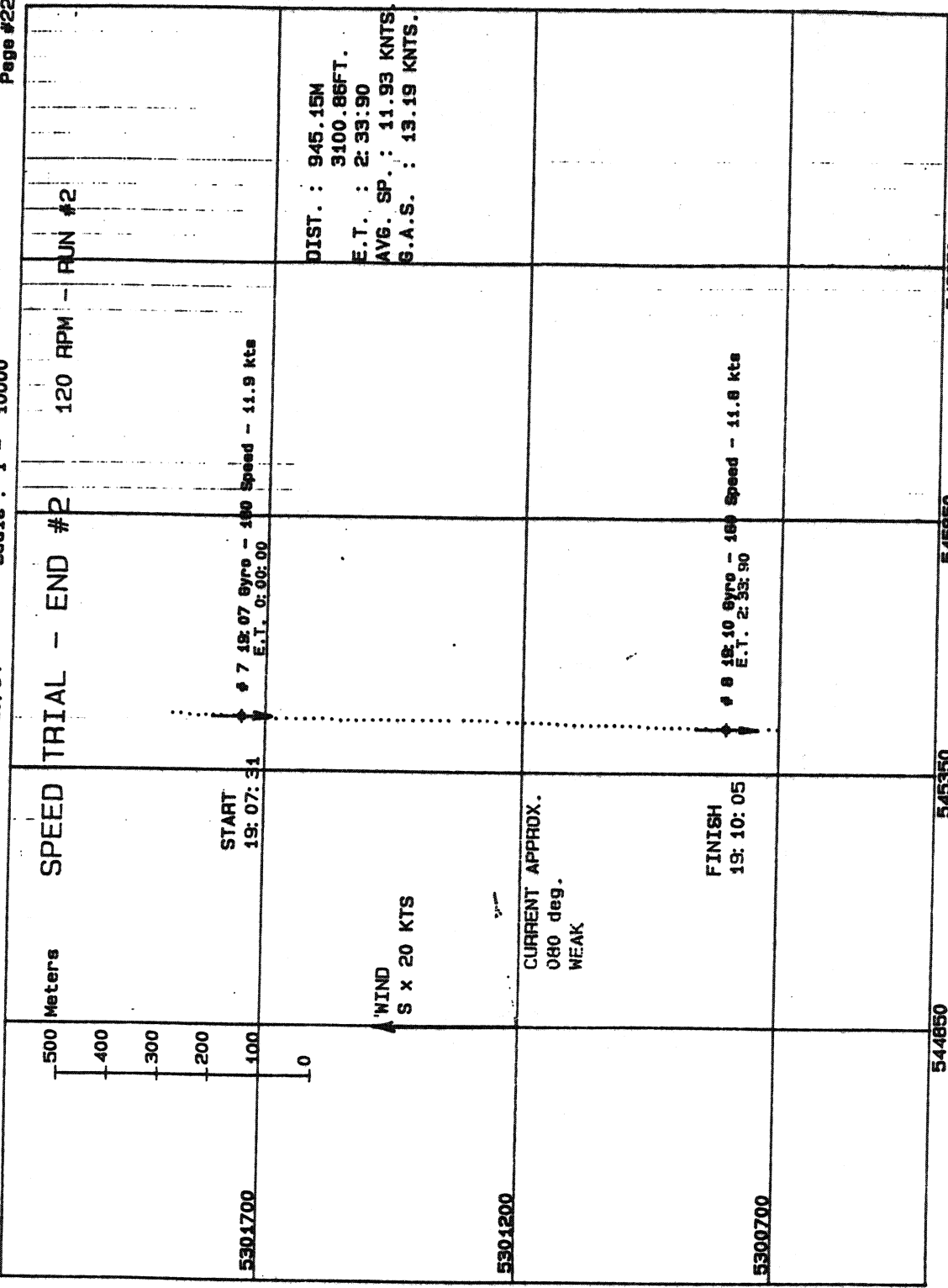
Mar 20/84

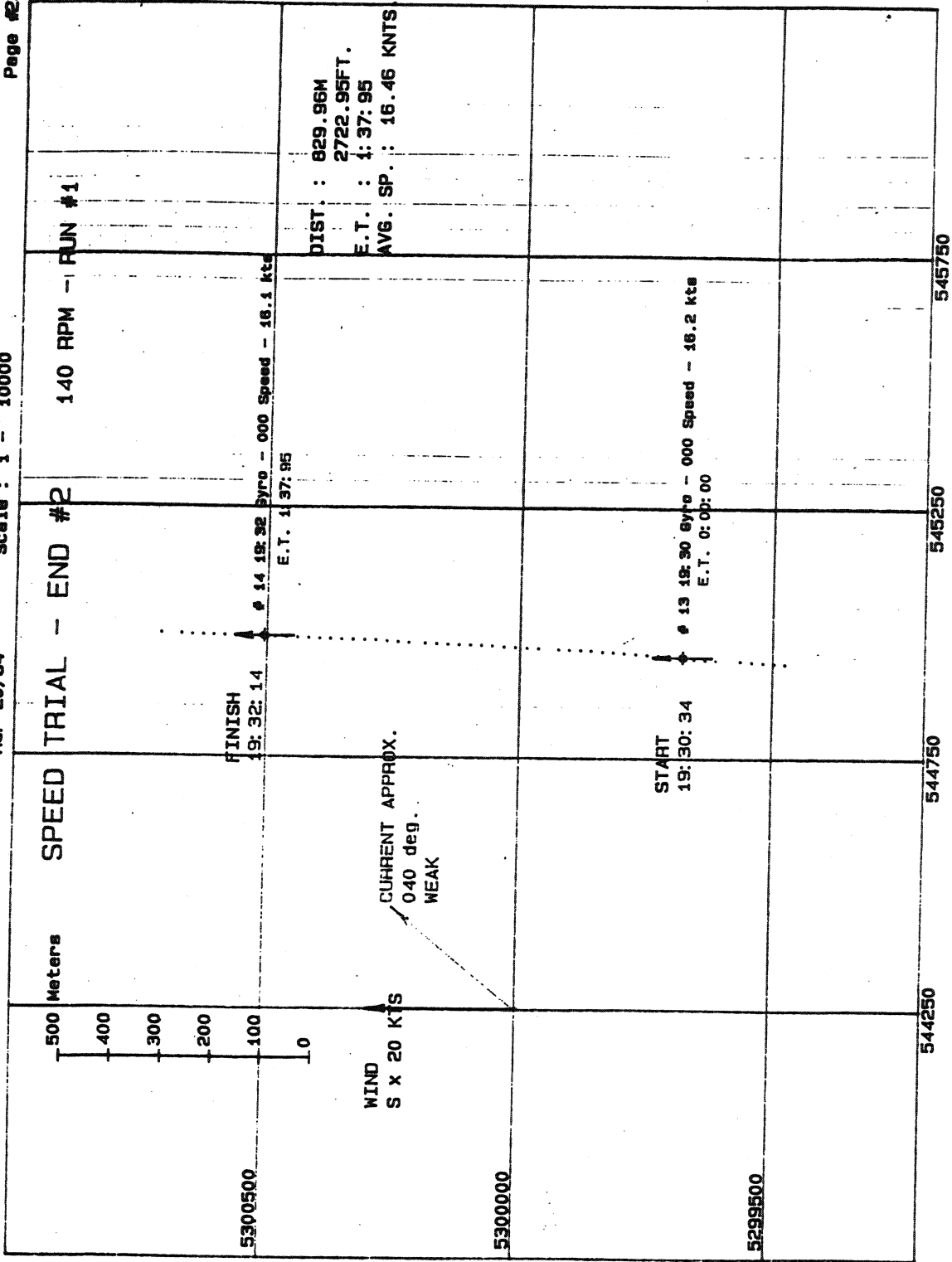
Scale : 1 - 10000

Page #21



461110





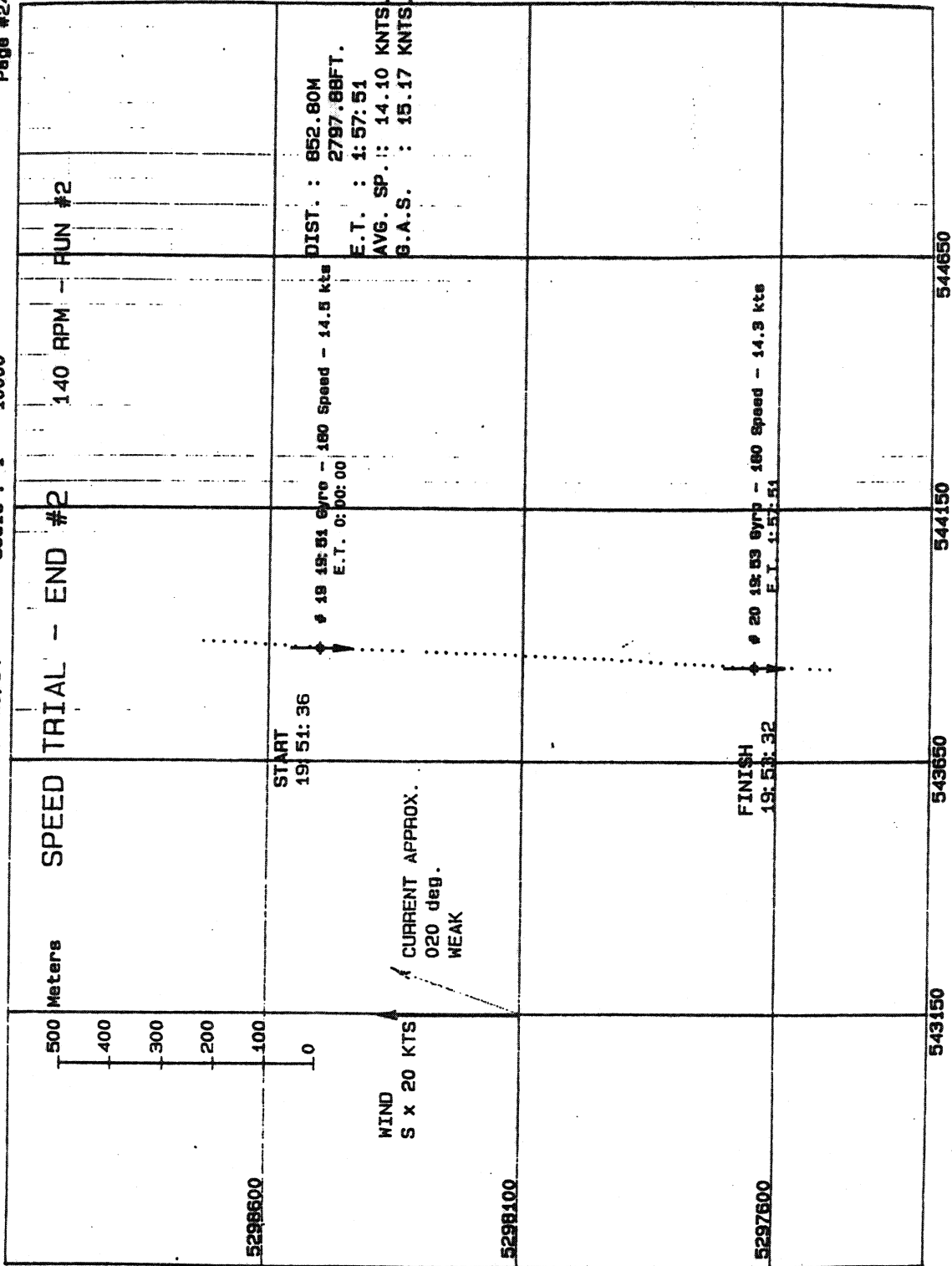
451010

See Trials - M. V. Yakima

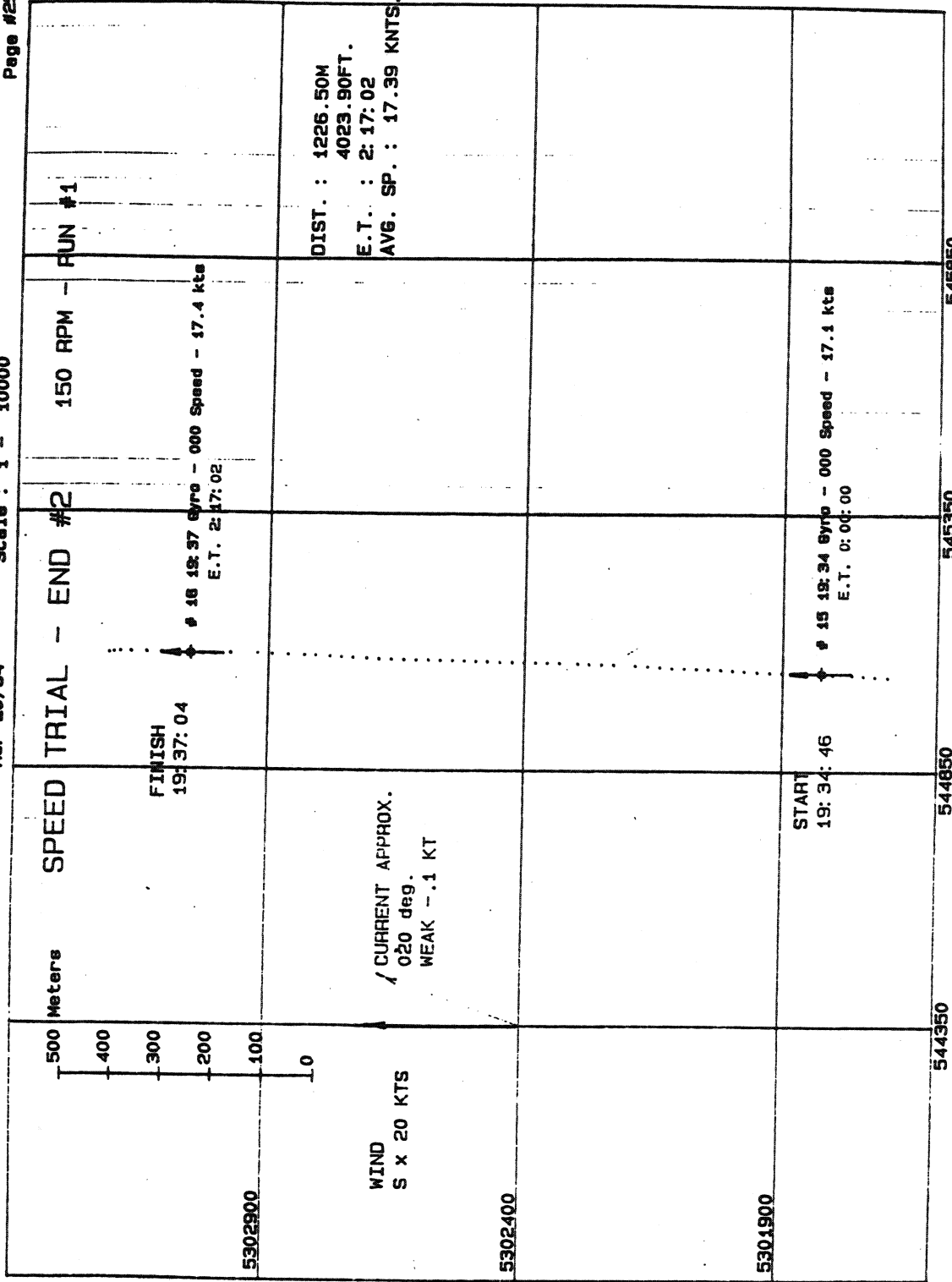
Mar 20/84

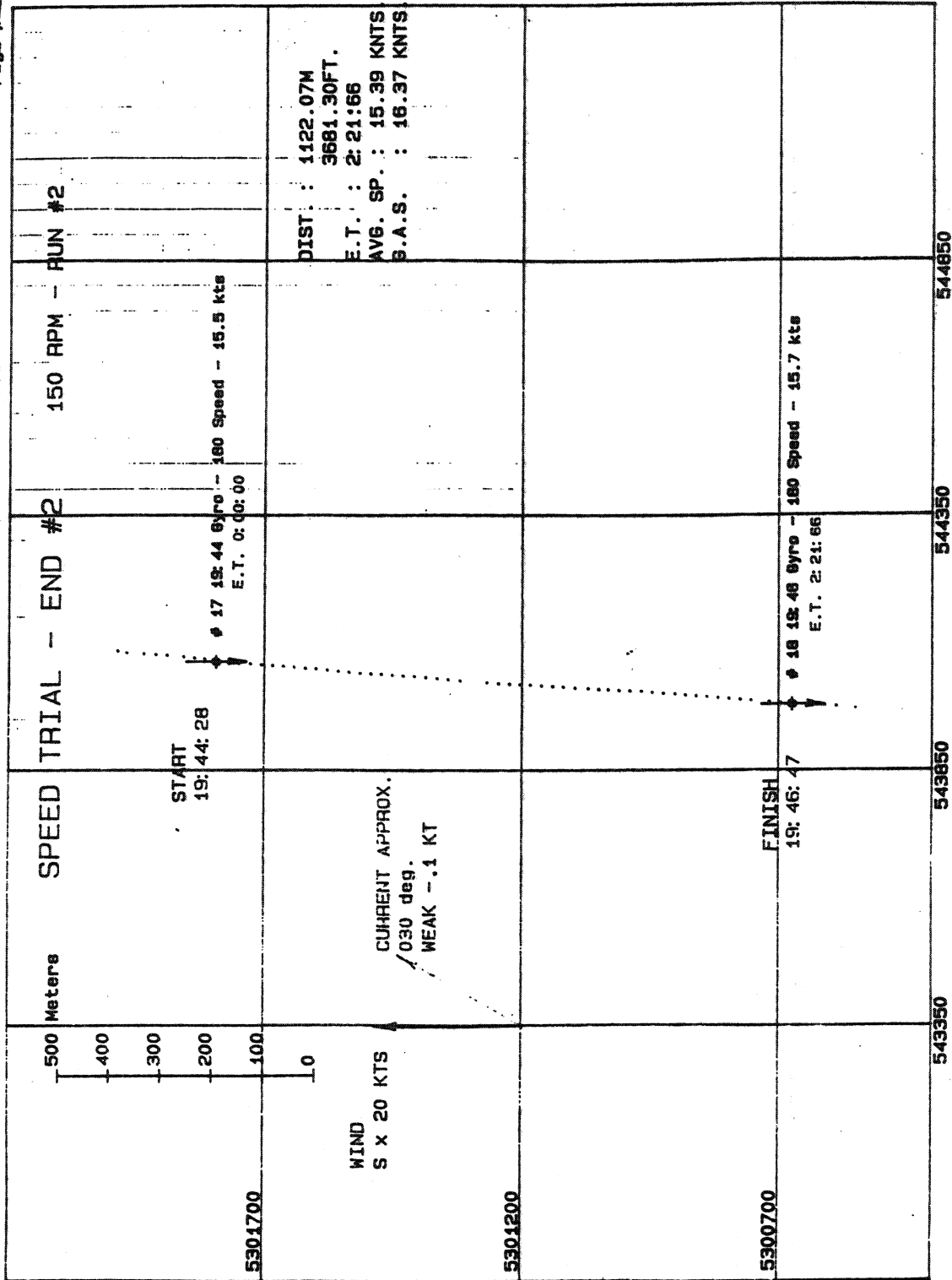
Scale : 1 - 10000

Page #24



4-1-10





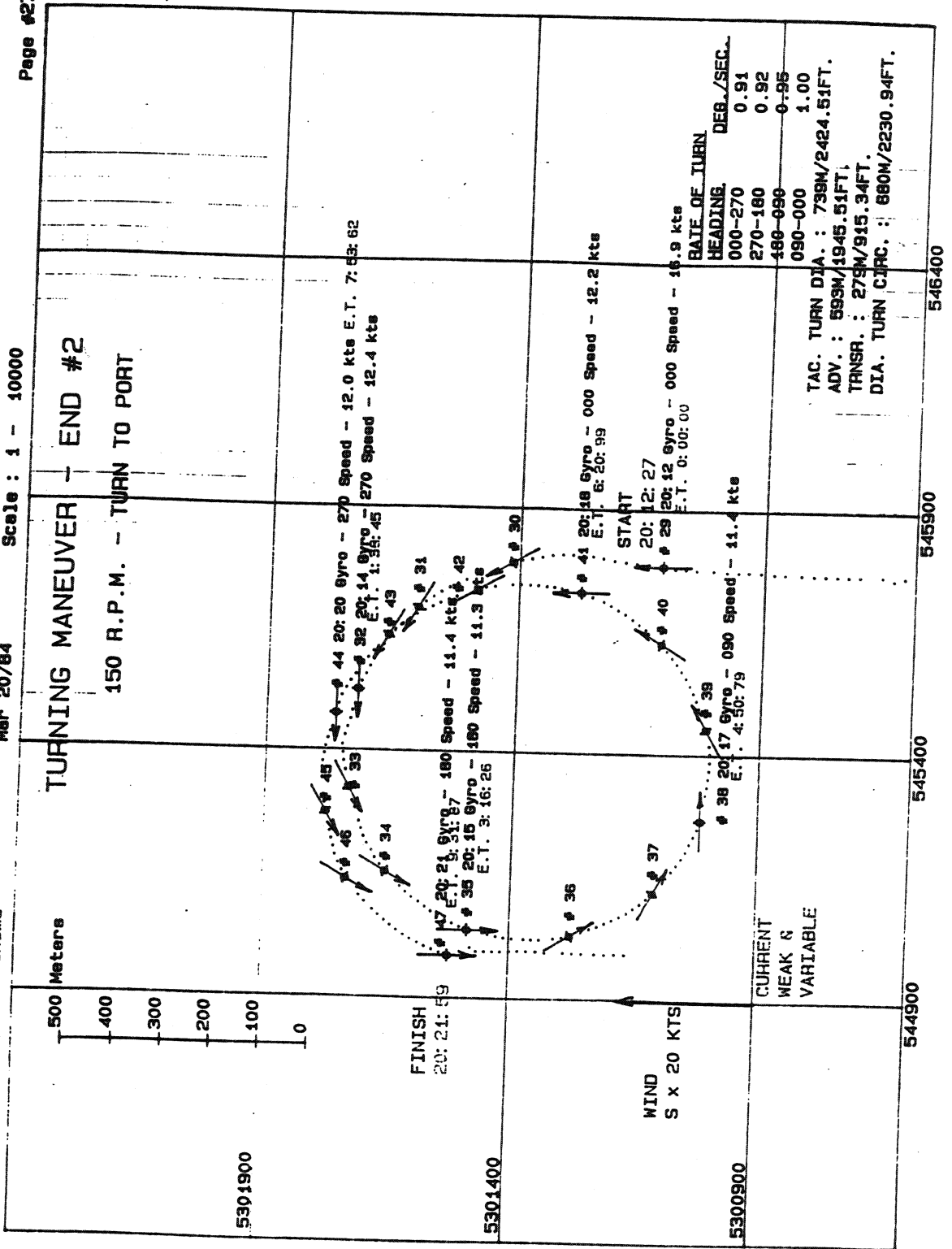
401110

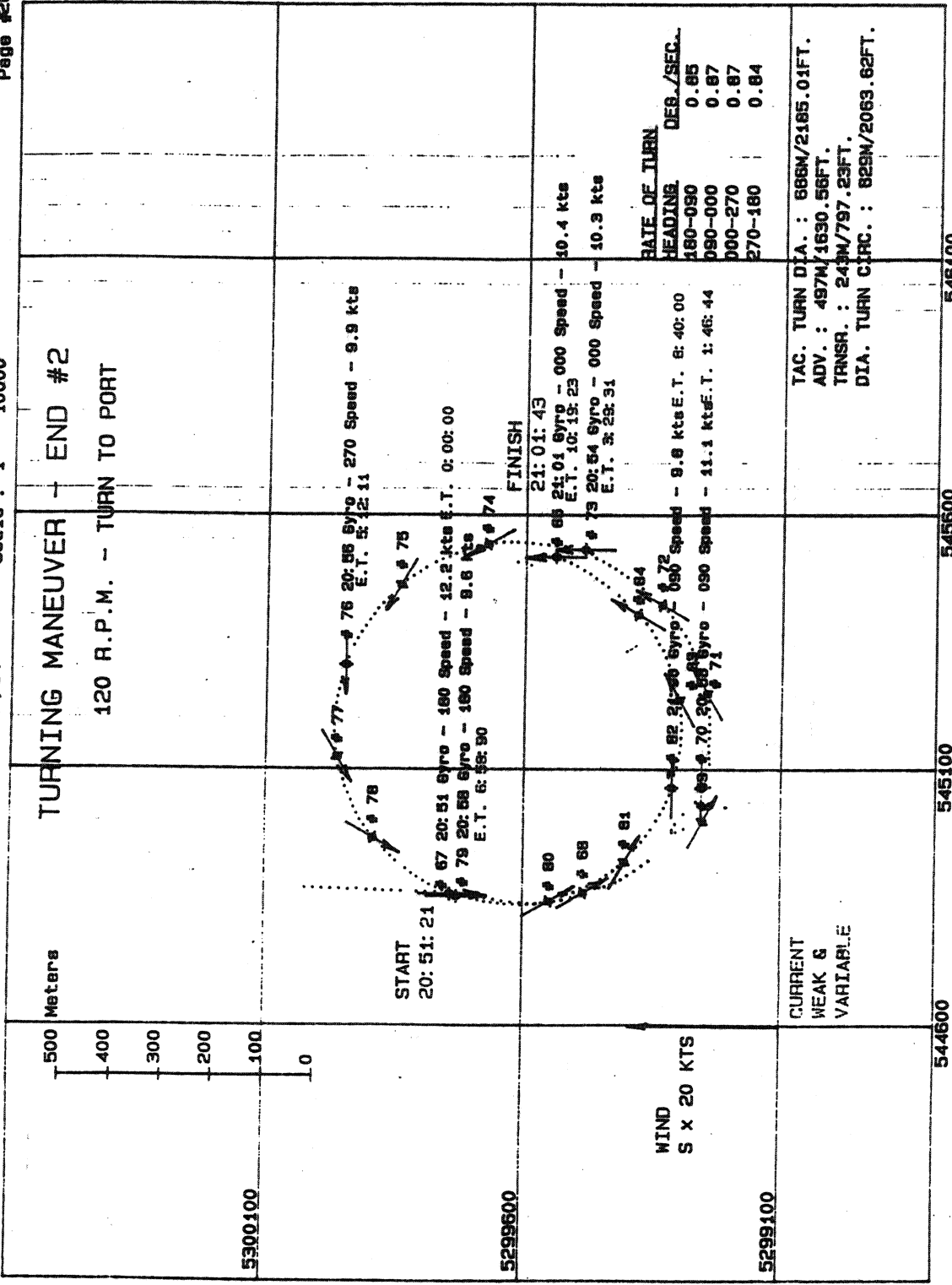
Sea Trials - M. V. Yakima

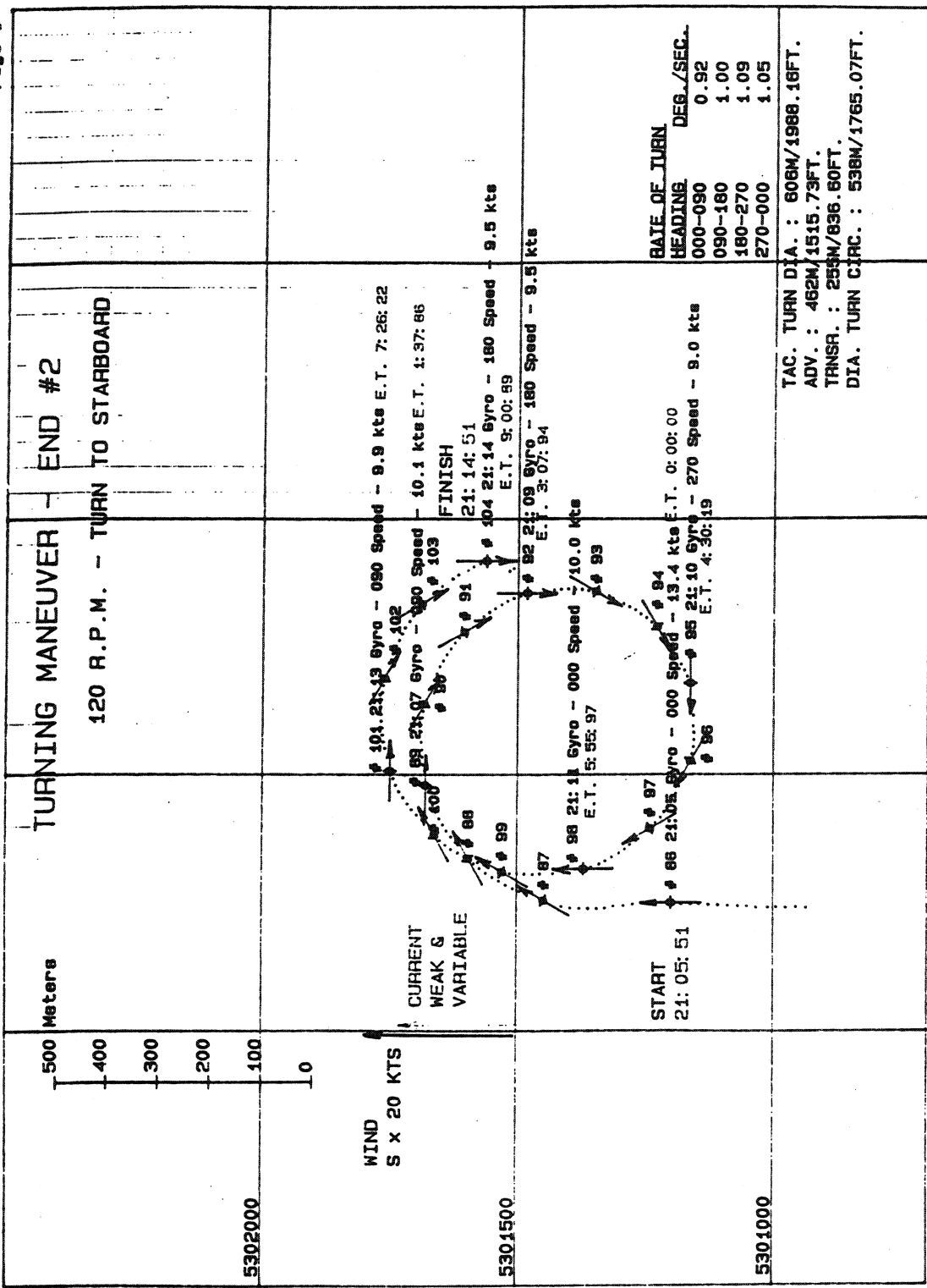
Mar 20/84

Scale: 1 - 10000

Page #27







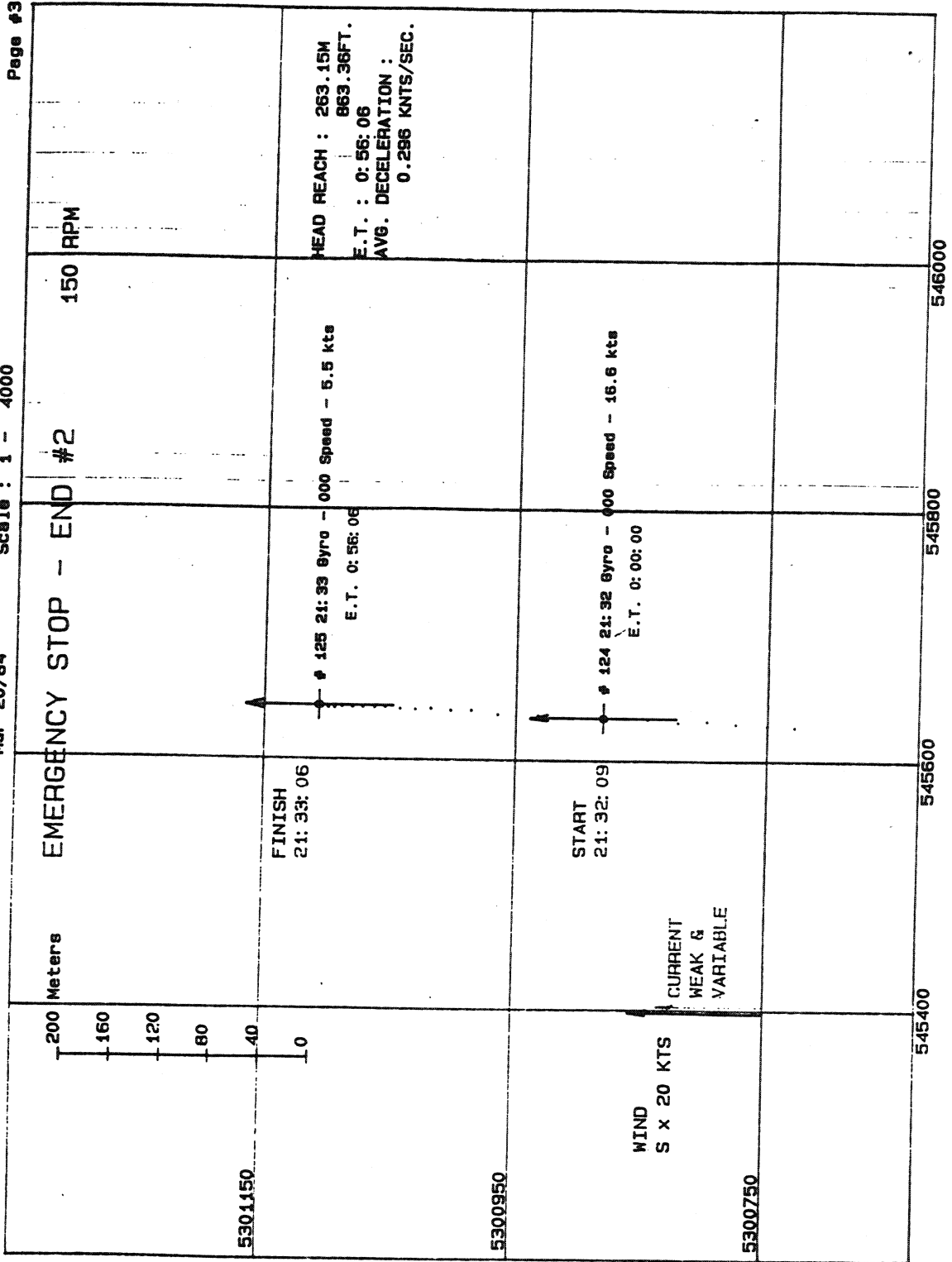
451009

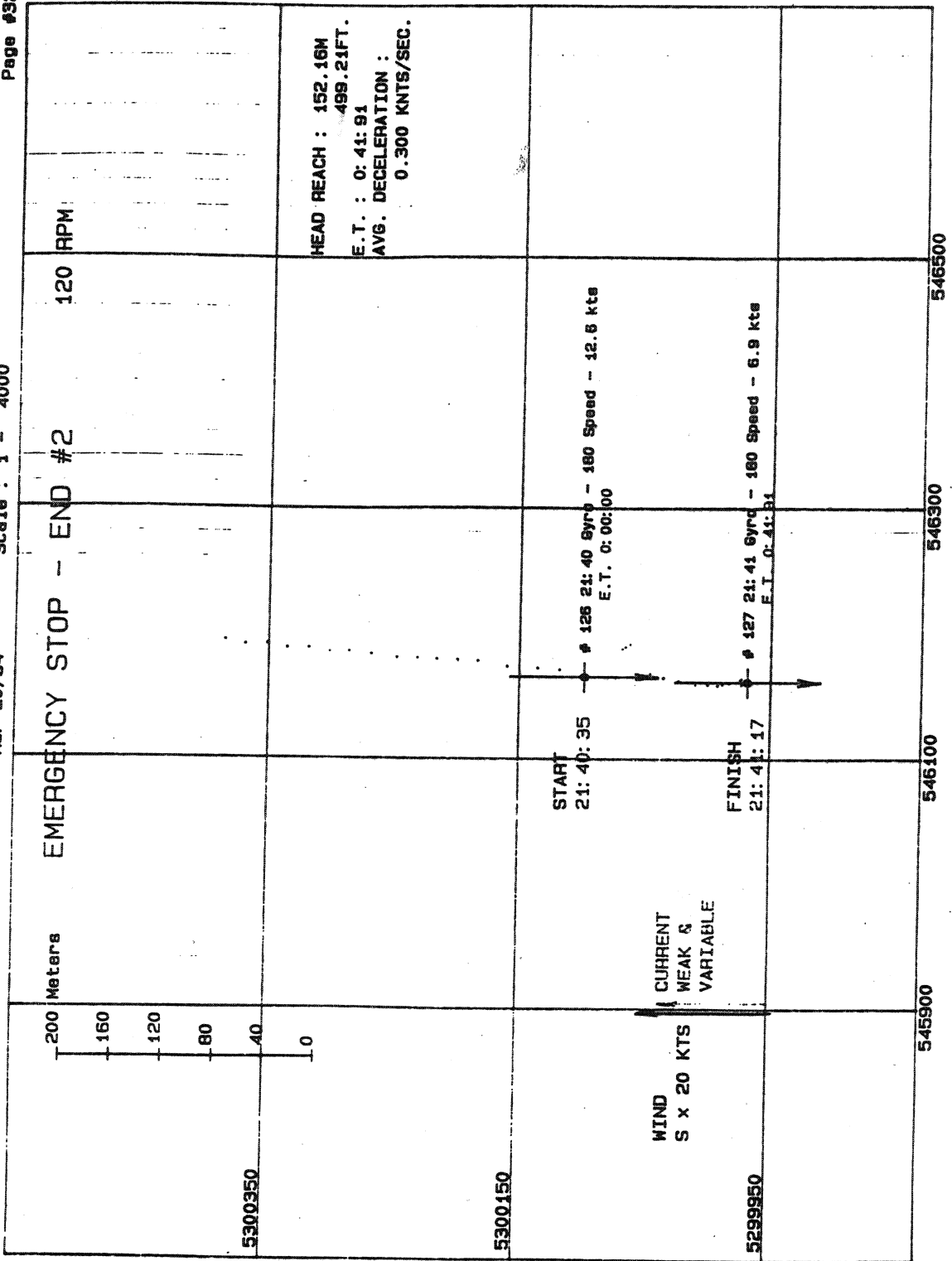
See Trials - M. V. Yakima

Mar 20/84

Scale : 1 - 4000

Page #31





SUPER CLASS MANEUVERING DATA

PILOTHOUSE NO.
IN COMMAND

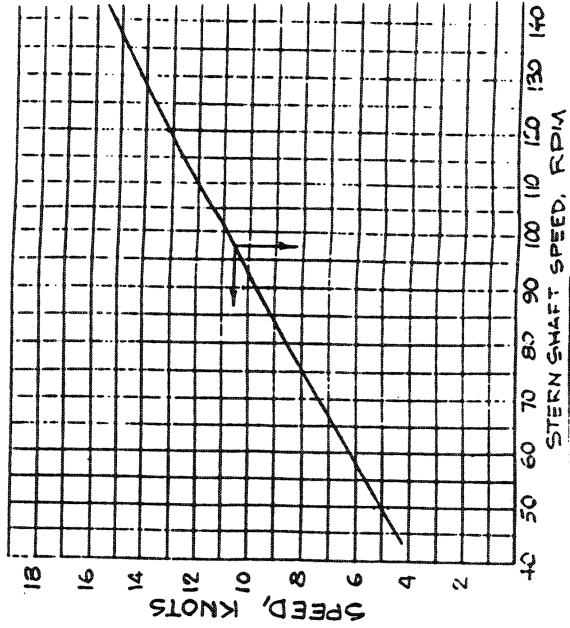
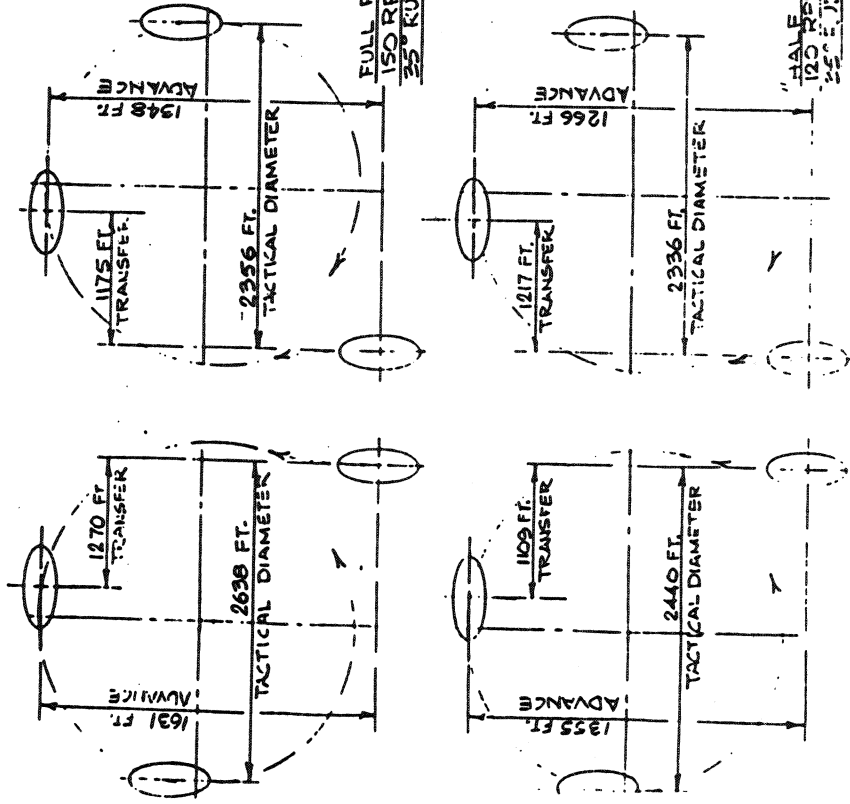
NOTE: DATA DERIVED FROM TEST BY OSN, LTD.,
MARCH 20, 1984, ON MV YAKIMA. DRAFT= 17'-2".
S.P. APPROX. 2800 TONS AT MOST AIDWAY BETWEEN
LIGHT SHIP (2363 TONS) AND FULL LOAD (3283 TONS)

WARNING:
THE RESPONSE OF THE
DIFFERENT FROM THAT SHOWN HERE IF ANY OF THE
FOLLOWING CONDITIONS UPON WHICH THE MANEUVERING
INFORMATION IS BASED ARE VARIED:

1. CALM WEATHER - WIND 10 KN OR LESS, CALM SEA
2. NO CURRENT
3. WATER DEPTH TWICE THE VESSEL'S DRAFT OR GREATER
4. CLEAN HULL
5. DIFFERENT DRAFT OR UNUSUAL TRIM

CRASH STOPS

INITIAL CONDITN	DEAD IN WATER		
RPM	SPEED	TIME	REACH
150	15.5 KN	59 SEC.	892 FT
120	13.1 KN	44 SEC.	570 FT



"SUPER" CLASS MANEUVERING DATA

PILOTHOUSE 1
IN COMMAND

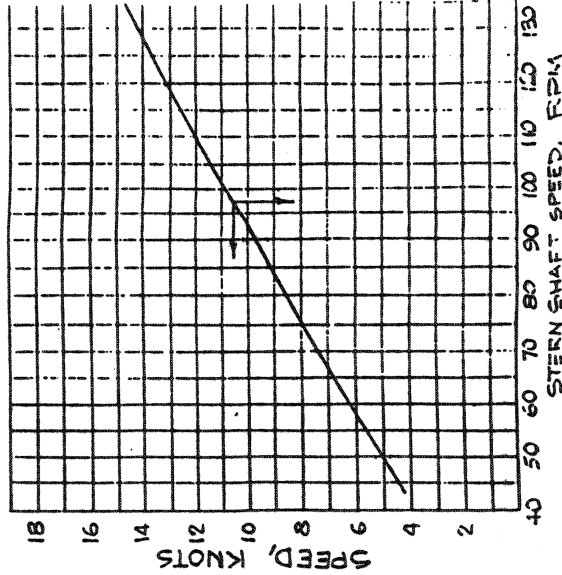
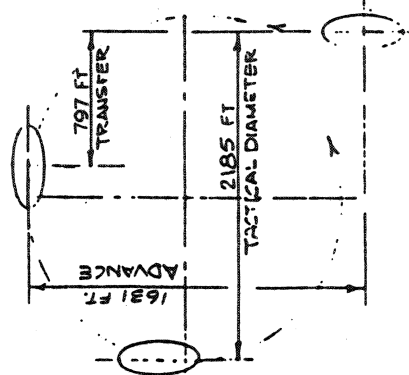
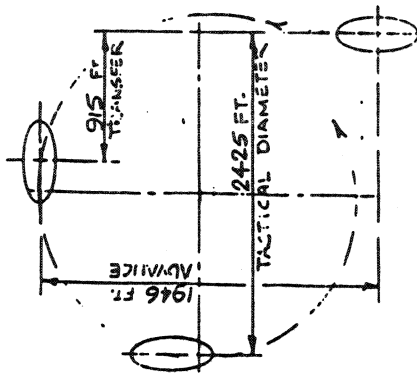
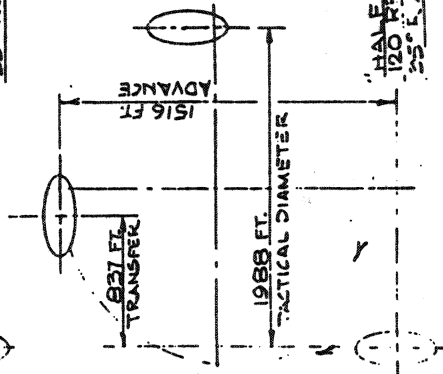
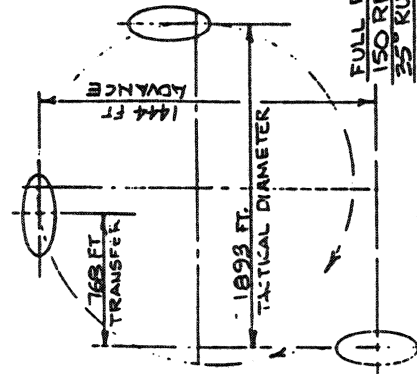
NOTE:
DATA DERIVED FROM TEST BY OSN, LTD.,
MARCH 20, 1984, ON MV YAKIMA. DRAFT = 17'-2".
DISP. APPROX. 2800 TONS ALMOST MIDWAY BETWEEN
LIGHT SHIP (2563 TONS) AND FULL LOAD (3283 TONS)

WARNING:
THE RESPONSE OF THE
DIFFERENT FROM THAT SHOWN HERE IF ANY OF THE
FOLLOWING CONDITIONS UPON WHICH THE MANEUVERING
INFORMATION IS BASED ARE VARIED:

1. CALM WEATHER - WIND 10 KN. OR LESS, CALM SEA
2. NO CURRENT
3. WATER DEPTH TWICE THE VESSEL'S DRAFT OR GREATER
4. CLEAN HULL
5. DIFFERENT DRAFT OR UNUSUAL TRIM

CRASH STOPS

INITIAL CONDITN	DEAD IN THE
RPM	SPEED TIME
150	65.5 KN 56 SEC 063
120	13.1 KN 42.58X 4.99



JUMBO CLASS

Super Crash Stops

Procedure

Operate the propulsion plant at maximum power and when speed becomes steady, record a line of data on the attached log sheets. Ring down "full astern" on the telegraph. Move the control wheel to absorb power from the bow motor and then to build up reversing current to the maximum power level. During the stop, use as little rudder as possible to maintain heading. After "dead in the water," ring "STOP" on the telegraph, then build up speed with half maximum power. At steady speed, record a line of data on the attached sheets. Then, ring down "full astern," and come to a stop, as before.

Repeat these tests with the other pilot house in command. Rerun any tests with phony results.

SUPER AND JUMBO CLASS

Speed Trials

Procedure

Operate the plant with all four main engines on-line. Build up to maximum allowable power, and when ship speed becomes steady, record a line of data on the attached data sheet. Turn the ship 180°, and when the ship speed becomes steady, record a line of data, as before.

Reduce power to half maximum power and repeat tests as above.

Select three other stern propeller speeds and repeat the tests above. One speed shall be between zero and half maximum power; one between half and full maximum power; and the third chosen to fill the bigger gap. Play this by seat of trousers.

Repeat series with each pilot house in command; ten runs total. Rerun any inconsistent tests.

SUPER AND JUMBO CLASS

Turning Circles

Procedure

Steer with wheel or lever. Make sure bow rudder is centered.

Operate the propulsion system at maximum power, and when ship speed becomes steady, record a line of data on the speed data log, and then execute a hard, 270° left turn. Record headings, speed, and machinery data on the attached log sheets at each 90° change in heading.

After the turn, get on course and let speed build up until steady. Record data as above and execute a hard, 270° RIGHT turn. Record data during turn as above.

Get back on course and build up speed with half maximum power. Repeat LEFT and RIGHT turns as above.

Repeat the whole process with the other pilot house in command. Rerun any tests with phony results.

APPENDIX I
VELOCITY AND ACCELERATION SAMPLE CALCULATIONS

This appendix provides sample calculations for the computation of final velocity for a WSF Super Class ferry that is drifting (zero propulsion force) from a given initial velocity. Equations 1, 2, and 3 are used. The vessel acceleration (or deceleration) is computed from the known force acting on the vessel, calculated from Equation 1, and from the vessel mass. This deceleration, along with initial velocity, is used to calculate subsequent velocities after travel over a known distance.

$$R_f/\text{Tons} = 1.21 (10)(1.31)(V/\sqrt{L}) \quad (1)$$

where R_f = total vessel resistance
 V = vessel velocity (ft/sec)
 L = vessel length (ft)

$$A = F/M \quad (2)$$

where A = vessel acceleration (or deceleration) (ft/sec²)
 F = net vessel force (lbs)
 M = vessel mass (lbs/ft/sec²)

$$V_1^2 = V_0^2 + 2 (A) (s) \quad (3)$$

where V_1^2 = vessel final velocity (ft/sec)
 V_0^2 = vessel initial velocity (ft/sec)
 A = vessel acceleration (or deceleration) (ft/sec²)
 s = distance travelled (ft)

SAMPLE CALCULATIONS FOR FINAL VELOCITY

$$1) \quad R_f/\text{Tons} = 1.21 (10)(1.31)(V/\sqrt{L})$$

where	R_t	=	vessel total resistance	varies	lbs
	Tons	=	vessel displacement	fixed	tons
	V	=	vessel velocity	varies	ft/sec
	L	=	vessel length	fixed	ft

Calculate R_t for $V_0 = 28.7$ ft/sec (17 knots)

$$\begin{aligned} R_f/\text{Tons} &= 1.21 (10)1.31(28.7/\sqrt{382.25}) \\ &= 16.7 \\ R_t &= 16.7 * 3283 \\ &= 54701 \text{ lbs} \end{aligned}$$

2) Acceleration

$$A = \frac{R}{M}$$

where A = vessel acceleration variable ft/sec²
R = vessel resistance force variable lbs
M = vessel mass fixed lbs/ft/sec²

Calculate A for R_f = 23939 lbs

Note: R_f = 23939 lbs from Appendix A for V = 28.71 ft/sec

$$A = \frac{23939}{228382.6}$$

$$A = 0.1048$$

3) Final Velocity

$$V_1^2 = V_0^2 + 2 * A * s$$

where V₁ = vessel final velocity variable ft/sec
V₀ = vessel initial velocity variable ft/sec
A = vessel acceleration variable ft/sec²
s = distance variable ft

Calculate V₁ for V₀ = 28.7 ft/sec and s = 500ft

$$V_1^2 = (28.7)^2 - 2 * 0.1408 * 500$$

$$V_1^2 = 683.5$$

$$V_1 = 26.1$$

The fixed values used in the above calculations are from Table I.1.

Table I.1 Vessel Data for WSF Super Class Ferries

Description	Value	Source
Length L	382.25 ft	WSF Brochure
Volumetric Displacement D	114905 ft ³ of sea water	Calculated from Equation 1 (App. A)
Weight Displacement W	3283 tons	Reference (1)
Mass W/g	228382.6 lb/ft/sec ²	Calculated
Prismatic Coefficient C _p	0.5409	Reference (2)
Block Coefficient C _b	0.3439	Reference (2)
Beam B	73.2 ft	WSF Brochure
Waterline Beam B	53.0 ft	Estimated
Draft T	17.25 feet	WSF Brochure
Wetted Surface S	18706 ft ²	Approximated from Equation 2 (App. A)
Density of sea water ρ	1.9905 lb sec ² /ft ⁴	Appendix B
Kinematic Viscosity of sea water ν	1.279x10 ⁻⁵ ft ² /sec	Appendix B
Gravitational Constant g	32.2 ft/sec ²	Constant

REFERENCES

1. Ishii, S. (1991). "Modifications to Ferry Landings to Accomodate Emergency Landings," Master's Thesis presented to the University of Washington, Seattle, WA.
1. Doebler, J.K. (1990). "A Proposal for the Installation of Hoistable Upper Car Decks for Issaquah Class Ferries," Master's Thesis presented to the University of Washington, Seattle, WA.

APPENDIX J
VELOCITY, ACCELERATION, AND
TOTAL RESISTANCE CALCULATIONS

These calculations represent computations required to calculate V_1 using Equation 3, for various values of V_0 , while a WSF Super Class ferry is drifting (zero propulsion force). The value for F , used in Equation 2, is first calculated from Equation 1, and represents the total force acting on the vessel. V_1 is calculated and becomes V_0 for the next iteration. The iterative approach is continued for an arbitrarily chosen range of 4,500 feet. (Note: 4,500 feet is approximately three quarters of a nautical mile).

$$R_f/\text{Tons} = 1.21 (10)(1.31)(V/\sqrt{L}) \quad (1)$$

where R_f = total vessel resistance
 V = vessel velocity (ft/sec)
 L = vessel length (ft)

$$A = F/M \quad (2)$$

where A = vessel acceleration (or deceleration) (ft/sec²)
 F = net vessel force (lbs)
 M = vessel mass (lbs/ft/sec²)

$$V_1^2 = V_0^2 + 2 (A) (s) \quad (3)$$

where V_1^2 = vessel final velocity (ft/sec)
 V_0^2 = vessel initial velocity (ft/sec)
 A = vessel acceleration (or deceleration) (ft/sec²)
 s = distance travelled (ft)

Table J-1. Velocity - Acceleration Calculations for Full Ahead - Zero Power

$$V_1^2 = V_0^2 + 2As$$

Mass = 228382.6 lbs/ft/sec²
 V₀ = 17.0 knots 28.7 fps
 L = 382.3 ft
 D = 3283.0 tons
 s = 500.0 feet

Distance feet	V ₀ knots	V ₀ fps	V/√L knots	R _v /Tons	R _t	A	V ₁
4450	17.0	28.7	0.9	16.7	54701	0.24	24.2
3950	14.3	24.2	0.7	11.0	36170	0.16	20.6
3450	12.2	20.6	0.6	8.0	26194	0.11	17.7
2950	10.5	17.7	0.5	6.1	19926	0.09	15.0
2450	8.9	15.0	0.5	4.8	15608	0.07	12.5
1950	7.4	12.5	0.4	3.8	12436	0.05	10.1
1450	6.0	10.1	0.3	3.0	9977	0.04	7.6
950	4.5	7.6	0.2	2.4	7962	0.03	4.8
450	2.8	4.8	0.1	1.9	6161	0.03	3.1
200	1.8	3.1	0.1	1.6	5272	0.02	1.6
50	1.0	1.6	0.0	1.4	4612	0.02	0.8
0	0.5	0.8	0.0	1.3	4277	0.02	0.0

APPENDIX K

**VELOCITY, ACCELERATION, AND TOTAL RESISTANCE
CALCULATIONS FOR POWER REDUCTION SCENARIOS**

These calculations represent computations required to calculate V_1 using Equation 3, for various values of V_0 , while a WSF Super Class ferry is decelerating after a power reduction of full ahead to slow ahead, to slow astern, and to full astern. The situation of a power reduction from full ahead to slow ahead is similar to a WSF vessel during a normal approach path; WSF vessels reduce power from full ahead to slow ahead at approximately one quarter mile from the landing structure. The total resistance force is calculated from Equation 1. The net force used in Equation 2 is calculated as total resistance minus a constant thrust. V_1 is calculated and becomes V_0 for the next iteration. The iterative approach is continued for an arbitrarily chosen range of approximately 4,500 feet. (Note: 4,500 feet is approximately three quarters of a nautical mile).

$$R_f/\text{Tons} = 1.21 (10)(1.31)(V/\sqrt{L}) \quad (1)$$

where R_f = total vessel resistance
 V = vessel velocity (ft/sec)
 L = vessel length (ft)

$$A = F/M \quad (2)$$

where A = vessel acceleration (or deceleration) (ft/sec²)
 F = net vessel force (lbs)
 M = vessel mass (lbs/ft/sec²)

$$V_1^2 = V_0^2 + 2 (A) (s) \quad (3)$$

where V_1^2 = vessel final velocity (ft/sec)
 V_0^2 = vessel initial velocity (ft/sec)
 A = vessel acceleration (or deceleration) (ft/sec²)
 s = distance travelled (ft)

Table K-1. Velocity - Acceleration Calculations for Full Ahead - Slow Ahead

$V_1^2 = V_0^2 + 2As$
 Mass = 228382.6 lbs/ft/sec²
 $V_0 = 17.0$ knots 28.7 fps
 $L = 382.3$ ft
 $D = 3283.0$ tons
 $s = 500.0$ feet

Distance feet	V_0 knots	V_0 fps	V/\sqrt{L} knots	R_f /Tons	R_t	Thrust	Net Force	A	V_1
5000	17.0	28.7	0.9	16.7	54701	10429	44272	0.19	25.1
4500	14.9	25.1	0.8	12.0	39365	10429	28936	0.13	22.4
4000	13.3	22.4	0.7	9.4	30861	10429	20432	0.09	20.4
3500	12.1	20.4	0.6	7.8	25496	10429	15067	0.07	18.7
3000	11.0	18.7	0.6	6.7	21847	10429	11418	0.05	17.3
2500	10.2	17.3	0.5	5.9	19240	10429	8811	0.04	16.1
2000	9.5	16.1	0.5	5.3	17312	10429	6883	0.03	15.2
1500	9.0	15.2	0.5	4.8	15853	10429	5424	0.02	14.3
1000	8.5	14.3	0.4	4.5	14729	10429	4300	0.02	13.7
500	8.1	13.7	0.4	4.2	13852	10429	3423	0.01	13.1
0	7.8	13.1	0.4	4.0	13162	10429	2733	0.01	12.7
	7.5	12.7	0.4	3.8	12615	10429	2186	0.01	12.3
	7.3	12.3	0.4	3.7	12180	10429	1751	0.01	11.9
	7.1	11.9	0.4	3.6	11833	10429	1404	0.01	11.7
	6.9	11.7	0.4	3.5	11555	10429	1126	0.00	11.5
	6.8	11.5	0.3	3.5	11333	10429	904	0.00	11.3
	6.7	11.3	0.3	3.4	11154	10429	725	0.00	11.2

R_f /Tons = $1.21 * 10(1.31 * V/\sqrt{L})$

Table K-2. Velocity - Acceleration Calculations for Slow Ahead - Slow Astern

$V_1^2 = V_0^2 + 2As$
 Mass = 228382.6 lbs/ft/sec²
 $V_0 = 13.0$ knots 22.0 fps
 $L = 382.3$ ft
 $D = 3283.0$ tons
 $s = 100.0$ ft

Distance feet	V_0 knots	V_0 fps	V/\sqrt{L} knots	R_f /Tons	R_t	Thrust	Net Force	A	V_1
1400	13.0	22.0	0.7	9.0	29519	-10429	39948	0.17	21.1
1300	12.5	21.1	0.6	8.3	27410	-10429	37839	0.17	20.3
1200	12.0	20.3	0.6	7.8	25481	-10429	35910	0.16	19.6
1100	11.6	19.6	0.6	7.2	23712	-10429	34141	0.15	18.8
1000	11.1	18.8	0.6	6.7	22081	-10429	32510	0.14	18.0
900	10.7	18.0	0.5	6.3	20574	-10429	31003	0.14	17.2
800	10.2	17.2	0.5	5.8	19176	-10429	29605	0.13	16.5
700	9.7	16.5	0.5	5.4	17875	-10429	28304	0.12	15.7
600	9.3	15.7	0.5	5.1	16659	-10429	27088	0.12	15.3
500	9.1	15.3	0.5	4.9	16087	-10429	26516	0.12	14.9
400	8.8	14.9	0.5	4.7	15533	-10429	25962	0.11	14.5
300	8.6	14.5	0.4	4.6	14995	-10429	25424	0.11	14.2
200	8.4	14.2	0.4	4.4	14473	-10429	24902	0.11	13.8
100	8.1	13.8	0.4	4.3	13966	-10429	24395	0.11	13.4
0	7.9	13.4	0.4	4.1	13473	-10429	23902	0.10	13.0

R_f /Tons = $1.21 * 10^{(1.31 * V * \sqrt{L})}$

Table K-3. Velocity - Acceleration Calculations for Full Ahead - Full Astern

$$V_1^2 = V_0^2 + 2As$$

- Mass = 228382.6 lbs/ft/sec²
- V₀ = 17.0 knots 28.7 fps
- L = 382.3 ft
- D = 3283.0 tons
- s = 100.0 feet

Distance feet	V ₀ knots	V ₀ fps	V ₁ /L knots	R _t /Tons	R _t	Thrust	Net Force	A	V ₁
1000	17.0	28.7	0.9	15.1	49448	-69752	119200	0.52	26.8
900	15.9	26.8	0.8	12.6	41321	-69752	111073	0.49	25.0
800	14.8	25.0	0.8	10.5	34534	-69752	104286	0.46	23.0
700	13.6	23.0	0.7	8.8	28795	-69752	98547	0.43	21.1
600	12.5	21.1	0.6	7.3	23889	-69752	93641	0.41	19.1
500	11.3	19.1	0.6	6.0	19655	-69752	89407	0.39	16.9
400	10.0	16.9	0.5	4.9	15960	-69752	85712	0.38	14.5
300	8.6	14.5	0.4	3.9	12697	-69752	82449	0.36	11.7
200	6.9	11.7	0.4	3.0	9759	-69752	79511	0.35	8.2
100	4.9	8.2	0.2	2.1	6992	-69752	76744	0.34	0.8
0	0.5	0.8	0.0	1.0	3426	-69752	73178	0.32	0.0

$$R/Tons = 1.21 * 12(0.31 * V\sqrt{L})$$

APPENDIX L
HEADREACH SAMPLE CALCULATIONS

This appendix provides sample calculations for the computation of headreach for a WSF Super Class ferry. Headreach is the distance travelled by a vessel in coming to a full stop from a full-ahead speed. Headreach is calculated using Equation 1. The Dynamic Potential, D_i , parameter used in Equation 1 is estimated from the curve presented in Figure L.1. To use this curve, R/T was taken as 0.8. R is resistance at full-ahead speed, and T is the full-astern thrust. Hence, the value of R/T was estimated as the RPM at full-ahead speed divided by the RPM at full-astern speed. With $R/T = 0.8$, D was estimated as 0.6.

$$s = D (M) V_1^2 / 2 (R) \quad (1)$$

where s = headreach (ft)

D = dynamic potential

M = vessel mass (lb-sec²/ft)

V_1 = initial vessel velocity (ft/sec)

R = vessel resistance and V_1 (lbs)

SAMPLE CALCULATIONS - HEADREACH FOR SUPER CLASS FERRIES

1) Dynamic Potential

$$R/T = 5470 \text{ lbs}/69752 \text{ lbs} = 0.8$$

R = resistance at approach speed variable (lbs)

T = full-astern thrust fixed (lbs)

From Figure 3.7, $D = 0.6$

2) Calculate s for $V_1 = 17$ knots

(note: 17 knots = 28.7 ft/sec, and $R = 54716$ lbs for $V = 28.7$ ft/sec)

$$s = (0.6) (228382.6 \text{ lb sec}^2/\text{ft}) (28.7 \text{ ft/sec})^2 / (2) (54716 \text{ lbs})$$

$$s = 1032.3 \text{ ft}$$

The fixed values used in the above calculations are from Table L.1

Table L.1 Vessel Data for WSF Super Class Ferries

Description	Value	Source
Length L	382.25 ft	WSF Brochure
Volumetric Displacement D	114905 ft ³ of sea water	Calculated from Equation 1 (App. A)
Weight Displacement W	3283 tons	Reference (1)
Mass W/g	228382.6 lb/ft/sec ²	Calculated
Prismatic Coefficient C _p	0.5409	Reference (2)
Block Coefficient C _b	0.3439	Reference (2)
Beam B	73.2 ft	WSF Brochure
Waterline Beam B	53.0 ft	Estimated
Draft T	17.25 feet	WSF Brochure
Wetted Surface S	18706 ft ²	Approximated from Equation 2 (App. A)
Density of sea water ρ	1.9905 lb sec ² /ft ⁴	Appendix B
Kinematic Viscosity of sea water υ	1.279x10-5 ft ² /sec	Appendix B
Gravitational Constant g	32.2 ft/sec ²	Constant

REFERENCES

1. Ishii, S. (1991). "Modifications to Ferry Landings to Accomodate Emergency Landings," Master's Thesis presented to the University of Washington, Seattle, WA.
2. Doebler, J.K. (1990). "A Proposal for the Installation of Hoistable Upper Car Decks for Issaquah Class Ferries," Master's Thesis presented to the University of Washington, Seattle, WA.

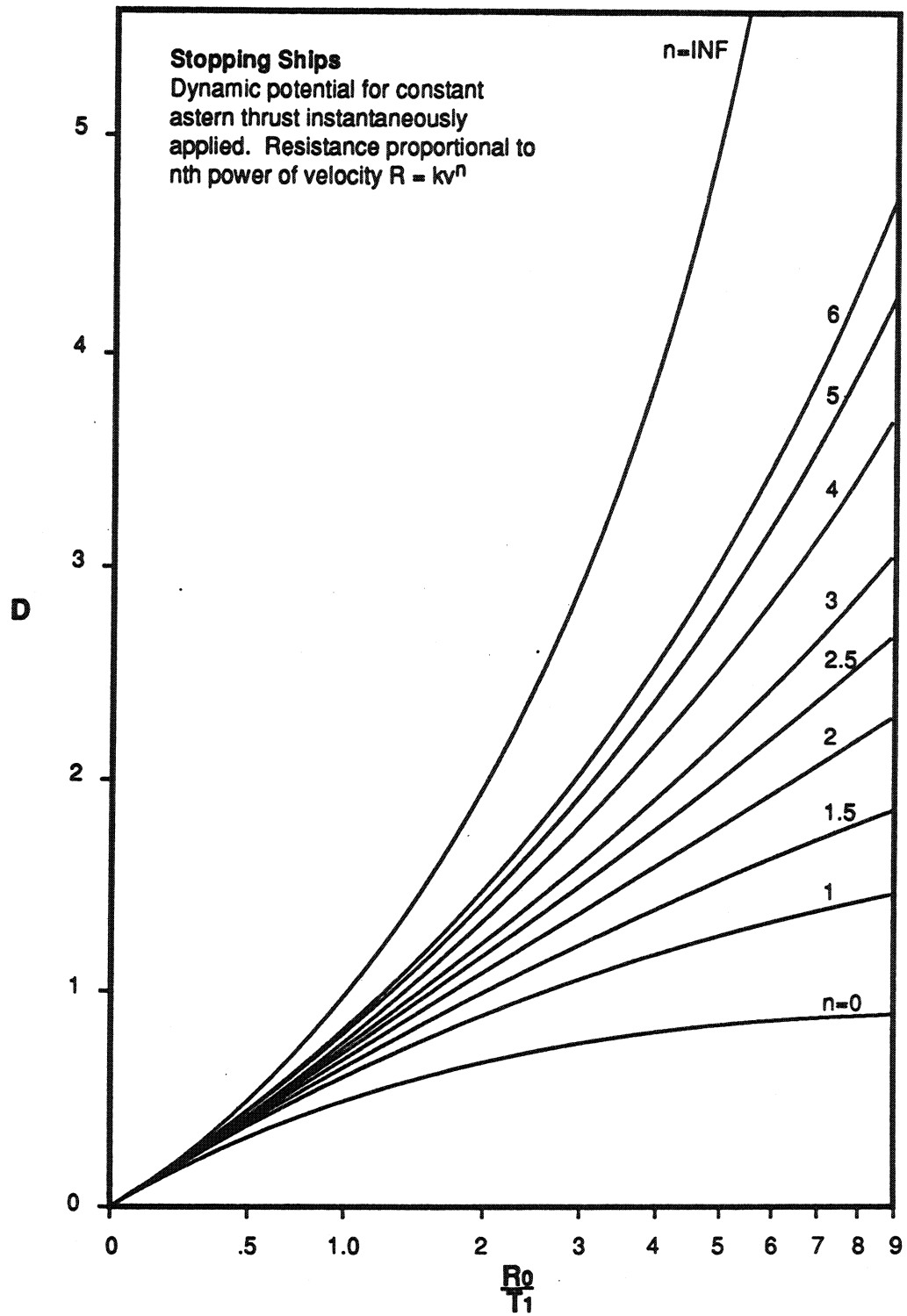


Figure L.1. Stopping Ships. Dynamic potential for constant astern thrust instantaneously applied. Resistance proportional to nth power of velocity (13)

APPENDIX M
DESCRIPTION OF SAN JUAN ISLANDS SAILING

To further understand the maneuvers of a ferry on a regular sailing, the research team took a trip aboard the *MV Hyak* in the San Juan Islands. During this scheduled sailing, the U.S. Coast Guard performed a quarterly inspection. The course of the ferry on this sailing was documented. Records of the maneuvers encountered on a regular sailing provide information to suggest possible full-scale measurements. Full-scale measurements during regular sailings provide quick, easy results to test simulated hypothetical incident scenarios. The following is a description of the voyage, and of the voyage's unique features that were a result of the Coast Guard inspections.

On June 22, 1992, the WSF Super Class Ferry, *MV Hyak* sailed from Anacortes to Orcas Island. The ferry left Anacortes at 10:45 am. Figure M-1 shows the approximate sailing route. The ferry stopped at Lopez Island, Shaw Island, and Orcas Island on the outbound trip. The return trip from Orcas Island to Anacortes was direct; it ended at Anacortes at 2:15 pm. The ferry was docked at Orcas Island for approximately one hour while the Coast Guard performed some of the required drills. Monday, June 22, 1992 was a clear, warm day with a slight breeze. Captain Terry Lee was in command.

Prior to departure, U.S. Coast Guard inspector, Lieutenant Juan Rosario, discussed the quarterly inspection procedures with Captain Lee. Captain Lee and Lieutenant Rosario agreed that Lieutenant Rosario would make the required inspection of the stationary features during the sailing, and that fire and rescue boat drills would be performed while the ferry was docked at Orcas Island. The stationary feature inspection covered fire extinguishers, the presence of emergency procedures manual, presence of life vests and other safety devices, verification of the posting of emergency signs, and confirmation that emergency communications equipment was functional. As the ferry departed from Anacortes, Captain Lee verified the engine RPM for various throttle settings from Wheelhouse #2. The readings are listed below.

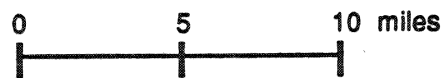
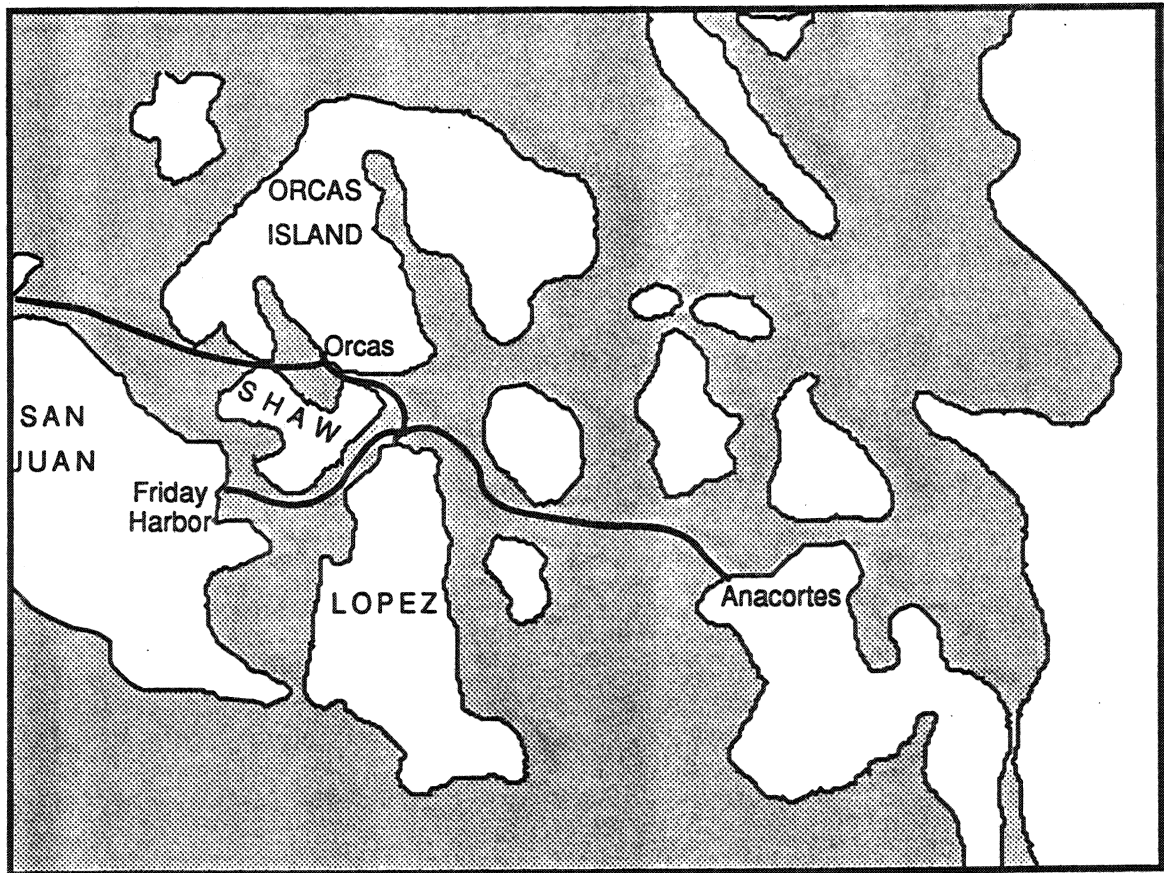


Figure M-1. San Juan Islands Route

Slow astern	50 - 60 RPM
Half astern	90 - 100 RPM
Full astern	120 RPM
Full ahead	120 - 130 RPM

The engine RPM for the same throttle settings, as displayed in the engine room, were as follows:

Slow astern	60 RPM
Half astern	100 RPM
Full astern	Maximum RPM
Slow ahead	50 RPM
Half ahead	80 RPM
Full ahead	145 RPM

Commanding from Wheelhouse #1, Captain Lee set a course for Lopez Island at a throttle setting of full ahead, travelling at a speed of approximately 17 knots. As the ferry approached the landing facility at Lopez Island, Captain Lee reduced the power to slow ahead at approximately five boat lengths from the dock (five boat lengths is approximately 2000 feet). The rudder was put over 20 degrees at approximately two boat lengths from the dock to align the ferry with the dock. The rudder angle was changed to 15 degrees right when the ferry was one boat length out. At the same time, the throttle setting was changed to slow astern, then half astern, then slow astern again as Captain Lee eased the ferry into its docking position. While docked, the throttle setting remained at slow ahead.

The departure from Lopez Island was atypical compared to the Kingston - Edmonds route. Figure M-2 shows the layout of the landing facility at Lopez Island, the surrounding geography, and the approximate course of the ferry into and away from Lopez Island. From Wheelhouse #1, Captain Lee backed away from the landing facility until in a position to swing onto the same general course as the outbound trip from Anacortes. With the throttle setting at half astern, and the rudder at 5 degrees left, the ferry travelled, in reverse, away from Lopez Island. When the ferry was approximately three boat lengths away from the landing facility, the power was changed from half astern to full ahead and the rudder was set to hard right. The change in power and rudder caused the ferry to rotate to the right

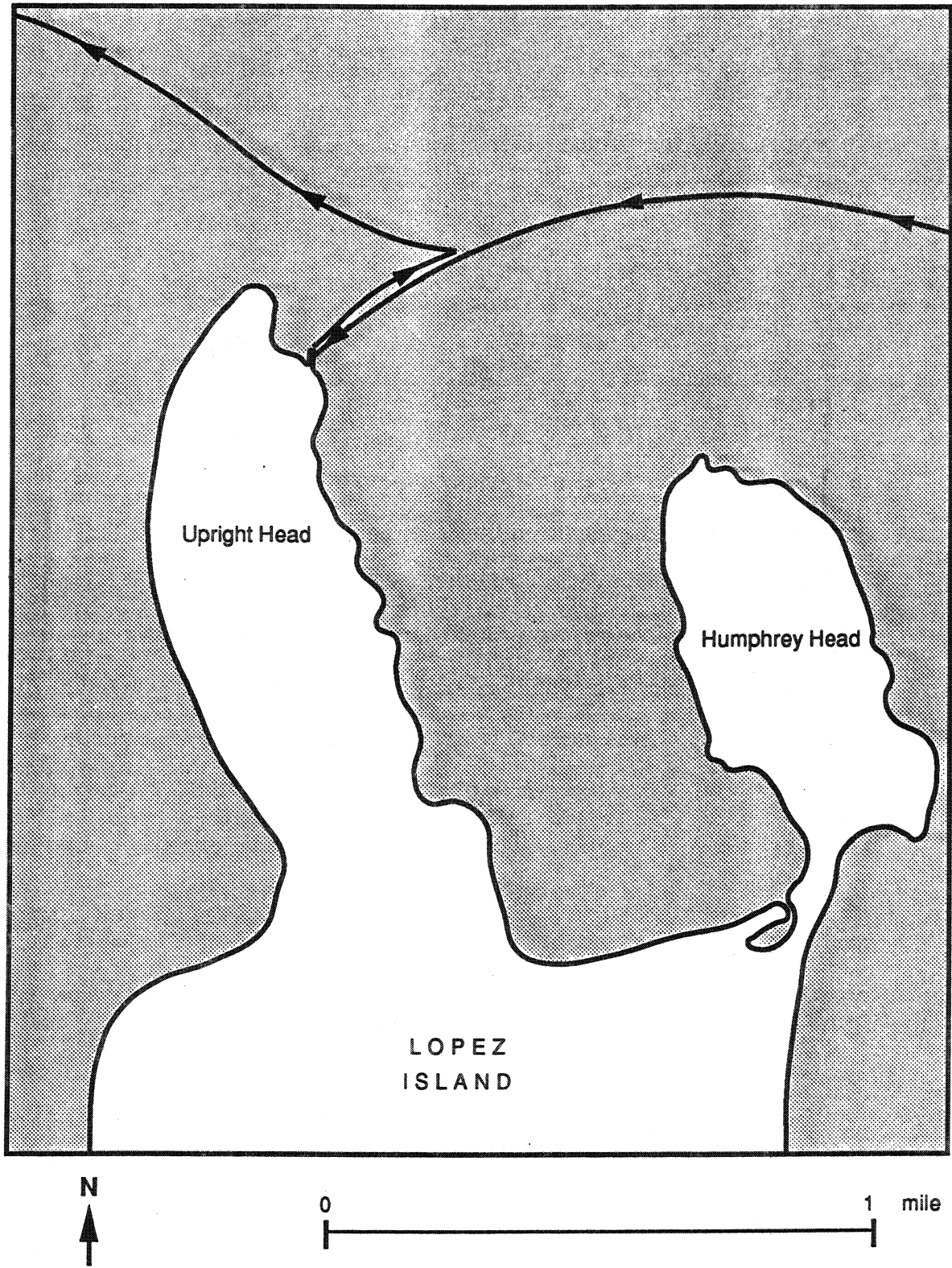


Figure M-2. Arrival and Departure at Lopez Island

without forward motion. When the ferry heading was such that it matched the heading (generally) of the original course, the rudder angle was set to 0 degrees and the ferry moved forward. The ferry resumed its original course and sailed toward Shaw Island at a speed of 17 knots.

The ferry sailed through a passage with Shaw Island to the south and Orcas Island to the north, en route to the Shaw Island terminal. Along this route, Captain Lee demonstrated the MV *Hyak*'s turning response. From Wheelhouse #1, Captain Lee set the rudder from 0 degrees to hard left (35 degrees). Within approximately thirty seconds, the ferry turned. Captain Lee then set the rudder to hard right (35 degrees). Again, within approximately 30 seconds, the ferry turned in the opposite direction. Captain Lee set the rudder back to 0 degrees and resumed course to Shaw Island.

On the approach to the landing facility at Shaw Island, Captain Lee slowed the ferry to slow ahead at approximately five boat lengths from the landing facility. Figure M-3 shows the approximate approach path at Shaw Island. On the approach, the rudder was set at 15 degrees left until the ferry was approximately three boat lengths away from the terminal, at which point the rudder was put over to hard left to position the ferry into the landing. The power was changed to slow astern at approximately two boat lengths from the dock. During the remaining distance, the power was alternated between slow astern and slow ahead until the ferry was docked.

The departure from Shaw Island terminal was similar to the departure from Lopez Island. Figure M-3 shows the approximate departure path from Shaw Island, and the approximate path toward Orcas Island. Once the ferry was travelling forward, it was turned to the right to proceed onto Orcas Island, a short distance from Shaw Island.

Captain Lee slowed the ferry from full ahead to slow ahead at approximately seven boat lengths from the Orcas Island terminal. He changed the power from slow ahead to slow astern for a distance of one boat length; he then set the throttle to stop at a distance of

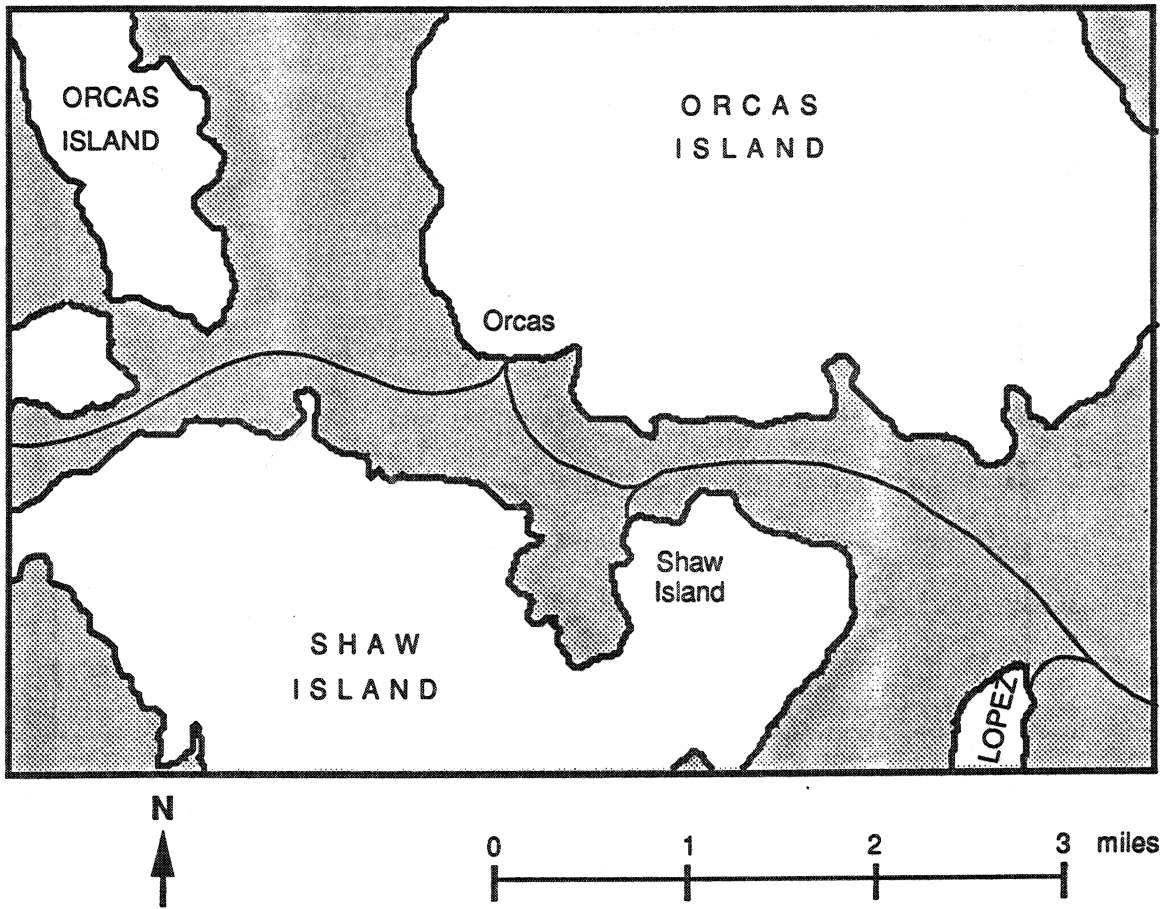


Figure M-3. Arrival and Departure at Shaw Island and at Orcas Island

five boat lengths (approximately) from the dock. In effect, the ferry coasted toward the dock from a distance of approximately five boat lengths. At a distance of one-half boat length the throttle was set to slow astern and the ferry docked as Captain Lee alternated the throttle setting between slow astern and slow ahead.

While docked at Orcas Island, the Coast Guard inspected the fire and the rescue boat drills performed by the crew of the MV *Hyak*. Briefly, the drills were performed as follows:

Fire Drill

After appropriate signals from the wheelhouse, in the form of whistles and bells, the crew mobilized to set positions. One crew member donned protective gear. Fire hoses were removed from the storage positions and activated, spraying water over the railing at an imaginary target. Fire extinguishers were removed from storage positions and aimed at imaginary targets. All fire doors and hatches were inspected. The equipment was then returned to storage.

Rescue Boat Drill

After appropriate signals from the wheel house, in the form of whistles and bells, the crew mobilized to set positions. The signals indicated a specific boat to be launched. The required rescue boat was lowered into the water and two crew members, equipped with life vests, entered the boat. The motor was started and the boat headed toward an imaginary target. The motor was turned off as the boat neared the imaginary target, and oars were used to return the boat to the ferry. The rescue boat was returned to its storage position aboard the ferry.

These drills were completed within one hour and the ferry left Orcas Island to return to Anacortes. The Captain commanded the ferry from Wheelhouse #2 during the return voyage. The ferry travelled at a speed of 17 knots.

The engine and control rooms were toured during the return voyage. An interview with the chief engineer revealed that the vessel response time, the time between the captain's throttle setting in the wheelhouse and the time the engine and vessel react, is a few seconds. During the control room tour, the engine speed corresponding to various throttle settings, as described above, was noted.

On approach to the Anacortes terminal, the ferry travelled approximately perpendicular to the landing facility's center line. As the path of the ferry intersected the projected center line of the landing facility, the ferry was turned 90 degrees to an approach path approximately parallel to the center line of the landing facility. The approach to the Anacortes terminal was similar to the approaches at other terminals. The ferry approached the landing facility at a constant heading. The MV *Hyak* docked at approximately 2:15 pm, thus ending the sailing.

